

STABLE NEARLY SELF-SIMILAR BLOWUP OF THE 2D BOUSSINESQ EQUATIONS WITH SMOOTH DATA

JIAJIE CHEN, THOMAS Y. HOU

ABSTRACT. Inspired by the numerical evidence of a potential 3D Euler singularity [54, 55], we prove finite time blowup of the 2D Boussinesq equations with boundary and smooth initial data of finite energy. There are several essential difficulties in proving finite time blowup of 2D Boussinesq equations with smooth initial data. One of the essential difficulties is to control a number of nonlocal terms that do not seem to offer any damping effect. Another essential difficulty is that the strong advection normal to the boundary introduces a large growth factor for the perturbation if we use weighted L^2 estimates. We overcome this difficulty by using a combination of a weighted L^∞ norm and a weighted $C^{1/2}$ norm, and develop sharp functional inequalities using the symmetry properties of the kernels and some techniques from optimal transport. Moreover we decompose the linearized operator into a leading order operator plus a finite rank operator. The leading order operator is designed in such a way that we can obtain sharp stability estimates. The contribution from the finite rank operator can be captured by an auxiliary variable and its contribution to linear stability can be estimated by constructing approximate solution in space-time. This enables us to establish nonlinear stability of the approximate self-similar profile and prove stable nearly self-similar blowup of the 2D Boussinesq equations with smooth initial data and boundary. In a forthcoming paper, we will extend our blowup analysis to prove finite time blowup of the axisymmetric Euler equations with smooth data and boundary by following our previous work [12].

1. INTRODUCTION

The question whether the 3D incompressible Euler equations can develop a finite time singularity from smooth initial data of finite energy is one of the most outstanding open questions in the theory of nonlinear partial differential equations and fluid dynamics. The main difficulty is due to the presence of the vortex stretching term in the vorticity equation:

$$(1.1) \quad \omega_t + \mathbf{u} \cdot \nabla \omega = \omega \cdot \nabla \mathbf{u},$$

where $\omega = \nabla \times \mathbf{u}$ is the *vorticity vector* of the fluid, and \mathbf{u} is related to ω via the *Biot-Savart law*. The velocity gradient $\nabla \mathbf{u}$ formally has the same scaling as vorticity ω . Thus the vortex stretching term has a quadratic nonlinearity in terms of vorticity. However, the nonlocal nature of the vortex stretching term can lead to dynamic depletion of the nonlinear vortex stretching, thus preventing a finite time blowup, see e.g. [18, 26, 46]. The interested readers may consult the excellent surveys [17, 35, 44, 49, 56] and the references therein.

In this paper, we study the 2D Boussinesq equations on the upper half space:

$$(1.2) \quad \omega_t + \mathbf{u} \cdot \nabla \omega = \theta_x,$$

$$(1.3) \quad \theta_t + \mathbf{u} \cdot \nabla \theta = 0,$$

where the velocity field $\mathbf{u} = (u, v)^T : \mathbb{R}_+^2 \times [0, T) \rightarrow \mathbb{R}_+^2$ is determined via the Biot-Savart law

$$(1.4) \quad -\Delta \psi = \omega, \quad u = -\psi_y, \quad v = \psi_x,$$

where ψ is the stream function. The no flow boundary condition at $y = 0$ reads

$$\psi(x, 0) = 0 \quad x \in \mathbb{R}.$$

It is well known that the 2D Boussinesq equations have the same scaling properties as those of the axisymmetric Euler equations away from the symmetry axis $r = 0$ [56].

The main result of this paper is a rigorous proof of the nearly self-similar blowup of the 2D incompressible Boussinesq equations with smooth initial data and boundary. The blowup

mechanism of the 2D Boussinesq equations with boundary is essentially the same as that of the 3D axisymmetric incompressible Euler equations with boundary. Our work is inspired by the computation of Luo-Hou [54, 55] in which they presented some convincing numerical evidence that the 3D axisymmetric Euler equations with smooth initial data and boundary develop a potential finite time singularity. Inspired by the recent breakthrough of Elgindi [27] (see also [28]) on the blowup of the axisymmetric Euler equations without swirl for $C^{1,\alpha}$ initial velocity, we have proved asymptotically self-similar blowup of the 2D Boussinesq equations and the nearly self-similar blowup of the 3D axisymmetric Euler equations with $C^{1,\alpha}$ velocity and boundary in [12]. The blowup analysis presented in [12] takes advantage of the $C^{1,\alpha}$ velocity in an essential way and does not generalize to prove the Luo-Hou blowup scenario with smooth initial data. The result presented in this paper provides the first rigorous proof of stable nearly self-similar blowup of the 2D Boussinesq equations with smooth data and boundary.

1.1. Some main ingredients in our analysis. We follow a general strategy that we have established in our previous works [12–14]. We first reformulate the problem of studying the finite time blowup of the 2D Boussinesq equations as the problem of proving nonlinear stability of an approximate steady state of the dynamic rescaling formulation. A very important first step is to construct an approximate steady state of the dynamic rescaling formulation with sufficiently small residual errors. We achieve this by decomposing the solution into a semi-analytic part that captures the far field behavior of the solution and a numerically computed part that has compact support. The approximate steady state gives an approximate self-similar profile. See more discussions in Section 5. We remark that there has been some recent exciting development of using a physics-informed neural network (PINN) to construct an approximate steady state of the 2D Boussinesq equations, see [75].

Establishing linear stability of the approximate steady state is the most crucial step in our blowup analysis for the 2D Boussinesq equations with smooth initial data. One essential difficulty is that the advection along the y direction for smooth initial data introduces a large growth factor if we use weighted L^2 energy estimates similar to [12–14, 27], see more discussions in Section 2. Such difficulty is absent in the analysis of 1D models [13, 14] and in the case of $C^{1,\alpha}$ initial velocity [12] since we gain a small factor α for the advection term. To overcome the destabilizing effect due to the y advection, we choose a weighted L^∞ norm, which allows us to extract the maximal amount of damping from the local terms without suffering from the destabilizing effect due to the y advection. In order to close the energy estimates, we use a combination of the weighted L^∞ norm and the weighted $C^{1/2}$ norm, which enables us to establish linear stability of the approximate steady state.

To estimate the nonlocal terms effectively, we derive sharp $C^{1/2}$ estimates for $\nabla \mathbf{u}$ using the symmetry properties of the kernels and some techniques from optimal transport. We note that novel functional inequalities on similar Biot-Savart laws have played a crucial role in the important works in [27, 48]. The authors identify the main term in the Biot-Savart law, which has a much simpler structure, and use it to control the velocity effectively. The sharp Hölder estimates play a similar role in our work. We decompose the Biot-Savart law into two parts. The main terms capture the most singular part of the Biot-Savart law, and the remaining terms are more regular. We can generalize these estimates to the weighted sharp $C^{1/2}$ estimate since the commutators between the singular weights and the velocity operators are more regular. Compared with [27, 48], our remaining terms are not small and cannot be controlled by *a-priori* estimates.

We decompose the linearized equations into three parts. The first part is the main part and differs from the linearized equations by a finite rank operator \mathcal{K} . We choose \mathcal{K} to capture the main contributions from the remaining terms in the Biot-Savart law and estimate \mathcal{K} in the second part. The stability analysis for the first part can be established using the new functional inequalities. The second part accounts for the contributions from \mathcal{K} to the linearized equations. Thanks to the finite rank structure of \mathcal{K} , we perform space-time estimates with computer assistance to obtain sharp stability estimates for the second part. The third part is

small and can be treated as a small perturbation. Note that the first part is not small since the linearized operator is not compact. By integrating these estimates, we establish linear stability.

The main result of this paper is stated by the informal theorem below. The more precise and stronger statement will be given by Theorem 2 in Section 2.

Theorem 1. *There is a family of smooth initial data (θ_0, ω_0) with θ_0 being even and ω_0 being odd, such that the solution of the Boussinesq equations (1.2)-(1.4) develops a singularity in finite time $T < +\infty$. The velocity field \mathbf{u}_0 has finite energy. The blowup solution $(\theta(t), \omega(t))$ is nearly self-similar in the sense that $(\theta(t), \omega(t))$ with suitable dynamic rescaling is close to an approximate blowup profile $\bar{\theta}, \bar{\omega}$ up to the blowup time. Moreover, the blowup is stable for initial data θ_0, ω_0 close to $\bar{\theta}, \bar{\omega}$ in some weighted L^∞ and $C^{1/2}$ norm.*

1.2. A novel framework of analysis with computer assistance. One of our main contributions is to introduce a novel framework of analysis that enables us to obtain sharp stability estimates by combining sharp functional inequalities, energy estimates, and approximate space-time solutions constructed numerically with rigorous error control. Such errors are treated as small perturbations in the energy estimates. Here we give a high level description of the linear stability analysis using this new framework of analysis. More discussions and motivation will be provided in Section 2. Let $\bar{\omega}, \bar{\theta}$ be an approximate steady state. We denote $W = (\omega, \theta_x, \theta_y)$ and decompose $W = \bar{W} + \tilde{W}$ with $\bar{W} = (\bar{\omega}, \bar{\theta}_x, \bar{\theta}_y)$. We further denote by \mathcal{L} the linearized operator around \bar{W} that governs the perturbation \tilde{W} in the dynamic rescaling formulation (see Section 2.5),

$$(1.5) \quad \tilde{W}_t = \mathcal{L}(\tilde{W}),$$

where we have neglected the contributions from the third part, the nonlinear terms and the residual error in the above linearized equation. We note that the coefficients of \mathcal{L} depend on the approximate steady state \bar{W} . We decompose the linearized operator \mathcal{L} into the main part \mathcal{L}_0 plus a finite rank perturbation \mathcal{K} , i.e

$$(1.6) \quad \mathcal{L} = \mathcal{L}_0 + \mathcal{K}.$$

The leading order operator \mathcal{L}_0 is constructed in such way that we can obtain sharp stability estimates and extract damping effect by using sharp functional inequalities.

We first perform energy estimates to extract the damping effect from the leading order operator \mathcal{L}_0 in the weighted L^∞ norm. By choosing appropriate singular weights, we can establish stability associated with \mathcal{L}_0 using the weighted L^∞ norm with a weak coupling to the weighted $C^{1/2}$ norm. Obtaining sharp energy estimates in the weighted $C^{1/2}$ norm is more challenging. To obtain a sharp bound in the weighted $C^{1/2}$ norm, we exploit the symmetry properties of the kernels and apply **optimal transport** along the horizontal and the vertical directions separately to obtain relatively sharp $C^{1/2}$ estimates. Since the contribution from the horizontal direction dominates that from the vertical direction, our strategy gives a relatively tight bound in the weighted $C^{1/2}$ norm.

To estimate the perturbed operator \mathcal{K} , we perform space-time estimates with computer assistance. We use the following toy model to illustrate the main ideas by considering \mathcal{K} as a rank-one operator $\mathcal{K}(\tilde{W}) = a(x)P(\tilde{W})$ for some nonlocal bounded linear operator P satisfying the properties (i) $P(\tilde{W})$ is constant in space and is only a function of time; (ii) $\|P(\tilde{W})\| \leq c\|\tilde{W}\|$. Given initial data \tilde{W}_0 , we decompose (1.5) as follows

$$(1.7) \quad \begin{aligned} \partial_t \tilde{W}_1(t) &= \mathcal{L}_0 \tilde{W}_1, & \tilde{W}_1(0) &= \tilde{W}_0, \\ \partial_t \tilde{W}_2(t) &= \mathcal{L} \tilde{W}_2 + a(x)P(\tilde{W}_1(t)), & \tilde{W}_2(0) &= 0. \end{aligned}$$

It is easy to see that $\tilde{W} = \tilde{W}_1 + \tilde{W}_2$ solves (1.5) with initial data \tilde{W}_0 since $\mathcal{L} = \mathcal{L}_0 + a(x)P$ by our assumption. By construction, the leading operator \mathcal{L}_0 has the desired structure that enables us to obtain sharp stability estimates. The second part \tilde{W}_2 is driven by the rank-one forcing term $a(x)P(\tilde{W}_1(t))$. Using Duhamel's principle, the fact that $P(\tilde{W}_1(t))$ is constant in space, we

yield

$$(1.8) \quad \widetilde{W}_2(t) = \int_0^t P(\widetilde{W}_1(s)) e^{\mathcal{L}(t-s)} a(x) ds.$$

Since $\widetilde{W}_1(t) = e^{\mathcal{L}_0(t)} \widetilde{W}_0$ decays in $L^\infty(\varphi)$ (ϕ is a singular weight), we can control $P(\widetilde{W}_1(s))$. If $e^{\mathcal{L}(t)} a(x)$ decays in $L^\infty(\varphi)$ for large t , we can show that $\widetilde{W}_2(t)$ also decays in $L^\infty(\varphi)$ and establish stability estimate of \widetilde{W}_2 .

A crucial idea in the estimate of \mathcal{K} is that we bridge the energy estimates and numerical PDEs via an approximate solution in space and time. To see this, we note that $e^{\mathcal{L}(t)} a(x)$ is equivalent to solving the linear evolution equation $v_t = \mathcal{L}(v)$ with initial data $v_0 = a(x)$. Due to the rapid decay of the linearized equation, we only need to solve this initial value problem using a numerical scheme up to a modest time T_1 and pad the solution beyond T_1 to be zero. The residual error of the numerical PDE in space and time is treated as a small perturbation in the energy estimates. We then construct an approximate solution by interpolating the solution in time by a cubic polynomial. The stability property of \widetilde{W}_1 allows us to control the numerical error in computing $e^{\mathcal{L}(t)} a(x)$ and obtain sharp stability estimates for \widetilde{W}_2 .

We remark that we only need to modify the linearized operator by a finite rank operator in a small sector near the boundary where we have the smallest amount of damping. We also add a few more terms to approximate the regular part of the solution in the bulk of the domain. The amount of damping improves significantly as we move away from the boundary and in the far field. Moreover, due to the decay of the far field solution \overline{W} , we only need to construct a finite rank operator $\widetilde{\mathcal{L}}$ in a finite size domain within this narrow sector. The rank of $\widetilde{\mathcal{L}}$ that we use is less than 50. The contributions from the finite rank operator require solving the linear PDE in space-time with a number of initial data, which can be implemented in full parallel. We have not explored the full potential of our method. If we try to perturb the linearized operator by a rank- N operator, we just need to solve the linearized evolution equation with N initial data, which can be solved very efficiently using a powerful parallel cluster.

Our stability analysis uses some quantities involving the approximate steady state. The grid values of these quantities are available with rigorous error bounds using interval arithmetic. Since we use piecewise polynomials to approximate the steady state, we can obtain rigorous bounds for the high order derivatives of the steady state. Such bounds in turn provide rigorous bounds for lower order derivatives, the pointwise values and various integrals involving the approximate steady state by using standard numerical analysis. The verification involves several case studies. We will present all the essential tools for verification in the Appendix and also in later sections, but will defer the actual verification steps of various quantities to the Supplementary Materials.

Our blowup analysis can be extended to prove finite time blowup of the axisymmetric Euler equations with smooth initial data and boundary (the Luo-Hou scenario). We can follow the same ideas presented in our previous work [12] by controlling the support of the vorticity to be in a small region that is close to the boundary and does not intersect the symmetry axis. The asymptotic scaling properties of the Biot-Savart kernels are essentially the same as those of the Biot-Savart kernels for the 2D Boussinesq equations after making appropriate changes of variables. Since the analysis is essentially the same, we do not present the analysis here.

1.3. Comparison between our method of analysis and the topological argument. Our method of analysis shares some similarity with the recently developed blowup analysis using a topological argument, see e.g. [58, 62–64]. In the topological argument, one also constructs a compact perturbation operator \mathcal{K} to the linearized operator \mathcal{L} . After subtracting the compact perturbation operator from the linearized operator, one can establish linear stability of the leading operator \mathcal{L}_0 in some Hilbert space. The compact perturbation operator can be approximated by a finite rank operator. Typically, this compact perturbation operator contains a number of unstable directions. A topological argument is used to show that there exists a stable trajectory leading to a finite time blowup, which avoids a finite number of unstable directions. This method has been used to prove unstable blowup of several nonlinear PDEs with great success.

The main difference between our method of analysis and the topological argument is in the way we estimate the finite rank operator \mathcal{K} . First of all, in our framework, we do not require the energy space to be a Hilbert space. The main innovation of our approach is that we develop a constructive method of analysis to establish stability of the finite rank operator by solving a finite number of decoupled linear PDEs in space-time with rigorous error control. This allows to establish linear stability of the original linearized operator \mathcal{L} . In comparison, a typical topological argument may only allow one to establish stability of the leading order operator \mathcal{L}_0 at the expenses of creating finitely many unstable directions induced by the finite rank operator \mathcal{K} . Such method is ideal if we expect to have unstable blowup. However, if we expect to have stable blowup as in the Luo-Hou blowup scenario, proving blowup with finitely many unstable directions for the Luo-Hou blowup scenario using a topological argument is not satisfactory.

The stability analysis presented in this paper can be substantially simplified if we have access to a very powerful parallel cluster with much faster CPUs. If the rank of the finite rank operator \mathcal{K} is sufficiently large and the residual errors can be made arbitrarily small, we can treat the third part of the linearized operator, the nonlinear terms and the residual errors as small perturbations, which can be essentially neglected in the stability analysis. We just need to focus on establishing linear stability of the leading order operator \mathcal{L}_0 . This provides a very powerful tool to give a constructive proof of stable nearly self-similar blowup for a large class of nonlinear PDEs with smooth initial data. Moreover, the computation of the finite rank operator can be done in full parallel and we only need to choose a low rank operator \mathcal{K} in our analysis.

1.4. Review of literature. There has been a lot of effort in studying potential singularity of the 3D Euler equations using various simplified models. In [55], the authors proposed the Hou-Luo model. This model captures many essential features observed in the Luo-Hou blowup scenario for the axisymmetric Euler equations. The blowup of the Hou-Luo model was first established in [15]. In [16, 38, 39, 50], the authors proposed several simplified models to study the Luo-Hou blowup scenario [54, 55] and established finite time blowup of these models. In these works, the velocity is determined by a simplified Biot-Savart law in a form similar to the key lemma in the seminal work of Kiselev-Sverak [48]. In [13], Chen-Hou-Huang proved the asymptotically self-similar blowup of the Hou-Luo model by extending the method of analysis established for the finite time blowup of the De Gregorio model by the same authors in [14]. In [30, 32], Elgindi and Jeong proved finite time singularity formation for the 2D Boussinesq and 3D axisymmetric Euler equations in a domain with a corner using $\mathcal{C}^{0,\alpha}$ data.

Several other 1D models, including the Constantin-Lax-Majda (CLM) model [19], the De Gregorio (DG) model [24, 25], the gCLM model [68] and the Hou-Li model [45], have been introduced to study the effect of advection and vortex stretching in the 3D Euler equations. Singularity formation from smooth initial data has been established for the CLM model in [19], for the DG model in [14], and for the gCLM model with various parameters in [5, 8, 10, 14, 29, 31]. In the viscous case, singularity formation of the gCLM model with some parameters has been established in [8, 70].

There has been some interesting recent results on the potential instability of the Euler blowup solutions, see [51, 72]. In a recent paper [11], we showed that the blowup solutions of the 2D Boussinesq and 3D Euler equations with $C^{1,\alpha}$ velocity considered in [12, 27] are also unstable using the notion of stability introduced in [51, 72]. These two seemingly contradictory results reflect the difference of the two approaches in studying the stability of 3D Euler blowup solutions. The linear stability analysis in [51, 72] is performed by directly linearizing the 3D Euler equations around a blowup solution in the original variables. It does not take into account the changes in the blowup time and the blowup exponent due to the change of the initial condition. Such information has been used in establishing the nonlinear stability of the blowup profile in [12, 27]. In [42, 43], Hou and Huang reported a potential two-scale traveling singularity for the 3D Euler equations in the interior domain. Inspired by the work reported in [42, 43], Hou discovered a new class of potential Euler singularity at the origin whose scaling properties are compatible with those of the Navier-Stokes equations [41]. Moreover, the Navier-Stokes equations with the same smooth initial data develop potentially singular solutions at the origin with maximum vorticity

increasing by a factor of 10^7 [40]. Various blowup criteria have been applied to provide strong support for this potentially singular behavior of the Navier-Stokes equations.

The rest of the paper is organized as follows. In Section 2, we provide detailed discussions and some key ingredients in establishing linear stability of an approximate profile using various simplified models. In Section 3, we show how to obtain sharp Hölder estimates using optimal transport. Section 4 is devoted to energy estimates and Section 5 is devoted to the construction of an approximate self-similar profile using the dynamic rescaling formulation. In Section 6, we demonstrate how to construct the leading order linearized operator \mathcal{L}_0 and the finite rank perturbation operator \mathcal{K} . Finally we show how to estimate the L^∞ and Hölder norms of the velocity in the regular case in Section 7. Some technical estimates and derivations are deferred to the Appendix.

2. LINEAR STABILITY ANALYSIS AND THE MAIN IDEAS

In this section, we will outline the main ingredients in our stability analysis by using the dynamic rescaling formulation for the 2D Boussinesq equations. The most essential part of our analysis lies in the linear stability. We need to use a number of techniques to extract the damping effect from the linearized operator around the approximate steady state of the dynamic rescaling equations and obtain sharp estimates of various nonlocal terms. Since the damping coefficient we obtain is relatively small, we need to construct an approximate steady state with a very small residual error. This is extremely challenging since the solution is supported on the upper half plane with a slowly decaying tail in the far field. We use analytic estimates and numerical analysis with rigorous error control to verify that the residual error is small in the energy norm. See more detailed discussions in Section 5 and the Supplementary Materials.

Passing from linear stability to nonlinear stability is relatively easier since the perturbation is quite small due to the small residual error. Yet we need to verify various inequalities involving the approximate steady state using the interval arithmetic [36, 67, 69] and numerical analysis with computer assistance. The most essential part of the linear stability analysis can be established based on the grid point values of the approximate steady state constructed on a relatively coarse grid, which does not involve the lengthy rigorous verification. The reader who is not interested in the rigorous verification can skip the lengthy verification process to be presented in the Supplementary Materials.

2.1. Notations and operators. The upper bar notation is reserved for the approximate steady state, e.g. $\bar{\omega}, \bar{\theta}$.

We introduce the notations for the nonlinear terms

$$(2.1) \quad \mathcal{N}_1 = -\mathbf{u} \cdot \nabla \omega + c_\omega \omega, \quad \mathcal{N}_2 = -\mathbf{u} \cdot \nabla \eta - u_x \eta - v_x \xi + 2c_\omega \eta, \quad \mathcal{N}_3 = -\mathbf{u} \cdot \nabla \xi - u_y \eta - v_y \xi + 2c_\omega \xi.$$

Without specification, \mathcal{N}_i depends on (ω, η, ξ) . Given the approximate steady state $\bar{\omega}, \bar{\theta}, \bar{c}_l, \bar{c}_\omega$, we denote by $\bar{\mathcal{F}}_i$ and $\bar{F}_\omega, \bar{F}_\theta$ the residual error

$$(2.2) \quad \begin{aligned} \bar{F}_\omega &= -(\bar{c}_l x + \bar{\mathbf{u}}) \cdot \nabla \bar{\omega} + \bar{\theta}_x + \bar{c}_\omega \bar{\omega}, & \bar{F}_\theta &= -(\bar{c}_l x + \bar{\mathbf{u}}) \cdot \nabla \bar{\theta} + \bar{c}_\theta \bar{\theta}, \\ \bar{\mathcal{F}}_1 &\triangleq \bar{F}_\omega, & \bar{\mathcal{F}}_2 &\triangleq \partial_x \bar{F}_\theta, & \bar{\mathcal{F}}_3 &\triangleq \partial_y \bar{F}_\theta. \end{aligned}$$

Notations. Denote by C_x^α, C_y^α the partial Hölder seminorms

$$(2.3) \quad [\omega]_{C_x^\alpha(D)} \triangleq \sup_{x, z \in D, x_2 = z_2} \frac{|\omega(x) - \omega(z)|}{|x_1 - z_1|^\alpha}, \quad [\omega]_{C_y^\alpha(D)} \triangleq \sup_{x, z \in D, x_1 = z_1} \frac{|\omega(x) - \omega(z)|}{|x_2 - z_2|^\alpha}.$$

Given a weight $g(h) : \mathbb{R}^2 \rightarrow \mathbb{R}_+$ that is $-\alpha$ -homogeneous, i.e. $g(\lambda h_1, \lambda h_2) = \lambda^{-\alpha} g(h)$, e.g., $g(h) = |h|^{-\alpha}$, we define the weighted Hölder seminorm

$$(2.4) \quad \|\omega\|_{C_g^\alpha(D)} = \sup_{x, z \in D} |(\omega(x) - \omega(z))g(x - z)|.$$

We will mostly use $D = \mathbb{R}_{++}^2$. In this case, we drop D to simplify the notations.

We define $\langle f, g \rangle$ the inner product in \mathbb{R}_{++}^2

$$(2.5) \quad \langle f, g \rangle = \int_{\mathbb{R}_{++}^2} f(x)g(x)dx.$$

2.2. Dynamic rescaling formulation. Following [12–14], we consider the dynamic rescaling formulation of the 2D Boussinesq equations. Let $\omega(x, t), \theta(x, t), \mathbf{u}(x, t)$ be the solutions of (1.2)–(1.4). Then it is easy to show that

$$(2.6) \quad \begin{aligned} \tilde{\omega}(x, \tau) &= C_\omega(\tau)\omega(C_l(\tau)x, t(\tau)), & \tilde{\theta}(x, \tau) &= C_\theta(\tau)\theta(C_l(\tau)x, t(\tau)), \\ \tilde{\mathbf{u}}(x, \tau) &= C_\omega(\tau)C_l(\tau)^{-1}\mathbf{u}(C_l(\tau)x, t(\tau)), \end{aligned}$$

are the solutions to the dynamic rescaling equations

$$(2.7) \quad \tilde{\omega}_\tau(x, \tau) + (c_l(\tau)\mathbf{x} + \tilde{\mathbf{u}}) \cdot \nabla \tilde{\omega} = c_\omega(\tau)\tilde{\omega} + \tilde{\theta}_x, \quad \tilde{\theta}_\tau(x, \tau) + (c_l(\tau)\mathbf{x} + \tilde{\mathbf{u}}) \cdot \nabla \tilde{\theta} = c_\theta\tilde{\theta},$$

where $\tilde{\mathbf{u}} = (\tilde{u}, \tilde{v})^T = \nabla^\perp(-\Delta)^{-1}\tilde{\omega}$, $\mathbf{x} = (x, y)^T$,

$$(2.8) \quad C_\omega(\tau) = \exp\left(\int_0^\tau c_\omega(s)d\tau\right), \quad C_l(\tau) = \exp\left(\int_0^\tau -c_l(s)ds\right), \quad C_\theta = \exp\left(\int_0^\tau c_\theta(s)d\tau\right),$$

$t(\tau) = \int_0^\tau C_\omega(s)d\tau$ and the rescaling parameters $c_l(\tau), c_\theta(\tau), c_\omega(\tau)$ satisfy [12]

$$(2.9) \quad c_\theta(\tau) = c_l(\tau) + 2c_\omega(\tau).$$

We have the freedom to choose the time-dependent scaling parameters $c_l(\tau)$ and $c_\omega(\tau)$ according to some normalization conditions. These two free scaling parameters are related to the fact that Boussinesq equations have scaling-invariant property with two parameters. The 3D Euler equations enjoy the same property. See [12]. After we determine the normalization conditions for $c_l(\tau)$ and $c_\omega(\tau)$, the dynamic rescaling equation is completely determined and the solution of the dynamic rescaling equation is equivalent to that of the original equation using the scaling relationship described in (2.6)–(2.8), as long as $c_l(\tau)$ and $c_\omega(\tau)$ remain finite.

We remark that the dynamic rescaling formulation was introduced in [52, 60] to study the self-similar blowup of the nonlinear Schrödinger equations. This formulation is also called the modulation technique in the literature and has been developed by Merle, Raphael, Martel, Zaag and others. It has been a very effective tool to analyze the formation of singularities for many problems like the nonlinear Schrödinger equation [47, 61], compressible Euler equations [2, 3], the nonlinear wave equation [66], the nonlinear heat equation [65], the generalized KdV equation [57], and other dispersive problems. Recently, this method has been applied to study singularity formation in incompressible fluids [12, 27] and related models [8–10, 14].

To simplify our presentation, we still use t to denote the rescaled time in (2.7) and simplify $\tilde{\omega}, \tilde{\theta}$ as ω, θ

$$(2.10) \quad \begin{aligned} \omega_t + (c_l x + \mathbf{u}) \cdot \nabla \omega &= \theta_x + c_\omega \omega, \\ \theta_t + (c_l x + \mathbf{u}) \cdot \nabla \theta &= c_\theta \theta. \end{aligned}$$

Following [13], we impose the following normalization conditions on c_ω, c_l

$$(2.11) \quad c_l = 2 \frac{\theta_{xx}(0)}{\omega_x(0)}, \quad c_\omega = \frac{1}{2}c_l + u_x(0), \quad c_\theta = c_l + 2c_\omega.$$

For smooth data, these two normalization conditions play the role of enforcing

$$(2.12) \quad \theta_{xx}(t, 0) = \theta_{xx}(0, 0), \quad \omega_x(t, 0) = \omega_x(0, 0)$$

for all time. In fact, we can derive the ODEs of $\theta_{xx}(t, 0)$ and $\omega_x(t, 0)$

$$\frac{d}{dt}\omega_x(t, 0) = (c_\omega - c_l - u_x(0))\omega_x(t, 0) + \theta_{xx}(t, 0), \quad \frac{d}{dt}\theta_{xx}(t, 0) = (c_\theta - 2(c_l + u_x(0)))\theta_{xx}(t, 0),$$

where we have used $v|_{y=0} = 0, v_x(t, 0) = 0$. Under the conditions (2.11), the right hand sides vanish.

2.3. Main Result. In this subsection, we will state our main result. We first introduce some notations and define our energy. Let $\psi_i, \varphi_i, \psi_{i,g}, g_i$ be the singular weights defined in (C.1), (C.2), (C.3), and $\mu_1, \mu_2, \tau_1, \tau_2, \mu_4$ be the parameters chosen in (C.4).

We define the energy E on three variables f_1, f_2, f_3 as follows

$$(2.13) \quad \begin{aligned} P_1 &= \max_{1 \leq i \leq 3} \|f_i \varphi_i\|_\infty, \quad P_2 = \max(\|f_1 \psi_1\|_{C_{g_1}^{1/2}}, \mu_1 \|f_2 \psi_2\|_{C_{g_2}^{1/2}}, \mu_2 \|f_3 \psi_3\|_{C_{g_3}^{1/2}}) \\ P_3 &= \tau_2 \max(\mu_2 \|f_1 \varphi_{g,1}\|_\infty, \|f_2 \varphi_{g,2}\|_\infty, \|f_3 \varphi_{g,3}\|_\infty), \\ P_4 &= \max\left(\frac{1}{65} |c_\omega(\omega)|, \frac{1}{10} |f_{2,xy}(0)|, \frac{1}{5} |f_{1,xy}(0)|\right), \quad E = \max(P_1, P_2, P_3, P_4). \end{aligned}$$

where $u_x(f)(0) = -\frac{4}{\pi} \int_{\mathbb{R}_2^{++}} \frac{y_1 y_2}{|y|^4} f(y) dy$.

Theorem 2. Let $(\bar{\theta}, \bar{\omega}, \bar{c}_l, \bar{c}_\omega)$ be the approximate self-similar profile constructed in Section 5 and $E_* = 5 \cdot 10^{-6}$. For even initial data $\theta_{0,x}$ and odd ω_0 of (2.10) with a small perturbation to $(\bar{\theta}, \bar{\omega})$ with $E(\omega_0 - \bar{\omega}, \theta_{0,x} - \bar{\theta}_x, \bar{\theta}_{0,y} - \bar{\theta}_y) < E_*$, we have

$$(2.14) \quad \|\omega - \bar{\omega}\|_{L^\infty}, \|\theta_x - \bar{\theta}_x\|_{L^\infty}, \|\theta_y - \bar{\theta}_y\|_\infty < 10^3 E_*, \quad |u_x(t, 0) - \bar{u}_x(0)|, |\bar{c}_\omega - c_\omega| < 100 E_*$$

for all time. In particular, we can choose smooth initial data $\omega_0, \theta_0 \in C_c^\infty$ in this class with finite energy $\|\mathbf{u}_0\|_{L^2} < +\infty$ such that the solution to the physical equations (1.2)-(1.4) with these initial data blows up in finite time T .

Remark 2.1. In our analysis, we decompose the nonlinear operator that governs the evolution of the perturbation into two parts. Correspondingly, we decompose the perturbation $\widetilde{W} = (\omega - \bar{\omega}, \theta_x - \bar{\theta}_x, \theta_y - \bar{\theta}_y)$ into two components, $\widetilde{W} = \widetilde{W}_1 + \widetilde{W}_2$, see Section 2.10.3 for the precise decomposition. At the linear level, the evolution of \widetilde{W}_1 is governed by a leading order operator \mathcal{L}_0 that enjoys sharp energy estimates after we subtract a finite rank operator. The perturbation \widetilde{W}_2 mainly captures the contributions from the finite rank perturbation operator. One advantage of using such decomposition is that \widetilde{W}_1 is only weakly coupled to \widetilde{W}_2 through the nonlinear terms and the residual errors, which are small. We can estimate the contributions of \widetilde{W}_2 to the linear stability by solving a finite number of linear PDEs in space and time and estimate the space-time residual errors via energy estimates. The stability of the leading order operator \mathcal{L}_0 enables us to control the residual errors arising from solving the linear PDEs in space and time rigorously. A crucial step in proving our main theorem is to establish the estimate $E_4(\widetilde{W}_1) < E_*$ with energy E_4 defined in (4.59). Note that $\widetilde{W}_1 = \widetilde{W}$ at $t = 0$ and the energy E_4 agrees with E at $t = 0$. See Sections 2.10, 4, and (4.8.5) for more discussions.

We will follow the framework in [12–14] to establish finite time blowup. It consists of the following steps: (a) construct approximate steady state to (2.10) with small residual error in suitable functional spaces; (b) perform linear and nonlinear stability analysis around the approximate steady state; (c) choose small perturbation in the energy space to obtain smooth initial data with finite energy and obtain finite time blowup using a rescaling argument and the stability results.

In the remaining of this section, we will outline some main ingredients in our blowup analysis by using a number of simplified models to illustrate and motivate the main ideas behind our method of analysis.

2.4. Basic properties of the approximate steady state. Following the ideas in [13, 14], we construct the approximate steady state $(\bar{\omega}, \bar{\theta}, \bar{c}_\omega, \bar{c}_l)$ of the dynamic rescaling equations (2.10), (2.11) by solving them numerically for a long enough time. In Figure 1, we plot the approximate steady state $\bar{\omega}, \bar{\theta}_x$. We plot the variable $\bar{\theta}_x$ rather than $\bar{\theta}$ since $\bar{\theta}$ grows in the far-field. Given the approximate steady state, we construct the numerical stream function $\bar{\psi}^N$ by solving the Poisson equations. Then we can derive the residual (2.2) up to the error in solving the Poisson equations. In Figure 2, we plot the piecewise rigorous bound of the weighted $L^\infty(\varphi_1)$ norm of $\bar{\mathcal{F}}_1$ and the $L^\infty(\varphi_2)$ norm of $\bar{\mathcal{F}}_2$. We remark that φ_1, φ_2 are very singular near $x = 0$ with leading order $|x|^{-2.9}, 0.385|x|^{-3}$. This is why the weighted $L^\infty(\varphi_1)$ norm of $\bar{\mathcal{F}}_1$ and the $L^\infty(\varphi_2)$ norm of $\bar{\mathcal{F}}_2$ are relatively large near the origin.

We observe that unweighted errors of $\bar{\mathcal{F}}_1, \bar{\mathcal{F}}_2$ are very small near the origin, less than $2 \cdot 10^{-12}$ since we use a uniform fine grid near the origin. In Figure 3, we plot the piecewise rigorous bound of the unweighted L^∞ norm of $\bar{\mathcal{F}}_1$ and the L^∞ norm of $\bar{\mathcal{F}}_2$ in a local domain near the origin. Note that the unweighted L^∞ norm of $\bar{\mathcal{F}}_1$ and the L^∞ norm of $\bar{\mathcal{F}}_2$ increase as $|x|$ increases. On the other hand, since the singular weights have a very mild growth rate in the far field of order $O(|x|^{1/16})$, the contributions from these weighted errors to the energy E_3 scale like $0.165 * |x|^{1/16} \|\bar{\mathcal{F}}_i\|_{L^\infty}$ ($i = 1, 2$). Thus the weighted L^∞ norm of $\bar{\mathcal{F}}_1$ and the L^∞ norm of $\bar{\mathcal{F}}_2$ only amplify the unweighted norms very mildly in the far field. Since the damping effect is stronger in the far field, we are able to close the energy estimates with the residual errors that we obtain. We defer the details of numerical computation to Section 5. Here, we list some important properties of the approximate steady state.

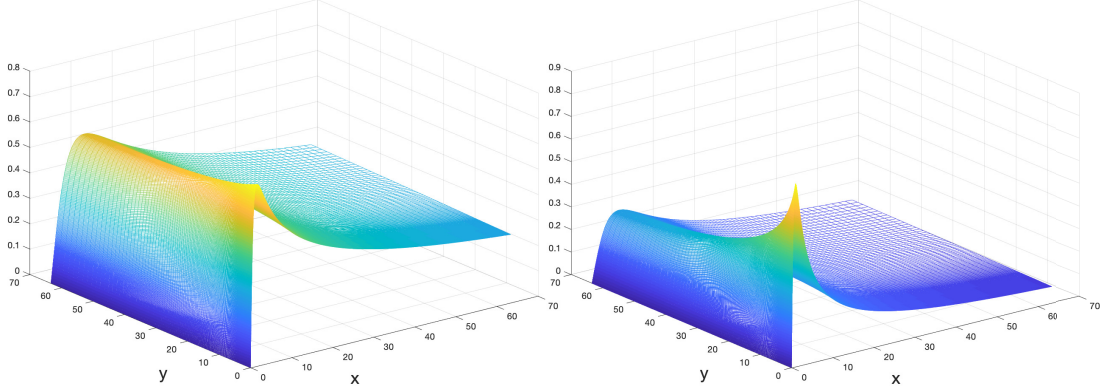


FIGURE 1. Approximate steady state in the near-field. Left figure: profile $\bar{\omega}$; right figure: $\bar{\theta}_x$.

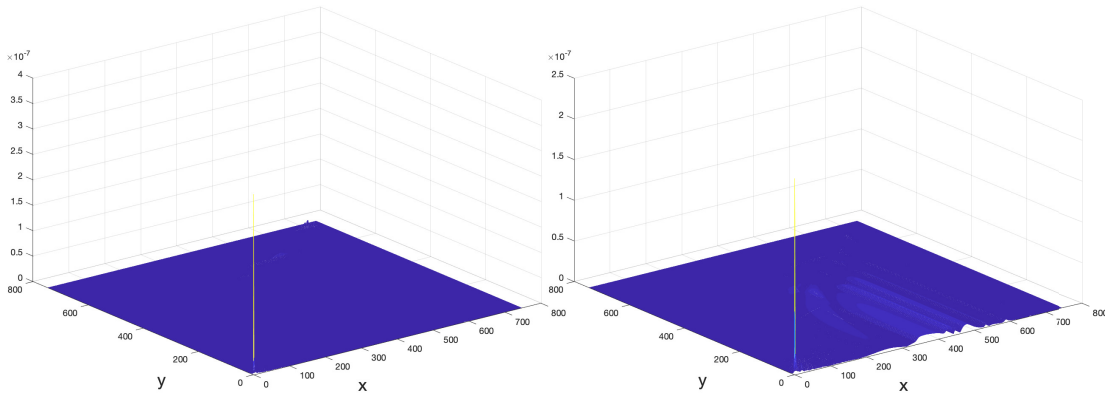


FIGURE 2. Weighted residual errors of the approximate steady state. Left figure: piecewise rigorous $L^\infty(\varphi_1)$ bound of \mathcal{F}_1 in the ω equation. Right figure: piecewise rigorous $L^\infty(\varphi_2)$ bound of \mathcal{F}_2 in the θ_x equation

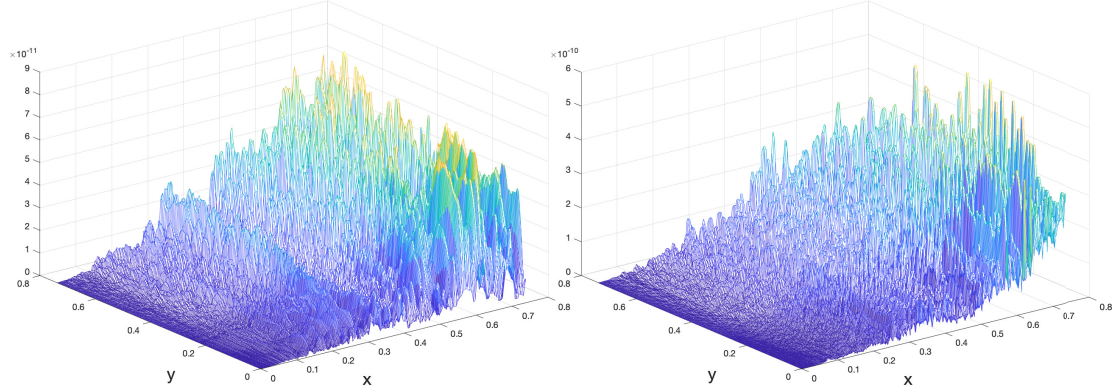


FIGURE 3. Unweighted residual errors of the approximate steady state. Left figure: piecewise rigorous L^∞ bound of \mathcal{F}_1 in the ω equation. Right figure: piecewise rigorous L^∞ bound of \mathcal{F}_2 in the θ_x equation.

Exponents. The exponents and the velocity near the origin satisfy

$$(2.15) \quad \bar{c}_l \approx 3.00649898, \quad \bar{c}_\omega \approx -1.02942516, \quad \bar{u}_x(0) \approx -2.532674, \quad \bar{v}_x(0) \approx 0.$$

We remark that the ratio $\bar{c}_l/\bar{c}_\omega \approx -2.9205600$ is very close to the one reported by Hou-Luo [54, 55].

Regularity and representation. The variables $\bar{\omega}, \bar{\psi}$ are odd in x and $\bar{\theta}$ is even in x . Denote by ψ the stream function. The approximate steady state $(\bar{\omega}, \bar{\theta}, \bar{\psi})$ is represented by piecewise fifth order polynomials $\bar{\omega}_2, \bar{\theta}_2, \bar{\psi}_2$ supported in $[0, D_1]^2$ with $D_1 \approx 10^{15}$, and semi-analytic parts $\bar{\omega}_1, \bar{\theta}_1, \bar{\psi}_1$ that capture the far-field behavior of the solutions

$$\bar{\omega} = \bar{\omega}_1 + \bar{\omega}_2, \quad \bar{\theta} = \bar{\theta}_1 + \bar{\theta}_2, \quad \bar{\psi} = \bar{\psi}_1 + \bar{\psi}_2.$$

See (5.2). In particular, we have $\bar{\omega}, \bar{\theta}, \bar{\psi} \in C^{4,1}$. The solution enjoys the decay rate

$$\bar{\omega} \sim r^\alpha, \quad \bar{\theta} \sim r^{1+2\alpha}, \quad \alpha \approx \bar{c}_\omega/\bar{c}_l.$$

Anisotropic. The solutions $\bar{\theta}$ and $\bar{\omega}$ are anisotropic in the sense that the y -derivative of the profile is much smaller than the x -derivative, especially in the near field:

$$(2.16) \quad |\bar{\theta}_y| < c_3 |\bar{\theta}_x|, \quad c_3 \approx 0.16, \quad |\bar{\omega}_y| < c_4 |\bar{\omega}_x|, \quad c_4 \approx 0.23,$$

for $(x, y) \in [0, 1]^2$. Note that the anisotropic property of the solutions has been observed for the $C^{1,\alpha}$ singular solution [12].

The advection. The advection in (2.10) satisfies the following important inequalities

$$\bar{c}_l x + \bar{u}(x, y) \geq c_1 x, \quad c_1 \approx 0.47, \quad \bar{c}_l y + \bar{v}(x, y) \geq c_2 y, \quad c_2 \approx 3,$$

for all $x, y \in \mathbb{R}_{++}^2$. For $x, y \in \mathbb{R}_{++}^2$ near the origin, we have

$$\bar{c}_l x + \bar{u}(x, y) \approx 0.47x, \quad c_1 y + \bar{v}(x, y) \approx 5.54y.$$

2.5. Linearized equations. Linearizing (2.10) around $(\bar{\omega}, \bar{\theta}, \bar{\mathbf{u}}, \bar{c}_l, \bar{c}_\omega)$, we yield

$$(2.17) \quad \begin{aligned} \omega_t &= -(\bar{c}_l x + \bar{\mathbf{u}}) \cdot \nabla \omega + \theta_x + \bar{c}_\omega \omega - \mathbf{u} \cdot \nabla \bar{\omega} + c_\omega \bar{\omega} + \bar{F}_\omega + N(\omega), \\ \theta_t &= -(\bar{c}_l x + \bar{\mathbf{u}}) \cdot \nabla \theta + \bar{c}_\theta \theta + c_\theta \bar{\theta} - \mathbf{u} \cdot \nabla \bar{\theta} + \bar{F}_\theta + N(\theta), \quad \mathbf{u} = \nabla^\perp (-\Delta)^{-1} \omega, \end{aligned}$$

where $\bar{F}_\omega, \bar{F}_\theta$ are the residual errors (2.2), and $N(\omega), N(\theta)$ are the nonlinear terms

$$(2.18) \quad N(\omega) = -\mathbf{u} \cdot \nabla \omega + c_\omega \omega = \mathcal{N}_1, \quad N(\theta) = -\mathbf{u} \cdot \nabla \theta + c_\theta \theta,$$

where we have used the notation \mathcal{N}_1 (2.1) and the following normalization conditions for the perturbing c_l, c_ω from (2.11)

$$(2.19) \quad c_\omega = u_x(0), \quad c_l \equiv 0, \quad c_\theta = c_l + 2c_\omega.$$

Since $\omega, \nabla\theta$ have similar regularity, we study the system of $(\omega, \theta_x, \theta_y)$ and denote

$$(2.20) \quad \eta = \theta_x, \quad \xi = \theta_y.$$

Taking derivatives on the θ equation in (2.17) and using the notations (2.1), (2.2), we obtain

$$(2.21) \quad \begin{aligned} \partial_t \eta &= -(\bar{c}_l x + \bar{\mathbf{u}}) \cdot \nabla \eta + (2\bar{c}_\omega - \bar{u}_x) \eta - \bar{v}_x \xi - \mathbf{u}_x \cdot \nabla \bar{\theta} - \mathbf{u} \cdot \nabla \bar{\theta}_x + 2c_\omega \bar{\theta}_x + \mathcal{N}_2 + \bar{\mathcal{F}}_2, \\ \partial_t \xi &= -(\bar{c}_l x + \bar{\mathbf{u}}) \cdot \nabla \xi + (2\bar{c}_\omega + \bar{u}_x) \xi - \bar{u}_y \eta - \mathbf{u}_y \cdot \nabla \bar{\theta} - \mathbf{u} \cdot \nabla \bar{\theta}_y + 2c_\omega \bar{\theta}_y + \mathcal{N}_3 + \bar{\mathcal{F}}_3, \end{aligned}$$

where we have used $c_\theta = c_l + 2c_\omega$. Due to the normalization conditions (2.12) and the odd symmetries of θ_x, ω we have the following vanishing conditions near the origin

$$(2.22) \quad \omega = O(|x|^2), \quad \theta_x = O(|x|^2), \quad \theta_y = O(|x|^2).$$

Analyzing the linear stability of the above system is extremely challenging since it contains several nonlocal terms, which are not small. We remark that numerical evidence of linear stability of the above system has been reported by Liu [53].

2.6. Main terms of the system. Firstly, we identify the main terms in the linearized equations (2.17), (2.21). As we will see later in the derivation of the damping terms, e.g., Section 2.7.2, we have larger damping factors away from the boundary. Moreover, the solution $(\bar{\omega}, \nabla \bar{\theta})$ decays in the far-field. Thus the most difficult region for the analysis is a sector Σ_S near the boundary, e.g. $(x, y) : |(x, y)| \leq 2, y/x \leq 0.1$.

2.6.1. Anisotropy of the solution. Since the solutions are anisotropic (2.16) in the near field, the coefficients involving the y -derivative of the solution, e.g., $\bar{\omega}_y, \bar{\theta}_y, \bar{\theta}_{xy}$, are relatively small.

For the $C^{1,\alpha}$ singular solution [12], the perturbation of θ is also anisotropic in the sense that θ_y enjoys much better estimate than that of θ_x since the damping term in the equation of θ_y is much larger. This also holds true in (2.17), (2.21) due to the flow structure: compression in the x -direction and outward flow in the y -direction. Indeed, since $\bar{u}_x(0) \approx -2.5$ near the origin and $\bar{c}_\omega \approx -1$ (2.15), we have

$$(2\bar{c}_\omega - \bar{u}_x)\eta \approx 0.5\eta, \quad (2\bar{c}_\omega + \bar{u}_x)\xi \approx -5.5\xi.$$

Therefore, these terms contribute to a growing term in the equation of η and a large damping term in the ξ equation. As a result, ξ enjoys much better stability estimate than η .

2.6.2. Weak coupling. Note that $\bar{v}_x \approx 0$ near 0 (2.15) and $\bar{v}(x, 0) = 0$ due to the boundary condition, \bar{v}_x is quite small in the near field and near the boundary. We will show ξ enjoys better estimate than η using the observation in Section 2.6.1. Therefore, the term $\bar{v}_x \xi$ in the η equation (2.21) is small in Σ_S . As a result, ξ is weakly coupled to the equation of η in the most difficult region of the analysis. This coupling structure between η and ξ is consistent with that of the $C^{1,\alpha}$ singular solution in [12], where $\bar{v}_x \xi$ is treated as a lower order term in the η equation.

Using the above analysis and dropping the smaller terms and the ξ equation, we identify the main terms in the linear part of the system (2.17)

$$(2.23) \quad \begin{aligned} \omega_t &= -(\bar{c}_l x + \bar{\mathbf{u}}) \cdot \nabla \omega + \eta + \bar{c}_\omega \omega - u \bar{\omega}_x + c_\omega \bar{\omega} + \mathcal{R}_\omega, \\ \partial_t \eta &= -(\bar{c}_l x + \bar{\mathbf{u}}) \cdot \nabla \eta + (2\bar{c}_\omega - \bar{u}_x)\eta - u_x \bar{\theta}_x - u \bar{\theta}_{xx} + 2c_\omega \bar{\theta}_x + \mathcal{R}_\eta, \end{aligned}$$

where $\mathcal{R}_\omega, \mathcal{R}_\eta$ denote the remaining terms in the equations. The above system is very similar to that in the Hou-Luo model [13]. Moreover, near the boundary, the coefficients $\bar{\omega}, \bar{\theta}$ are very similar. We will show that the contribution of the lower order linear terms to the energy estimate is small compared to the main term, e.g. about or less than 1/10 of that in the near field.

2.7. The local parts and functional spaces. To understand the linear stability, we first focus on the local terms in the main system (2.23)

$$(2.24) \quad \begin{aligned} \partial_t \omega + (\bar{c}_l x + \bar{\mathbf{u}}) \cdot \nabla \omega &= \bar{c}_\omega \omega + \eta + \mathcal{R}_{\omega,loc}, \\ \partial_t \eta + (\bar{c}_l x + \bar{\mathbf{u}}) \cdot \nabla \eta &= (\bar{c}_\omega - \bar{u}_x) \eta + \mathcal{R}_{\eta,loc}, \end{aligned}$$

and design the functional spaces for stability analysis, where $\mathcal{R}_{\omega,loc}$, $\mathcal{R}_{\eta,loc}$ denote other terms in (2.17), (2.21), (2.23).

Following [12–14], we will perform weighted energy estimate in some suitable space X and derive the damping terms in the weighted energy estimate from the above local terms, especially the advection term $(\bar{c}_l x + \bar{\mathbf{u}}) \cdot \nabla f$. See Section 2 in [14] for an example. The principle of choosing the appropriate energy space X is the following [13]. Firstly, the local part of the linearized equations should be stable in space X . Secondly, we can estimate the nonlocal terms in X effectively.

In [12–14], the linear stability analysis is based on some weighted L^2 spaces with singular weight near the origin. In these works, one of the major advantages of the weighted L^2 space over other weighted Sobolev spaces is that one can explore nonlocal quadratic cancellation among the local and nonlocal terms to obtain sharp estimates of the nonlocal terms. In [13, 14], an additional advantage is that one can use the L^2 isometry of the Hilbert transform to control the nonlocal terms effectively. We note that the Riesz transform $\nabla \mathbf{u} = \nabla \nabla^\perp (-\Delta)^{-1} \omega$ in the 2D Boussinesq (2.17) also enjoys several sharp L^2 estimate, e.g. $\|\partial_{xy} (-\Delta)^{-1} u\|_{L^2} \leq \|\omega\|_{L^2}$. Yet, we will use a toy example to show that a weighted L^2 space may not be suitable for the stability analysis due to the y -advection $(\bar{c}_l y + \bar{v}) \partial_y f$.

2.7.1. A toy model for the local term. To understand the behavior of the local terms in (2.24), we approximate the system (2.24) near the origin by the following model in \mathbb{R}_2^{++}

$$(2.25) \quad \begin{aligned} \omega_t + (a_1 x \partial_x + a_2 y \partial_y) \omega &= -\omega + \eta, \\ \eta_t + (a_1 x \partial_x + a_2 y \partial_y) \eta &= a_3 \eta, \quad a_1 = 0.5, \quad a_2 = 5.5, \quad a_3 = 0.5, \end{aligned}$$

with ω, η being odd in x , where we have used (2.15) to obtain approximations

$$\bar{c}_l x + \bar{u} \approx (\bar{c}_l + \bar{u}_x(0))x \approx 0.5x, \quad \bar{c}_l y + \bar{v} \approx 5.5y, \quad 2\bar{c}_\omega - \bar{u}_x(0) \approx 0.5.$$

Weighted L^2 spaces. The first attempt for stability analysis is to perform weighted L^2 estimate with singular weight $\varphi = x^{-\alpha} y^{-\beta}$ and some $\alpha, \beta > 0$ following [12–14]. Due to the symmetry in x , we focus on $D = \mathbb{R}_2^{++}$. For the η equation, using integration by parts and a direct computation yield

$$\frac{1}{2} \frac{d}{dt} \int_D \eta^2 \varphi = \int_D \eta (a_3 \eta - a_1 x \partial_x \eta - a_2 y \partial_y \eta) \varphi = \int_D \left(a_3 \varphi + \frac{1}{2} a_1 (x \varphi)_x + \frac{1}{2} a_2 (y \varphi)_y \right) \eta^2.$$

Since $(x\varphi)_x = (1 - \alpha)\varphi$, $(y\varphi)_y = (1 - \beta)\varphi$, we get

$$\frac{1}{2} \frac{d}{dt} \int_D \eta^2 \varphi = a(\alpha, \beta) \int_D \eta^2 \varphi, \quad a = a_3 + \frac{1}{2} a_1 (1 - \alpha) + \frac{1}{2} a_2 (1 - \beta).$$

Notice that ω, η do not vanish near the boundary $y = 0$, we need to choose $\beta < 1$ so that the energy is well-defined. This implies that the y -advection $a_2 y \partial_y f$ contributes to a growing factor in the energy estimate. Moreover, we cannot choose β sufficiently close to 1 in our stability analysis of (2.17), (2.21) since we will need to estimate the weighted norm of the nonlocal term, e.g. $u_x \bar{\theta}_x$ in (2.21). If β is close to 1, since u_x does not vanishes near $y = 0$, we expect a very poor estimate: $\|u_x \varphi^{1/2}\|_2 \leq C(1 - \beta)^{-1/2} \|\omega \varphi^{1/2}\|_2$.

Since $a_2 = \frac{11}{2}$ is much larger than $a_1 = \frac{1}{2}$, to obtain a damping factor $a(\alpha, \beta) < 0$, we need to pick α sufficiently large. For example, if $\beta = 0$, to obtain $a(\alpha, \beta) \leq 0$, we need

$$\frac{1}{2} + \frac{1}{4}(1 - \alpha) + \frac{11}{4} \leq 0, \quad \alpha \geq 14.$$

This means that we need to choose a very singular weight near the origin. Yet, the perturbation ω, η in (2.17), (2.21) does not vanishes to such a high order near the origin (2.22). Another

type of weight is $\varphi = x^{-\alpha}y^{-\beta}(x^2 + y^2)^{-\gamma/2}$. Similar computation yields that for $\beta = 0$, to get a damping factor, $\alpha + \gamma$ need to be sufficiently large.

Thus, the y -advection in (2.17), (2.21) can contribute to a large growing factor to the energy estimate. This is a new difficulty that is absent in [12–14].

A potential L^2 based approach to derive the damping term is to perform sufficiently high order H^k estimate. Taking a partial derivative $\partial_x^i \partial_y^j$ plays a role similar to a singular weight $x^{-i}y^{-j}$. Yet, this approach can lead to many more terms in the system (2.17), (2.21), e.g. $\partial_x^i(u_x \bar{\theta}_x)$, which can be difficult to control. Moreover, constructing an approximate steady state with a small residual error in H^k with $k \geq 14$ is extremely challenging.

Weighted L^∞ space. Instead of weighted L^2 spaces, one can try weighted L^p spaces. In particular, we can use weighted L^∞ estimates to take advantage of the transport structure. Suppose that $\varphi = r^{-\gamma}$, $r = (x^2 + y^2)^{1/2}$. Multiplying the η equation with φ and a direct calculation yield

$$(2.26) \quad \partial_t(\eta\varphi) + (a_1x\partial_x + a_2y\partial_y)(\eta\varphi) = (a_3\varphi + a_1x\partial_x\varphi + a_2y\partial_y\varphi)\eta \triangleq a(\gamma)\eta\varphi,$$

Since $x\partial_x\varphi = -\gamma x^2r^{-\gamma-2}$, $y\partial_y\varphi = -\gamma y^2r^{-\gamma-2}$ and $a_2 \geq a_1$, we get

$$(2.27) \quad a(\gamma) = a_3 + \frac{a_1x\partial_x\varphi + a_2y\partial_y}{\varphi} = a_3 - \gamma \frac{a_1x^2 + a_2y^2}{x^2 + y^2} \leq a_3 - a_1\gamma.$$

Since $a_1 = 0.5$, $a_2 = 5.5$, $a_3 = 0.5$, to obtain a damping factor $a(\gamma) \leq 0$, we can choose $\gamma \geq 1$. Notice that for the system (2.17), (2.21), ω, η vanish at least quadratically near 0 (2.22). Therefore, we can choose $\gamma \geq 2$ to derive the damping terms in the η equation.

For the system in (2.25), performing L^∞ estimate with weight $\varphi = r^{-\gamma}$ with $\gamma > 1$ on both equations, we get

$$(2.28) \quad \frac{d}{dt} \|\omega\varphi\|_\infty \leq (-1 - a_1\gamma) \|\omega\varphi\|_\infty + \|\eta\varphi\|_\infty, \quad \frac{d}{dt} \|\eta\varphi\|_\infty \leq (a_3 - a_1\gamma) \|\eta\varphi\|_\infty.$$

It is easy to further obtain that $\max(\|\omega\varphi\|_\infty, \|\eta\varphi\|_\infty)$ decays exponentially fast.

From (2.27), since a_2 is much larger than a_1 , as the ratio $\lambda = y/x$ increases, we get a much larger damping factor

$$a(\gamma, \lambda) = a_3 - \gamma \frac{a_1 + a_2\lambda^2}{1 + \lambda^2}, \quad a(\gamma, 0) = a_3 - a_1\gamma = \frac{1}{2} - \frac{1}{2}\gamma, \quad a(\gamma, \infty) = a_3 - \gamma a_2 = \frac{1}{2} - \frac{11}{2}\gamma.$$

Weighted Hölder estimate. There is one drawback of applying the weighted L^∞ estimate to (2.17), (2.21). Since (2.21) contains $\nabla \mathbf{u} = \nabla \nabla^\perp(-\Delta)^{-1}\omega$ and the Riesz transform is not bounded from $L^\infty \rightarrow L^\infty$, we cannot close the estimates using the weighted L^∞ space. To overcome this difficulty, we perform weighted Hölder C^α estimates. We will use the following simple identity repeatedly.

Lemma 2.2. *Suppose that f satisfies*

$$(2.29) \quad \partial_t f + b(x) \cdot \nabla f = c(x)f(x) + \mathcal{R}, \quad x \in \mathbb{R}_+^2.$$

Given some weights $g(x_1, x_2)$ even in x_1, x_2 and φ , we denote the operator δ and function F

$$\delta(p)(x, z) = p(x) - p(z), \quad F(x, z, t) = \delta(f\varphi)(x, z)g(x - z), \quad d(x) = c(x) + \frac{b \cdot \nabla \varphi}{\varphi}, \quad x, z \in \mathbb{R}_+^2.$$

Then we have

$$(2.30) \quad \begin{aligned} \partial_t F + (b(x) \cdot \nabla_x + b(z) \cdot \nabla_z)F &= (d(x) + \frac{(b(x) - b(z)) \cdot (\nabla g)(x - z)}{g(x - z)})F \\ &\quad + (d(x) - d(z))g(x - z)(f\varphi)(z) + \delta(\mathcal{R}\varphi)(x, z)g(x - z). \end{aligned}$$

The proof is based on a direct calculation and is deferred to Appendix A.1. We treat the first term on the right hand side of (2.30) as a damping term. The term $\frac{b \cdot \nabla \varphi}{\varphi}$ in $d(x)$ is the damping term from the singular weight $\varphi(x)$. In (2.31) below, we show that the term

$$\frac{(b(x) - b(z)) \cdot (\nabla g)(x - z)}{g(x - z)}F$$

has a negative coefficient and is also a damping term. It comes from the Hölder function g .

Next, we apply the computation in Lemma 2.2 to the η equation in (2.25). Denote

$$\varphi_2 = |x|^{-\gamma_2}, \quad g(h) = |h|^{-\alpha}, \quad h \in \mathbb{R}^2, \quad b(x) = (a_1 x_1, a_2 x_2), \quad F = ((\eta \varphi_2)(x) - (\eta \varphi_2)(z))g(x - z)$$

for $x = (x_1, x_2), z = (z_1, z_2) \in \mathbb{R}_+^2$. Using the identity (2.27) and definitions of g, b , we get

$$\begin{aligned} d(x) &= a_3 + \frac{b(x) \cdot \nabla \varphi_2}{\varphi_2} = a(\gamma_2), \quad h_i \partial_i g = -\alpha \frac{h_i^2}{|h|^{2+\alpha}} = -\alpha \frac{h_i^2}{|h|^2} g, \\ b(x) - b(z) &= (a_1(x_1 - z_1), a_2(x_2 - z_2)). \end{aligned}$$

Thus, we obtain that $\frac{(b(x) - b(z)) \cdot (\nabla g)(x - z)}{g(x - z)} F$ is a damping term

$$(2.31) \quad \frac{(b(x) - b(z)) \cdot (\nabla g)(x - z)}{g(x - z)} F = -\alpha \frac{a_1(x_1 - z_1)^2 + a_2(x_2 - z_2)^2}{|x - z|^2} F \triangleq e(\alpha, x, z) F,$$

where

$$e(\alpha, x, z) = -\alpha \frac{a_1(x_1 - z_1)^2 + a_2(x_2 - z_2)^2}{|x - z|^2}.$$

Using Lemma 2.2 with $\mathcal{R} = 0$, we yield

$$\partial_t F + (b(x) \nabla_x + b(z) \nabla_z) F = (a(\gamma_2)(x) + e(\alpha, x, z)) F + (a(\gamma_2)(x) - a(\gamma_2)(z)) g(x - z) (f \varphi_2)(z).$$

Clearly, we have $e(\alpha, x, z) \leq -\alpha a_1$. For the last term in the above equation, from definition (2.27), $d(x) = a(\gamma_2)(x)$ is not in C^α . Yet, we can estimate $I_4 = (a(\gamma_2)(x) - a(\gamma_2)(z))g(x - z)|z|^\alpha$. In fact, since $a(\gamma_2)(x)|x|^\alpha, |x|^\alpha \in C^\alpha$, we can rewrite I_4 as follows

$$I_4 = (a(\gamma_2)(x)|x|^\alpha - a(\gamma_2)(z)|z|^\alpha)g(|x - z|) + a(\gamma_2)(x)(|z|^\alpha - |x|^\alpha)g(|x - z|),$$

which is bounded. By combining the $L^\infty(|x|^{-\gamma})$ estimate of η with $\gamma = \gamma_2 + \alpha$ and $\varphi_2|x|^{-\alpha} = |x|^{-\gamma_2 - \alpha} = |x|^{-\gamma}$, we can control the last term

$$|(a(\gamma_2)(x) - a(\gamma_2)(z))g(x - z)\eta\varphi_2(z)| \leq \|\eta|z|^{-\gamma}\|_\infty \cdot \|(a(\gamma_2)(x) - a(\gamma_2)(z))g(x - z)|z|^\alpha\|_\infty.$$

Recall $a(\gamma_2) \leq a_3 - a_1\gamma_2, d(\alpha) \leq -a_1\alpha$. From the above estimate, we obtain

$$\frac{d}{dt} \|F\|_{L^\infty(x, z)} \leq (a_3 - a_1(\gamma_2 + \alpha)) \|F\|_{L^\infty(x, z)} + \|\eta|z|^{-\gamma}\|_\infty \cdot \|(a(\gamma_2)(x) - a(\gamma_2)(z))g(x - z)|z|^\alpha\|_\infty.$$

The above estimate provides a weighted C^α estimate for η . Since $a_1 = a_3 = 1/2$, by choosing $\gamma_2 + \alpha = \gamma > 1$ and combining the above estimate and (2.28), we can establish the stability estimate for the model problem in a combination of weighted L^∞ and C^α spaces.

2.7.2. Anisotropy of the flow and the most difficult scenario. The system (2.17), (2.21) is much more complicated than the model problem (2.25) since it involves variables coefficients and several nonlocal terms. Similar to [12–14], we will design the weight as linear combination of different powers $|x|^{-\alpha_i}$ to take into account the behavior in the near field and the far field.

From the above analysis of the model problem, (2.27), and (2.31), we see that the estimate is anisotropic in x and y . In the near field, from (2.27), if y/x is not small, we get a much larger damping term. Therefore, the most difficult region for the estimate is $y/x = 0$, which corresponds to the boundary.

From (2.31), we also get a much larger damping factor if $|x_2 - z_2|/|x_1 - z_1|$ is large. This implies that the Hölder estimate in y direction enjoys much better estimates than those in the x direction. Therefore, the most difficult part of the estimate lies in the Hölder estimate in the horizontal estimate. We will exploit the structure of the flow in designing the energy functional and stability analysis. See Section 4.1.1.

2.7.3. *Functional spaces and energy.* Motivated by the above analysis, we will design the functional spaces X as a combination of weighted L^∞ and C^α spaces with $\alpha = \frac{1}{2}$.

Denote $f_1 = \omega, f_2 = \eta, f_3 = \xi$. In the weighted L^∞ estimate, we choose singular weights $\varphi_i, i = 1, 2, 3$ and will estimate $f_i\varphi_i$ in L^∞ . In the weighted Hölder estimate, we will choose singular weights $\psi_1(x), \psi_2(x), \psi_3(x)$ even in x_1 and $-1/2$ -homogeneous functions $g_i(h)$ equivalent to $|h|^{-1/2}$ and estimate $\|f_i\psi_i\|_{C_{g_i}^\alpha}$ (2.4). This quantity is equivalent to the Hölder seminorm $\|f_i\psi_i\|_{C^{1/2}}$.

From the discussion in Section 2.6.1, $[f_i]_{C_y^{1/2}}$ enjoys better estimate than that of $[f_i]_{C_x^{1/2}}$. To exploit this property, we choose anisotropic weight $g_i(h)$ such that $g(0, 1)$ is stronger than $g(1, 0)$, e.g. $g(h) = \frac{1}{(|h_1| + 0.5|h_2|)^{1/2}}$. We refer more details to Section 4.

2.7.4. *Estimates of the Hölder norm in \mathbb{R}_{++}^2 .* To simplify our energy estimate, using the symmetry of f_i in the x direction, we only perform Hölder estimates in the first quadrant. This allows us to control

$$I_x = \frac{(f_i\psi_i)(x_1, x_2) - (f_i\psi_i)(z_1, x_2)}{|x_1 - z_1|^{1/2}}, \quad I_y = \frac{(f_i\psi_i)(x_1, x_2) - (f_i\psi_i)(x_1, z_2)}{|x_2 - z_2|^{1/2}},$$

for $x = (x_1, x_2), (z_1, x_2), (x_1, z_2) \in \mathbb{R}_{++}^2$. Due to the symmetry in the x direction, we have $|I_y(x_1, x_2, z_2)| = |I_y(-x_1, x_2, z_2)|$ and obtain the Hölder estimate in the y direction, i.e. control of I_y for all pair $(x_1, x_2), (x_1, z_2) \in \mathbb{R}^2$. The above quantities do not control the Hölder estimate in the x direction for all pair x, z . It only allows us to control the difference when $(x_1, x_2), (z_1, x_2)$ are in the same quadrant since $|I_x(x_1, z_1, x_2)| = |I_x(-x_1, -z_1, x_2)|$.

However, to control the Hölder norm of $\nabla \mathbf{u}(\omega)$ in \mathbb{R}_{++}^2 , since $\nabla \mathbf{u}(\omega)$ is nonlocal, we need to control the Hölder norm of ω in the whole \mathbb{R}_+^2 . To further control $I_x(\omega)$ with $x_1 z_1 < 0$, we consider $x_1 < 0 < z_1$. In this case, since $\omega\psi$ is odd and $|x_1 - z_1| = |x_1| + |z_1|$ we have

$$\begin{aligned} \frac{|(\omega\psi_1)(-x_1, x_2) + (\omega\psi_1)(z_1, x_2)|}{|x_1 - z_1|^{1/2}} &\leq \max\left(\frac{2|(\omega\psi_1)(-x_1, x_2)|}{|2x_1|^{1/2}}, \frac{2|(\omega\psi_1)(z_1, x_2)|}{|2z_1|^{1/2}}\right) \frac{|x_1|^{1/2} + |z_1|^{1/2}}{(2|x_1| + 2|z_1|)^{1/2}} \\ &\leq \max\left(\frac{2|(\omega\psi_1)(-x_1, x_2)|}{|2x_1|^{1/2}}, \frac{2|(\omega\psi_1)(z_1, x_2)|}{|2z_1|^{1/2}}\right), \end{aligned} \tag{2.32}$$

where we have used the Cauchy-Schwarz inequality in the last inequality. Therefore, it suffices to further control $\|\omega\psi_1|x_1|^{-1/2}\|_{L^\infty}$, which will be done by performing a L^∞ estimate.

We remark that we do not need to estimate $\|\eta\psi_2|x_1|^{-1/2}\|_{L^\infty}$ and $\|\xi\psi_3|x_1|^{-1/2}\|_{L^\infty}$.

Remark 2.3. In fact, from the Hölder estimate in \mathbb{R}_{++}^2 , we can also control $I_x(x_1, z_1, x_2)$ for $x_1 < 0 < z_1$ and $x_2 = z_2$. Using the fact that $|I_x(x_1, 0, x_2)| = (|\omega\psi_1(x)|)|x_1|^{-1/2}$ and the above inequality, for $x_1 < 0 < z_1$, we get

$$|I_x(x_1, z_1, x_2)| \leq \max_x \sqrt{2}|I_x(x_1, 0, x_2)|.$$

However, we need to pay a factor $\sqrt{2}$. For this reason, we estimate $\|\eta\psi_2|x_1|^{-1/2}\|_{L^\infty}$ directly.

Several weighted L^∞ estimates. To establish the linear stability, we will first choose weights φ_i that has faster decay, e.g. $\varphi_i \sim |x|^{-\beta}$ with large β for large $|x|$. This allows us to obtain a larger damping factor. For example, from (2.27), $a(\gamma)$ is larger if γ is larger. To close the nonlinear estimate, we need to control $\|\nabla \mathbf{u}\|_{L^\infty}, \|\omega\|_{L^\infty}, \|\nabla \theta\|_{L^\infty}$. Since the weight φ_i is weaker than $O(1)$ in the far-field, we cannot control these L^∞ quantities using $\|f_i\varphi_i\|_{L^\infty}, \|f_i\psi_i\|_{C^{1/2}}$. Thus, we further choose weights $\varphi_{g,i}$ growing in the far-field and estimate $f_i\varphi_{g,i}$. We also need to estimate $\|\omega\psi_1|x_1|^{-1/2}\|_{L^\infty}$, as discussed in Section 2.7.4.

Note that similar idea of obtaining weighted estimate in the stability analysis through a few intermediate steps has been used in our previous work [12].

The functional spaces of the perturbation. From the above discussions, we will estimate the following quantities in \mathbb{R}_{++}^2

$$\|f_i\varphi_i\|_{L^\infty}, \quad \|f_i\psi_i\|_{C_g^{1/2}}, \quad \|f_i\varphi_{g,i}\|_{L^\infty}, \quad \|\omega\psi_1|x_1|^{-1/2}\|_{L^\infty},$$

where $f_1 = \omega, f_2 = \eta, f_3 = \xi$, and $\|\cdot\|_{C_g^{1/2}}$ is defined in (2.4). In view of Lemma A.2, we will design our final energy E in the form of $\max(\mu_i F_i)$ with F_i being one of the above quantities and some weights μ_i . We will determine the weights later. See more details in Section 4.

2.7.5. Vanishing order of the perturbation. From (2.22), the perturbation ω, η, ξ vanishes quadratically near $x = 0$. To obtain larger damping factors, from the model problem (2.25) and (2.27), we can choose a larger γ . We will decompose the perturbation f_i into two parts

$$f_i = f_{i,1} + f_{i,2},$$

where $f_{i,1}$ captures the main part of f_i and vanishes to the order $O(|x|^3)$ near $x = 0$, and $f_{i,2}$ accounts for the contribution from some finite rank operators. For example, if we choose $\omega_2 = \omega_{xy}(0)xy\chi(x, y)$ for some cutoff function $\chi \in C_c^\infty$ with $\chi = 1$ near $x = 0$, then $\omega_1 = \omega - \omega_2 = O(|x|^3)$ near 0. In this problem, cubic vanishing order is good enough for our stability analysis. See more discussions in Section 2.10.4 and (2.75).

We will perform energy estimates on $f_{i,1}$ and use space-time estimates for $f_{i,2}$.

2.8. Estimate the nonlocal terms $\nabla \mathbf{u}$. In the stability analysis, we need to estimate the nonlocal terms $\mathbf{u}, \nabla \mathbf{u}$ in (2.17), (2.21). One disadvantage of performing energy estimates in the new functional space is that we lose the L^2 isometry property for the nonlocal velocity: e.g. $\|\nabla \mathbf{u}\|_2 = \|\omega\|_2, \|\nabla \mathbf{u}_x\|_2 = \|\omega_x\|_2$, which can be obtained using the elliptic equation $-\Delta\psi = \omega$ and integration by parts. Although we have standard C^α estimates for the Riesz transform $\nabla \nabla^\perp (-\Delta)^{-1}\omega$, the constants usually are not given explicitly, and they are not sharp enough for our purposes.

Strategies. Our strategies to estimate the nonlocal terms are the following. For the nonlocal terms that are of order ω , e.g., $\nabla \mathbf{u} = \nabla \nabla^\perp (-\Delta)^{-1}\omega$, and their localized version (3.4), we develop sharp functional inequalities to estimate them. Due to the localization of the kernel, we will gain a small factor in the weighted L^∞ estimate. For the more regular nonlocal terms, e.g., \mathbf{u} , we will approximate them by finite rank operators F_u . We further develop a crucial decomposition of the equations (2.17), (2.21) that enable us to estimate the contribution of these finite rank operators separately using computer assistance. See Section 2.9.

To obtain sharp C^α estimates for $\nabla \mathbf{u}$, we have a crucial observation that we can use techniques from optimal transport. This is another reason why we choose a weighted $C^{1/2}$ space in the energy estimates. Note that optimal transport has been applied to establish many sharp functional inequalities and study functional inequalities in details, e.g., the reverse Brascamp-Lieb inequality [1], the Sobolev and Gagliardo-Nirenberg inequalities [20], the isoperimetric inequalities [34]. See also the excellent books [73, 74] for more details.

We focus on u_x from $u_x \bar{\theta}_x$ in the main system (2.23). This term is the most difficult nonlocal term to estimate since other nonlocal terms in (2.24) are related to $\mathbf{u} = (u, v)$ and are more regular. We note that in the leading order system for the $C^{1,\alpha}$ singular solution [12], $u_x \bar{\theta}_x$ is also the main nonlocal term. The coefficients of other nonlocal terms involving $\mathbf{u}, \nabla \mathbf{u}$, e.g. $-u\bar{\omega}_x, -u\bar{\theta}_{xx}, v_x\bar{\theta}_y$, contain a small factor α , which makes the estimates much easier.

Denote by $u_x(x, a, b)$ the localized version of u_x

$$(2.33) \quad u_x(x, a, b) \triangleq -\frac{1}{\pi} P.V. \int_{|x_1 - y_1| \leq a, |x_2 - y_2| \leq b} K_1(x - y) W(y) dy, \quad K_1(s) = \frac{s_1 s_2}{|s|^4},$$

where W is an odd extension of ω in y from \mathbb{R}_+^2 to \mathbb{R}^2 (3.3).

We decompose u_x into two parts $u_x = u_{x,S} + u_{x,R}$ with $u_{x,S}(x) = u_x(x, a, b)$ for some $a, b > 0$. The main term $u_{x,S}$ captures the most singular part of u_x in the Biot-Savart law, and the remaining term $u_{x,R}$ is more regular. Using the odd symmetry property of $K(s)$ in s_1, s_2 and some techniques from optimal transport, we establish sharp estimates for the singular term

$u_{x,S}$ in Lemma 3.1 uniformly in a, b . Similarly, we have established a sharp estimate of u_x in the $C_y^{1/2}$ seminorm and the estimates of u_y, v_x in the Hölder seminorms. To estimate the regular part $u_{x,R}$, we follow the previous strategy.

2.8.1. Weighted estimates. In the stability analysis, we need to estimate the weighted L^∞ and C^α norm of the nonlocal terms. We focus on estimating the Hölder norm of $u_x\psi$. We observe that the commutator

$$\begin{aligned} [u_x(\cdot, a, b), \psi](\omega) &\triangleq u_x(\omega)(x, a, b)\psi(x) - u_x(\omega\psi)(x, a, b) \\ &= -\frac{1}{\pi} \int_{|x_1-y_1| \leq a, |x_2-y_2| \leq b} K_1(x-y)W(y)(\psi(x) - \psi(y))dy \end{aligned}$$

is more regular. Therefore, we have the decomposition

$$(2.34) \quad u_x(\omega)(x, a, b)\psi = u_x(\omega\psi)(x, a, b) + [u_x(\cdot, a, b), \psi](\omega).$$

For the first term on the right hand side, we can apply the sharp Hölder estimate in Section 3. Given that ω is in some weighted L^∞ space, since $K_1(x-y)(\psi(x) - \psi(y))$ has a singularity of order $\frac{1}{|x-y|}$, the second term is log-Lipschitz and is more regular than the first term. Therefore, we can estimate its $C^{1/2}$ seminorm by the weighted L^∞ norm of ω . In particular, if a and b are small, we obtain a small factor of order $(\max(a, b))^{1/2}$ in this estimate.

To understand if we can obtain linear stability using a combination of weighted L^∞ and $C^{1/2}$ space, we consider the Hölder estimate where $|x - z|$ is very small in Section 2.8.2. To understand our overall strategy of the energy estimate, we will study a model problem in Section 2.8.3, which also motivates the localization of the velocity.

2.8.2. The singular scenario. We rewrite (2.17), (2.21) and keep the local terms and the nonlocal terms that are of the same order of $\omega, \nabla\theta$

$$\begin{aligned} \omega_t &= -(\bar{c}_l x + \bar{\mathbf{u}}) \cdot \nabla \omega + \bar{c}_\omega \omega + \eta + \mathcal{R}_1, \\ (2.35) \quad \eta_t &= -(\bar{c}_l x + \bar{\mathbf{u}}) \cdot \nabla \eta + (2\bar{c}_\omega - \bar{u}_x)\eta - (u_x - \hat{u}_x)\bar{\theta}_x - (v_x - \hat{v}_x)\bar{\theta}_y + \mathcal{R}_2. \end{aligned}$$

Here \hat{u}_x, \hat{v}_x approximate u_x, v_x near 0:

$$(2.36) \quad \hat{u}_x = (u_x(0) + C_{u_x}(x)\mathcal{K}_{00})\chi(x), \quad \hat{v}_x = C_{v_x}(x)\mathcal{K}_{00}\chi$$

The above approximation can be obtained by Taylor expansions and satisfies

$$(2.37) \quad u_x - \hat{u}_x = O(|x|^{5/2}), \quad v_x - \hat{v}_x = O(|x|^{5/2}),$$

for $\omega = O(|x|^{5/2})$ near $x = 0$. The above vanishing order can be justified for the perturbation ω in our energy class. The functions $C_{u_x}(x), C_{v_x}(x)$ and operators \mathcal{K}_{00} are defined in (2.80) and (2.79), and χ is some compactly supported cutoff function with $\chi = 1$ near $x = 0$. The above approximation is a simplification of the approximation of the velocity in Section 2.11. For ω vanishes $O(|x|^3)$ near $x = 0$, the new term $\hat{u}_x\bar{\theta}_x + \hat{v}_x\bar{\theta}_y$ in (2.39) can be seen as a finite rank operator. We will use the ideas to be introduced in Sections 2.9 and 2.10 to decompose the system and perturb the equations by some finite rank operators.

We assume that the remaining terms $\mathcal{R}_1, \mathcal{R}_2$ have vanishing order $O(|x|^3)$ near $x = 0$. For initial perturbation with vanishing order $\omega_0, \eta_0 = O(|x|^3)$ near $x = 0$, using (2.37), we obtain that these vanishing conditions can be preserved. Note that, in general, the solution to the original system (2.17), (2.21) only vanishes quadratically (2.22), and does not satisfy cubic vanishing conditions. We will perform a correction near $x = 0$ so that $\omega, \eta = O(|x|^3)$ near $x = 0$. See Sections 2.7.5 and 2.10.

In the Hölder estimate with x, z close enough, we will show below that (2.35) can be seen as the leading order system. We also move the term $\bar{v}_x\xi$ in the η equation to the remaining term due to the weak coupling discussed in Section 2.6.2.

Goal of the estimates and heuristic. In the following weighted Hölder estimates, we will show that if $|x - z|$ is sufficiently small with $x_2 = z_2$, we can treat the nonlocal terms $u_x - \hat{u}_x, v_x - \hat{v}_x$ as perturbations with size $2.55[\omega\psi_1]_{C_x^{1/2}}, 2.53\|(\omega\psi_1)g_1\|_{L^\infty}$, respectively, using the sharp estimates in Lemmas 3.1 and 3.4.

This can be understood heuristically. Since $x_2 = z_2$ and $|x_1 - z_1|$ is small, we can interpret the following estimates as taking a half derivative D on (2.39). If D applies to a regular term, which is Lipschitz, we almost get 0. If D acts on the nonlocal terms, e.g. $u_x - \hat{u}_x$, since \hat{u}_x is more regular and $[u_x]_{C_x^{1/2}}$ can be bounded using Lemma 3.1, we treat it as $2.55[\omega\psi_1]_{C_x^{1/2}}$. If D applies to the local term, we can simply apply the derivations in Section 2.7.1.

Following [12–14], we design the singular weights by choosing different powers to take care of the behaviors in the near field and the far field. We use the weights (C.1) for the Hölder estimate, which satisfies

$$(2.38) \quad \psi_1 \sim |x|^{-2}, \quad \psi_2 \sim p_1|x|^{-5/2}$$

near $x = 0$ for some parameter p_1 .

Next, we perform the weighted $C^{1/2}$ estimate. Denote

$$\bar{b}(x) = (\bar{c}_l x + \bar{u}, \bar{c}_l y + \bar{v}).$$

Derivations for the local terms. Applying Lemma 2.2, we get

$$(2.39) \quad \begin{aligned} \partial_t \delta(\omega\psi_1)g_1 + (\bar{b}(x) \cdot \nabla_x + \bar{b}(z) \cdot \nabla_z)(\delta(\omega\psi_1)g_1) &= \bar{e}_1(x, z)\delta(\omega\psi_1)g_1 \\ &+ \delta(\eta\psi_1)g_1(x - z) + \delta(\bar{d}_1)g_1(x - z)(\omega\psi_1)(z) + \delta(\mathcal{R}_1\psi_1)g_1(x - z), \\ \partial_t \delta(\eta\psi_2)g_2 + (\bar{b}(x) \cdot \nabla_x + \bar{b}(z) \cdot \nabla_z)(\delta(\eta\psi_2)g_2) &= \bar{e}_2(x, z)\delta(\eta\psi_2)g_2 \\ &- \delta((u_x - \hat{u}_x)\bar{\theta}_x\psi_2 + (v_x - \hat{v}_x)\bar{\theta}_y\psi_2)g_2 + \delta(\bar{d}_2)g_2(x - z)(\eta\psi_2)(z) + \delta(\mathcal{R}_2\psi_2)g_2(x - z) \end{aligned}$$

where $g_1 = g_1(x - z), \delta f = f(x) - f(z)$ for a function f ,

$$(2.40) \quad \begin{aligned} \bar{d}_1 &= \bar{c}_\omega + \frac{\bar{b} \cdot \nabla \varphi_1}{\varphi_1}, \quad \bar{e}_1(x, z) = \bar{d}_1(x) + \frac{(\bar{b}(x) - \bar{b}(z))(\nabla g_1)(x - z)}{g_1(x - z)}, \\ \bar{d}_2 &= 2\bar{c}_\omega - \bar{u}_x + \frac{\bar{b} \cdot \nabla \varphi_2}{\varphi_2}, \quad \bar{e}_2(x, z) = \bar{d}_2 + \frac{(\bar{b}(x) - \bar{b}(z))(\nabla g_2)(x - z)}{g_2(x - z)}. \end{aligned}$$

We consider the difficult scenario discussed in Section 2.7.2, i.e. for x, z with $x_2 = z_2$, and the most singular scenario where x and z are sufficiently close. We will discuss how to handle the more regular case where $|x - z|$ is not small later. We also neglect the nonlinear terms N_ω, N_θ and the residual $\bar{F}_\omega, \bar{F}_\theta$.

Estimate the nonlocal terms. Suppose that $\omega\varphi_1, \eta\varphi_2 \in L^\infty$ and $\delta(\omega\psi_1)g_1, \delta(\eta\psi_2)g_2 \in L^\infty$. We consider $|x - z|$ sufficiently small compared to $\min(1, |x|)$ with $x_2 = z_2$. To estimate $\delta_2((u_x - \hat{u}_x)\bar{\theta}_x\psi_2)g_2$, we introduce $A(x) = \bar{\theta}_x \frac{\psi_2}{\psi_1}$ and rewrite the difference as follows

$$\begin{aligned} \delta((u_x - \hat{u}_x)\bar{\theta}_x\psi_2)g_2 &= \delta((u_x - \hat{u}_x)\psi_1 A(x))g_2 \\ &= (\delta((u_x - \hat{u}_x)\psi_1)A(x) + (u_x - \hat{u}_x)(z)\psi_1(z)\delta(A))g_2 \triangleq I + II. \end{aligned}$$

The second term II can be seen as a regular term since the half derivative acts on the coefficient. Indeed, if x is away from the origin, the coefficient $\bar{\theta}_x \frac{\psi_2}{\psi_1}$ is Lipschitz. Since $|x - z|$ is sufficiently small and $(u_x - \hat{u}_x)\psi_1$ is bounded (2.37), (2.38), in this case, we get $|II| \approx 0$. For x close to the origin, using the fact that $\bar{\theta}_x$ is odd and smooth, (2.37), and (2.38), we obtain that

$$(2.41) \quad \bar{\theta}_x \frac{\psi_2}{\psi_1} \sim x|x|^{-1/2} \quad x \text{ near } 0, \quad \bar{\theta}_x \frac{\psi_2}{\psi_1} \in C^{1/2}.$$

Since $|x - z|, |x|$ are small, we get $(u_x - \hat{u}_x)(z)\psi_1(z) = O(|z|^{1/2})$ near $z = 0$, which is also small. Thus, we get

$$|(u_x - \hat{u}_x)(z)\psi_1(z)\delta(A))g_2| \lesssim |(u_x - \hat{u}_x)(z)\psi_1(z)||A||_{C^{1/2}} \lesssim |z|^{1/2}(\|\omega\varphi_1\|_{L^\infty} + \|\omega\psi_1\|_{C^{1/2}}) \approx 0.$$

Next, we focus on I . For x away from the origin, the weight ψ is nonsingular and $|A(x)| \lesssim 1$. Recall that the commutator $[u_x, \psi_1](\omega)$ is more regular and \hat{u}_x (2.36) is regular. Applying the above argument to estimate the regular term, Lemma 3.1 to estimate $u_x(\omega\psi_1)$, and using $g_2(x_1 - z_1, 0) = |x_1 - z_1|^{-1/2}$, we get

$$(2.42) \quad I \approx \delta(u_x(\omega)\psi_1)g_2A(x) \approx \delta(u_x(\omega\psi_1))g_2A(x),$$

which can be bounded by

$$2.55[\omega\psi_1]_{C_x^{1/2}}|\bar{\theta}_x \frac{\psi_2}{\psi_1}(x)|.$$

In the above approximation, we used the same argument as that for II to show the estimate of some regular term is small. The estimate is more involved for x near the origin due to the singular weight. In this case, we need to use the scaling symmetry of u_x and decompose $u_x = u_x(x, a, b) + u_x^R$ with size of the singular region (a, b) proportional to x . We can obtain the following estimate

$$|\delta((u_x - \hat{u}_x)\psi_1)| \cdot |x_1 - z_1|^{-1/2} \leq C_1(x, z)[\omega\psi_1]_{C_x^{1/2}} + C_2(x, z)\|\omega\varphi_1\|_{L^\infty}$$

with $C_1(x, z)$ close to 2.55 and $C_2(x, z)$ uniformly bounded for small x, z . The most singular part in $\delta((u_x - \hat{u}_x)\psi_1)$ can be estimated using Lemma 3.1. The regular part can be controlled using the weighted L^∞ norm of ω . These constants C_1, C_2 can be estimated effectively by computing suitable integrals, and we will discuss them in details in Section 7. Now since $A(z) \lesssim |z|^{1/2}$ (2.41), in the case near the origin, we have better estimate

$$|I| \lesssim |x|^{1/2}(C_1(x, z)[\omega\psi_1]_{C_x^{1/2}} + C_2(x, z)\|\omega\varphi_1\|_{L^\infty}) \approx 0.$$

Note that if we fix $x \neq 0$ and then consider $|z_1 - x_1| \rightarrow 0$, it is easy to justify the above estimate by using the argument around (2.42). Similarly, we have

$$\delta(v_x \bar{\theta}_y \psi_2)g_2 \approx \delta(v_x(\omega\psi_1))|x_1 - z_1|^{-1/2}\bar{\theta}_y \frac{\psi_2}{\psi_1} \triangleq m, \quad m \leq 2.53\|\delta(\omega\psi_1)g_1\|_{L^\infty} \left| \bar{\theta}_y \frac{\psi_2}{\psi_1}(x) \right|,$$

where the constant 2.53 comes from applying Lemma 3.4 by optimizing the parameter τ and using

$$[\omega]_{C_x^{1/2}} \leq \|\omega\psi_1\|_{C_g^{1/2}}, \quad [\omega]_{C_y^{1/2}} \leq \frac{1}{1.718}\|\omega\psi_1\|_{C_g^{1/2}},$$

to further simplify the upper bound in Lemma 3.4, where $\|\cdot\|_{C_g^{1/2}}$ is defined in (2.4).

Estimate the regular and remaining terms. For $|x - z|$ sufficiently small, the more regular term vanishes in this estimate. For example, for $u\bar{\omega}_x$ in (2.17), in our energy estimate for the Boussinesq equations, we will approximate \mathbf{u} using some finite rank operators $\hat{\mathbf{u}}$ similar to (2.36) and estimate $(u - \hat{u})\bar{\omega}_x$, which vanishes cubically near $x = 0$. See Sections 2.10 and 2.11. We can control the log-Lipschitz norm or $C^{4/5}$ norm of u in some weighted space using $\|\omega\varphi_1\|_{L^\infty}$. Thus, for $|x - z|$ sufficiently small, we get

$$\frac{|((u - \hat{u})\bar{\omega}_x\psi_1)(x) - ((u - \hat{u})\bar{\omega}_x\psi_1)(z)|}{|x - z|^{1/2}} \leq C(x, z)\|\omega\varphi_1\|_{L^\infty},$$

with $C(x, z) \rightarrow 0$ if we fix x and take $|z - x| \rightarrow 0$. The same idea applies to other regular terms in (2.39), e.g.

$$\delta(\bar{d}_1)g_1(x - z)(\omega\psi_1), \quad \delta(\bar{d}_2)g_2(x - z)(\eta\psi_2).$$

For $\delta(\eta\psi_1)g_1$ in the ω equation (2.39), we get

$$\delta(\psi_1\theta_x)g_1 = \delta\left(\frac{\psi_1}{\psi_2}\theta_x\psi_2\right)g_1 \approx \frac{\psi_1}{\psi_2}(x)\delta(\theta_x\psi_2)|x_1 - z_1|^{-1/2} \triangleq m_1, \quad |m_1| \leq \left|\frac{\psi_1}{\psi_2}(x)\right|[\theta_x\psi_2]_{C_x^{1/2}}.$$

We remark that, if $z_1 = x_1$, all the above approximations become *equality* since the difference $\delta(f)|x - z|^{-1/2}$ becomes 0 for f being locally Lipschitz around x .

Summarize the estimates. For $x_2 = z_2$ with $|x_1 - z_1|$ sufficiently small, the damping terms \bar{e}_1, \bar{e}_2 in (2.39) can be simplified as

$$\bar{e}_i(x) = \bar{d}_i(x) - \frac{1}{2} \frac{\bar{b}_1(x) - \bar{b}_1(z)}{x_1 - z_1} \approx \bar{d}_i(x) - \frac{1}{2} \partial_1 \bar{b}_1(x) = \bar{d}_i(x) - \frac{1}{2} (\bar{c}_l + \bar{u}_x(x)).$$

Therefore, we derive

$$\begin{aligned} \partial_t \delta(\omega \psi_1) g_1 + (\bar{b}(x) \cdot \nabla_x + \bar{b}(z) \cdot \nabla_z) \delta(\omega \psi_1) g_1 &= \bar{e}_1 \delta(\omega \psi_1) g_1 + B_1(x, z) + \mathcal{R}_3, \\ \partial_t \mu_1 \delta(\eta \psi_2) g_2 + (\bar{b}(x) \cdot \nabla_x + \bar{b}(z) \cdot \nabla_z) \mu_1 \delta(\eta \psi_2) g_2 &= \bar{e}_2 \mu_1 \delta(\eta \psi_2) g_2 + \mu_1 B_2(x, z) + \mu_1 \mathcal{R}_4, \end{aligned}$$

where B_i denotes the linear terms in (2.39) except for $\bar{v}_x \xi$, and $\mathcal{R}_3, \mathcal{R}_4$ denote the remaining terms coming from the nonlinear terms, the residual, and the terms related to ξ . Here, we have multiplied the η equation with an additional parameter

$$(2.43) \quad \mu_1 = 0.668.$$

The role of μ_1 is to change the weights between $\delta(\omega \psi_1) g_1, \delta(\eta \psi_2) g_2$ in the energy estimate so that the damping term dominates. See Lemma A.2. When $x_2 = z_2$ with $|x_1 - z_1| \rightarrow 0$, from the above estimate, we have

(2.44)

$$|B_1(x, x)| \leq \left| \frac{\psi_1}{\mu_1 \psi_2}(x) \right| \mu_1 [\theta_x \psi_2]_{C_x^{1/2}}, \quad \mu_1 |B_2(x, x)| \leq \mu_1 (2.55 |\bar{\theta}_x| + 2.53 |\bar{\theta}_y|) \frac{\psi_2}{\psi_1}(x) \|\omega \psi_1\|_{C_g^{1/2}}.$$

In view of (A.6) and Lemma A.2, if in each equation, the coefficient of the damping term is larger than that of the bad term, then we can obtain stability. Indeed, these conditions are satisfied: we have

$$(2.45) \quad \bar{e}_i + S_i \leq -c_i, \quad S_1 = \left| \frac{\psi_1}{\mu_1 \psi_2}(x) \right|, \quad S_2 = \mu_1 (2.55 |\bar{\theta}_x| + 2.53 |\bar{\theta}_y|) \frac{\psi_2}{\psi_1}(x),$$

for some $c_1, c_2 > 0$. In Figure 4, we plot the grid point values of S_1, S_2 defined in (2.45), which are the upper bounds of $B_1, \mu_1 B_2$ in (2.44), and $-\bar{e}_1, -\bar{e}_2$ on the boundary $y = 0$ for small x . Note that the estimates away from the boundary and for large x are much better due to the larger damping from $\frac{\bar{b} \cdot \nabla \psi_i}{\psi_i}$ and the decay of the profile. See Section 2.7.2.

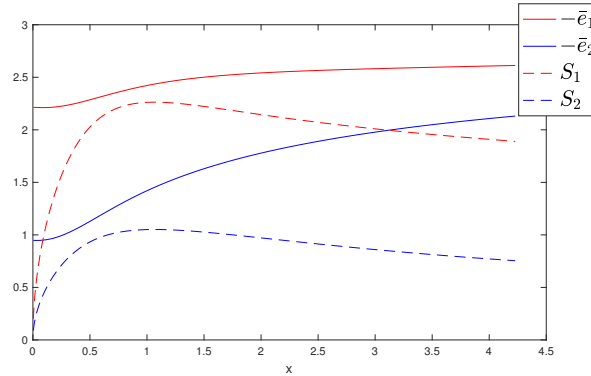


FIGURE 4. Coefficients \bar{e}_1, \bar{e}_2 of the damping terms and the estimates of the bad terms B_1, B_2

For $|x - z|$ sufficiently small but with other ratio $|x_2 - z_2|/|x_1 - z_1|$, from Sectin 2.7.2, we can obtain a larger damping term from $\frac{\delta \bar{b} \cdot \nabla g_i}{g_i}$ in (2.40) and obtain better estimates. Using the sharp functional inequalities in Section 3, we can also verify that the damping terms dominate.

The remaining step is to show that when $|x - z|$ is not small, these conditions are also satisfied. We remark that for larger $|x - z|$, the constants in the Hölder estimates improve. See the discussion below Remark 2.5 and Lemmas 3.1-3.4. We will show later that the constants in the Hölder estimates for the bad terms do not increase too much for $|x - z|$ not too small.

Remark 2.4. We remark that to obtain the stability condition (2.45), one can choose weights similar to ψ_1, ψ_2 with other parameters, or other weights. In view of the model and derivations in Section 2.7.1, the gap $-c_i - (\bar{e}_i + S_i)$ is larger if one chooses weight $|x|^\gamma$ with smaller γ . In ψ_1, ψ_2 (C.1), the power with the largest exponent is $|x|^{1/6}$, which leads to a smaller gap. Note that to close the nonlinear estimates, we need to control the L^∞ norm of $\omega, \eta, \xi, \nabla \mathbf{u}$. We choose this growing weight so that we have a stronger control of the solution in the far-field, which leads to smaller constants in the nonlinear estimates and makes it easier to control the nonlinear estimates.

2.8.3. A model problem for localized velocity and energy estimate. We consider the following model problem to illustrate the ideas of our overall energy estimate and motivate the localization of velocity (2.33)

$$(2.46) \quad \omega_t = -d(x)\omega + a(x)u_x(\omega, \varepsilon)(x).$$

Here $u_x(\omega, \varepsilon)$ denotes the localized velocity $u_x(\omega, a, b)$ (2.33) with $b = a = \varepsilon$. We assume

$$(2.47) \quad -d(x) + m|a(x)| \leq -c_1 < 0, \quad -d(x) \leq -c_2 < 0, \quad d(x), |a(x)|, \|d\|_{C^{1/2}}, \|a\|_{C^{1/2}} \leq c_3,$$

for some constant $c_1, c_2, c_3 > 0$, where $m = \max(C_1(\infty), \frac{1}{2}C_1(\infty) + C_2(\infty)) \leq 2.64$. The constants $C_1(\cdot), C_2(\cdot)$ are defined in Lemmas 3.1, 3.3. From Lemmas 3.1, 3.3, we have

$$(2.48) \quad \|u_x(x, a, b)\|_{C^{1/2}} \leq m\|\omega\|_{C^{1/2}},$$

uniformly for any a, b . The first condition in (2.47) corresponds to (2.45) and means that the damping term dominates in the Hölder estimate if $|x - y|$ is very small.

In (2.46), we remove the transport terms. Since in the weighted energy estimate, it contributes to the damping terms (see Sections 2.7.1, 2.8.2), in this model, we incorporate this effect in the damping terms $-d(x)\omega$ for simplicity. The nonlocal term $u_x(\omega, \varepsilon)$ models other nonlocal terms $\nabla \mathbf{u}$ in (2.17), (2.21). We remove the more regular nonlocal terms in (2.17), (2.21), e.g. \mathbf{u}, c_ω , and the nonsingular part $u_{x,R} = u_x - u_x(\omega, \varepsilon)$, which will be estimated using the methods in Section 2.9 and 2.10.

We argue that if ε is small enough, we can establish the stability analysis. In the following estimate, C will be some absolute constant independent of the above parameters. For L^∞ estimate, using the definition of $u_x(\omega, \varepsilon)$ (2.33) and the Hölder norm of ω , we get

$$(2.49) \quad |u_x(\omega, \varepsilon)(x)| \leq C\varepsilon^{1/2}\|\omega\|_{C^{1/2}}, \quad \frac{d}{dt}\|\omega\|_{L^\infty} \leq -c_2\|\omega\|_{L^\infty} + Cc_3\varepsilon^{1/2}\|\omega\|_{C^{1/2}}.$$

The above L^∞ estimate is almost closed since we have a small parameter ε . For any x, z , denote $\delta(f)(x, z) = f(x) - f(z)$. In the Hölder estimate, using (2.47), and a direct calculation, we yield

$$-\frac{\delta(d\omega)(x, z)}{|x - z|^{1/2}} = -d(x)\frac{\delta(\omega)}{|x - z|^{1/2}} - \frac{d(x) - d(z)}{|x - z|^{1/2}}\omega(z), \quad \left| \frac{d(x) - d(z)}{|x - z|^{1/2}}\omega(z) \right| \leq c_3\|\omega\|_{L^\infty}.$$

For $a(x)u_x(x, \varepsilon)$, using (2.47), (2.48), and the above L^∞ estimate on u_x , we obtain

$$\left| \frac{\delta(au_x(\omega, \varepsilon))}{|x - z|^{1/2}} \right| \leq a(x)\left| \frac{\delta(u_x(\omega, \varepsilon))}{|x - z|^{1/2}} \right| + \left| \frac{a(x) - a(z)}{|x - z|^{1/2}} \right| |u_x(\omega, \varepsilon)(z)| \leq |a(x)|m\|\omega\|_{C^{1/2}} + Cc_3\varepsilon^{1/2}\|\omega\|_{C^{1/2}}.$$

It follows

$$(2.50) \quad \partial_t \frac{\delta\omega}{|x - z|^{1/2}} = -d(x)\frac{\delta\omega}{|x - z|^{1/2}} + B(x, z), \quad |B(x, z)| \leq (|a(x)|m + Cc_3\varepsilon^{1/2})\|\omega\|_{C^{1/2}} + c_3\|\omega\|_{L^\infty}.$$

Multiplying both sides by $\frac{\delta\omega}{|x - z|^{1/2}}$ and taking $|\frac{\delta\omega}{|x - z|^{1/2}}| \leq \|\omega\|_{C^{1/2}}$, we derive

$$\begin{aligned} \frac{1}{2}\partial_t \frac{(\delta\omega)^2}{|x - z|} &\leq -(d(x) - |a(x)|m - Cc_3\varepsilon^{1/2})\frac{(\delta\omega)^2}{|x - z|} \\ &\quad + (|a(x)|m + Cc_3\varepsilon^{1/2})(\|\omega\|_{C^{1/2}}^2 - \frac{(\delta\omega)^2}{|x - z|}) + c_3\|\omega\|_{L^\infty}\|\omega\|_{C^{1/2}}. \end{aligned}$$

Suppose that ε is small enough such that $Cc_3\varepsilon^{1/2} < \frac{c_1}{2}$. From (2.47), we have $d(x) - |a(x)|m - Cc_3\varepsilon^{1/2} \geq \frac{c_1}{2}$. Evaluating at the maximizer (x_*, z_*) and using $\|\omega\|_{C^{1/2}}^2 - \frac{(\delta\omega(x_*, z_*))^2}{|x_* - z_*|} = 0$, we get (2.51)

$$\frac{1}{2} \frac{d}{dt} \|\omega\|_{C^{1/2}}^2 \leq -\frac{c_1}{2} \|\omega\|_{C^{1/2}}^2 + c_3 \|\omega\|_{L^\infty} \|\omega\|_{C^{1/2}}, \quad \frac{d}{dt} \|\omega\|_{C^{1/2}} \leq -\frac{c_1}{2} \|\omega\|_{C^{1/2}} + c_3 \|\omega\|_{L^\infty}.$$

Combining the above estimate and the L^∞ estimate (2.49), for ε small enough such that

$$Cc_3\varepsilon^{1/2}c_3 < \frac{c_2c_1}{2},$$

using Lemma A.1 with $n = 2$ and $(F_1, F_2) = (\|\omega\|_{L^\infty}, \|\omega\|_{C^{1/2}})$, we obtain that

$$(2.52) \quad \frac{d}{dt} E \leq -\lambda E, \quad E = \max(\|\omega\|_{L^\infty}, \tau \|\omega\|_{C^{1/2}}), \quad \tau = \sqrt{\frac{Cc_3\varepsilon^{1/2}c_1/2}{c_3c_2}} = \sqrt{\frac{C\varepsilon^{1/2}c_1/2}{c_2}},$$

for some $\lambda > 0$. The above inequality for ε is from (A.2), and we have chosen $\tau = \mu_2$ offered in Lemma A.1. We prove the desired stability.

Interpretation of the estimates. From the estimate (2.52), we see that the weight of $\|\omega\|_{C^{1/2}}$ in the energy is smaller due to the factor $\varepsilon^{1/2}$. Since the L^∞ estimate (2.49) is almost closed, we can formally treat $\|\omega\|_{L^\infty}$ as an a-priori estimate. We choose the weight $\tau \sim \varepsilon^{1/4}$ so that $c_3\|\omega\|_{L^\infty}$ and $Cc_3\varepsilon^{1/4}\|\omega\|_{C^{1/2}}$ in (2.51) are balanced. Then for ε small enough, we can close the Hölder estimate. In our energy estimate of (2.17), (2.21), we will approximate the regular terms so that we can establish the L^∞ estimate with a small cost of the Hölder norm of ω similar to (2.49).

For the localized velocity, we show in Lemmas 3.1-3.4 that the constants in the Hölder estimates decrease if the distance $|x - z|$ increases. This improvement allows us to show that the worst scenario for the Hölder stability estimate occurs when $|x - z|$ is small.

Remark 2.5. Our energy estimate to be presented later follows ideas similar to those mentioned above. Yet, since it involves variable coefficients and several singular weights, the estimates are more technical. We will also track the constants and choosing the weight, e.g. τ in (2.52), much more carefully so that we do not need to choose ε to be too small, or approximate the regular terms using finite rank operators with a very high rank to get a small approximation error in a suitable norm. This will reduce our computation cost significantly. See Sections 2.9 and 2.10. The choice of the parameters in the above example are only used to illustrate the ideas.

2.9. A toy model with a nonlocal term. In this section, we use a model problem to illustrate the ideas of stability analysis of a linearized equation perturbed from a simpler linearized equation. In Section 2.10, we will apply these ideas to decompose the system (2.17), (2.21) and estimate the more regular nonlocal terms in (2.17), (2.21), e.g. $\mathbf{u} \cdot \nabla \bar{\omega}$.

We consider the following model

$$(2.53) \quad f_t = -b(x) \cdot \nabla f + d(x)f + a(x)P(f) \triangleq \mathcal{L}f$$

in \mathbb{R}_2^{++} , where the functions $b(x), d(x), a(x)$ are given and

$$b_i(x) \geq c_i x_i, c_i > 0, \quad P(f) = \int_{\mathbb{R}_2^{++}} f g dx,$$

for some time-independent function g . The terms $b(x) \cdot \nabla f, d(x)f$ model the local terms in (2.17), (2.21), and the rank one operator $a(x)P(f)$ models the nonlocal terms. We want to understand the long time behavior and the stability of the above model.

If the nonlocal term $a(x)P(f)$ is absent, we can follow the derivations in Section 2.7.1 to perform stability analysis. We assume that

$$(2.54) \quad f_t = -b(x) \cdot \nabla f + d(x)f \triangleq \mathcal{L}_0 f$$

is linearly stable in $L^\infty(\varphi)$ with some singular weight φ . Can we use this information to study (2.53)? Given initial data f_0 , a natural attempt is to use the Duhamel principle to represent

the solution to (2.53)

$$(2.55) \quad f(t) = e^{\mathcal{L}_0 t} f_0 + \int_0^t e^{\mathcal{L}_0(t-s)} (a(x) P(f(s))) ds = e^{\mathcal{L}_0 t} f_0 + \int_0^t P(f(s)) e^{\mathcal{L}_0(t-s)} a(x) ds,$$

where $e^{\mathcal{L}_0 t} g$ represents the solution to (2.54) at time t from initial data g , and we have used the fact that $P(f(s))$ is constant in space in the second equality. Although we know that $e^{\mathcal{L}_0 t} f_0$ and $e^{\mathcal{L}_0(t-s)} a(x)$ decay in $L^\infty(\varphi)$ due to the stability, if $a(x)$ is not small, the nonlocal term $P(f(s))$ and the contribution from the integral can lead to the growth of $f(t)$. In this case, it is not clear if $f(t)$ decays in some norm for large time.

Another attempt is to project f onto some space Y orthogonal to $g(x)$ or $a(x)$ so that the contribution from the nonlocal term is 0 in Y . However, since our estimate is L^∞ -based rather than L^2 -based, the orthogonal structure and projection are not compatible with these estimates.

2.9.1. Rank-one perturbation. Since (2.53) is a rank one perturbation of (2.54), we expect that the solution f to (2.53) can be decomposed as $f = f_1 + f_2$, where the main part f_1 has behavior similar to the solution of (2.54) and f_2 can be seen as a low rank correction. In particular, we draw inspiration from the Sherman-Morrison formula [71] in linear algebra. Given an invertible square matrix $A \in \mathbb{R}^{n \times n}$ and column vectors $u, v \in \mathbb{R}^n$, the matrix $A + uv^T$ is invertible if and only if $1 + v^T A^{-1} u \neq 0$. In this case,

$$(2.56) \quad (A + uv^T)^{-1} = A^{-1} - \frac{A^{-1}uv^T A^{-1}}{1 + v^T A^{-1} u}.$$

This formula shows that to check the invertibility of the perturbed matrix, it suffices to test the action of A^{-1} on these perturbed directions u, v . Now, we generalize this idea to study (2.53) from (2.54). Given initial data f_0 , we decompose (2.53) as follows

$$(2.57) \quad \begin{aligned} \partial_t f_1(t) &= \mathcal{L}_0 f_1, & f_1(0) &= f_0, \\ \partial_t f_2(t) &= \mathcal{L} f_2 + a(x) P(f_1(t)), & f_2(0) &= 0. \end{aligned}$$

It is easy to see that $f_1 + f_2$ solves (2.53) with initial data f_0 . The first part f_1 satisfies (2.54). The second part f_2 is driven by the rank-one forcing term $a(x)P(f_1(t))$. Using the Duhamel principle, the fact that $P(f_1(t))$ is constant in space, and derivations similar to (2.55), we yield

$$(2.58) \quad f_2(t) = \int_0^t P(f_1(s)) e^{\mathcal{L}(t-s)} a(x) ds.$$

Since $f_1(t) = e^{\mathcal{L}_0 t} f_0$ decays in $L^\infty(\varphi)$, we can control $P(f_1(s))$. If $e^{\mathcal{L}t} a(x)$ decays in $L^\infty(\varphi)$ for large t , we can show that $f_2(t)$ also decays in $L^\infty(\varphi)$ and establish stability estimate of f_2 .

Remark 2.6. The initial data f_0 can be an arbitrary function in some weighted space. By choosing zero initial data for f_2 and using the fact that $P(f_1(s))$ is a scalar, we can solve f_2 for an arbitrary forcing coefficient $P(f_1(s))$.

Let us compare the above decomposition with (2.56). The operators $\mathcal{L}_0, \mathcal{L}$ and rank-one perturbation $a(x)P(f)$ are analogs of $A, A + uv^T$ and uv^T . The stability of \mathcal{L} is analogous to the invertibility of $A + uv^T$. Testing the stability of \mathcal{L} from initial data $a(x)$ or the decay of $e^{\mathcal{L}(t-s)} a(x)$ is similar to testing A^{-1} on the directions u, v so that $1 + v^T A^{-1} u \neq 0$.

Similar idea also appears in the celebrated $T(1)$ [22] and $T(b)$ [23, 59] theorems in Harmonic analysis. Roughly, it states that for a linear operator T associated with a standard kernel K , proving the L^2 boundedness of T reduces to testing T on 1 or on some function b . In our model problem, using energy estimate to establish the stability of (2.54) is similar to extracting certain properties of T from a standard kernel. Further, testing the operators \mathcal{L} on the perturbations to obtain its stability is similar to testing T on 1 or b to obtain the L^2 boundedness of T .

2.9.2. Constructing approximate solution to f_2 and a perturbed operator. In this section, we discuss how to verify the decay of $e^{\mathcal{L}t} a$. Though the operator \mathcal{L} and function a are given, it is difficult to prove decay estimates of $e^{\mathcal{L}t} a$ in the weighted norm analytically since \mathcal{L} involves a nonlocal term. In our application to the Boussinesq system, analyzing $e^{\mathcal{L}t} a$ analytically is even more challenging since the operator \mathcal{L} and the nonlocal terms are much more complicated.

An alternative approach is to solve (2.53) numerically from initial data $a(x)$ to obtain an approximate solution $\hat{g}(t, x)$. Then by showing the error $e^{\mathcal{L}t}a - \hat{g}(t, x)$ is small in the weighted norm with a singular weight and verifying the decay of $\hat{g}(t)$, we obtain the decay estimates of $e^{\mathcal{L}t}a$. The difficulty lies in estimating the error in the weighted norm rigorously. The standard *a-priori* error estimate provides the following estimate

$$|e^{\mathcal{L}t}a(x) - \hat{g}(t, x)| \leq C_1(h^m + k^n)e^{C_2 t},$$

for some constants C_1, C_2 depending on $a(x)$ and \mathcal{L} , where h is the mesh size, k is the time step in the computation, and m, n relate to the order of the numerical scheme. However, the constants are not easy to estimate and can be quite large, and the above estimate does not account the round off error. Since the solution can have a slow decay in \mathbb{R}_+^2 , our computation domain can be very large. As a result, choosing a very small mesh size h in the computation may not be practical. Moreover, t is not small since we want to obtain decay estimates of $e^{\mathcal{L}t}a$ for suitably large t , e.g., $t \geq 10$. The above estimate is not practical.

Instead, we seek *a-posteriori* error estimate. Firstly, we solve (2.53) numerically and obtain a numerical solution $\hat{g}(t_k, x)$ at time t_k , which is represented by piecewise polynomials and thus defined globally in x . Then we interpolate the solution $\hat{g}(t_k, x)$ in time t using piecewise cubic polynomials to obtain solution $\hat{g}(t, x)$ defined on $[0, T] \times \mathbb{R}_+^2$. Then we introduce the residual error and a residual operator \mathcal{R} related to the nonlocal term $P(f_1(t))$ in (2.57)

$$(2.59) \quad \begin{aligned} e(t, x) &\triangleq (\partial_t - \mathcal{L})\hat{g}, \quad e_0(x) = \hat{g}(0) - g_0, \quad g_0 = a(x) \\ \mathcal{R}(f_1, t) &= P(f_1(t))e_0(x) + \int_0^t P(f_1(s))e(t-s, x)ds. \end{aligned}$$

Since \hat{g} is defined everywhere in space and time, we can estimate $e(t, x)$ and $e_0(x)$.

Now, using the approximate solution $\hat{g}(t, x)$ for $e^{\mathcal{L}t}g_0$, we can construct the approximate solution to the f_2 -equation in (2.57) based on (2.58)

$$(2.60) \quad \hat{f}_2(t) = \int_0^t P(f_1(s))\hat{g}(t-s)ds.$$

By definition and (2.59), we have

$$\begin{aligned} (\partial_t - \mathcal{L})\hat{f}_2 &= P(f_1(t))\hat{g}(0) + \int_0^t P(f_1(s))(\partial_t - \mathcal{L})\hat{g}(t-s)ds \\ &= P(f_1(t))(a(x) + e_0) + \int_0^t P(f_1(s))e(t-s, x)ds = P(f_1(t))a(x) + \mathcal{R}(f_1, t). \end{aligned}$$

If the error $e(t, x)$ and e_0 are small, we can show that the norm of the residual operator is small in some suitable functional space

$$(2.61) \quad \|\mathcal{R}(f_1, t)\|_X \leq \varepsilon \|f_1\|_X, \quad \varepsilon \ll 1.$$

Now, we modify the decomposition (2.57) as follows ($f = f_1 + \hat{f}_2$)

$$(2.62) \quad \begin{aligned} \partial_t f_1 &= \mathcal{L}_0 f_1 - \mathcal{R}(f_1, t), \quad f_1(0) = f_0, \\ \partial_t \hat{f}_2 &= \mathcal{L} \hat{f}_2 + a(x)P(f_1(t)) + \mathcal{R}(f_1, t). \end{aligned}$$

We remark that the solution (2.60) constructed by the numerical solution \hat{g} solves the second equation *exactly*. Now, due to the smallness (2.60), we can apply the stability estimate of \mathcal{L}_0 and treat $\mathcal{R}(f_1, t)$ as perturbation to obtain stability estimate of f_1 .

Remark 2.7. We should compare the original problem (2.53) with (2.62). By performing the decomposition (2.57), (2.62), constructing an approximating solution \hat{g} to $e^{\mathcal{L}t}a(x)$, and testing its decay, we replace a difficult nonlocal term in (2.53) by a small error term $\mathcal{R}(f_1, t)$ in (2.62) that can be treated as a small perturbation. Moreover, we do not need to assume any specific form about the rank-one operator $a(x)P(f_1(t))$.

2.10. Finite rank perturbations to the linearized operators. We generalize the idea in the previous section to the Boussinesq equations. Using the ideas in (2.9), we can modify the operators in (2.17), (2.21) by a finite rank operator \mathcal{K} with rank N by testing these operators on N suitable functions. Then we perform energy estimate on $\mathcal{L} - \mathcal{K}$. These finite rank operators approximate the contributions from the more regular terms in (2.17), (2.21), e.g., $\mathbf{u} \cdot \nabla \bar{\omega}$, $\mathbf{u} \cdot \nabla \bar{\theta}_x$, which we neglect in Section 2.8. The more regular terms can be seen as compact operators of ω in some suitable weighted spaces.

Since we will perform weighted estimates with singular weights near $x = 0$, it is useful to rewrite (2.17), (2.21) such that each term has the right vanishing order. We introduce the following notations [12, 13]

$$(2.63) \quad \tilde{u} = u - u_x(0)x, \quad \tilde{v} \triangleq v - v_y(0)y = v + u_x(0)y.$$

Since $\omega_x(0) = 0$ (2.22), $\omega_x(0) = -\Delta \psi_x(0)$, $\psi(x, 0) = 0$, and ψ is odd in x , we yield

$$\psi = O(|x|^4), \quad \tilde{u} = O(|x|^3), \quad \tilde{v} = O(|x|^3), \quad \nabla \tilde{\mathbf{u}} = O(|x|^2),$$

for perturbations that are regular enough. Recall $c_\omega = u_x(0)$ (2.19). Using $\tilde{u}_x = u_x - u_x(0)$, $\tilde{u}_y = u_y$, $\tilde{v}_x = v_x$, $\tilde{v}_y = v_y + u_x(0)$,

$$\begin{aligned} -\mathbf{u} \cdot \nabla \bar{\omega} + c_\omega \bar{\omega} &= -\tilde{\mathbf{u}} \cdot \nabla \bar{\omega} + c_\omega (\bar{\omega} - x\bar{\omega}_x + y\bar{\omega}_y), \\ -\mathbf{u} \cdot \nabla \bar{\theta}_x - \mathbf{u}_x \cdot \bar{\theta} + 2c_\omega \bar{\theta}_x &= -\tilde{\mathbf{u}} \cdot \nabla \bar{\theta}_x - \tilde{\mathbf{u}}_x \cdot \nabla \bar{\theta} + c_\omega (\bar{\theta}_x - x\bar{\theta}_{xx} + y\bar{\theta}_{xy}), \\ -\mathbf{u} \cdot \nabla \bar{\theta}_y - \mathbf{u}_y \cdot \nabla \bar{\theta} + 2c_\omega \bar{\theta}_y &= -\tilde{\mathbf{u}} \cdot \nabla \bar{\theta}_y - \tilde{\mathbf{u}}_y \cdot \nabla \bar{\theta} + c_\omega (\bar{\theta}_y - x\bar{\theta}_{xy} + y\bar{\theta}_{yy}), \end{aligned}$$

and denoting

$$(2.64) \quad \bar{f}_{c_\omega,1} = \bar{\omega} - x\bar{\omega}_x + y\bar{\omega}_y, \quad \bar{f}_{c_\omega,2} = \bar{\theta}_x - x\bar{\theta}_{xx} + y\bar{\theta}_{xy}, \quad \bar{f}_{c_\omega,3} = 3\bar{\theta}_y - x\bar{\theta}_{xy} + y\bar{\theta}_{yy},$$

we can rewrite (2.17), (2.21) as follows

$$\begin{aligned} (2.65) \quad \partial_t \omega &= -(\bar{c}_l x + \tilde{\mathbf{u}}) \cdot \nabla \omega + \bar{c}_\omega \omega + \eta - \tilde{\mathbf{u}} \cdot \nabla \bar{\omega} + c_\omega \bar{f}_{c_\omega,1} + \mathcal{N}_1 + \bar{\mathcal{F}}_1 \triangleq \mathcal{L}_1 + \mathcal{N}_1 + \bar{\mathcal{F}}_1, \\ \partial_t \eta &= -(\bar{c}_l x + \tilde{\mathbf{u}}) \cdot \nabla \eta + (2\bar{c}_\omega - \bar{u}_x)\eta - \bar{v}_x \xi - \tilde{\mathbf{u}}_x \cdot \nabla \bar{\theta} - \tilde{\mathbf{u}} \cdot \nabla \bar{\theta}_x + c_\omega \bar{f}_{c_\omega,2} \\ &\quad + \partial_x (N_\theta + \bar{F}_\theta) \triangleq \mathcal{L}_2 + \mathcal{N}_2 + \bar{\mathcal{F}}_2, \\ \partial_t \xi &= -(\bar{c}_l x + \tilde{\mathbf{u}}) \cdot \nabla \xi + (2\bar{c}_\omega - \bar{u}_x)\xi - \bar{u}_y \eta - \tilde{\mathbf{u}}_y \cdot \nabla \bar{\theta} - \tilde{\mathbf{u}} \cdot \nabla \bar{\theta}_y + c_\omega \bar{f}_{c_\omega,3} \\ &\quad + \partial_y (N_\theta + \bar{F}_\theta) \triangleq \mathcal{L}_3 + \mathcal{N}_3 + \bar{\mathcal{F}}_3. \end{aligned}$$

The nonlocal terms $c_\omega \bar{f}_{c_\omega,i}$, $-\tilde{\mathbf{u}} \cdot \nabla f$ for $f = \bar{\omega}, \bar{\theta}_x, \bar{\theta}_y$, and $\nabla \tilde{\mathbf{u}}_R$, the nonsingular part of the integral, are more regular than ω . We will choose finite rank operators to approximate them.

2.10.1. Correction near the origin. We discuss in Section 2.7.5 that to obtain better stability factors, we choose more singular weights for the stability analysis. We consider the following corrections

$$\begin{aligned} (2.66) \quad \mathcal{K}_{1i}(\omega) &\triangleq c_\omega(\omega) \bar{f}_{c_\omega,1}, \\ NF_1(\omega, \eta, \xi) &= (c_\omega \omega_{xy}(0) + \partial_{xy} \bar{\mathcal{F}}_1(0)) f_{\chi,1}, \quad f_{\chi,1} \triangleq xy\chi, \\ NF_2(\omega, \eta, \xi) &= (c_\omega \eta_{xy}(0) + \partial_{xy} \bar{\mathcal{F}}_2(0)) f_{\chi,2}, \quad f_{\chi,2} \triangleq xy\chi, \\ NF_3(\omega, \eta, \xi) &= (c_\omega \xi_{xx}(0) + \partial_{xx} \bar{\mathcal{F}}_3(0)) f_{\chi,3}, \quad f_{\chi,3} \triangleq \frac{x^2}{2}\chi, \end{aligned}$$

where χ is some cutoff function with $\chi = 1$ near $x = 0$ defined later. The operator \mathcal{K}_{1i} is correction to the linear part, and NF_i is correction to the nonlinear term, and the residual in (2.65), respectively. After subtracting \mathcal{K}_{1i} and NF_i from (2.65), the resulting equations preserve the vanishing conditions $\omega, \eta, \xi = O(|x|^3)$.

We can derive the ODE for $\omega_{xy}(0), \theta_{xxy}(0)$ using (2.10)

$$\begin{aligned} (2.67) \quad \frac{d}{dt} \omega_{xy}(0) &= (-2c_l + c_\omega) \omega_{xy}(0) - \omega_x^2(0) + \theta_{xxy}(0), \\ \frac{d}{dt} \theta_{xxy}(0) &= (-2c_l + 2c_\omega - u_x(0)) \theta_{xxy}(0) - 2\omega_x(0) \theta_{xx}(0). \end{aligned}$$

Since $\omega_x(0), \theta_{xx}(0)$ are preserved (2.12), to estimate $\omega_{xy}(0), \theta_{xxy}(0)$, using (2.67), we only need to control $c_l, c_\omega, u_x(0)$ rather than some higher order norm of ω, θ , e.g. $\|\omega\|_{C^2}, \|\theta\|_{C^3}$.

2.10.2. *Approximation of the velocity.* For $f = u, v, u_x, u_y, v_x, v_y$, we will construct in (2.89), (2.82), (2.88) in Section 2.11 the finite rank approximations \hat{f} for \tilde{f} so that we get smaller constants C in the weighted estimate of $\tilde{f} - \hat{f}$ using the energy $\|\omega\varphi\|_{L^\infty}, \|\omega\psi_1\|_{C_x^{1/2}}, \|\omega\psi_1\|_{C_y^{1/2}}$.

We remark that for these operators, we do not have

$$\partial_x^i \partial_y^j \hat{u} = \widehat{\partial_x^i \partial_y^j u}, \quad \partial_x^i \partial_y^j \hat{v} = \widehat{\partial_x^i \partial_y^j v},$$

for $i + j = 1$. These approximations contribute to the following finite rank operators

$$(2.68) \quad \mathcal{K}_{21} = -\hat{\tilde{\mathbf{u}}} \cdot \nabla \bar{\omega}, \quad \mathcal{K}_{22} = -\hat{\tilde{\mathbf{u}}}_x \cdot \nabla \bar{\theta} - \hat{\tilde{\mathbf{u}}} \cdot \bar{\nabla} \theta_x, \quad \mathcal{K}_{23} = -\hat{\tilde{\mathbf{u}}}_y \cdot \nabla \bar{\theta} - \hat{\tilde{\mathbf{u}}} \cdot \nabla \bar{\theta}_y,$$

which are designed to capture the contributions from the regular nonlocal terms. We defer the construction of \mathcal{K}_{2i} to Section 2.11.

The linearized operators in (2.65) perturbed by these finite rank operators are similar to the one in Section 2.8.3, which we can estimate following the ideas in Section 2.8.3. This stability estimate serves as the role of stability estimate of \mathcal{L}_0 in the model problem in Section 2.9. Then we further test the original operators in (2.65) on these finite rank operators using the ideas in Section 2.9 and next section to close the stability analysis.

2.10.3. *Decomposition of the system.* Denote $W_1 = (\omega_1, \eta_1, \xi_1), W_2 = (\omega_2, \eta_2, \xi_2)$. Recall the notations (2.1) and (2.2). Following Section 2.9 and (2.57), we decompose (2.65) as follows

$$(2.69) \quad \begin{aligned} \partial_t W_{1,i} &= (\mathcal{L}_i - \mathcal{K}_{1i} - \mathcal{K}_{2i}) W_1 + \mathcal{N}_i(W_1 + W_2) + \bar{\mathcal{F}}_i - NF(W_1 + W_2), \\ \partial_t W_{2,i} &= \mathcal{L}_i W_2 + \mathcal{K}_{1i}(W_1) + \mathcal{K}_{2i}(W_1) + NF_i(W_1 + W_2), \\ W_1|_{t=0} &= (\omega_0, \eta_0, \xi_0), \quad W_2|_{t=0} = (0, 0, 0), \end{aligned}$$

with ω_0, η_0, ξ_0 being the initial perturbation with vanishing order $O(|x|^3)$.

Firstly, we show that $W = W_1 + W_2$ solves (2.65) with initial data $= (\omega_0, \eta_0, \xi_0)$. A direct calculation yields

$$\partial_t(W_1 + W_2) = \mathcal{L}_i(W_1 + W_2) + \mathcal{N}_i(W_1 + W_2) + \bar{\mathcal{F}}_i,$$

which are the same equations as (2.65). Since $W_1 + W_2$ has initial data $(\omega_0, \eta_0, \xi_0)$, $W_1 + W_2$ solves (2.65) with the given initial data. Using the definitions (2.66) and a Taylor expansion near $x = 0$, we obtain that the vanishing conditions $\omega_1, \eta_1, \xi_1 = O(|x|^3)$ are preserved.

Remark 2.8. Although $W_{1,2} + W_{2,2} = \theta_x, W_{1,3} + W_{2,3} = \theta_y$, since the finite rank operators \mathcal{K}_{ij} we choose do not satisfy similar partial derivative relations, the solution to (2.69) does not satisfy $\partial_y W_{i,2} = \partial_x W_{i,3}$ for $i = 1$ or $i = 2$.

Let us motivate the decomposition (2.69). At the linear level, we choose finite rank operators $\mathcal{K}_{1i}, \mathcal{K}_{2i}$ to approximate \mathcal{L}_i . Then $\mathcal{L}_i - \mathcal{K}_{1i} - \mathcal{K}_{2i}, \mathcal{L}_i$ serve as the $\mathcal{L}_0, \mathcal{L}$ operators in the model problem (2.54), (2.53), respectively. The decomposition of the solutions W_1, W_2 is similar to (2.57). Since we want to perform energy estimate on W_1 using more singular weights, we correct the nonlinear terms and the forcing terms in the first equation in (2.69). Although $NF_i(W_1 + W_2)$ involves nonlinear factors, e.g. $c_\omega(\omega_1 + \omega_2)\partial_{xy}(\omega_1 + \omega_2)(0)$, since these factors are constant in space, we can still apply Duhamel's formula in (2.55) to $NF_i(W_1 + W_2)$, i.e.,

$$\int_0^t e^{\mathcal{L}(t-s)} \left(c_\omega \partial_{xy}(\omega_1(s) + \omega_2(s))(0) \bar{f} \right) ds = \int_0^t c_\omega \partial_{xy}(\omega_1(s) + \omega_2(s))(0) e^{\mathcal{L}(t-s)} \bar{f} ds,$$

and obtain the formula of W_2 in (2.69).

Avoiding the loss of derivatives. Note that in the equation of W_1 in (2.69), it contains the nonlinear terms $\mathbf{u}(W_1 + W_2) \cdot \nabla(W_1 + W_2)$. In general, the term $\mathbf{u} \cdot \nabla W_2$ can lead to loss of derivatives. We overcome this difficulty by constructing smoother W_2 . Note that W_2 in (2.69) is driven by the forcing terms of the following forms

$$(2.70) \quad \sum_{1 \leq i \leq N} a_i(W_1, W_2)(t) f_i$$

for some N , time-dependent scalars (independent of x) $a_i(W_1, W_2)(t)$, and time-independent functions f_i , e.g. $c_\omega(W_1) \bar{f}_{c_\omega, i}$ in (2.66). By choosing smoother f_i in the approximation, we can obtain solution W_2 smooth enough for our energy estimates.

2.10.4. Constructing the approximate solution of W_2 and modifying the decomposition. Following the ideas in Section 2.9.2, instead of solving the W_2 equations in (2.69) exactly, we solve them with an error term. Assume that we have the following representations for the operators

$$\vec{\mathcal{K}}_{1j}(W_1) + \vec{\mathcal{K}}_{2j}(W_1) = \sum_{1 \leq i \leq n_1} a_i(W_1)(t) \bar{F}_{ij},$$

where $\vec{\mathcal{K}}_{i \cdot} = (\mathcal{K}_{i1}, \mathcal{K}_{i2}, \mathcal{K}_{i3})$, $\bar{F}_i(x) = (\bar{f}_{i,1}(x), \bar{f}_{i,2}(x), \bar{f}_{i,3}(x)) : \mathbb{R}_+^2 \rightarrow \mathbb{R} \times \mathbb{R} \times \mathbb{R}$, and $a_i(W_1)(t)$ is some linear functional on W_1 . For example, the formula (2.66) can be written as

$$a(W_1)(t)(\bar{f}_{c_\omega, 1}, \bar{f}_{c_\omega, 2}, \bar{f}_{c_\omega, 3}), \quad a(W_1)(t) = c_\omega(W_1) = u_x(W_1(t))(0),$$

where we have used (2.19) for c_ω . Recall the operators NF_i and functions $f_{\chi, i}$ from (2.66). Writing (2.66) as vectors, we have

$$(2.71) \quad \begin{aligned} NF(\omega) &= (c_\omega \partial_{xy} \omega(0) + \partial_{xy} \bar{\mathcal{F}}_1(0))(f_{\chi, 1}, 0, 0) + (c_\omega \partial_{xy} \eta(0) + \partial_{xy} \bar{\mathcal{F}}_2(0))(0, f_{\chi, 2}, 0) \\ &\quad + (c_\omega \partial_{xx} \xi(0) + \partial_{xx} \bar{\mathcal{F}}_3(0))(0, 0, f_{\chi, 3}) \triangleq \sum_{1 \leq i \leq 3} a_{nl, i}(\omega(t)) F_{\chi, i}, \end{aligned}$$

where

$$(2.72) \quad a_{nl, \cdot} = (c_\omega \partial_{xy} \omega(0) + \partial_{xy} \bar{\mathcal{F}}_1(0), c_\omega \partial_{xy} \eta(0) + \partial_{xy} \bar{\mathcal{F}}_2(0), c_\omega \partial_{xx} \xi(0) + \partial_{xx} \bar{\mathcal{F}}_3(0)), \quad F_{\chi, i} = f_{\chi, i} e_i,$$

and e_1, e_2, e_3 are the standard basis for \mathbb{R}^3 . Denote by $\hat{F}_i(t, x)$ and $\hat{F}_{\chi, i}(t, x)$ the approximation of $e^{\mathcal{L}t} \bar{F}_i$ and $e^{\mathcal{L}t} \bar{F}_{\chi, i}$. Following (2.59) and (2.60), and using the idea in (2.70), we construct the approximate solution to W_2 in (2.69) as follows

$$(2.73) \quad \hat{W}_2(t) = \sum_{i \leq n_1} \int_0^t a_i(W_1(s)) \hat{F}_i(t-s) ds + \sum_{i \leq 3} \int_0^t a_{nl, i}(W_1(s) + \hat{W}_2(s)) \hat{F}_{\chi, i}(t-s) ds.$$

We introduce the residual operator

$$(2.74) \quad \begin{aligned} \mathcal{R}_l(W_1) &\triangleq \sum_{i=1}^{n_1} \left(a_i(W_1(t))(\hat{F}_i(0) - \bar{F}_i) + \int_0^t a_i(W_1(s))((\partial_t - \mathcal{L})\hat{F}_i)(t-s) ds \right), \\ \mathcal{R}_{nl}(W) &\triangleq \sum_{i=1}^3 \left(a_{nl, i}(W(t))(\hat{F}_{\chi, i}(0) - \bar{F}_{\chi, i}) + \int_0^t a_{nl, i}(W(s))((\partial_t - \mathcal{L})\hat{F}_{\chi, i})(t-s) ds \right), \\ \mathcal{R}(W_1, \hat{W}_2) &\triangleq \mathcal{R}_l(W_1) + \mathcal{R}_{nl}(W_1 + \hat{W}_2), \end{aligned}$$

where $\mathcal{R}_l, \mathcal{R}_{nl}$ denote the linear and the nonlinear parts, respectively. Note that $\mathcal{R}(W_1, \hat{W}_2)(x)$ is a vector in \mathbb{R}^3 .

Remark 2.9. We remark that given W_1 and $\hat{F}_i, \hat{F}_{\chi, i}$, the solution \hat{W}_2 (2.73) is not completely determined since the second part depends on \hat{W}_2 . At the linear level, the solution \hat{W}_2 (2.73) is determined. Since the second part depends on \hat{W}_2 nonlinearly, we will show that it is small relative to the linear part using a bootstrap argument. Therefore, we can still use (2.73) to estimate \hat{W}_2 .

Similar to (2.62), using the above operators, we modify the decomposition (2.69) as follows

$$(2.75) \quad \begin{aligned} \partial_t W_{1,i} &= (\mathcal{L}_i - \mathcal{K}_{1i} - \mathcal{K}_{2i})(W_1) + \mathcal{N}_i(W_1 + \hat{W}_2) + \bar{\mathcal{F}}_i - NF_i(W_1 + \hat{W}_2) - \mathcal{R}_i(W_1, \hat{W}_2), \\ \partial_t \hat{W}_{2,i} &= \mathcal{L}_i \hat{W}_2 + \mathcal{K}_{1i}(W_1) + \mathcal{K}_{2i}(W_1) + NF_i(W_1 + \hat{W}_2) + \mathcal{R}_i(W_1, \hat{W}_2), \\ W_1|_{t=0} &= (\omega_0, \eta_0, \xi_0), \quad \hat{W}_2|_{t=0} = (0, 0, 0), \end{aligned}$$

where $\mathcal{R} = (\mathcal{R}_1, \mathcal{R}_2, \mathcal{R}_3)$. The above decomposition is a nonlinear generalization of (2.62). We solve the \hat{W}_2 equation using the formula (2.73) *exactly*. It is easy to see that $W_1 + \hat{W}_2$ solves (2.65) from initial data $(\omega_0, \eta_0, \xi_0)$. If the error in (2.74), e.g. $\hat{F}_i(0) - \bar{F}_i$, $(\partial_t - \mathcal{L})\hat{F}_i$, is small, we expect that the following estimates for \mathcal{R} :

$$\|\mathcal{R}(W_1, \hat{W}_2)\|_X \leq \varepsilon(\|W_1\|_X + \|W_1 + \hat{W}_2\|_X^2 + \bar{\varepsilon})$$

in some suitable weighted space X with very small $\varepsilon, \bar{\varepsilon}$, where the second and the third terms come from the estimate of $a_{nl,i}(W_1 + \hat{W}_2)$ defined in (2.71). Since $\bar{\mathcal{F}}_i$ is the residual error of the profile, for $i+j=2$, $\partial_x^i \partial_y^j \bar{\mathcal{F}}(0)$ is small and contributes to the small factor $\bar{\varepsilon}$. Thus, the residual operator \mathcal{R} can be treated as a small perturbation in (2.75). In particular, at the linear level, \hat{W}_2 does not appear in the W_1 equation.

We will construct approximate solution \hat{F}_i and $\hat{F}_{\chi,i}$ so that the error vanishes cubically near $x=0$:

$$(2.76) \quad \hat{F}_i(0) - \bar{F}_i, \quad (\partial_t - \mathcal{L})\hat{F}_i = O(|x|^3), \quad \hat{F}_{\chi,i}(0) - \bar{F}_{\chi,i}, \quad (\partial_t - \mathcal{L})\hat{F}_{\chi,i} = O(|x|^3).$$

We will discuss how to construct these approximate solution and estimate these errors in the weighted functional spaces for the energy estimate rigorously in Section 6.

For initial perturbation $\omega_0, \eta_0, \xi_0 = O(|x|^3)$, from the definitions (2.66) and the above vanishing order of the error, we obtain that the vanishing conditions $\omega_1, \eta_1, \xi_1 = O(|x|^3)$ are preserved. Thus, we can perform energy estimates on W_1 using singular weights of order $|x|^{-3}$ near $x=0$. See Section 2.7.5 for more discussions on the vanishing order. We will perform the energy estimates in Section 4.

Remark 2.10. Since \hat{F}_i is the numerical solution to $\partial_t F_i = \mathcal{L} F_i$, the above error terms (2.76) are small. Since the solution is smooth enough, in principle, by choosing a high order numerical scheme with sufficiently small mesh size and timestep, one can make the error term to be arbitrarily small. In such a case, the residual operators in (2.74), (2.75) are also sufficiently small compared to the perturbation W_1, W .

2.11. Approximating the regular part of the velocity. We want to construct a finite rank approximation $\mathcal{K}(\omega)$ of $\int_{\mathbb{R}^2} K_f(x-y)\omega(y)dy$, where K_f is the kernel for $\partial_x^i \partial_y^j (-\Delta)^{-1}\omega, i+j \leq 2$, so that we can estimate

$$(2.77) \quad \left| \int_{\mathbb{R}^2} K_f(x-y)\omega(y)dy - \mathcal{K}(\omega) \right| \leq C_1(x)\|\omega\varphi_1\|_{L^\infty} + C_2(x)\|\omega\psi_1\|_{C_x^{1/2}} + C_3(x)\|\omega\psi_1\|_{C_y^{1/2}},$$

with small constant $C_1(x), C_2(x), C_3(x)$ for some given weights, where the Hölder seminorms $C_x^{1/2}, C_y^{1/2}$ are defined in (2.3).

Since $K_f(z)$ is smooth away from $z=0$, a natural approach is to approximate the nonsingular part of $K(x-y)$ by interpolating $K(x-y)$ on finite many points x_i :

$$K(x-y)\mathbf{1}_{|x-y|\geq\varepsilon} \approx \sum_{1 \leq i \leq n} \chi_i(x)K(x_i-y)\mathbf{1}_{|x_i-y|\geq\varepsilon},$$

where χ_i is some cutoff function localized to x_i . The above right hand sides lead to the finite rank operator

$$(2.78) \quad \mathcal{K}(\omega) = \sum_{i=1}^n \chi_i(x) \int K(x_i-y)\mathbf{1}_{|x_i-y|\geq\varepsilon}\omega(y)dy.$$

We will construct the bulk part of the approximation in Section 2.11.2 based on (2.78). Due to the decay of the coefficients of $\mathbf{u}, \nabla \mathbf{u}$ in (2.65), e.g. $\nabla \bar{\omega}$ in $\mathbf{u} \cdot \nabla \bar{\omega}$, $\bar{\nabla} \theta_x$ in $\nabla \mathbf{u} \cdot \nabla \theta_x$, these nonlocal terms are small for large $|x|$. Thus, we only need to approximate $\mathbf{u}, \nabla \mathbf{u}$ for x in the

near field, especially for x close to the boundary due to the anisotropy of the flow. See Section 2.7.2.

Regularity of the velocity. For $\mathbf{u} = \nabla^\perp(-\Delta)^{-1}\omega$, given ω in some weighted space $L^\infty(\varphi)$, \mathbf{u} is log-Lipschitz. Thus we can approximate $\mathbf{u}(x)$ in $C^\beta \cap L^\infty$ for any $\beta < 1$ by interpolating discrete points $\mathbf{u}(x_i)$, $i = 1, 2, \dots, n$ with n sufficiently large. The $C^\beta \cap L^\infty$ norm of the approximation error can be bounded by $c\|\omega\varphi\|_\infty$ with a small constant c . Similarly, for $\nabla\mathbf{u} = \nabla\nabla^\perp(-\Delta)^{-1}\omega$, given ω in some weighted L^∞ space, the nonsingular part of $\nabla\mathbf{u}$, $K(z)\mathbf{1}_{|z|\geq\varepsilon} * \omega$, is Lipschitz. Thus we can approximate it in $C^{1/2} \cap L^\infty$. Since $\nabla\mathbf{u} = \nabla\nabla^\perp(-\Delta)^{-1}\omega$ is not bounded from L^∞ to L^∞ , for the singular part of $\nabla\mathbf{u}$, $K(z)\mathbf{1}_{|z|\leq\varepsilon} * \omega$, we need to use the Hölder regularity of ω to control it. These motivate (2.77).

2.11.1. *Approximation near 0.* Since we will perform weighted energy estimates with singular weights and the velocity $\mathbf{u}, \nabla\mathbf{u}$ do not vanish near $x = 0$ with high order, we first approximate $\mathbf{u}, \nabla\mathbf{u}$ by its leading order behavior at $x = 0$.

In our energy estimate, we consider perturbation ω with vanishing order $O(|x|^{2+\alpha})$ for some $\alpha > 0$ near $x = 0$. Recall $-\Delta\psi = \omega$ and $\mathbf{u} = \nabla^\perp\psi$. Using Taylor expansion and

$$0 = \omega_x(0) = -\psi_{xxx}(0) - \psi_{xyy}(0), \quad 0 = \omega_{xy}(0) = -\psi_{xxxy}(0) - \psi_{xyyy}(0),$$

we get

$$\psi(x, y) = \psi_{xy}(0)xy + \frac{1}{6}(\psi_{xxxy}(0)x^3y + \psi_{xyyy}(0)xy^3) + h.o.t. = \psi_{xy}(0)xy + \frac{1}{6}\psi_{xxxy}(0)(x^3y - xy^3) + h.o.t.$$

We can represent $\psi_{xxxy}(0)$ as an integral of ω

$$(2.79) \quad \psi_{xxxy}(0) = \frac{2}{\pi} \int_{\mathbb{R}_{++}^2} \omega(y)K_{00}(y)dy, \quad K_{00}(y) \triangleq \frac{24y_1y_2(y_1^2 - y_2^2)}{|y|^8}, \quad \mathcal{K}_{00}(\omega) \triangleq \frac{1}{\pi} \int_{\mathbb{R}_{++}^2} K_{00}(y)\omega(y)dy.$$

For $\omega = O(|x|^{2+\alpha})$ with a suitable decay, the above integral is well-defined. By definition, we have $\psi_{xxxy}(0) = 2\mathcal{K}_{00}$. Here and below, we use \mathcal{K}_{00} as a short hand notation for $\mathcal{K}_{00}(\omega)$. Note that $u_x(0) = -\psi_{xy}(0)$. Using the above formulas, near 0, the leading order term for $\nabla\mathbf{u}$ and \mathbf{u} are given by

$$\begin{aligned} u &= -\psi_y = u_x(0)x - \left(\frac{1}{3}x^3 - xy^2\right)\mathcal{K}_{00} + h.o.t., \quad v = \psi_x = -u_x(0)y + \left(x^2y - \frac{1}{3}y^3\right)\mathcal{K}_{00} + h.o.t., \\ u_x &= u_x(0) - (x^2 - y^2)\mathcal{K}_{00} + h.o.t., \quad v_x = 2xy\mathcal{K}_{00} + h.o.t., \quad u_y = -\psi_{yy} = -2xy\mathcal{K}_{00} + h.o.t. \end{aligned}$$

By introducing

$$(2.80) \quad \begin{aligned} C_{u0} &= x, & C_{v0} &= -y, & C_{u_x0} &= 1, & C_{u_y0} &= C_{v_x0} = 0, \\ C_u &= -\left(\frac{1}{3}x^3 - x^2y\right), & C_v &= x^2y - \frac{1}{3}y^3, \\ C_{u_x} &= -(x^2 - y^2), & C_{v_x} &= 2xy, & C_{u_y} &= -2xy, \end{aligned}$$

we can rewrite the above leading order formulas as

$$(2.81) \quad f(x, y) = u_x(0)C_{f0}(x, y) + \mathcal{K}_{00}C_f(x, y) + h.o.t., \quad f = u, v, u_x, v_x, u_y.$$

For v_y , we will use $v_y = -u_x$ to estimate it. We will localize the above leading order terms to construct the approximation term near 0 in the next subsection.

2.11.2. *Approximation along the boundary.* Let χ be the cutoff function constructed in (F.1) and $\tilde{\chi} = 1 - \chi$. They satisfy

$$\chi(x) = 0, \quad \tilde{\chi}(x) = 1, \quad x \leq 0, \quad \chi(x) = 1, \quad \tilde{\chi}(x) = 0, \quad x \geq 1.$$

Given $0 < x_0 < x_1 < \dots < x_n < x_{n+1}$ and $y_0 > 0$, we construct the cutoff functions

$$\chi_0 = \tilde{\chi}\left(\frac{x - x_0}{x_1 - x_0}\right)\tilde{\chi}\left(\frac{y - y_0}{y_0}\right), \quad \chi_i = \left(\chi\left(\frac{x - x_{i-1}}{x_i - x_{i-1}}\right)\mathbf{1}_{x \leq x_i} + \tilde{\chi}\left(\frac{x - x_i}{x_{i+1} - x_i}\right)\mathbf{1}_{x \geq x_i}\right)\tilde{\chi}\left(\frac{y - y_0}{y_0}\right), \quad 1 \leq i \leq n.$$

We impose the cutoff function $\tilde{\chi}(\frac{y-y_0}{y_0})$ so that χ_i is supported near $y = 0$. By definition, for $x \leq x_n, y \leq y_0$, we have

$$\sum_{i \leq n} \chi_i(x, y) = 1.$$

We want to approximate $\mathbf{u}, \nabla \mathbf{u}$ such that the remainders $\mathbf{u} - \mathbf{u}_{app}$ vanish near $x = 0$ with high order. See Section 2.11.1. To preserve these vanishing orders in the approximations and obtain smoother approximations, we consider the following approximation, which modifies (2.78)

$$(2.82) \quad \hat{f}_1(x, y) \triangleq C_{f0}(x, y)u_x(0) + \hat{f}_{10}(x, y), \quad \hat{f}_{10} \triangleq C_f(x, y) \left(\mathcal{K}_{00}\chi_0(x, y) + \sum_{1 \leq i \leq n} \frac{1}{C_f(x_i, 0)} \chi_i(x, y) \hat{f}(x_i, 0) \right),$$

where

$$(2.83) \quad \hat{f}(x_i, 0) = \int_{y \in \mathbb{R}^2, \max(|y_1 - x_i, y_2|) \geq t_i} K_f((x_i, 0) - y) \omega(y) dy - C_{f0}(x_i, 0)u_x(0),$$

and K_f is the kernel for $f = u, v, u_x, v_x, u_y$, and functions C_{f0} and C_f are the coefficients of the leading order approximations of $\partial_x^i \partial_y^j \psi$ near $x = 0$. See (2.81) and (2.80). We add the functions $C_f(x, y)$ in (2.82) so that \hat{f}_1 has the same vanishing order as that of f .

We construct the above approximations along the boundary for u, u_x . For v, v_x, u_y , since the associated coefficients are relatively small, e.g. $\bar{\omega}_y$ in $v\bar{\omega}_y$ and $\bar{\theta}_y$ in $v_x\bar{\theta}_y$ (2.65), we only construct the approximation term $C_f(x, y)\mathcal{K}_{00}\chi_0(x, y)$ near 0. Now, by definition, we have

$$(2.84) \quad \begin{aligned} f(x_i, 0) - \hat{f}_1(x_i, 0) &= f(x_i, 0) - C_{f0}(x_i, 0)u_x(0) - \hat{f}(x_i, 0), \quad 0 \leq i \leq n \\ f(x, y) - \hat{f}_1(x, y) &= f(x, y) - C_{f0}(x, y)u_x(0) - C_f(x, y)\mathcal{K}_{00}, \quad \text{for } x \leq x_0, y \leq y_0, \end{aligned}$$

The first identity shows that \hat{f}_1 is an interpolation of the non-singular part of $K_f * \omega$, which is similar to (2.78). Here, we consider a weighted version of (2.78) with weight $C_f(x)$ so that the approximation has the right vanishing order near $x = 0$. The second identity shows that near $x = 0$, the approximation \hat{f}_1 captures the leading order behavior of f near $x = 0$ (2.81). Thus, \hat{f}_1 can approximate f near the points $(0, 0), (x_i, 0), 0 \leq i \leq n$.

2.11.3. Approximation in the far-field. To improve the far-field estimate, instead of using $u_x(0)$ to approximate $u, v, \partial u$ (2.83), we use the truncated version of $u_x(0)$

$$I_n \triangleq -\frac{4}{\pi} \int_{\max(y_1, y_2) \geq R_n} \frac{y_1 y_2}{|y|^4} \omega(y) dy.$$

Note that the above approximation is similar to the leading order term of the velocity derived in [48]. For $f = u, v, u_x, v_y$, the leading order part of the kernel $K(s) = -\frac{1}{\pi} \frac{s_1 s_2}{|s|^4}$ with symmetrization is given by

$$(2.85) \quad K^{sym}(x, y) = K(x - y) + K(x + y) - K(x_1 - y_1, x_2 + y_2) - K(x_1 + y_1, x_2 - y_2) = -\frac{4}{\pi} \frac{y_1 y_2}{|y|^4} + l.o.t.$$

for $\max|y_i| \geq C \max|x_i|$ with large C . For $f = u, v, v_y$, using a similar argument, we can show that the leading order part of the associated kernel K_f is

$$(2.86) \quad K_f^{sym} = -C_{f0} \frac{4}{\pi} \frac{y_1 y_2}{|y|^4} + l.o.t.$$

for $\max|y_i| \geq C \max|x_i|$ with large C , where C_{f0} is defined in (2.80). When $|y|$ is small and $|x|$ is large, the function $-\frac{4}{\pi} \frac{y_1 y_2}{|y|^4}$ does not approximate $K^{sym}(x, y)$ well, and thus we truncate it. Note that the operator

$$(2.87) \quad \int_{\max|y_i| \geq C \max|x_i|} -\frac{y_1 y_2}{|y|^4} \omega(y) dy$$

does not have a finite rank due to the hard cutoff function $\mathbf{1}_{|y| \geq C|x|}$. To approximate it by a finite rank operators, we approximate $\mathbf{1}_{|y| \geq C|x|}$ by a smooth cutoff function

$$g(x, y) = \sum_i \mathbf{1}_{|y_1| \vee |y_2| \geq R_i} \chi_i(x)$$

such that $\chi_i(x)$ is localized to the domain with $|x|$ comparable R_i . Then for x close to R_i , we obtain $g(x, y) \approx \mathbf{1}_{|y_1| \vee |y_2| \geq R_i} \approx \mathbf{1}_{|y_1| \vee |y_2| \geq |x|}$.

More specifically, given $R_0 < R_2 < \dots < R_m$, we construct cutoff functions as follows

$$\begin{aligned} \chi_i^R(x, y) &= \tilde{\chi}\left(\frac{x - R_i}{R_{i+1} - R_i}\right) \tilde{\chi}\left(\frac{y - R_i}{R_{i+1} - R_i}\right) - \tilde{\chi}\left(\frac{x - R_{i-1}}{R_i - R_{i-1}}\right) \tilde{\chi}\left(\frac{y - R_{i-1}}{R_i - R_{i-1}}\right), \quad 1 \leq i \leq m-1, \\ \chi_m^R(x, y) &= 1 - \tilde{\chi}\left(\frac{x - R_{m-1}}{R_m - R_{m-1}}\right) \tilde{\chi}\left(\frac{y - R_{m-1}}{R_m - R_{m-1}}\right). \end{aligned}$$

By definition, χ_i^R is supported in the annulus $[0, R_{i+1}]^2 \setminus [0, R_{i-1}]^2$, $1 \leq i \leq m-1$, and $\chi_m^R = 1$ for $\max(x, y) \geq R_m$. Moreover, we have $\sum_{i \leq m} \chi_i^R(x, y) = 1$ for $\max(x, y) \geq R_1$. Now, we construct the second approximation

$$(2.88) \quad \hat{f}_2(x, y) = C_{f0}(x, y)(1 - \chi_{tot}(x, y)) \left(\sum_{1 \leq i \leq m} \chi_i^R(x, y)(I_i - u_x(0)) \right),$$

where $\chi_{tot}(x, y)$ is the sum of the cutoff functions for the first approximation in Section 2.11.2:

$$\chi_{tot}(x, y) = \sum_{0 \leq i \leq n} \chi_i(x, y).$$

For $\chi_{tot}(x, y) = 0$ and $x = R_i, y \in [0, R_i]$, from (2.83), we get $\hat{f}_1 = C_{f0}(x)u_x(0), \hat{f}_2 = C_{f0}(I_i - u_x(0))$,

$$\begin{aligned} f - \hat{f}_1 - \hat{f}_2 &= f - C_{f0}u_x(0) - C_{f0}(I_i - u_x(0)) = \int (K_f(x - y)\omega(y)dy - C_{f0}I_i \\ &= \int_{\mathbb{R}_{++}^2} (K_f^{sym}(x, y) + \frac{4}{\pi}C_{f0}(x)\frac{y_1 y_2}{|y|^4} \mathbf{1}_{\max(|y_1|, |y_2|) \geq R_i})\omega(y)dy, \end{aligned}$$

where K_f^{sym} is the symmetrized kernel. Therefore, for large $|x|$, the approximation $\hat{f}_1 + \hat{f}_2$ can be seen as a smooth interpolation of the main term related to (2.86), (2.87) with $C = 1$. In view of the leading order structure (2.85), (2.86), we can obtain a better estimate of the above integral than the original integral without approximation.

Remark 2.11. We remark that the lower order term in (2.85), (2.86) is about $|x|/|y|$ of the main term, which is not small if $|y|$ and $|x|$ are comparable. As a result, the above finite rank approximation (2.88) can only approximate part of the integral in f . Nevertheless, it allows us to obtain a better estimate of $f - \hat{f}_1 - \hat{f}_2$ than f , which is sufficient for our purpose.

Combining (2.82), (2.88), we construct the following approximation for $f = \mathbf{u}, \nabla \mathbf{u}$ and for $\tilde{f} = f - C_{f0}u_x(0)$

$$(2.89) \quad \hat{f}(\omega) \triangleq \hat{f}_1(\omega) + \hat{f}_2(\omega), \quad \tilde{\hat{f}} \triangleq \hat{f}(\omega) - C_{f0}u_x(0) = \hat{f}_{10}(\omega) + \hat{f}_2(\omega),$$

where the notations \tilde{u}, \tilde{v} are introduced in (2.63). Clearly, $\hat{f}, \tilde{\hat{f}}$ is a finite rank operator of ω .

We list the parameters x_i, t_i, R_i in the above approximations in Appendix C.2. To obtain sharp estimate of the constants in (2.77) and $\mathbf{u} - \hat{\mathbf{u}}, \nabla \mathbf{u} - \widehat{\nabla \mathbf{u}}$ in the energy estimates, which are important for us to reduce the number of approximation terms and obtain sharp energy estimates, we will estimate the integrals with computer assistance. We will discuss them in details in Section 7.

We remark that we do not need to construct too many approximaton terms. The total number of approximation terms we choose is less than 50.

3. SHARP HÖLDER ESTIMATE VIA OPTIMAL TRANSPORT

In this section, we derive the sharp Hölder $C^{1/2}$ estimate for $\nabla \mathbf{u}$ using the symmetry properties of the kernels and some techniques from optimal transport. We note that novel functional inequalities on similar Biot-Savart laws have played a crucial role in the important works [27, 48]. Those estimates enable the authors to control the velocity effectively. The sharp Hölder estimates play a similar role in our work.

To obtain the Hölder estimate of $\nabla \mathbf{u}$ in \mathbb{R}_2^{++} , the natural approach is to estimate $\nabla \mathbf{u}(x) - \nabla \mathbf{u}(z)$ for all pairs $x, z \in \mathbb{R}_{++}^2$, which has a dimension of 4. It is very difficult to obtain a sharp estimate since the kernel in $\nabla \mathbf{u}(x) - \nabla \mathbf{u}(z)$ for arbitrary x, z has a complicated sign structure and destroys some symmetry properties of the kernels in $\nabla \nabla(-\Delta)^{-1}$. Instead, we will estimate the $C_x^{1/2}$ and $C_y^{1/2}$ seminorms (2.3) due to the following important observations. Firstly, the linearized operators (2.17), (2.21) are anisotropic in x and y . See Section 2.7.2. We have much larger damping factors along the y direction. Therefore, a sharp Hölder estimate of $\nabla \mathbf{u}$ in the x direction, i.e. $[\nabla \mathbf{u}]_{C_x^{1/2}}$ is much more important. Secondly, if we estimate the $C_x^{1/2}$ or $C_y^{1/2}$ seminorm (2.3), where we assume $x_1 = z_1$ or $x_2 = z_2$, we reduce the dimension of (x, z) from 4 to 3. Moreover, the kernel in $\nabla \mathbf{u}(x) - \nabla \mathbf{u}(z)$ enjoys better symmetry properties and the sign properties are much simpler. These properties allow us to reduce estimating the 2D integral into estimating many 1D integrals. After we estimate $[\nabla \mathbf{u}]_{C_x^{1/2}}, [\nabla \mathbf{u}]_{C_y^{1/2}}$, using the triangle inequality, we can obtain the estimate of $\|\nabla \mathbf{u}\|_{C^{1/2}}$.

The kernels associated with ∇u are given by

$$(3.1) \quad K_1(y) \triangleq \frac{y_1 y_2}{|y|^4}, \quad K_2(y) \triangleq \frac{1}{2} \frac{y_1^2 - y_2^2}{|y|^4}, \quad G(y) = -\frac{1}{2} \log |y|,$$

where $\frac{1}{\pi} G$ is the Green function of $-\Delta$ in \mathbb{R}^2 . Note that $\partial_1 \partial_2 G = K_1$, $\partial_1^2 G = K_2$.

Denote by $K_{i,s}$ the symmetrized kernel

$$(3.2) \quad K_{i,s}(x, y) \triangleq K_i(x - y) - K_i(x_1 + y_1, x_2 - y_2) - K_i(x_1 - y_1, x_2 + y_2) + K_i(x + y).$$

Consider the odd extension of ω in y from \mathbb{R}_2^+ to \mathbb{R}_2

$$(3.3) \quad W(y) = \omega(y) \text{ for } y_2 \geq 0, \quad W(y) = -\omega(y_1, -y_2) \text{ for } y_2 < 0.$$

W is odd in both y_1 and y_2 variables. Clearly, u_x can be written as

$$u_x(x) = -\frac{1}{\pi} \int_{\mathbb{R}^2} K_1(x - y) W(y) dy = -\frac{1}{\pi} \int_{\mathbb{R}_2^{++}} \omega(y) K_{1,s}(x, y) dy.$$

For any $a, b_1, b_2 > 0$, we consider the localized velocity

$$(3.4) \quad \begin{aligned} u_x(x, a, b_1, b_2) &\triangleq -\frac{1}{2\pi} P.V. \int_{|x_1 - y_1| \leq a, -b_1 \leq x_2 - y_2 \leq b_2} \frac{2(x_1 - y_1)(x_2 - y_2)}{|x - y|^2} \omega(y) dy, \\ u_y(x, a) &\triangleq \frac{1}{2\pi} P.V. \int_{|x_1 - y_1| \leq a, |x_2 - y_2| \leq a} \frac{(x_1 - y_1)^2 - (x_2 - y_2)^2}{|x - y|^4} \omega(y) dy + \frac{\omega(x)}{2}, \\ v_x(x, a) &\triangleq \frac{1}{2\pi} P.V. \int_{|x_1 - y_1| \leq a, |x_2 - y_2| \leq a} \frac{(x_1 - y_1)^2 - (x_2 - y_2)^2}{|x - y|^4} \omega(y) dy - \frac{\omega(x)}{2}. \end{aligned}$$

In particular, if $b_1 = b_2 = b$, we simplify $u_x(x, a, b_1, b_2)$ as $u_x(x, a, b)$; if $b_1 = b_2 = a$, we further simplify $u_x(x, a, b_1, b_2)$ as $u_x(x, a)$.

Denote by $d_x(f, x, z), d_y(f, x, z)$ the Hölder difference

$$(3.5) \quad d_x(f, x, z) \triangleq \frac{|f(x) - f(z)|}{|x_1 - z_1|^{1/2}}, \quad d_y(f, x, z) \triangleq \frac{|f(x) - f(z)|}{|x_2 - z_2|^{1/2}}.$$

3.1. The Hölder estimates of the velocity. We have the following important estimates for $\nabla \mathbf{u}$. We will discuss the ideas in Section 3.2 and the proof in Sections 3.3, 3.4, and Appendix B. We localize the velocity in (3.4) to obtain improvement of the constant $C_1(\frac{b}{|x-z|})$ when $|x - z|$ is large.

Lemma 3.1 (Estimate of $\|u_x\|_{C_x^{1/2}}$). *For any $b_1, b_2 > 0, a \geq \frac{1}{2}|x_1 - z_1|, x = (x_1, x_2), z = (z_1, x_2) \in \mathbb{R}_2^+$, we have*

$$\frac{|u_x(x, a, b_1, b_2) - u_x(z, a, b_1, b_2)|}{|x - z|^{1/2}} \leq C_1 \left(\frac{b}{|x - z|} \right) \|\omega\|_{C_x^{1/2}},$$

where $b = \max(b_1, b_2)$ and $C_1(a)$ is an increasing function given by

$$C_1(b) = \frac{4}{\pi} \left| \int_0^b ds_2 \int_{f(s_2)}^{\infty} |T(s_1, s_2) - s_1|^{1/2} \Delta(s_1, s_2) ds_1 \right|,$$

$$\Delta(s_1, s_2) = \frac{(s_1 + 1/2)s_2}{((s_1 + 1/2)^2 + s_2^2)^2} - \frac{(s_1 - 1/2)s_2}{((s_1 - 1/2)^2 + s_2^2)^2}.$$

Here, $f(s_2)$ is the unique solution in $[0, \infty)$ satisfying $\Delta(f(s_2), s_2) = 0$ and $T(s_1, s_2)$ is the unique solution in $[0, s_2)$ that solves

$$\int_{T(s_1, s_2)}^{s_1} \Delta(s_1, s_2) ds_1 = 0,$$

for $s_1 > f(s_2)$. In particular, $T(s_1, s_2)$ can be obtained explicitly by solving a cubic equation and $C_1(b) \leq 2.55$ for any $b > 0$.

Remark 3.2. The above Lemma can be further generalized to the localized velocity $\omega * K_1(s) \mathbf{1}_{-a_1 \leq s \leq a_2, -b_1 \leq s_2 \leq b_2}$, i.e., we do not need $a_1 = a_2$ in (3.4). The proof follows from the same argument. Yet, we will only use the special case $a_1 = a_2$ in our later estimates.

The upper bounds in the following Lemmas involve $[\omega]_{C_x^{1/2}}$ and $[\omega]_{C_y^{1/2}}$. We will further bound it using the energy norm. To obtain the sharp estimate, we will optimize the choice of τ .

Lemma 3.3 (Estimate of $\|u_x\|_{C_y^{1/2}}$). *For any $a, b \geq 1, x = (x_1, x_2), z = (x_1, z_2) \in \mathbb{R}_2^+$, we have*

$$\frac{|u_x(x, a, b) - u_x(z, a, b)|}{|x - z|^{1/2}} \leq \frac{1}{2} C_1 \left(\frac{a}{|x - z|} \right) \|\omega\|_{C_y^{1/2}} + C_2 \left(\frac{a}{|x - z|} \right) \|\omega\|_{C_x^{1/2}},$$

where $C_1(a)$ is defined in the previous Lemma and $C_2(a)$ is given by

$$C_2(a) = \frac{\sqrt{2}}{\pi} \int_0^a \int_0^{\infty} y_1^{1/2} \left| \frac{y_1(1/2 - y_2)}{(y_1^2 + (1/2 - y_2)^2)^2} + \frac{y_1(1/2 + y_2)}{(y_1^2 + (1/2 + y_2)^2)^2} \right| dy.$$

In particular, $C_2(a) \leq \frac{4.26}{\pi}$.

Next we estimate the other kernel. We remark that for $u_y(x, a)$ and $v_x(y, a)$, the estimates are different due to the local term related to ω (3.4).

Lemma 3.4 ($C_x^{1/2}$ estimate of u_y, v_x). *For any $a \geq 1, x = (x_1, x_2), z = (z_1, x_2) \in \mathbb{R}_2^+$ and $\tau > 0$, we have*

$$\frac{|v_x(x, a) - v_x(z, a)|}{|x - z|^{1/2}} \leq \frac{1}{\pi} C_1(\tau) \max(\|\omega\|_{C_x^{1/2}}, \tau^{-1} \|\omega\|_{C_y^{1/2}}^{1/2}),$$

$$\frac{|u_y(x, a) - u_y(z, a)|}{|x - z|^{1/2}} \leq \frac{1}{\pi} C_2(\tau) \max(\|\omega\|_{C_x^{1/2}}, \tau^{-1} \|\omega\|_{C_y^{1/2}}^{1/2}),$$

for some constant $C_1(\tau), C_2(\tau) > 0$, where $C_1(0.589) = 7.94$ and $C_2(0.589) = 5.32$. The above estimates can be improved for a smaller window size a and the corresponding constant can be computed.

In the proof of the above Lemma, we provide the upper bounds for $C_1(\tau), C_2(\tau)$, which can be computed. Although the estimates are equivalent for different τ , we choose τ according to the weight g_1 in Hölder seminorm $[\omega \psi_1]_{C_{g_1}^{1/2}}$. In practice, we choose $\tau = g_1(0, 1)/g_1(1, 0)$ which is close to 0.589.

In general, the localized $C_y^{1/2}$ estimate does not hold for u_y due to the presence of the boundary and the discontinuity of W cross $y = 0$. Thus, we consider the estimate without localizing the kernel.

Lemma 3.5 ($C_y^{1/2}$ estimate of u_y, v_x). For $x = (x_1, x_2), z = (x_1, z_2) \in \mathbb{R}_2^+$ and any $\tau > 0$, we have

$$\begin{aligned} \frac{|v_x(x, \infty) - v_x(z, \infty)|}{|x - z|^{1/2}} &\leq \frac{C_3(\tau)}{\pi} \max(\|\omega\|_{C_x^{1/2}}, \tau^{-1} \|\omega\|_{C_y^{1/2}}), \\ \frac{|u_y(x, \infty) - u_y(z, \infty)|}{|x - z|^{1/2}} &\leq \frac{C_4(\tau)}{\pi} \max(\|\omega\|_{C_x^{1/2}}, \tau^{-1} \|\omega\|_{C_y^{1/2}}), \end{aligned}$$

for some constant $C_3(\tau), C_4(\tau) > 0$. We have $C_3(0.589) = 8.14, C_4(0.589) = 8.14$.

3.2. Connection to optimal transport and ideas of the proof. A key observation is that the Hölder estimate is related to an optimal transport problem. We illustrate the ideas by proving a sharp Hölder estimate of the Hilbert transform. The Hilbert transform can be seen as an approximation of $u_x(\omega)$, which is exact if $\omega(x, y)$ is constant in y [15, 54].

We estimate $\frac{1}{|x-z|^{1/2}} |Hf(x) - Hf(z)|$ by $\|f\|_{\dot{C}^{1/2}}$. Due to translation and scaling symmetry, we can assume $x = 1, z = -1$ without loss of generality. Then we need to estimate

$$(3.6) \quad S = Hf(1) - Hf(-1) = \frac{1}{\pi} \int_{\mathbb{R}} \left(\frac{1}{1-y} + \frac{1}{1+y} \right) f(y) dy = \frac{2}{\pi} \int_{\mathbb{R}} \frac{1}{1-y^2} f(y) dy.$$

The kernel $k(y) = \frac{2}{1-y^2}$ is positive on $(-1, 1)$ and negative for $|y| > 1$, and satisfies $\int k(y) dy = 0$.

Denote $k^{\pm}(y) = \max(\pm k(y), 0)$. An estimate of S using $\sup \frac{|f(x) - f(z)|}{|x-z|^{1/2}}$ is equivalent to estimating the transportation cost of moving the positive region of $k(y)$ with measure $k^+(y) dy$ to its negative region with measure $k^-(y) dy$ with distant function $c(x, y) = |x - y|^{1/2}$.

For example, if $k(y) = \delta_1(y) + \delta_2(y) - \delta_3(y) - \delta_4(y)$, where $\delta_a(x)$ is the Dirac function centered at a , then we get

$$|\int k(y) f(y) dy| = |f(1) + f(2) - f(3) - f(4)| \leq |f(2) - f(3)| + |f(1) - f(4)| \leq (\sqrt{1} + \sqrt{3}) \|f\|_{C^{1/2}}.$$

The above estimate can be interpreted as moving the mass from 2 to 3 and 1 to 4 with cost function $|x - y|^{1/2} \|f\|_{C^{1/2}}$. Using the language of optimal transport, to obtain sharp estimate of S (3.6), we are seeking a measurable map T such that $T \# k_+ dy = k_- dy$, where $(T \# \mu)(A) = \mu(T(A))$ for a measurable set A , and the following cost

$$C(T) = \int_{k(y) \geq 0} |T(y) - y|^{1/2} k(y) dy \|f\|_{C^{1/2}}$$

is as small as possible. Based on the above discussion, we have the following transportation lemma, which will be used repeatedly in the Hölder estimate.

Lemma 3.6 (Transportation Lemma). Suppose that there exists $c \in (a, b)$ such that $f < 0$ on (a, c) , $f > 0$ on (c, b) , $f|x - c|^{1/2} \in L_{loc}^1$ with $\int_a^b f(x) dx = 0$. For $g \in C_x^{1/2}(a, b)$, we have

$$\left| \int_a^b f(x) g(x) dx \right| \leq \int_c^b |f(x)| |x - T(x)|^{1/2} dx [g]_{C_x^{1/2}} = \int_a^c |f(x)| |x - T(x)|^{1/2} dx [g]_{C_x^{1/2}},$$

where $T(x)$ solves $\int_x^{T(x)} f(s) ds = 0$.

The estimate of $\int f g$ in terms of $[g]_{C_x^{1/2}}$ can be interpreted as transporting the negative part of f to its positive part with distant function $c(x, y) = |x - y|^{1/2}$.

Proof. Firstly, we want to understand how to construct the map T . Note that for $x_1 < x_2 < x_3 < x_4$, we have

$$\begin{aligned} &|\int (\delta_{x_1} + \delta_{x_2} - \delta_{x_3} - \delta_{x_4}) g(x) dx| = |g(x_1) + g(x_2) - g(x_3) - g(x_4)| \\ &\leq \min(|x_1 - x_3|^{1/2} + |x_2 - x_4|^{1/2}, |x_1 - x_4|^{1/2} + |x_2 - x_3|^{1/2}) [g]_{C_x^{1/2}} \\ &= (|x_1 - x_4|^{1/2} + |x_2 - x_3|^{1/2}) [g]_{C_x^{1/2}}. \end{aligned}$$

The above estimate indicates that to find an optimal map T moving $(\delta_{x_1} + \delta_{x_2}) dx$ to $(\delta_{x_3} + \delta_{x_4}) dx$ with cost $|x - y|^{1/2}$, we should choose $T(x_1) = x_4, T(x_2) = x_3$, which implies that $T(x)$ is

decreasing in x . Due to conservation of mass and the sign properties of f , a natural construction of $T : (a, c) \rightarrow (c, b)$ is given by

$$(3.7) \quad \int_x^{T(x)} f(x)dx = 0,$$

for $x < c$, which implies $T'(x)f(T(x)) = f(x)$ for smooth f . The idea of the above map is to move the mass in the positive region to its closest negative region that has not been occupied due to the monotonicity of T . Using a change of variable $y = T(x) : (a, c) \rightarrow (c, b]$, we get

$$\int_c^b f(x)g(x)dx = - \int_a^c f(T(x))g(T(x))T'(x)dx = - \int_a^c f(x)g(T(x))dx.$$

It follows

$$\left| \int_a^b f g \right| = \left| \int_a^c f(x)(g(T(x)) - g(x))dx \right| \leq \int_a^c |f(x)| |T(x) - x|^{1/2} dx [g]_{C_x^{1/2}}.$$

Similarly, we can define $T : (c, b) \rightarrow (a, c)$ by solving $\int_{T(x)}^x f(s)ds = 0$, which is also equivalent to (3.7). The first inequality in Lemma 3.6 follows from the same argument. \square

3.2.1. $C^{1/2}$ estimate of the Hilbert transform. Now, we apply Lemma 3.6 with $f = k(y), g = f(y)$ to estimate (3.6). For any $y > 0$, we construct the transportation map $T(y)$ by solving

$$0 = \int_x^{T(x)} k(y)dy = \int_x^{T(x)} \frac{1}{1-y^2} dy = 0,$$

which implies

$$\frac{x+1}{1-x} = \frac{T+1}{T-1}, \quad T(x) = \frac{1}{x},$$

where we have used $T(x) > 1$ if $x < 1$ and $T(x) < 1$ if $x > 1$ due to the sign of $\frac{1}{1-y^2}$. This map also applies to $y < 0$. Using this map, we yield

$$\begin{aligned} |S| &= \left| \frac{2}{\pi} \int_{y>1} k(y)(f(y) - f(T(y)))dy + \frac{2}{\pi} \int_{y<-1} k(y)(f(y) - f(T(y)))dy \right| \\ &\leq \frac{4}{\pi} \int_{y>1} |k(y)| |y - T(y)|^{1/2} dy \|f\|_{C^{1/2}} = \frac{4}{\pi} \int_{y>1} \frac{1}{|y^2 - 1|} \frac{|y^2 - 1|^{1/2}}{|y|^{1/2}} dy \|f\|_{C^{1/2}} \\ &= \|f\|_{C^{1/2}} \frac{4}{\pi} \int_{y>1} \frac{1}{|y^2 - 1|^{1/2} y^{1/2}} dy = C \|f\|_{C^{1/2}}. \end{aligned}$$

The above formula is an example of the derivation in Lemma 3.6. The constant C can be estimated. It follows

$$(3.8) \quad \frac{S}{|x - z|^{1/2}} \leq \frac{C}{\sqrt{2}} \|f\|_{C^{1/2}}, \quad \frac{C}{\sqrt{2}} \approx \frac{7.4}{\pi} \approx 2.37.$$

Since x, z are arbitrary, we yield $\|Hf\|_{C^{1/2}} \leq \frac{C}{\sqrt{2}}$.

Remark 3.7. Note that the Hilbert transform satisfies $H(Hf) = -f$. It implies that the sharp constant in $\|Hf\|_{C^{1/2}} \leq C \|f\|_{C^{1/2}}$ satisfies $C \geq 1$. Thus, the above estimate does not overestimate too much.

In the following subsections, we prove Lemmas 3.1, 3.3 for u_x , which is the most singular nonlocal term in (2.23). The proofs of Lemmas 3.4, 3.5 are similar but technical, which are deferred to Appendix B.

To apply Lemma 3.6 to the Hölder estimate of $\nabla \mathbf{u}$, which involves 2D integrals, we need two steps. Firstly, we identify the sign of the kernel K in the integral of $\nabla \mathbf{u}(x) - \nabla \mathbf{u}(z)$. Next, we fix a variable in the 2D integral in one direction, e.g. fix $x = a$, and then apply Lemma 3.6 to estimate the 1D integral in the other direction, e.g., on the line $\{(a, y) : y \in \mathbb{R}\}$. One may generalize Lemma 3.6 to 2D and construct the 2D optimal transport map directly. Yet, the domain where the kernel K is positive or negative is complicated. To avoid this difficulty, we build the 2D transport map using the 1D Lemma 3.6 repeatedly. The odd symmetry of the

kernel $K_1(s)$ in s_1 enables us to apply this approach to obtain sharp estimate of u_x effectively. See Remark 3.8.

3.3. Estimate of $[u_x]_{C_x^{1/2}}$. In the $C_x^{1/2}$ estimate of u_x , we have $x_2 = z_2$. In the case without localization of the kernel, using the scaling symmetry and translation invariance, we only need to estimate the following

$$(3.9) \quad u_x\left(\frac{1}{2}, x_2\right) - u_x\left(-\frac{1}{2}, x_2\right) = -\frac{1}{\pi} P.V. \int_{\mathbb{R}^2} K(s) W(s_1, x_2 - s_2) ds$$

for any x_2 , where W is an odd extension of ω from \mathbb{R}_+^2 to \mathbb{R}^2 , and $K(s)$ is given by

$$(3.10) \quad K(s) = K_1\left(s_1 + \frac{1}{2}, s_2\right) - K_1\left(s_1 - \frac{1}{2}, s_2\right) = \frac{(s_1 + \frac{1}{2})s_2}{((s_1 + \frac{1}{2})^2 + s_2^2)^2} - \frac{(s_1 - \frac{1}{2})s_2}{((s_1 - \frac{1}{2})^2 + s_2^2)^2}.$$

Since $K(s)$ is odd in s_2 , we consider $s_2 \geq 0$ without loss of generality. We will only use the Hölder seminorm of W , $[W]_{C_x^{1/2}}$, to estimate the above quantity. Note that $[W]_{C_x^{1/2}(\mathbb{R}^2)} = [\omega]_{C_x^{1/2}(\mathbb{R}_+^2)}$. Without loss of generality, we can assume that $x_2 = 0$.

A direct calculation yields

$$K(s) = \frac{\Delta_1(s_1, s_2)}{((s_1 + \frac{1}{2})^2 + s_2^2)^2((s_1 - \frac{1}{2})^2 + s_2^2)^2}, \quad \Delta_1 = s_2^4 - 2s_1^2s_2^2 - 3s_1^4 + \frac{1}{2}s_1^2 + \frac{1}{2}s_2^2 + \frac{1}{16}.$$

For fixed s_2 , $\Delta_1(s_1, s_2) = 0$ implies

$$(3.11) \quad s_1 = f(s_2) = \left(\frac{\frac{1}{2} - 2s_2^2 + \sqrt{16s_2^4 + 4s_2^2 + 1}}{6} \right)^{1/2}.$$

Moreover, for $s_1, s_2 \geq 0$, it is easy to see that $\Delta_1(s_1, s_2) \geq 0$ if and only if

$$(3.12) \quad K(s_1, s_2) \geq 0 \text{ for } s_1 \in [0, f(s_2)], \quad K(s_1, s_2) \leq 0 \text{ for } s_1 \geq f(s_2).$$

Note that the sign changes if $s_2 \leq 0$ since K is odd in s_2 . Since K_1 is odd in s_1 , we get

$$\begin{aligned} \int_0^\infty K(s_1, s_2) ds_1 &= \int_0^\infty K_1\left(s_1 + \frac{1}{2}, s_2\right) - K_1\left(s_1 - \frac{1}{2}, s_2\right) ds_1 \\ &= \int_{1/2}^\infty K_1(s_1, s_2) ds_1 - \int_{-1/2}^\infty K_1(s_1, s_2) ds_1 = - \int_{-1/2}^{1/2} K_1(s_1, s_2) ds_1 = 0. \end{aligned}$$

To estimate the integral in (3.9), we first fix s_2 and then apply Lemma 3.6 to estimate (3.13)

$$I(s_2) = \int_{\mathbb{R}} K(s_1, s_2) W(s_1, x_2 - s_2) ds_1 = \left(\int_{\mathbb{R}_-} + \int_{\mathbb{R}_+} \right) K(s_1, s_2) W(s_1, x_2 - s_2) ds_1 \triangleq I_-(s_2) + I_+(s_2).$$

We do so for the following reason. Near the singularity, from Taylor expansion of (3.11): $s_1 = \frac{1}{2} + O(s_2^4)$, the curve Γ separating the positive and negative region of $K(s)$ is close to a straight line in the vertical direction. Similar to the idea below (3.7), an effective plan in 2D should move the mass in the positive region to its closest possible negative region that has not been occupied. Based on this idea, we expect that an effective 2D transport plan $(x, y) \rightarrow T(x, y)$ is orthogonal to the curve Γ and thus almost parallel to the x direction.

Remark 3.8. The fact that near the singularity $s = (\pm \frac{1}{2}, 0)$, the curve Γ is almost vertical is due to the odd symmetry of $K_1(s_1, s_2)$ in s_1 . In fact, from (3.10), for s close to $(\frac{1}{2}, 0)$, we have $K(s) \approx -K_1(s_1 - \frac{1}{2}, s_2)$, whose sign is determined by $\text{sgn}(s_1 - \frac{1}{2})$.

Since $K(s_1, s_2)$ is even in s_2 , we can estimate $I_+(s_2), I_-(s_2)$ in the same way. To apply Lemma 3.6, we first construct $T(\cdot, s_2)$ on $[0, \infty)$ by solving

$$(3.14) \quad \int_{T(s_1, s_2)}^{s_1} K(t, s_2) dt = 0.$$

We will show later that this equation has a unique solution of T on $[0, \infty]$ for $s_1 > 0$. Then applying Lemma 3.6 to $I_+(s_2)$ and using $[W]_{C_x^{1/2}} = [\omega]_{C_x^{1/2}}$, we get

$$|I_+(s_2)| \leq [\omega]_{C_x^{1/2}} \left| \int_{f(s_2)}^{\infty} K(s_1, s_2) |T(s_1, s_2) - s_1|^{1/2} ds_1 \right| \triangleq M(s_2).$$

Since $K(s_1, s_2)$ is even in s_2 , the estimate of $I_-(s_2)$ in (3.13) is the same: $I_-(s_2) \leq M(s_2)$. Since $K(s)$ is odd in s_1 , from (3.14), we get $T(s_1, -s_2) = T(s_1, s_2)$. Therefore, the estimate of $I(s_1, s_2)$ is the same as $I(s_1, -s_2)$: $|I(s_1, s_2)| \leq 2M(|s_2|)$. Integrating the estimate of $I(s)$ over s_2 , we yield

$$\left| -\frac{1}{\pi} P.V. \int_{\mathbb{R}^2} K(s) W(s_1, x_2 - s_2) ds \right| \leq \frac{4}{\pi} [\omega]_{C_x^{1/2}} \left| \int_0^{\infty} ds_2 \int_{f(s_2)}^{\infty} K(s_1, s_2) |T(s_1, s_2) - s_1|^{1/2} ds_1 \right|,$$

which along with (3.9) prove Lemma 3.1 in the case of $a = b_1 = b_2 = \infty$.

3.3.1. *Formula of T .* From (3.10) and $\frac{xy}{(x^2+y^2)^2} = -\frac{1}{2} \partial_x \frac{y}{x^2+y^2}$, equation (3.14) is equivalent to

$$s_2 \left(\frac{1}{(T + \frac{1}{2})^2 + s_2^2} - \frac{1}{(T - \frac{1}{2})^2 + s_2^2} \right) = s_2 \left(\frac{1}{(s_1 + \frac{1}{2})^2 + s_2^2} - \frac{1}{(s_1 - \frac{1}{2})^2 + s_2^2} \right)$$

where we have simplified $T(s_1, s_2)$ as T . For $s_2 \neq 0$, expanding the identity yields

$$(3.15) \quad 0 = -1 - 8Ts_1 + 16Ts_1(T^2 + Ts_1 + s_1^2) - 8s_2^2(1 - 4s_1T + 2s_2^2).$$

The above equation is cubic in T , and thus can be solved explicitly. In Appendix B.3, for fixed s_2 and $s_1 > 0$, we show that it has a unique solution on $[[0, \infty)$ using the discriminant of the cubic solution. We also study the properties of $T(s_1, s_2)$, which allows us to estimate a sharp bound for $C_1(b)$ in Lemma 3.1.

Remark 3.9. In the special case where $\omega(x, y)$ is constant in y , we have $u_x(\omega)(x, 0) = H\omega(x)$, which has been observed in [15, 54]. Thus, the optimal constant in Lemma 3.1 must be larger than that of the Hilbert transform (3.8). Here, the upper $C_1(b) \leq 2.55$ is very close to that the Hilbert transform $C/\sqrt{2} \approx 2.37$ (3.8), which reflects the effectiveness of the optimal transport approach to estimate the sharp constant.

3.3.2. *Localized estimate of u_x .* Next, we estimate $u_x(x, a, b_1, b_2) - u_x(z, a, b_1, b_2)$ with $x_2 = z_2$ using $[W]_{C_x^{1/2}}$. The estimate consists of following steps. Firstly, we identify the sign of the kernel similar to those between (3.9) and (3.11). Secondly, we construct the transportation map along the x direction and derive the transportation cost. Thirdly, we compare the transportation cost in the case of kernel localization with that without kernel localization using the properties of the transportation maps, and show that the cost with kernel localization is smaller than that without using kernel localization.

Without loss of generality, we assume $x_1 = \frac{1}{2}, z_1 = -\frac{1}{2}, x_2 = 0$. Denote

$$I_a \triangleq [-a, a], \quad I_b = [-b_1, b_2], \quad Q \triangleq I_a \times I_b, \quad b = \max(b_1, b_2),$$

Since we assume $a \geq \frac{1}{2}|x_1 - z_1|$ in Lemma 3.1, we have

$$(3.16) \quad a \geq 1/2.$$

The kernel associated with $u_x(\frac{1}{2}, x_2) - u_x(-\frac{1}{2}, x_2)$ (3.4) becomes

$$(3.17) \quad \begin{aligned} K_{a,b}(s_1, s_2) &= \mathbf{1}_{s_2 \in I_b} \left(\frac{(s_1 + \frac{1}{2})s_2}{((s_1 + \frac{1}{2})^2 + s_2^2)^2} \mathbf{1}_{s_1 + \frac{1}{2} \in I_a} - \frac{(s_1 - \frac{1}{2})s_2}{((s_1 - \frac{1}{2})^2 + s_2^2)^2} \mathbf{1}_{s_1 - \frac{1}{2} \in I_a} \right) \\ &= ((K_1(s_1 + 1/2, s_2) - K_1(s_1 - 1/2, s_2)) \mathbf{1}_{s_1 + 1/2 \in Q} \\ &\quad - K_1(s_1 - 1/2, s_2) (\mathbf{1}_{s_1 - 1/2 \in Q} - \mathbf{1}_{s_1 + 1/2 \in Q})). \end{aligned}$$

Since $a \geq \frac{1}{2}$ and $K_1(s)$ is odd in s_1 , for fixed s_2 , we have

$$\int_0^{\infty} K_{a,b}(s_1, s_2) ds_1 = \left(\int_{1/2}^a - \int_{-1/2}^a \right) K_1(s) ds_1 = - \int_{-1/2}^{1/2} K_1(s) ds_1 = 0, \quad \int_{-\infty}^0 K_{a,b}(s_1, s_2) ds_1 = 0.$$

Similar to the case without localization, for each s_2 , we consider the transportation from the positive part of $K_{a,b}$ to its negative part. Firstly, we identify the sign of $K_{a,b}$. We restrict to $s_2 \in [-b_1, b_2]$ and $s_2 \neq 0$ since otherwise $K_{a,b} = 0$. We focus on $s_1, s_2 \geq 0$ and the estimate for $s_1 < 0$ or $s_2 < 0$ is the same. Since $a > -\frac{1}{2}$, we always have

$$(3.18) \quad s_1 \pm 1/2 > -a, \quad \text{for } s_1 \geq 0.$$

Thus, for $s_1 \geq 0$, we can neglect the constraint $s_1 \pm \frac{1}{2} \geq -a$ in the localization in (3.17).

Case 1: $a \in (1/2, 1]$. Clearly, $K_{a,b}(s_1, s_2) > 0$ for $s_1 < \frac{1}{2}$ since both kernels in (3.17) are non-negative. For $s_1 \geq \frac{1}{2}$, since $a \leq 1$, we get

$$K_{a,b}(s_1, s_2) = -K_1(s_1 - \frac{1}{2}, s_2) \mathbf{1}_{s-1/2 \in Q} \leq 0.$$

In this case, we denote $s_c(s_2) = \frac{1}{2}$.

Case 2: $a \in (1, f(s_2) + \frac{1}{2})$. Recall $f(s_2)$ from (3.11). For $s_1 > a - \frac{1}{2} > \frac{1}{2}$, we get

$$K_{a,b} = -K_1(s_1 - \frac{1}{2}, s_2) \mathbf{1}_{s-1/2 \in Q} \leq 0.$$

For $s_1 \leq a - \frac{1}{2} < f(s_2)$, using (3.12) and $s_1 + \frac{1}{2} \leq a$, we obtain

$$K_{a,b} = K_1(s_1 + \frac{1}{2}, s_2) - K_1(s_1 - \frac{1}{2}, s_2) \geq 0.$$

We denote $s_c(s_2) = a - \frac{1}{2}$.

Case 3: $a \geq f(s_2) + \frac{1}{2}$. For $s_1 < f(s_2)$, using (3.12) and $s_1 \pm \frac{1}{2} < a$, we get

$$K_{a,b} = K_1(s_1 + \frac{1}{2}, s_2) - K_1(s_1 - \frac{1}{2}, s_2) \geq 0.$$

For $s_1 \geq f(s_2) > \frac{1}{2}$, since $K_1(s_1 + \frac{1}{2}, s_2) - K_1(s_1 - \frac{1}{2}, s_2) \leq 0$ (3.12) and

$$\mathbf{1}_{s-1/2 \in Q} - \mathbf{1}_{s+1/2 \in Q} = \mathbf{1}_{s_1-1/2 \leq a} - \mathbf{1}_{s+1/2 \leq a} \geq 0,$$

we get

$$K_{a,b} \leq -K_1(s_1 - 1/2, s_2) (\mathbf{1}_{s-1/2 \in Q} - \mathbf{1}_{s+1/2 \in Q}) \leq 0.$$

We denote $s_c(s_2) = f(s_2)$. In summary, for fixed s_2 , we define

$$(3.19) \quad \begin{aligned} s_c(s_2) &= \frac{1}{2}, \quad \text{if } a \in (\frac{1}{2}, 1], \quad s_c(s_2) = a - \frac{1}{2}, \quad \text{if } a \in (1, f(s_2) + \frac{1}{2}), \\ s_c(s_2) &= f(s_2), \quad \text{if } a \geq f(s_2) + 1/2, \end{aligned}$$

which satisfies

$$(3.20) \quad K_{a,b}(s_1, s_2) \geq 0, \quad s_1 \in [0, s_c], \quad K_{a,b}(s_1, s_2) \leq 0, \quad s_1 \in [s_c, \infty], \quad s_c(s_2) \leq f(s_2),$$

where the last inequality follows from the definition of s_c and $f(s_2) \geq \frac{1}{2}$ (3.11).

In each case $i = 1, 2, 3$, we construct the transport map by solving

$$(3.21) \quad \int_{T_i(s_1, s_2)}^{s_1} K_{a,b}(x, s_2) dx = 0, \quad T_i \leq a + \frac{1}{2}.$$

We add the restriction $T_i \leq a + \frac{1}{2}$ since $K_{a,b}(s) = 0$ for $s_1 > a + \frac{1}{2}$ by definition (3.17). Applying Lemma 3.6 in the s_1 direction and using $K_{a,b}(s) = 0$ for $|s_2| \geq b$, we yield

$$I_i \triangleq \left| \int_{s_1 \geq 0, s_2 \geq 0} K_{a,b}(s_1, s_2) \omega(s_1, -s_2) ds \right| \leq \int_0^b \int_0^{s_c(s_2)} |K_{a,b}(s)| |T_i(s) - s_1|^{1/2} ds \cdot [\omega]_{C_x^{1/2}}.$$

3.3.3. *Comparison of the cost.* Next, we show that the cost can be bounded uniformly by the cost of the case without localization

$$(3.22) \quad I_i \leq \int_0^b \int_{f(s_2)}^{\infty} |K(s)| |T(s) - s_1|^{1/2} ds \cdot [\omega]_{C_x^{1/2}} \triangleq I.$$

where T is defined in (3.14). It suffices to prove

$$(3.23) \quad J_i \triangleq \int_0^{s_c(s_2)} |K_{a,b}(s)| |T_i(s) - s_1|^{1/2} ds \leq \int_0^{f(s_2)} |K(s)| |T(s) - s_1|^{1/2} ds$$

for any s_2 . We focus on $|s_2| \leq a$ and $s_2 \neq 0$. The intuition behind the above inequality is that if the mass is localized, we should get “cheaper” transportation cost than the case without localization since the transportation distance is shorter. To justify these heuristics, we compare the kernels and will prove

$$(3.24) \quad |K_{a,b}(s)| \leq |K(s)|, \quad s_1 \in [0, s_c(s_2)],$$

and use (3.14) and (3.21) to compare T_i and T

$$(3.25) \quad s_1 \leq s_c(s_2) \leq T_i(s) \leq T(s), \quad s_1 \in [0, s_c(s_2)]$$

and thus $T_i(s) - s_1 \leq T(s) - s_1$. Clearly, inequality (3.23) follows from (3.24) and (3.25).

Compare the kernels. From (3.20) and (3.12), since $s_c(s_2) \leq f(s_2)$, we get $K_{a,b}(s), K(s) \geq 0$ for $s_1 \in [0, s_c(s_2)]$. Hence, for fixed $s_2 \in [-b_1, b_2]$, (3.24) is equivalent to

$$0 \leq K(s) - K_{a,b}(s) = K_1(s_1 + \frac{1}{2}, s_2)(1 - \mathbf{1}_{s_1+1/2 \in I_a}) - K_1(s_1 - \frac{1}{2}, s_2)(1 - \mathbf{1}_{s_1-1/2 \in I_a}) \triangleq I.$$

From the definition of (3.19) and (3.18), for $s_1 \in [0, s_c(s_2)]$, we have

$$s_1 \pm 1/2 \geq -a, \quad s_1 - 1/2 \leq a, \quad 1 - \mathbf{1}_{s_1-1/2 \in I_a} = 0,$$

which along with $K_1(s_1 + \frac{1}{2}, s_2) \geq 0$ (3.17) implies (3.24)

$$I = K_1(s_1 + \frac{1}{2}, s_2)(1 - \mathbf{1}_{s_1+1/2 \in I_a}) \geq 0.$$

Remark 3.10. In the above derivations, we consider $s_2 \geq 0$. If $s_2 \leq 0$, one needs to track the sign to prove inequality (3.24).

Compare the maps. To prove (3.25), our idea is to use the equations (3.14), (3.21) and the sign of the kernels $K_{a,b}, K$ to compare T_i and T .

We fix $s_2 > 0$ in the following derivations. To simplify the notation, we simplify $T(s_1, s_2)$ as $T(s_1)$ in some places. Since T_i, T (3.14), (3.21) are decreasing and $s_c(s_2)$ is a fixed point for $T_i(\cdot, s_2)$, for $s_1 \leq s_c(s_2)$, we get

$$(3.26) \quad T_i(s_1, s_2) \geq T_i(s_c(s_2), s_2) = s_c(s_2), \quad T(s_1, s_2) \geq T(f(s_2), s_2) = f(s_2) \geq s_c(s_2).$$

Moreover, from (3.14), (3.21), we have

$$(3.27) \quad T_i(T_i(s_1)) = s_1, \quad T(T(s_1)) = s_1.$$

Denote

$$(3.28) \quad K^\pm = K(s_1 \pm \frac{1}{2}, s_2), \quad K_{a,b}^+ = K_1(s_1 + \frac{1}{2}, s_2) \mathbf{1}_{s_1+\frac{1}{2} \leq a}, \quad K_{a,b}^- = K_1(s_1 - \frac{1}{2}, s_2) \mathbf{1}_{s_1-\frac{1}{2} \leq a}.$$

We remark that K^- is not non-negative but K^+ is positive. By definition, we have

$$(3.29) \quad \begin{aligned} K_{a,b} &= K_{a,b}^+ - K_{a,b}^-, & K &= K^+ - K^-. \\ K^+(s) &\geq 0, \quad s_1, s_2 \geq 0, & K^-(s) &\geq 0, \quad s_1 \geq 1/2, s_2 \geq 0. \end{aligned}$$

Next, we study each case in the order of 3, 2, 1 to prove (3.25).

Case 3: $a \geq f(s_2) + \frac{1}{2}$. In this case, recall $s_c(s_2) = f(s_2)$ from (3.19).

For $s_1 \leq a - \frac{1}{2}$, we get $K_{a,b} = K$ (3.17). Hence, equations (3.14) and (3.21) are the same for $s_1 \leq a - 1/2$, and we get

$$(3.30) \quad T_3(s_1, s_2) = T(s_1, s_2), \quad s_1 \in [T(a - \frac{1}{2}), a - \frac{1}{2}].$$

It follows (3.25) for $s_1 \in [T(a - 1/2), f(s_2)]$. We recall that from (3.26), $a - 1/2 \geq f(s_2)$ and $T(a - 1/2) = T_3(a - 1/2)$, we have

$$(3.31) \quad T(a - 1/2) \leq T(f(s_2)) = f(s_2) \leq a - 1/2, \quad T(s_1), T_3(s_1) \geq a - 1/2, \quad s_1 \leq T(a - 1/2).$$

Next, we compare $T(s_1), T_3(s_1)$ for $s_1 < T(a - 1/2) \leq f(s_2)$. From (3.14), (3.21), and $T(a - 1/2) = T_3(a - 1/2) \leq a - 1/2$, we have

$$\int_{T(a-1/2)}^{a-1/2} K(s) ds_1 = \int_{T_3(a-1/2)}^{a-1/2} K_{a,b}(s) ds_1 = \int_{T(a-1/2)}^{a-1/2} K_{a,b}(s) ds_1 = 0.$$

Moreover, from (3.17) and (3.21), we have

$$\begin{aligned} K_{a,b}(t, s_2) &= -K_{a,b}^-(t, s_2) = -K^-(t, s_2), \quad t \in [a - 1/2, T_3(s_1)] \subset [1 - 1/2, a + 1/2], \\ K_{a,b}(t, s_2) &= K(t, s_2), \quad s_1 \leq T(a - 1/2) \leq a - 1/2. \end{aligned}$$

Plugging the above identities in (3.14), (3.21) for $s_1 \leq T(a - 1/2)$, we yield

$$\begin{aligned} 0 &= \int_{s_1}^{T(s_1)} K(t, s_2) dt = \int_{s_1}^{T(a-1/2)} K(t, s_2) + \int_{a-1/2}^T K(t, s_2) dt, \\ 0 &= \int_{s_1}^{T_3(s_1)} K_{a,b}(t, s_2) dt = \int_{s_1}^{T(a-1/2)} K(t, s_2) - \int_{a-1/2}^{T_3(s_1)} K^-(t, s_2) dt. \end{aligned}$$

Note that $K = K^+ - K^-$. Calculating the difference between the two identities yields

$$0 = \int_{a-1/2}^{T(s_1)} (K^+ - K^-) ds + \int_{a-1/2}^{T_3(s_1)} K^- = \int_{a-1/2}^{T(s_1)} K^+ ds_1 + \int_{T(s_1)}^{T_3(s_1)} K^- ds_1.$$

Recall $s_2 \neq 0$ and from (3.31), we obtain $T_3(s_1), T(s_1) \geq a - 1/2 \geq 1/2$. From (3.29), we yield $K^+ > 0$ and $K^- > 0$ for $s_1 \geq \min(a - 1/2, T_3, T)$. Since T is decreasing and

$$T(s_1) \geq T(T(a - 1/2)) = a - 1/2, \quad s_1 \leq T(a - 1/2),$$

the first integral is non-negative. We prove $T(s_1) \geq T_3(s_1)$ for $s_1 \leq T(a - 1/2)$, which along with (3.30) implies (3.25).

The proof in the case 1,2 is completely similar.

Case 2: $a \in (1, f(s_2) + \frac{1}{2})$. Recall $s_c(s_2) = a - \frac{1}{2} \leq f(s_2)$ from (3.19) and (3.26). For any $s_1 \leq a - \frac{1}{2} \leq f(s_2)$, using (3.14), (3.21), and an argument similar to that in case 3, we yield

$$\begin{aligned} 0 &= \int_{s_1}^{T_2(s_1)} K_{a,b}(t, s_2) dt = \int_{s_1}^{a-1/2} K(t, s_2) dt - \int_{a-1/2}^{T_2(s_1)} K^-(t, s_2) dt, \\ 0 &= \int_{s_1}^{T(s_1)} K(t, s_2) dt = \int_{s_1}^{a-1/2} K(t, s_2) dt + \int_{a-1/2}^{T(s_1)} (K^+ - K^-)(t, s_2) dt, \end{aligned}$$

where we have used $K_{a,b}(t, s_2) = -K^-(t, s_2)$ for $t \geq a - 1/2$ (3.17), (3.28) in the second equality.

Comparing the difference between two identities yields

$$0 = \int_{a-1/2}^{T(s_1)} K^+ - K^-(t, s_2) dt + \int_{a-1/2}^{T_2(s_1)} K^-(t, s_2) dt = \int_{a-1/2}^{T(s_1)} K^+(t, s_2) dt + \int_{T(s_1)}^{T_2(s_1)} K^-(t, s_2) dt.$$

Recall from (3.26) that $T(s_1), T_2(s_1) \geq s_c(s_2) = a - 1/2$ for $s_1 \leq a - 1/2$. For $s_2 \neq 0$ and $s_1 \geq \min(T, T_2, a - 1/2) = a - 1/2 > 1/2$, we have $K^- > 0, K^+ > 0$ (3.29). We obtain $T(s_1) \geq T_2(s_1)$, which implies (3.25).

Case 1: $a \in (1/2, 1]$. In this case, $s_c(s_2) = \frac{1}{2} < f(s_2)$. From (3.17), we yield

$$\begin{aligned} 0 &\leq K_{a,b} = \mathbf{1}_{s_1+1/2 \leq a} K_1(s_1 + 1/2, s_2) - K_1(s_1 - 1/2, s_2) \\ &\leq K_1(s_1 + 1/2, s_2) - K_1(s_1 - 1/2, s_2) = K, \quad s_1 \in [0, 1/2], \end{aligned}$$

$$K_{a,b} = -K_1(s_1 - 1/2, s_2) = -K^-(s_1, s_2), \quad K^-(s_1, s_2) \geq 0, \quad s_1 \in [1/2, a + 1/2].$$

For any $s_1 < \frac{1}{2}$ and $s_2 \neq 0$, from (3.26), we get $T_1(s_1) \geq 1/2, T(s_1) \geq f(s_2) > 1/2$. Using (3.14), (3.21) and the above estimates for $K_{a,b}$, we yield

$$0 = \int_{s_1}^{1/2} K_{a,b}(t, s_2) dt - \int_{1/2}^{T_1(s_1)} K^-(t, s_2) dt = \int_{s_1}^{1/2} K(t, s_2) dt + \int_{1/2}^T (K^+ - K^-)(t, s_2) dt.$$

It follows

$$0 = \int_0^{1/2} (K - K_{a,b})(t, s_2) dt + \int_{1/2}^T K^+ + \int_T^{T_1} K^-(t, s_2) dt \triangleq II_1 + II_2 + II_3.$$

From (3.24) and $K_{a,b}, K > 0$ on $t \in [0, s_c(s_2)] = [0, 1/2]$, we get $II_1 \geq 0$. Note that $K^-, K^+ > 0$ for $s_1 > 1/2$ (3.12), (3.20). Since $T_1, T > 1/2$, we must obtain $T(s_1) \geq T_1(s_1)$, which implies (3.25).

We have proved (3.25) in all three cases, which implies $|T(s) - s_1| \geq |T_i(s) - s_1|$. Combining this estimate and (3.24), we prove (3.22) and conclude the proof of Lemma 3.1.

3.4. Estimate of $[u_x]_{C_y^{1/2}}$.

Firstly, we note that $b_1 = b_2 = b$ and $x_1 = z_1$ in this case.

Without loss of generality, we assume $z_2 = m + 1/2, x_2 = m - 1/2$ and $x_1 = y_1 = 0$ for some $m \geq 1/2$. We have

$$u_x(z) - u_x(x) = \frac{1}{\pi} \int_{\mathbb{R}^2} W(y) \left(K_{a,b}(y_1, y_2 - (m - 1/2)) - K_{a,b}(y_1, y_2 - (m + 1/2)) \right) dy,$$

where W is the odd extension of ω in \mathbb{R}^2 (3.3). Note that W is not Hölder in the y -direction near $y_2 = 0$, we cannot use the same method as that in the estimate of $[u_x]_{C_x^{1/2}}$. On the other hand, since $W \in C_y^{1/2}(\mathbb{R} \times [m, \infty))$, we can apply the previous method to obtain

$$\left| \frac{1}{\pi} \int_{y_2 \geq m} W(y) (K_{a,b}(y_1, y_2 - (m - 1/2)) - K_{a,b}(y_1, y_2 - (m + 1/2))) dy \right| \leq \frac{1}{2} C_1(a) \|\omega\|_{C_y^{1/2}}.$$

Rotating the coordinate by 90 degree, we obtain the case studied in Section 3.3.

It remains to estimate

$$\begin{aligned} I(b) &= \frac{1}{\pi} \int_{y_2 \leq m} W(y) (K_{a,b}(y_1, y_2 - (m - 1/2)) - K_{a,b}(y_1, y_2 - (m + 1/2))) dy \\ &= \frac{1}{\pi} \int_{y_2 \leq 0} W(y_1, y_2 + m) (K_{a,b}(y_1, y_2 + 1/2) - K_{a,b}(y_1, y_2 - 1/2)) dy. \end{aligned}$$

Since W is not Hölder continuous across $y = 0$, we use $[W]_{C_x^{1/2}}$ to control I . Our idea is to compare the integral $I(b)$ with the case $b = \infty, I(\infty)$. To do so, we need a monotonicity Lemma.

Lemma 3.11. *Suppose $f, fg \in L^1$ and $g \geq 0$ is monotone increasing on $[0, \infty]$. For any $0 \leq k \leq b \leq c$, we have*

$$\int_{b-k}^{b+k} |f(x - k)|g(x) dx \leq \int_{b-k}^{c-k} |f(x - k) - f(x + k)|g(x) dx + \int_{c-k}^{c+k} |f(x - k)|g(x) dx.$$

Proof. Denote by R, L the right and the left hand side of the above inequality, respectively. We have

$$\begin{aligned} R - L &\geq \int_{b-k}^{c-k} (|f(x - k)| - |f(x + k)|)g(x) dx + \int_{c-k}^{c+k} |f(x - k)|g(x) dx - \int_{b-k}^{b+k} |f(x - k)|g(x) dx \\ &= \int_{b+k}^{c+k} |f(x - k)|g(x) dx - \int_{b-k}^{c-k} |f(x + k)|g(x) dx = \int_b^c |f(x)| (g(x + k) - g(x - k)) dx. \end{aligned}$$

Since g is increasing on $[0, \infty)$, we prove $R \geq L$. \square

Now, we are in a position to estimate I . Since $K_{a,b}(y_1, y_2)$ is odd in y_1 , we yield

$$|I| \leq \frac{1}{\pi} \int_{y_2 \leq 0, y_1 \geq 0} \sqrt{2y_1} |K_{a,b}(y_1, y_2 + 1/2) - K_{a,b}(y_1, y_2 - 1/2)| dy \cdot [\omega]_{C_x^{1/2}}.$$

For a fixed y_1 with $|y_1| \leq a$ and $b \geq 1/2$, using the definition of $K_{a,b}$ (3.4), the odd symmetry $K_{a,b}(y_1, y_2 + 1/2) - K_{a,b}(y_1, y_2 - 1/2)$ in y_2 , and Lemma 3.11 with $k = 1/2$ and $c = \infty$, we get

$$\begin{aligned} & \int_{y_2 \leq 0} |K_{a,b}(y_1, y_2 + 1/2) - K_{a,b}(y_1, y_2 - 1/2)| dy_2 \\ &= \int_{y_2 \geq 0} |K_{a,b}(y_1, y_2 + 1/2) - K_{a,b}(y_1, y_2 - 1/2)| dy_2 \\ &= \int_0^{b-1/2} |K_1(y_1, y_2 + 1/2) - K_1(y_1, y_2 - 1/2)| dy_2 + \int_{b-1/2}^{b+1/2} |K_1(y_1, y_2 - 1/2)| dy_2 \\ &\leq \int_0^\infty |K_1(y_1, y_2 + 1/2) - K_1(y_1, y_2 - 1/2)| dy_2. \end{aligned}$$

Since $K_{a,b}(y) = 0$ for $|y_1| \geq a$, integrating the above inequality in y_1 from 0 to a , we prove

$$|I| \leq \frac{1}{\pi} \int_0^a \int_0^\infty \sqrt{2y_1} |K_1(y_1, y_2 + 1/2) - K_1(y_1, y_2 - 1/2)| dy \cdot [\omega]_{C_x^{1/2}}.$$

4. ENERGY ESTIMATES

Recall the decomposition (2.75) in Section 2.10. In this section, we perform energy estimates of W_1 following the ideas and some derivations in Sections 2.7.1, 2.8.2, 2.8.3. The goal of the energy estimates is to control several weighted L^∞ norms of ω, η, ξ and their weighted Hölder norms and establish the estimates (A.6) for the coefficients in the estimates. The condition (A.6) means that the damping term is stronger than the bad terms. Then we can further establish stability using the stability Lemma A.2.

4.1. The main equation. After choosing a suitable approximation for the velocity \mathbf{u} and using the approach described in Section 2.10, the main equations (2.75) for ω_1, η_1, ξ_1 read

$$\begin{aligned} (4.1) \quad & \partial_t \omega_1 + (\bar{c}_l x + \bar{\mathbf{u}} + \mathbf{u}(\omega)) \cdot \nabla \omega_1 = \bar{c}_\omega \omega_1 + \eta_1 - \mathbf{u}_A(\omega_1) \cdot \nabla \bar{\omega}, \\ & \partial_t \eta_1 + (\bar{c}_l x + \bar{\mathbf{u}} + \mathbf{u}(\omega)) \cdot \nabla \eta_1 = (2\bar{c}_\omega - \bar{u}_x) \eta_1 - \bar{v}_x \xi_1 - \mathbf{u}_A \cdot \nabla \bar{\theta}_x - \mathbf{u}_{x,A} \cdot \nabla \bar{\theta}, \\ & \partial_t \xi_1 + (\bar{c}_l x + \bar{\mathbf{u}} + \mathbf{u}(\omega)) \cdot \nabla \xi_1 = (2\bar{c}_\omega - \bar{v}_x) \xi_1 - \bar{u}_y \eta_1 - \mathbf{u}_A \cdot \nabla \bar{\theta}_y - \mathbf{u}_{y,A} \cdot \nabla \bar{\theta}, \end{aligned}$$

where $\bar{\mathbf{u}} = (\bar{u}, \bar{v})$, and $\mathbf{u}_A(\omega_1)$ is the velocity after subtracting the approximation term $\tilde{\mathbf{u}}$ defined in (2.82), (2.88), (2.89), (2.68)

$$(4.2) \quad \mathbf{u}_A(f) \triangleq \tilde{\mathbf{u}}(f) - \tilde{\mathbf{u}}(f), \quad \mathbf{u}_{x,A} \triangleq \tilde{\mathbf{u}}_x(f) - \tilde{\mathbf{u}}_x(f), \quad \mathbf{u}_{y,A} \triangleq \tilde{\mathbf{u}}_y(f) - \tilde{\mathbf{u}}_y(f).$$

Note that we do not have $\partial_x \mathbf{u}_A = \mathbf{u}_{x,A}$ since we choose the approximations for $\mathbf{u}, \mathbf{u}_x, \mathbf{u}_y$ separately. Similarly, we do not have $\partial_y \eta_1 = \partial_x \xi_1$. We make these finite rank perturbations to the velocity and the linearized equations by subtracting \mathcal{K}_{2i} (2.68) from \mathcal{L} in (2.75). We also remove the $c_\omega \bar{f}_{\chi,i}$ terms (2.66) in (2.65) by subtracting \mathcal{K}_{1i} from \mathcal{L} in (2.75). We adopt the notation from (2.75)

$$(4.3) \quad W_{1,1} = \omega_1, \quad W_{1,2} = \eta_1, \quad W_{1,3} = \xi_1.$$

Since we will perform weighted L^∞ and $C^{1/2}$ estimate on ω_1, η_1, ξ_1 , we also include the advection terms $\mathbf{u}(\omega) \cdot \nabla f$ from the nonlinear part in the above system. At this stage, we have dropped the remaining term $\mathcal{R}_i, NF(W_1 + W_2)$, part of the nonlinear terms \mathcal{N}_i , the error term $\bar{\mathcal{F}}_i$ in (2.75) to simplify the presentation.

For initial perturbations that satisfy $\omega_{1,0}, \eta_{1,0}, \xi_{1,0} = O(|x|^3)$, the system (2.75) preserve these vanishing orders. See more discussions in Section 2.10.4.

We introduce $\mathcal{T}_d(\rho)$, $d_i(\varphi)$ to denote the coefficients of the damping terms and $b(x)$ to denote the coefficient of the advection

$$(4.4) \quad \begin{aligned} b(x) &= \bar{c}_l x + \bar{\mathbf{u}} + \mathbf{u}, & \mathcal{T}_d(\rho) &= \rho^{-1} \left((\bar{c}_l x + \bar{\mathbf{u}} + \mathbf{u}) \cdot \nabla \rho \right) = \rho^{-1} (b \cdot \nabla \rho), \\ d_1(\rho) &= \mathcal{T}_d(\rho) + \bar{c}_\omega, & d_2(\rho) &= \mathcal{T}_d(\rho) + 2\bar{c}_\omega - \bar{u}_x, & d_3(\rho) &= \mathcal{T}_d(\rho) + 2\bar{c}_\omega + \bar{u}_x. \end{aligned}$$

The terms $d_i(\rho)$ appear naturally in the weighted $L^\infty(\rho)$ estimates of $W_{1,i}$. See below (4.6).

In the equation of $W_{1,i}$, we treat the terms other than the local terms of $W_{1,i}$ in (4.1) as bad terms

$$(4.5) \quad \begin{aligned} B_1(x) &\triangleq \eta_1 - \mathbf{u}_A(\omega_1) \cdot \nabla \bar{\omega}, & B_2(x) &\triangleq -\bar{v}_x \xi_1 - \mathbf{u}_A \cdot \nabla \bar{\theta}_x - \mathbf{u}_{x,A} \cdot \nabla \bar{\theta}, \\ B_3(x) &\triangleq -\bar{u}_y \eta_1 - \mathbf{u}_A \cdot \nabla \bar{\theta}_y - \mathbf{u}_{y,A} \cdot \nabla \bar{\theta}. \end{aligned}$$

With the above notations, we can simplify (4.1) as follows

$$\partial_t W_{1,i} + b \cdot \nabla W_{1,i} = d_i(1) W_{1,i} + B_i,$$

where $d_i(1)$ acts on constant function 1 and $\mathcal{T}_d(1) = 0$. The weighted quantity enjoys the following estimate

$$(4.6) \quad \partial_t (W_{1,i} \rho) + b \cdot \nabla (W_{1,i} \rho) = d_i(\rho) W_{1,i} + B_i \rho.$$

We choose the following weights for the weighted $C^{1/2}$ estimate

$$(4.7) \quad \begin{aligned} \psi_1 &= p_{11}|x|^{-2} + p_{12}|x|^{-1/2} + p_{13}|x|^{-1/6}, \\ \psi_i &= p_{i1}|x|^{-5/2} + p_{i2}|x|^{-1} + p_{i3}|x|^{-1/2} + p_{i4}|x|^{1/6}, \quad i = 2, 3, \end{aligned}$$

where p_{ij} are given in (C.1). The above weights can be determined by the analysis of the singular scenario in Section 2.8.2, where we consider the Hölder estimate for any pair $x, z \in \mathbb{R}_2^{++}$ with $x_2 = z_2$ and $|x - z|$ being sufficiently small.

Remark 4.1. The reader should not confuse the weights ψ_i with the notation for the stream function $(-\Delta)^{-1}\omega$. In this paper, we rarely use the stream function.

From Section 2.8.2, we know that in the scenario when $x_2 = z_2$ and $|x - z|$ is sufficiently small, we have enough damping to obtain the stability estimate. See (2.45) and (A.6) in Lemma A.2. To estimate the more regular case when $|x - z|$ is not small, we need to control the weighted L^∞ norm of ω_1, η_1, ξ_1 . We will follow the ideas in Sections 2.8.3 2.10 to first show that the weighted L^∞ estimates with suitable weights are almost close. We then combine the L^∞ and $C^{1/2}$ estimates to close the stability estimate. We will show that in the more regular case when $|x - z|$ is not small, the damping factor in the Hölder estimate, i.e., λ in (A.6), is similar or even larger than c_1, c_2 in (2.45). Therefore, from c_1, c_2 in (2.45), we can get a good estimate of the stability factor $\lambda_* \approx c_1, c_2$ in our overall energy estimates based on (A.6) and Lemma A.2

$$(4.8) \quad \lambda_* \in [0.06, 0.12].$$

4.1.1. Guidelines of choosing the Hölder weights. To choose the parameters in the above weights (C.1), we first choose different powers so that we can control the solution in the near-field and the far-field. Then we choose the coefficients p_{ij} such that we can obtain the damping terms from the local parts following the derivations in the weighted Hölder estimates in Section 2.7.1. Next, we use the estimates in Section 2.8.2 and treat the nonlocal terms as bad terms (4.5). We further optimize the coefficients so that we can obtain (2.45) with c_1, c_2 as large as possible. These ideas are similar to those presented in [13], and we refer to [13] for more discussions.

After we determine the weight ψ_i , we further determine the weights g_i in the Hölder norm $\|(W_{1,i} \psi_i(x) - W_{1,i} \psi_i(z)) g_i(x - z)\|_\infty$ by studying the Hölder estimates with $|x - z|$ being sufficiently small. In this case, similar to the analysis in Section 2.8.2, the more regular terms vanish. We use Lemma 3.1-Lemma 3.5 and the triangle inequality

$$g(x - z) |f(x) - f(z)| \leq g(x - z) (|f(x_1, x_2) - f(z_1, x_2)| + |f(z_1, x_2) - f(x_2, z_2)|)$$

to estimate the Hölder norm of $\nabla \mathbf{u}$. In general, applying the triangle inequality in the Hölder estimate leads to a larger constant. For example, if $|f(x_1, a) - f(z_1, a)| \leq A|x_1 - z_1|^{1/2}$ for any a, x_1, z_1 and $|f(a, x_2) - f(a, z_2)| \leq A|x_2 - z_2|^{1/2}$ for any a, x_2, z_2 , then

$$\frac{|f(x) - f(z)|}{|x - z|^{1/2}} \leq A \frac{h_1^{1/2} + h_2^{1/2}}{|h_1^2 + h_2^2|^{1/4}}, \quad h_i = x_i - z_i.$$

The upper bound can be $\sqrt{2}A$ if $h_1 = h_2$, which leads to an additional factor $\sqrt{2}$. One way to avoid this overestimate is to choose

$$(4.9) \quad g(h_1, h_2) = (|h_1|^{1/2} + c|h_2|^{1/2})^{-1}.$$

for some constant c in the weighted Hölder estimate. In the above example, one can choose $c = 1$ and obtain $g(x - z)|f(x) - f(z)| \leq A$ for any x, z . However, in the weighted Hölder estimate, we want to obtain a damping factor from the weight g

$$d_g = g(x - z)^{-1} (b(x) - b(z)) \cdot (\nabla g)(x - z) < 0, \quad b(x) = \bar{c}_l x + \bar{\mathbf{u}} + \mathbf{u}.$$

See (2.30). Yet, for the weight (4.9), d_g can be positive and even unbounded since $(\partial_1 g)(0, h_2) = \infty$ and $b_1(x) - b_1(z) \neq 0$ when $x_1 = z_1$. To overcome this difficulty, we perturb the weight (4.9) by considering

$$(4.10) \quad g_i(h) = q_{i0}(h)g_{i0}(1, 0)^{-1}, \quad g_{i0}(h) = (\sqrt{|h_1| + q_{i1}|h_2|} + q_{i3}\sqrt{|h_2| + q_{i2}|h_1|})^{-1},$$

for some small q_{i1}, q_{i2} . We divide the factor $g_{i0}(1, 0)$ to normalize $g_i(1, 0) = 1$. To exploit the anisotropy of the flow (see Section 2.7.2), we choose $q_{i3} < 1$. The parameters q_{ij} are given in (C.1).

We remark that we still have a larger constant when we estimate $g(x - z)(\nabla \mathbf{u}(x) - \nabla \mathbf{u}(z))$ for general (x, z) than the case $x_1 = z_1$ or $x_2 = z_2$. Yet, since we also gain more damping from the above d_g when $|x_2 - z_2|/|x_1 - z_1|$ is not too small, we can still show that the damping term dominates other nonlocal terms.

For η and ξ , we choose the same weight: $g_3(h) = g_2(h)$. To determine the parameters g_{ij} , we first find $x \in \mathbb{R}_2^{++}$ such that we have the least damping in case when $|x - z|$ is sufficiently small with $x_2 = z_2$. That is, we find x_* such that the left hand side of (2.45) achieves the maximum at x_* . Then at such point, we perform the Hölder estimates with other ratio $|z_2 - x_2|/|z_1 - x_1|$ and keeping $|x - z|$ small. We choose q_{ij} so that the damping factor is larger than or close to the one in the case of $x_2 = z_2$.

4.2. Ideas of estimating the nonlocal terms. In the energy estimates, we need to perform weighted L^∞ and Hölder estimates on the velocity $\mathbf{u}_A, \mathbf{u}_{A,x}, \mathbf{u}_{A,y}$ (4.2) given that $\omega_1 \varphi_1 \in L^\infty, \omega_1 \psi_1 \in C^{1/2}$ for some weights φ_1, ψ_1 . For $f = \mathbf{u}_A, (\nabla \mathbf{u})_A$, it can be written as

$$I(f)(x) = \int_{\mathbb{R}^2} K_f(x, y) \Omega_1(y) dy,$$

for some kernel K_f , where Ω_1 is the odd extension of ω_1 in y from \mathbb{R}_+^2 to \mathbb{R}^2 (3.3). In the case without the approximation terms, the formulas of $\nabla \mathbf{u}$ are given in (3.4). For $f = \mathbf{u}_A$, the kernel involves $\nabla^\perp \log |y|$ and has a singularity of order $|x|^{-1}$, which is locally integrable. To obtain a sharp weighted estimate of \mathbf{u}_A with some singular weight ρ , since Ω_1 is odd in y_1, y_2 , we symmetrize the kernel and then apply the L^∞ estimate

$$(4.11) \quad \begin{aligned} K_f^{sym}(x, y) &= K_f(x, y) - K_f(x, -y_1, y_2) - K_f(x, y_1, -y_2) + K_f(x, y), \\ |\rho(x)I(\mathbf{u})(x)| &= \rho(x) \left| \int_{\mathbb{R}_{++}^2} K_{\mathbf{u}}^{sym} \omega_1(y) dy \right| \leq \rho(x) \int_{\mathbb{R}_{++}^2} |K_{\mathbf{u}}^{sym}| \varphi_1^{-1}(y) dy \cdot \|\omega_1 \varphi_1\|_{L^\infty} \\ &\triangleq \rho(x) C(\mathbf{u}, x) \|\omega_1 \varphi_1\|_{L^\infty}, \end{aligned}$$

where $C(\mathbf{u}, x)$ denotes the last integral on the second line. The above estimate is sharp in the sense that for a fixed x , the equality can be achieved if $\omega \varphi_1(y) = C \text{sgn}(K^{sym}(x, y))$ for some constant C . For a given weight φ_1 , the constant $C(\mathbf{u}, x)$ is independent of ω_1 and is an integral of some explicit function. We can estimate it effectively for *all* x using the scaling symmetry of the kernel and numerical computation with rigorous error estimates.

For $f = (\nabla \mathbf{u})_A$, the kernel has a singularity of order $|x|^{-2}$, which is not integrable near the singularity. We decompose the integral $I(f)$ into the nonsingular part (NS) and the singular part (S) with singular region R centered around x with radius $r(x)$

$$(4.12) \quad \begin{aligned} I(f) &= I_{NS}(f) + I_S(f), \quad R(x) = \{y : \max_{i=1,2} |x_i - y_i| \leq r(x)\}. \\ I_{NS}(f) &= \int_{R^c} K_f(x, y) \Omega_1(y) dy, \quad I_S(f) = \int_R K_f(x, y) \Omega_1(y) dy. \end{aligned}$$

In the weighted L^∞ estimate of $(\nabla \mathbf{u})_A$, for I_{NS} , we use the above idea and $\|\omega \varphi_1\|_{L^\infty}$ to control it. For the singular part, we further decompose it using the identity related to the commutator, e.g., (2.34). We apply the above L^∞ estimate (4.11) to the regular term. The singular term related to $\nabla \mathbf{u}(\omega \psi_1)$ is estimated using $\|\omega \psi_1\|_{C^{1/2}}$. For example, we have the following estimate

$$\begin{aligned} \int_{|s_1|, |s_2| \leq \tau} \frac{s_1 s_2}{|s|^4} (\omega \psi_1)(x - s) ds &= \int_{0 \leq s_1 \leq s_2, |s_2| \leq \tau} \frac{s_1 s_2}{|s|^4} ((\omega \psi_1)(x - s) - (\omega \psi_1)(x_1 + s_1, x_2 - s_2)) ds \\ &\leq C \tau^{1/2} [\omega \psi_1]_{C_x^{1/2}}, \end{aligned}$$

where C is some constant related to the kernel and is independent of τ . In short, we can estimate $\rho I(f)$ with some singular weight as follows

$$(4.13) \quad |\rho(x) I(f)(x)| \leq C_1(x) \|\omega \varphi_1\|_{L^\infty} + C_2(x) [\omega \psi_1]_{C_x^{1/2}} + C_3(x) [\omega \psi_1]_{C_y^{1/2}},$$

for some constant $C_i(x)$. We will further bound the right hand side using the energy.

The weighted Hölder estimate is more involved. For $(\nabla \mathbf{u})_A$, we again decompose it into the regular part and the singular part. For the singular part, we will use the sharp Hölder estimates in Lemma 3.1-Lemma 3.5. For the nonsingular part, it is locally Lipschitz. We can estimate its Lipschitz norm by computing suitable integrals and using ideas similar to the above. The estimate for \mathbf{u}_A is easier since it is more regular. We refer the details to Section 7.

4.2.1. Scaling symmetry and rescaled integral. In the above computation of the integrals, e.g., (4.11), there are two singularities. Firstly, the weight $\rho(x)$ is singular near 0, which can amplify the error in the computation of the integral $\int_{\mathbb{R}_2^+} |K_{\mathbf{u}}^{sym}(x, y) \rho(y)| dy$ significantly. Secondly, the kernel $K_{\mathbf{u}}(x, y)$ is singular near $y = x$. In the case of ∇u , the associated kernel is singular of order 2. If there are only a few x , one can design a mesh that is adapted to the singularity $y = x$ and then apply the standard quadrature rule. However, it is very difficult to apply this method to compute the integrals for all x . A crucial observation is that the kernel $K(x, y)$ enjoys scaling symmetry, which enables us to restrict the singularity x in a finite domain away from 0 by choosing suitable rescaling.

Denote $f_\lambda(x) \triangleq f(\lambda x)$. We consider the kernels about ∇u , which are singular of order 2 and satisfy $K(\lambda x, \lambda y) = \lambda^{-2} K(x, y)$. For λ to be chosen, applying a change of variables $y = \lambda \hat{y}, x = \lambda \hat{x}$, we get

$$\rho(x) \int_{\mathbb{R}_2^{++}} K^{sym}(x, y) \omega(y) dy = \rho(\lambda \hat{x}) \int_{\mathbb{R}_2^{++}} K^{sym}(\lambda \hat{x}, \lambda \hat{y}) \omega(\lambda \hat{y}) \lambda^2 d\hat{y} = \rho_\lambda(\hat{x}) \int_{\mathbb{R}_2^{++}} K^{sym}(\hat{x}, \hat{y}) \omega_\lambda(\hat{y}) d\hat{y}.$$

Now, applying the L^∞ estimates, we obtain

$$|\rho(x) \int_{\mathbb{R}_2^{++}} K^{sym}(x, y) \omega(y) dy| \leq \|\omega_\lambda \varphi_{1,\lambda}\|_{L^\infty} \rho_\lambda(\hat{x}) \int_{\mathbb{R}_2^{++}} |K^{sym}(\hat{x}, \hat{y})| \varphi_{1,\lambda}(\hat{y})^{-1} d\hat{y}.$$

Note that $\|\omega_\lambda \varphi_\lambda\|_{L^\infty} = \|\omega \varphi\|_{L^\infty}$. Hence, to establish the estimate, it suffices to compute the rescaled integral. The advantage of the above integral compared to the one without rescaling is that the integral is singular at the rescaled point \hat{x} , which can be restricted to some finite domain by choosing suitable rescaling parameter λ . As a result, we can design an adaptive mesh which is dense in the $O(1)$ region to compute the integrals and we do not need to remesh in the computation of integrals with different \hat{x} . In addition, \hat{x} can be chosen to be away from 0, e.g. $|\hat{x}| \asymp 1$, so that $\rho_\lambda(\hat{x})$ is not singular in \hat{x} . For example, we can write $|x|^{-2} = \lambda^{-2} |\hat{x}|^{-2}$ by

choosing $\lambda = |x|/|\hat{x}|$ with $|\hat{x}| \asymp 1$. The above rescaling argument enables us to overcome the difficulties caused by the singularities in our computation. We refer more details to Section 7.

4.3. Weighted L^∞ estimate with decaying weights. Recall the discussion of several weighted L^∞ estimates after Remark 2.3. We first perform energy estimate with decaying weights in the weighted L^∞ estimate so that we have more damping in the energy estimates. See the weighted L^∞ estimate in the model problem in Section 2.7.1 for more motivations. We choose the following weights

$$(4.14) \quad \begin{aligned} \varphi_1 &= (p_{41}|x|^{-2.4} + p_{42}|x|^{-1/2})|x_1|^{-1/2} + p_{43}|x|^{-1/6}, \quad \varphi_4 = \psi_1|x_1|^{-1/2}, \\ \varphi_{i-3} &= (p_{i1}|x|^{-5/2} + p_{i2}|x|^{-3/2} + p_{i3}|x|^{-1/6})|x_1|^{-1/2} + p_{i4}|x|^{-1/4} + p_{i5}|x|^{1/7}, \quad i = 5, 6, \end{aligned}$$

for the weighted L^∞ estimate with parameters p_{ij} given in (C.2). We apply ψ_1, φ_1 for $\omega, \psi_2, \varphi_2$ for η , and ψ_3, φ_3 for ξ . We will use φ_4 in Section 4.5.2 for an additional weighted L^∞ estimate of ω_1 . We will discuss the ideas of choosing φ_i in Section 4.3.3.

Using the weights φ_1, ψ_1 , we can estimate the constants in the weighted estimate of $\mathbf{u}_A, (\nabla \mathbf{u})_A$ $C_{ij,k}$ in (4.11), (4.13) using the ideas in Section 4.2

$$(4.15) \quad |\rho_{ij} f_{ij}(x)| \leq C_{ij,1}(x) \|\omega \varphi_1\|_\infty + C_{ij,2}(x) [\omega \psi_1]_{C_x^{1/2}} + C_{ij,3}(x) [\omega \psi_1]_{C_y^{1/2}},$$

where $f_{01} = u_A, f_{10} = v_A, f_{11} = u_{x,A}$, etc. We use these indices since $u = -\partial_y \psi, v = \partial_x \psi, u_x = -\partial_x \partial_y \psi$ etc, where ψ is the stream function. We add the weight ρ_{ij} to capture the vanishing order and decays of $\mathbf{u}_A, \nabla \mathbf{u}_A$

$$(4.16) \quad \rho_{10} = \rho_{01} = |x|^{-3} + |x|^{-7/6}, \quad \rho_{ij} = \psi_1, \quad i + j = 2.$$

For $(\nabla \mathbf{u})_A$, we choose $\rho_{ij} = \psi_1, i + j = 2$, since we need to estimate $(\nabla \mathbf{u})_A \psi_1$ using the Hölder norm of $\omega_1 \psi_1$ and $\nabla \mathbf{u}$ and ω_1 are of the same order. To control \mathbf{u}_A , we do not need to use the Hölder seminorm and have

$$(4.17) \quad C_{ij,2}(x) = C_{ij,3}(x) = 0, \quad i + j = 1.$$

4.3.1. Piecewise upper bounds. In practice, we discretize a very large domain $[0, D]^2$ in \mathbb{R}_2^{++} using the mesh y in Section 5 to compute the profiles. Using the method in Section 7, we can estimate $\mathbf{u}_A, \nabla \mathbf{u}_A$ uniformly in each grid $[y_i, y_{i+1}] \times [y_j, y_{j+1}]$. In particular, $C_{ij,1}, C_{ij,2}, C_{ij,3}$ in the upper bound (4.14) are piecewise constants. Then we can track these bounds using $n \times n$ matrices. The estimate in the far-field $x \notin [0, D]^2$ is straightforward since the coefficients of the nonlocal terms in (4.1) have fast decay. The same ideas apply to all other estimates.

Operators and functions. To simplify the notations, we introduce some operators and functions. We define

$$(4.18) \quad \begin{aligned} \mathcal{T}_u(f)(x) &= C_{01,1}|f_x| + C_{10,1}|f_y|, \quad C(\mathbf{u}_x, i) \triangleq C_{11,i}|\bar{\theta}_x| + C_{20,i}|\bar{\theta}_y|, \\ C(\mathbf{u}_y, i) &\triangleq C_{02,i}|\bar{\theta}_x| + C_{11,i}|\bar{\theta}_y|, \quad C(f, a) \triangleq C(f, 1)a_1 + C(f, 2)a_2 + C(f, 3)a_3, \end{aligned}$$

for $\mu \in \mathbb{R}^3$ and $f = \mathbf{u}_x$ or $f = \mathbf{u}_y$. We will use \mathcal{T}_u for the estimate of the $\mathbf{u}_A \cdot \nabla f, C(\mathbf{u}_x, i)$ for $\mathbf{u}_{A,x} \cdot \nabla \bar{\theta}$, and $C(\mathbf{u}_y, i)$ for $\mathbf{u}_{A,y} \cdot \nabla \bar{\theta}$. Note that $C(f, \mu)$ is linear in μ .

Following the derivations in the weighted L^∞ estimate in Section 2.7.1 and using (4.6), we have the following estimates for $W_{1,i} = \omega_1, \eta_1, \xi_1$ (4.3) in (4.1)

$$(4.19) \quad \partial_t(W_{1,i} \varphi_i) + (\bar{c}_t x + \bar{\mathbf{u}} + \mathbf{u}) \cdot \nabla(W_{1,i} \varphi_i) = -d_i(\varphi_i) W_{1,i} \varphi_i + B_i(x),$$

where we have used the operators (4.4) $d_i(\cdot)$ to denote the coefficient of the damping terms, and $B_i(x)$ are the bad terms defined in (4.5). We estimate $B_i(x)$ directly using the above estimates

for the nonlocal terms

$$\begin{aligned}
(4.20) \quad |B_1(x)| &\leq \frac{\varphi_1}{\varphi_2} \|\eta_1 \varphi_2\|_\infty + \frac{\varphi_1}{\rho_{10}} \mathcal{T}_u(\bar{\omega}) \|\omega_1 \varphi_1\|_\infty, \\
|B_2(x)| &\leq \frac{\varphi_2}{\varphi_3} |\bar{v}_x| \|\xi_1 \varphi_3\|_\infty + \frac{\varphi_2}{\rho_{10}} \mathcal{T}_u(\bar{\theta}_x) \|\omega_1 \varphi_1\|_\infty \\
&\quad + \frac{\varphi_2}{\psi_1} (C(\mathbf{u}_x, 1) \|\omega_1 \varphi_1\|_\infty + C(\mathbf{u}_x, 2) [\omega_1 \psi_1]_{C_x^{1/2}} + C(\mathbf{u}_x, 3) [\omega_1 \psi_1]_{C_y^{1/2}}), \\
|B_3(x)| &\leq \frac{\varphi_3}{\varphi_2} |\bar{u}_y| \|\eta_1 \varphi_2\|_\infty + \frac{\varphi_3}{\rho_{10}} \mathcal{T}_u(\bar{\theta}_y) \|\omega_1 \varphi_1\|_\infty \\
&\quad + \frac{\varphi_3}{\psi_1} (C(\mathbf{u}_x, 1) \|\omega_1 \varphi_1\|_\infty + C(\mathbf{u}_x, 2) [\omega_1 \psi_1]_{C_x^{1/2}} + C(\mathbf{u}_x, 3) [\omega_1 \psi_1]_{C_y^{1/2}}).
\end{aligned}$$

4.3.2. *Weights between the L^∞ norm and the Hölder norm.* We cannot close the L^∞ estimate since the estimate of $\nabla \mathbf{u}_A$ involves the Hölder seminorm of ω_1 . If we neglect the Hölder seminorm, we indeed obtain stability for the L^∞ estimate with energy $\max_i \|W_{1,i} \varphi_i\|_\infty$ by checking the condition (A.6). For example, for the η equation, we have

$$-d_2(\varphi_2) - \frac{\varphi_2}{\varphi_3} |\bar{v}_x| - \frac{\varphi_2}{\rho_{10}} \mathcal{T}_u(\bar{\theta}_x) - \frac{\varphi_2}{\psi_1} C(\mathbf{u}_x, 1) \geq \lambda > 0,$$

for some λ . To close our weighted L^∞ and Hölder estimate using Lemma A.2, we need to choose the weights μ_i among different norms such that (A.6) holds.

Recall the weighted Hölder norm from (2.4). We introduce the first energy

$$(4.21) \quad E_1(t) = \max(\max_i \|W_{1,i} \varphi_i\|_\infty, \tau_1^{-1} \|\omega_1 \psi_1\|_{C_{g_1}^{1/2}}).$$

Since $g_1(h_1, 0) = |h_1|^{-1/2}, g_1(0, h_2) = g_1(0, 1)|h_2|^{-1/2}$ (4.10), we obtain

$$E_1(t) \geq \tau_1^{-1} \|\omega_1 \psi_1\|_{C_{g_1}^{1/2}} \geq \tau_1^{-1} [\omega_1 \psi_1]_{C_x^{1/2}}, \quad \tau_1^{-1} g_1(0, 1) [\omega_1 \psi_1]_{C_y^{1/2}}.$$

Using $E_1(t)$ and the notation (4.18), we can simplify the estimate (4.15) for $\nabla \mathbf{u}_A$ as follows (4.22)

$$|\rho_{ij} f_{ij}| \leq (C(f_{ij}, 1) + C(f_{ij}, 2) \tau_1 + C(f_{ij}, 3) \tau_1 g_1(0, 1)^{-1}) E_1 = E_1 \cdot C(f_{ij}, (1, \tau_1, \tau_1 g_1(0, 1)^{-1})).$$

Similarly, the bound in B_i can be simplified as follows

$$C(f, 2) [\omega_1 \psi_1]_{C_x^{1/2}} + C(f, 3) [\omega_1 \psi_1]_{C_y^{1/2}} \leq \tau_1 C(f, (0, 1, g_1(0, 1)^{-1})) E_1(t), \quad f = \mathbf{u}_x, \mathbf{u}_y,$$

where $C(f, \mu)$ is defined in (4.18). The constraint (A.6) for the η equation becomes

$$(4.23) \quad \left(-d_2(\varphi_2) - \frac{\varphi_2}{\varphi_3} |\bar{v}_x| - \frac{\varphi_2}{\rho_{10}} \mathcal{T}_u(\bar{\theta}_x) - \frac{\varphi_2}{\psi_1} C(\mathbf{u}_x, 1) \right) - \tau_1 \frac{\varphi_2}{\psi_1} C(\mathbf{u}_x, (0, 1, g_1(0, 1)^{-1})) \geq \lambda.$$

Similarly, we have another constraint for τ_1 from the estimate of ξ_1 . We want to obtain an overall stability factor λ_* (4.8) and thus choose $\lambda \approx \bar{\lambda}_*$. We choose the largest τ_1 such that the inequality (4.23) and a similar inequality for ξ_1 hold. The idea to choose large τ_1 (or small τ_1^{-1}) is similar to that in (2.52) for the model problem, where the weight τ for the Hölder norm is small. We choose the largest τ_1 so that in the Hölder estimate for $\tau_1^{-1} \omega \psi_1$, we have the small factor τ_1^{-1} associated with the weighted L^∞ norm $\max_i \|W_{1,i} \varphi_i\|_\infty$ in (A.6). In our estimate, we can choose

$$(4.24) \quad \tau_1 = 5.$$

Although τ_1 is not very large, it is enough for us to show that the estimate of the more regular case in the Hölder estimate, i.e. $|x - z|$ is not very small, is similar to or even better than that in the singular case when $|x - z|$ is small. There are two reasons. Firstly, we get the above small factor τ_1^{-1} when we estimate the more regular terms using the weighted L^∞ norm. Secondly, as $|x - z|$ increases, due to our localized estimates in Lemmas 3.1-3.4, the constants in the estimates of the nonlocal terms decrease. Note that from (4.23), choosing a larger τ_1 requires better estimates on the nonlocal terms, e.g., smaller $C(\mathbf{u}_x, i)$. For this reason, we need to approximate the nonlocal terms \mathbf{u} with finite rank operators with a higher rank, which increases the computation cost. Due to this consideration, we choose a moderate τ_1 .

Due to the anisotropy of the flow (see Section 2.7.2), we have a larger damping factors d_i away from the boundary. Due to the decay of the solution, the coefficients in the estimates of the nonlocal terms become smaller. Thus, we can focus on the near-field and the boundary to test the conditions (A.6) for given weights and the approximations of $\mathbf{u}, \nabla \mathbf{u}$ that we choose in Section 2.11.

In Figure 5, we plot the coefficients of the damping terms, e.g. $-d_2(\varphi_2)$ (4.23), and the estimates of the bad terms, i.e. the sum of the terms with negative sign (4.23), and the remaining damping factors (the left hand side of (4.23)) on the grid points along the boundary. The ξ variable enjoys a much better estimates near the boundary, so we do not plot it.

We choose the approximation terms $\hat{\mathbf{u}}, \widehat{\nabla \mathbf{u}}$ for $\mathbf{u}, \nabla \mathbf{u}$ along the boundary in Section 2.11 such that the weighted estimates of $\mathbf{u} - \hat{\mathbf{u}}, \nabla \mathbf{u} - \widehat{\nabla \mathbf{u}}$ are small. Near the center of the approximation terms, x_i in (2.82), we have better estimates of the bad terms. In Figure 5, the points x_i are the local minimum of the blue dashed curve. Since the coefficients of the nonlocal terms (4.1), e.g., $\bar{\omega}_x, \bar{\theta}_x$, decay for large x , we do not need to construct the approximations for large x .

We choose φ_1 slightly weaker than φ_2 near the origin (4.14) such that $\varphi_1/\varphi_2 \|\eta_1 \varphi_2\|_\infty$ is small, and we can obtain large stability factors for both ω and η , which are larger than 0.7. This allows us to control a larger weighted residual error near the origin.

In Figure 6, we plot the stability factors, e.g., the left hand side of (4.23), in the weighted L^∞ estimates of ω_1, η_1 . Due to the anisotropy of the flow, the damping terms and the stability factors are much larger if the angle y/x is large. See Section 2.7.2.

Note that we only use these plots to visualize the estimates. To justify the inequalities (4.23), we follow the methods in [13, 14] and derive piecewise bounds of different functions based on the estimates of the approximate steady state and the weights in Appendices E, C.3.

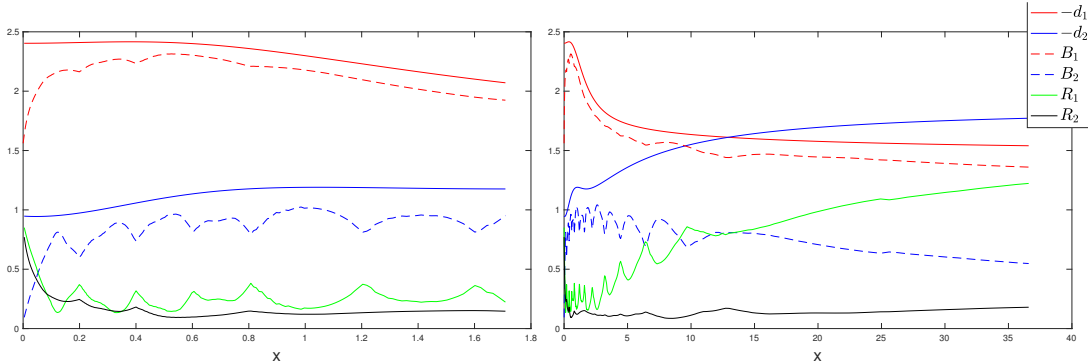


FIGURE 5. Weighted L^∞ estimates with slowly decay weights. Left figure: estimates near 0, $x \in [0, 1.8]$; Right figure: estimates in a larger domain, $x \in [0, 35]$. The red curves shows the coefficient of the damping term $-d_1(\varphi_1)$, and the estimate of B_1 ; the blue curves are for $-d_2(\varphi_2), B_2$ in the estimates of η_1 . The green and the black curves are the stability factors in the estimate of ω_1 and η_1 .

4.3.3. Order of choosing the parameters. We have discussed how to choose the Hölder estimate in Section 4.1.1. For φ_i , we first choose the weight φ_1 for ω_1 consisting of different powers to take into account the vanishing order of ω_1 near 0 and its decay in the far field. We add the power $|x_1|^{-1/2}$ in $\varphi_1, \varphi_2, \varphi_3$ (4.14) since we need to control $\|\omega_1 |x_1|^{-1/2} \psi_1\|_\infty$ for the Hölder estimate. See Section 2.7.4. In the estimate of $\omega_1 |x_1|^{-1/2} \psi_1$, we need to control $\eta_1 |x_1|^{-1/2} \psi_1$ and other weighted quantities with weights singular at $x_1 = 0$. Thus, we add the weight $|x_1|^{-1/2}$ in φ_i . We adjust the parameters in φ_1 so that we have a good damping factor $d_1(x)$ from the local term for ω_1 . Then we can estimate the nonlocal terms and the constants (4.15). Once we obtain the estimates for $\nabla \mathbf{u}_A, \mathbf{u}_A$, we choose the exponents of different powers in φ_2 and adjust the parameters so that we have better stability factors in the weighted L^∞ estimate and choose

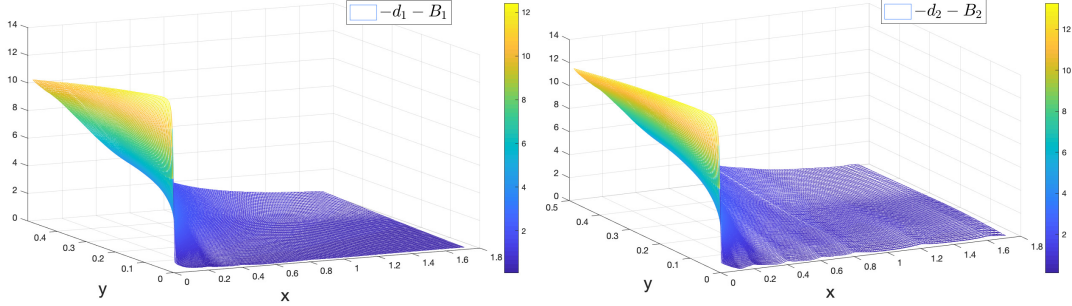


FIGURE 6. Weighted L^∞ estimates in the near-field. Left: stability factors in the estimate of ω_1 . Right: stability factor in the estimate of η_1 .

a larger τ_1 (4.23). Since the equations of ξ_1 and η_1 are similar, we choose the same combination of powers in φ_2 and φ_3 (4.14). Moreover, since ξ_1 is weakly coupled with ω_1 and η_1 (see Section 2.6.2), we determine the parameters in φ_3 after we obtain φ_1, φ_2 .

4.4. Weighted Hölder estimates. Recall the weights ψ_i for ω_1, η_1, ξ_1 (C.1) and $g_i(h)$ (4.10) in the weighted $C^{1/2}$ estimates, the notation $W_{1,i}$ (4.3), and the simplified equation (4.6). The goal of the weighted Hölder estimate is to control $\|W_{1,i}\psi_i\|_{C_{g_i}^{1/2}}$, where $\|\cdot\|_{C_{g_i}^{1/2}}$ is defined in (2.4), which along with the weighted L^∞ estimate, we can control the second energy

$$(4.25) \quad E_2(t) \triangleq \max(E_1(t), \tau_1^{-1} \max(\|W_{1,1}\psi_1\|_{C_{g_1}^{1/2}}, \mu_1 \|W_{1,2}\psi_2\|_{C_{g_2}^{1/2}}, \mu_2 \|W_{1,3}\psi_3\|_{C_{g_3}^{1/2}}))$$

for the weights μ_1, μ_2 determined by analyzing the most singular scenario in Section 2.8.2 (2.43). They are given in (C.4). In fact, these factors can be absorbed in the definition of ψ_2, ψ_3 . We have normalized the coefficient of the most singular power in ψ_1 as 1.

Following the derivations in the weighted Hölder estimate in Section 2.7.1 and using (4.6) and Lemma 2.2, we derive the following for $W_{1,i}\psi_i$ and any $x, z \in \mathbb{R}_{++}^2$

$$(4.26) \quad \begin{aligned} \partial_t H_i + (b(x) \cdot \nabla_x + b(z) \cdot \nabla_z) H_i &= \left((d_i(\psi_i) W_{1,i}\psi_i)(x) - (d_i(\psi_i) W_{1,i}\psi_i)(z) \right) g_i(x-z) \\ &\quad + d_{g,i} H_i + \left((B_i\psi_i)(x) - (B_i\psi_i)(z) \right) g_i(x-z) \triangleq I_1 + I_2 + I_3 \triangleq R_i, \end{aligned}$$

where $b(x)$ is the coefficient of the advection (4.4), $d_{g,i}$ is the damping factor from g_i in the Hölder estimate, and J_i, H_i are given below

(4.27)

$$J_i \triangleq W_{1,i}\psi_i, \quad H_i(x, z) = (J_i(x) - J_i(z))g_i(x-z), \quad d_{g,i} \triangleq \frac{(b(x) - b(z)) \cdot (\nabla g_i)(x-z)}{g_i(x-z)}.$$

The factor d_i is defined in (4.4)

$$(4.28) \quad d_1(\psi_1) = \mathcal{T}_d(\psi_1) + \bar{c}_\omega, \quad d_2(\psi_2) = \mathcal{T}_d(\psi_2) + 2\bar{c}_\omega - \bar{u}_x, \quad d_3(\psi_3) = \mathcal{T}_d(\psi_3) + 2\bar{c}_\omega + \bar{u}_x,$$

and B_i is the bad term defined in (4.5).

We note that the second term I_2 in (4.26) is already a damping term. See Section 2.7.1 and discussion below Lemma 2.2. To further simplify the notation, we introduce

$$(4.29) \quad a_i(x) = d_i(\psi_i)(x), \quad \delta(f)(x, z) = f(x) - f(z).$$

We also drop the dependence of $\delta(f)$ on x, z when there is no confusion. Using the above notation we get

$$(4.30) \quad \delta(fg) = (fg)(x) - (fg)(z) = f(x)\delta(g) + \delta(f)g(z).$$

4.4.1. Estimate the explicit coefficients. In the Hölder estimates, we need to estimate $(\bar{p}q)(x) - (\bar{p}q)(z)g(x - z)$ for some coefficient \bar{p} , perturbation q , e.g. $q = \omega_1, \eta_1$, and some weight g , e.g. $g = g_i$. The coefficient \bar{p} only depends on the weights ψ_i, φ_i and the approximate steady state. In particular, locally, \bar{p} is smooth enough. We can estimate $g(x - z)\delta(\bar{p})$ effectively using the method in Appendix G. Note that the approximate steady state, weights and their derivatives can be estimated effectively using the method in Appendices E, C.3. In practice, we estimate the piecewise $C_x^{1/2}$ and $C_y^{1/2}$ seminorms of $\bar{p}(x)$, and then use the triangle inequality to obtain the estimate of $g(x - z)\delta(\bar{p})$. Namely, given x, z , we have

$$(4.31) \quad \begin{aligned} |p(x_1, x_2) - p(z_1, z_2)| &\leq |p(x_1, x_2) - p(z_1, x_2)| + |p(z_1, x_2) - p(z_1, z_2)| \\ &\leq |x_1 - z_1|^{1/2} A(x_1, x_2, z_1) + |x_2 - z_2|^{1/2} B(z_1, x_2, z_2), \end{aligned}$$

for some constants A, B . We discretize the domain \mathbb{R}_{++}^2 using the same mesh $y_0 < y_1 < \dots, y_n$ in our computation for the profile in Section 5 and estimate these constants for $x \in Q_1, z \in Q_2$ for different grids uniformly. These piecewise Hölder estimates of a function can be established using the methods in Appendices G.6, G.7. Therefore, can track the piecewise bounds $A(x_1, x_2, z_1)$ for x_1, x_2, z_1 in each cube $I_i \times I_j \times I_k, I_i = [y_i, y_{i+1}]$ using $n \times n \times n$ matrices.

In general, such an estimate has some overestimates. Yet, since the problem is anisotropic in x and y direction, in the worst case scenario where $|x_2 - z_2|$ is much smaller than $|x_1 - z_1|$, this simple estimate is effective. See also Section 4.1.1.

Although the weights ψ_i, φ_i are singular near $x = 0$, from the estimates in the most singular scenario in Section 2.8.2 (see Figure 4), we have better estimates near $x = 0$. Thus, the difficult region in our estimate is x away from 0, e.g. x around 0.5. In such a case, we can simply treat the weights ψ_i, φ_i as smooth functions.

Now, using (4.30), we obtain

$$P \triangleq \delta(\bar{p}q)g(x - z) = (\bar{p}(x)\delta(q) + \delta(\bar{p})q(z))g(x - z) \triangleq P_1 + P_2.$$

The second term is more regular. We can use the weighted L^∞ norm of q to control it. For the first term, we bound it using the weighted Hölder (semi)norm. Below, we discuss different cases. In all cases, the estimate of P_2 is much smaller than that of P_1 . Moreover, we have another decomposition

$$P = (\bar{p}(z)\delta(q) + \delta(\bar{p})q(x))g(x - z) \triangleq \tilde{P}_1 + \tilde{P}_2.$$

For x, z not sufficiently close, these two decompositions lead to two different estimates. We will optimize two estimates.

4.4.2. Estimate of I_1 . Recall I_1 from (4.26). Note that $H_i = \delta(J_i)g_i(x - z)$ is the energy we want to control. We have

$$(4.32) \quad \begin{aligned} I_1 &= \delta(a_i J_i)g_i(x - z) = (a_i(x)\delta(J_i) + \delta(a_i)J_i(z))g_i(x - z) \\ &= a_i(x)H_i + \delta(a_i)g_i(x - z)J_i(z) \triangleq I_{11} + I_{12}. \end{aligned}$$

The first term is a damping term. Note that we can control $J_i(x)$ using the weighted L^∞ norm in the energy E_1 (4.21)

$$|J_i(z)| = |(W_{1,i}\psi_i)(z)| \leq \|W_{1,i}\varphi_i\|_\infty \frac{\psi_i(z)}{\varphi_i(z)} \leq E_1 \frac{\psi_i(z)}{\varphi_i(z)}.$$

Since a_i is explicit and a given function, we follow Section 4.4.1 and estimate $\delta(a_i)g_i(x - z)$ using the method in Appendix G. In particular, when $|x - z|$ is small, $\delta(a_i)g_i(x - z)$ is very small. It follows

$$(4.33) \quad |I_{12}| \leq |\delta(a_i)g_i(x - z)| \frac{\psi_i(z)}{\varphi_i(z)} E_1.$$

Similarly, we have

$$(4.34) \quad I_1 = \tilde{I}_{11} + \tilde{I}_{12}, \quad \tilde{I}_{11} = a_i(z)H_i, \quad |\tilde{I}_{12}| \leq |\delta(a_i)g_i(x - z)| \frac{\psi_i(x)}{\varphi_i(x)} E_1.$$

We choose one of the above estimates according to the relative size of the following terms

$$(4.35) \quad m_1 = a_i(x) + \tau_1^{-1} |\delta(a_i)g_i(x-z)| \frac{\psi_i(z)}{\varphi_i(z)}, \quad m_2 = a_i(z) + \tau_1^{-1} |\delta(a_i)g_i(x-z)| \frac{\psi_i(x)}{\varphi_i(x)},$$

where τ_1 is the ratio between the L^∞ and $C^{1/2}$ norm in the energy. We use the decomposition (4.32) and its estimates if m_1 is smaller. We choose (4.34) if m_2 is smaller. We remark that this optimization is similar to maximize the left hand side of (A.6) (the sign is different), and allows us to obtain better stability factor. We will use similar optimizations several times to get better stability factors. Following the discussions and ideas in Section 4.4.1, we can track the piecewise bounds of the above functions and estimates, e.g. $a_i, \tau_1^{-1} |\delta(a_i)g_i(x-z)| \frac{\psi_i(z)}{\varphi_i(z)}$.

4.4.3. Estimate of I_3 . Recall I_3 from (4.26) and B_i from (4.5). The term B_i involves both the local term and nonlocal terms. We treat them as bad terms and estimate them separately.

Estimate of the local part. We focus on η_1 in B_1 . Other terms $-\bar{v}_x \xi_1$ in B_2 , $-\bar{u}_y \eta_1$ in B_3 (4.5) can be estimated similarly. Note that the weights are different for ω_1, η_1 . We rewrite the difference as follows

$$\delta(\eta_1 \psi_1) g_1(x-z) = \delta(\eta_1 \psi_2) \frac{\psi_1}{\psi_2} g_1(x-z) = \left(\delta(\eta_1 \psi_2) \frac{\psi_1}{\psi_2}(x) + (\eta_1 \psi_2)(z) \delta\left(\frac{\psi_1}{\psi_2}\right) \right) g_1(x-z) \triangleq P_1 + P_2.$$

The term P_2 is more regular. We follow Section 4.4.1 to estimate $\delta\left(\frac{\psi_1}{\psi_2}\right) g_1(x-z)$. Using the weighted L^∞ norm of η_1 and the energy E_2 (4.25), we obtain

$$(4.36) \quad |P_2| \leq \|\eta_1 \varphi_2\|_\infty \frac{\psi_2(z)}{\varphi_2(z)} \left| \delta\left(\frac{\psi_1}{\psi_2}\right) g_1(x-z) \right| \leq E_2 \frac{\psi_2(z)}{\varphi_2(z)} \left| \delta\left(\frac{\psi_1}{\psi_2}\right) g_1(x-z) \right|.$$

Following Section 4.4.1, we can track the piecewise bound of the coefficient in the above upper bound. For P_1 , we have

$$(4.37) \quad \begin{aligned} |P_1| &\leq \frac{\psi_1}{\psi_2}(x) \frac{g_1(x-z)}{g_2(x-z)} |\delta(\eta_1 \psi_2) g_2(x-z)| \leq \frac{\psi_1}{\psi_2}(x) \left| \frac{g_1(x-z)}{g_2(x-z)} \right| \|\eta_1 \psi_2\|_{C_{g_2}^{1/2}} \\ &\leq \frac{\psi_1}{\psi_2}(x) \left| \frac{g_1(x-z)}{g_2(x-z)} \right| E_2 \tau_1 \mu_2^{-1}, \end{aligned}$$

where we have used the energy E_2 (4.25) in the last inequality. We note that in the estimate of $\tau_1^{-1} \|\omega_1 \psi_1\|_{C_{g_2}^{1/2}}$, we have the term $\tau_1^{-1} P_1$. The weight τ_1^{-1} cancels τ_1 in the above upper bound.

Note that g_1 and g_2 are equivalent to $|h|^{-1/2}$ and homogeneous of order $-1/2$. The quantity $\left| \frac{g_1(x-z)}{g_2(x-z)} \right|$ only depends on the ratio between $x_1 - z_1, x_2 - z_2$. We also track this ratio.

For large $|x-z|$, we have a trivial estimate

$$|\delta(\eta_1 \psi_1) g_1(x-z)| \leq \|\eta_1 \varphi_2\|_\infty \left(\frac{\psi_1}{\varphi_2}(x) + \frac{\psi_1}{\varphi_2}(z) \right) g_1(x-z) \leq E_2 \left(\frac{\psi_1}{\varphi_2}(x) + \frac{\psi_1}{\varphi_2}(z) \right) g_1(x-z).$$

Estimate of the nonlocal part. To control the nonlocal terms in B_i , we use the sharp $C_x^{1/2}$ and $C_y^{1/2}$ estimates in Section 3 for the most singular part and the estimates in Section 7 for the more regular part. We focus on the estimate of $-u_{x,A} \bar{\theta}_x$ in B_2 (4.5), which contributes to the largest part in the estimate. Firstly, we have

$$\delta(u_{x,A} \bar{\theta}_x) = \delta(u_{x,A}) \bar{\theta}_x(x) + u_{x,A}(z) \delta(\bar{\theta}_x) \triangleq P_3 + P_4.$$

The term P_4 is more regular. For $u_{x,A}(z)$, we use the estimate in Section 4.3. For $\delta(\bar{\theta}_x)$, we follow Section 4.4.1. In particular, we have

$$(4.38) \quad |P_4| = |u_{x,A}(x) \delta(\bar{\theta}_x)| \leq E_1 (C_1(x, z) |x_1 - z_1|^{1/2} + C_2(x, z) |x_2 - z_2|^{1/2}),$$

for some functions $C_i(x, z)$ depending on the weights and the profile. See Section 4.3.1. Again, we can obtain piecewise upper bound of these functions.

For P_3 , using the triangle inequality, we have

$$|u_{x,A}(x) - u_{x,A}(z)| = |u_{x,A}(x_1, x_2) - u_{x,A}(z_1, x_2)| + |u_{x,A}(z_1, x_2) - u_{x,A}(z_1, z_2)|$$

Applying the $C_x^{1/2}$ and $C_y^{1/2}$ estimate in Section 3, 7 to P_{51}, P_{52} , respectively, we obtain

$$\begin{aligned} (4.39) \quad |u_{x,A}(x) - u_{x,A}(z)| &\leq C_3(x, z)|x_1 - z_1|^{1/2} + C_4(x, z)|x_1 - z_1|^{1/2} \max(\tau_1 \|\omega_1 \varphi_1\|_\infty, [\omega_1 \psi_1]_{C_{g_1}}^{1/2}) \\ &\leq (C_3(x, z)|x_1 - z_1|^{1/2} + C_4(x, z)|x_1 - z_1|^{1/2})\tau_1^{-1} E_2, \end{aligned}$$

for some constants C_3, C_4 only depending on the weight and the profile. We remark that the constants C_3, C_4 are very close to the constants provided by the sharp Hölder estimate in Section 3. Again, we can obtain these piecewise uppers and track them. See Section 4.3.1.

When $|x - z|$ is not small, we can apply the triangle inequality and the L^∞ estimate of $u_{x,A}$ in Section 4.3 to obtain another bound.

In practice, we only need to apply the above Hölder estimate when $|x|$ and $|z|$ are comparable and $|x - z|$ is very small, e.g. $|x| \leq |z| \leq 1.2|x|$. Beyond such a range, the L^∞ estimate already provides better estimate.

4.4.4. Summarize the estimates. In summary, for the right hand sides in (4.26), when x, z are close, we can obtain the following estimates

$$R_i = (d_{g,i}(x, z) + a_i(p))H_i + \tilde{B}_i, \quad \tilde{B}_i = \hat{I}_{12} + \delta(B_i \psi_i)g_i(x - z),$$

where \tilde{B}_i is the combination of the term \hat{I}_{12} (4.32) or (4.34) and I_3 , and we can estimate it as follows,

$$(4.40) \quad |\tilde{B}_i| \leq \left((|x_1 - z_1|^{1/2} A_1(x, z) + |x_2 - z_2|^{1/2} A_2(x, z))g_i(x - z) + A_3(x, z) \frac{g_i(x - z)}{g_{k_i}(x - z)} \right) E_2$$

with $(p, \hat{I}_{12}) = (x, I_{12})$ or (z, \tilde{I}_{12}) depending on the size of m_1, m_2 in (4.35), $(k_1, k_2, k_3) = (2, 3, 2)$. The term $A_3(x, z) \frac{g_i(x - z)}{g_{k_i}(x - z)}$ comes from the estimate of the local terms, e.g. (4.37), the term $|x_1 - z_1|^{1/2} A_1(x, z) + |x_2 - z_2|^{1/2} A_2(x, z)$ bounds the estimate of the nonlocal terms, e.g. (4.39), and the regular terms such as (4.33), (4.36), (4.38) using the method (4.31). We remark that we can obtain piecewise upper bound of the coefficients A_i in the above estimates and can track them using matrices. See Sections 4.3.1, 4.4.1.

Checking the stability conditions. According to Lemma A.2, to obtain linear stability, we need to check the conditions (A.6). We use the following method to check such a condition. We discretize a large domain $[0, D]^2$ into small grids $Q_{ij} = I_i \times I_j$ using the same mesh $y_0 < y_1 < \dots < y_n$ as that in Section 5. We have piecewise bounds for the coefficients A_i (4.40) in each pair of grids $x \in Q_{ij}, z \in Q_{kl}$.

Firstly, we fix the locations of x, z to some grids: $x \in Q_1, z \in Q_2$. Then we can derive the bound $A_i(x, z)$. We still need to control the different $x - z$. One observation is that given A_i is constant in $Q_1 \times Q_2$, the upper bound in (4.40) is 0-homogeneous in $x - z$. Thus, we only need to further consider the ratio between $r_1 = x_1 - z_1, r_2 = x_2 - z_2$. Similar considerations apply to the damping factors $d_{g,i}$ (4.26). We consider four different cases depending on the sign of r_1/r_2 and the size between $|r_1|, |r_2|$. We focus on the $r_1/r_2 > 0$ and $r_2 \leq r_1$ to illustrate the ideas. In such a case, we can normalize $r_1 = 1$ and $0 \leq r_2 \leq 1$. Now the problem reduces to checking the inequality in 1D. Since these functions have monotone properties, e.g. $g_i(1, r_2)$ is decreasing in r_2 , these inequalities can be checked by partitioning $r_2 \in [0, 1]$ into smaller intervals $r_2 \in [b_i, b_{i+1}], 0 = \beta_0 < \beta_1 < \dots < \beta_N = 1$.

Note that when $|x - z|$ is far away, we will have much better estimate due to the improvement from the sharp Hölder estimates in Lemmas 3.1-3.4. In practice, for $x \in Q_{i_1, i_2}, z \in Q_{j_1, j_2}$ with $\max(|i_1 - j_1|, |i_2 - j_2|) \geq 20$, we already have much better stability factors.

In Figure 7, we plot the estimates for the grid point along the boundary with $r_2/r_1 = 0$. Here, we consider $x \in I_i \times I_0, z \in I_j \times I_0$, where $I_i = [y_i, y_{i+1}]$ is a small interval. It is the case where we have the smallest damping. Other cases with small $j - i$ are similar and the estimate is better. The estimate of the bad terms in the η_1 equation is very close to the one in the most singular scenario based on the sharp inequalities. In some cases, we have better estimates since $|x - z|$ is far away and the improvement of constants for the localized the velocity from Lemmas

3.1-3.4. For larger ratio $|r_2/r_1|$, we have larger stability factors due to the anisotropy of the flow. See Section 2.7.2. We have designed the weights g_i to exploit this properties.

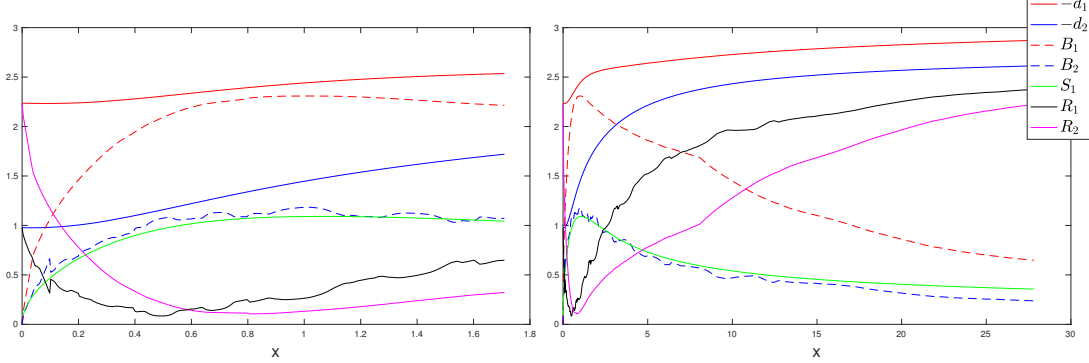


FIGURE 7. Weighted Hölder estimates. Left figure: estimates near 0, $x \in [0, 1.8]$; Right figure: estimates in a larger domain, $x \in [0, 30]$. The red curves shows the coefficient of the damping term for $\delta(W_{1,1}\psi_1)g_1(x - z)$ and the estimate of the bad terms; the blue curves are for the Hölder estimate of $W_{1,2}\psi_2$. The green curve is the same estimated as that in the most singular scenario based on the sharp inequalities. The magenta and the black curves are the stability factors in the Hölder estimate for ω_1, η_1 . The stability factors are larger than 0.08.

In Figure 8, we consider $x \in I_i \times I_0, z \in I_j \times I_0$ with $j - i = 10$. The stability factor for η_1 shown by the black curve becomes much larger and is larger than 0.3.

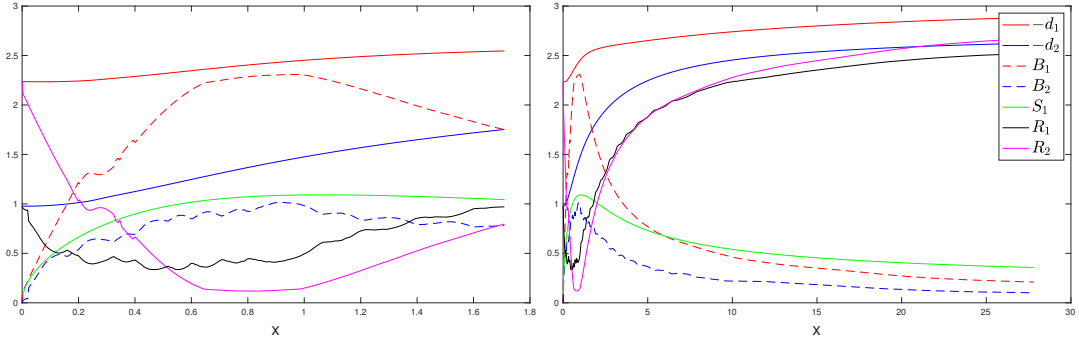


FIGURE 8. Weighted Hölder estimates with larger $|x - z|$

We refer the full details of the verification to the upcoming Supplementary Materials.

4.5. Additional Weighted L^∞ estimates.

4.5.1. *Weighted L^∞ estimates with growing weights.* To close the nonlinear estimate in (2.65), (2.75), we need to control $\|\omega\|_\infty, \|\nabla\theta\|_\infty, \|W_{1,i}\|_\infty$. The quantities we estimate in the previous sections only allow us to control ω_1 in the near field since the singular weight φ_1 decays in the far field, see (4.14). To obtain better control of $W_{1,i}$ in the far-field, we perform similar weighted L^∞ energy estimates on $W_{1,i}\varphi_{gi}$ with a different weight φ_{gi} that grows faster than φ_i in the far-field, $i = 1, 2, 3$.

We choose the following weights φ_{gi}

$$(4.41) \quad \begin{aligned} \varphi_{g1} &= \varphi_1 + p_{71}|x|^{1/16}, \quad \varphi_{g2} = \varphi_2 + p_{81}|x|^{1/4}, \\ \varphi_{g3} &= (p_{31}|x|^{-5/2} + p_{32}|x|^{-3/2} + p_{33}|x|^{-1/6})|x_1|^{-1/2} + p_{34}|x|^{-1/4} + p_{91}|x|^{1/7} + p_{92}|x|^{1/4}. \end{aligned}$$

The subscript “g” is short for “grow”. For $\varphi_{g1}, \varphi_{g2}$, we simply add the powers $|x|^{1/16}, |x|^{1/4}$, which grow faster than φ_1, φ_2 , respectively. For φ_{g3} , we also add the power $|x|^{1/4}$. In addition, we modify the coefficients of $|x|^{1/7}$ in φ_3 (4.14). Other parts of φ_{g3} are the same as φ_3 in (4.14). The parameters are given in (C.3). Since we can close the weighted L^∞ and $C^{1/2}$ estimates at the linear level, we can establish the stability estimate for $W_{1,i}\varphi_{gi}$ for φ_{gi} close to φ_i .

We remark that to determine these parameters, especially p_{71} , we first use the estimate of the nonlocal terms in (4.15), (4.22) and then perform energy estimates similar to those in Section 4.3. By checking the stability condition for $\|W_{1,i}\varphi_{gi}\|_\infty$, we can determine the value of p_{71} . To improve the estimates, we further use $\|\omega_1\varphi_{g1}\|_\infty$ and the Hölder norm of $\omega_1\psi_1$ to derive another estimate of $\mathbf{u}_A, \nabla \mathbf{u}_A$

$$(4.42) \quad |\rho_{ij}f_{ij}(x)| \leq C_{gij,1}(x)\|\omega\varphi_{g1}\|_\infty + C_{gij,2}(x)[\omega\psi_1]_{C_x^{1/2}} + C_{gij,3}(x)[\omega\psi_1]_{C_y^{1/2}},$$

where g is short for “grow”, $f_{01} = u_A, f_{10} = v_A$, etc similar to those in (4.15). Similar to (4.17), we have

$$(4.43) \quad C_{gij,2}(x) = C_{gij,3}(x) = 0, \quad i + j = 1.$$

For some weights τ_2, μ_4 to be determined, we consider a new energy

$$(4.44) \quad E_3(t) = \max \left(E_2(t), \tau_2 \max(\mu_2\|\omega_1\varphi_{g1}\|_\infty, \|\eta_1\varphi_{g,2}\|_\infty, \|\xi_1\varphi_{g,3}\|_\infty) \right).$$

where $E_2(t)$ is defined in (4.25). The parameters τ_2, μ_4 are chosen in (C.4).

With these weights τ_2, μ_4 , we can simplify the above bound similar to (4.22)

$$|\rho_{ij}f_{ij}(x)| \leq (C_{gij,1}(x)(\tau_2\mu_4)^{-1} + C_{gij,2}(x)\tau_1 + C_{gij,3}(x)\tau_1 g_1(0,1)^{-1})E_3(t).$$

Combining the above estimate and (4.22) and using $E_3 \geq E_1$, we yield

$$(4.45) \quad |\rho_{ij}f_{ij}(x)| \leq C_{gij}(\tau_2\mu_4)(x)E_3(t)$$

$$C_{gij}(\tau)(x) = \min(C_{gij,1}(x)\tau^{-1} + C_{gij,2}(x)\tau_1 + C_{gij,3}(x)\tau_1 g_1(0,1)^{-1}, C(f_{ij}, [1, \tau_1, \tau_1 g_1(0,1)^{-1}])).$$

Here, since τ_1 has been chosen, C_{gij} only depends on the weight $\tau_2\mu_4$. Since φ_{g1} grows faster than φ_1 in the far field, the above estimates provide better estimates of $\mathbf{u}_A, \nabla \mathbf{u}_A$ in the far-field.

Now, following the derivations and estimates in Section 4.3, we obtain

$$(4.46) \quad \partial_t(W_{1,i}\varphi_{gi}) + (\bar{c}_l x + \bar{\mathbf{u}} + \mathbf{u}) \cdot \nabla(W_{1,i}\varphi_{gi}) = -d_{gi}(x)W_{1,i}\varphi_{gi} + B_{gi}(x),$$

where the damping terms d_i are given by

$$(4.47) \quad d_{g1}(x) = \mathcal{T}_d(\varphi_{g1}) + \bar{c}_\omega, \quad d_{g2}(x) = \mathcal{T}_d(\varphi_{g2}) + 2\bar{c}_\omega - \bar{u}_x, \quad d_{g3}(x) = \mathcal{T}_d(\varphi_{g3}) + 2\bar{c}_\omega + \bar{u}_x,$$

and \mathcal{T}_d is defined in (4.4). To estimate the local terms, e.g. η in (4.1), we have

$$|\varphi_{g1}\eta| \leq \varphi_{g1}(\varphi_2^{-1}\|\eta_1\varphi_2\|_\infty \wedge \tau_2^{-1}\varphi_{g2}^{-1}\|\tau_2\eta\varphi_{g2}\|_\infty) \leq \varphi_{g1}(\varphi_2^{-1} \wedge \tau_2^{-1}\varphi_{g2}^{-1})E_3(t).$$

where $a \wedge b = \min(a, b)$. Similarly, we have

$$|\varphi_{g2}\bar{v}_x\xi_1| \leq \varphi_{g2}|\bar{v}_x|(\varphi_3^{-1} \wedge \tau_2^{-1}\varphi_{g3}^{-1})E_3, \quad |\varphi_{g3}\bar{u}_y\eta_1| \leq \varphi_{g3}|\bar{u}_y|(\varphi_2^{-1} \wedge \tau_2^{-1}\varphi_{g2}^{-1})E_3.$$

For the nonlocal terms $\mathbf{u}_A, \nabla \mathbf{u}_A$, we apply (4.45). To simplify the notation, we introduce an operator $\mathcal{T}_{u,g}$ similar to \mathcal{T}_u in (4.18)

$$(4.48) \quad \mathcal{T}_{u,g}(f, \tau) = C_{g01}(\tau)|f_x| + C_{g01}(\tau)|f_y|$$

to control $\mathbf{u}_A \cdot \nabla f$.

We obtain the following estimate for the remaining terms

$$\begin{aligned}
 |B_{gi}(x)| &\leq A_{gi}(x)E_3(t), \quad i = 1, 2, 3, \\
 A_{g1} &= \varphi_{g1}(\varphi_2^{-1} \wedge \tau_2^{-1} \varphi_{g2}^{-1}) + \frac{\varphi_{g1}}{\rho_{01}} \mathcal{T}_{u,g}(\bar{\omega}, \tau_2 \mu_4), \\
 (4.49) \quad A_{g2} &= \varphi_{g2} |\bar{v}_x| (\varphi_3^{-1} \wedge \tau_2^{-1} \varphi_{g3}^{-1}) + \frac{\varphi_{g2}}{\rho_{10}} \mathcal{T}_{u,g}(\bar{\theta}_x, \tau_2 \mu_4) + \frac{\varphi_{g2}}{\psi_1} (C_{g11} |\bar{\theta}_x| + C_{g20} |\bar{\theta}_y|), \\
 A_{g3} &= \varphi_{g3} |\bar{u}_y| (\varphi_2^{-1} \wedge \tau_2^{-1} \varphi_{g2}^{-1}) + \frac{\varphi_{g3}}{\rho_{10}} \mathcal{T}_{u,g}(\bar{\theta}_y, \tau_2 \mu_4) + \frac{\varphi_{g3}}{\psi_1} (C_{g02} |\bar{\theta}_x| + C_{g11} |\bar{\theta}_y|).
 \end{aligned}$$

In the above estimates, C_{gij} depends on $\tau_2 \mu_4$ (4.45). Now, the inequality (A.6) for $\|W_{1,i} \varphi_{gi}\|_\infty$ with weights $(\tau_2 \mu_4, \tau_2, \tau_2)$ reads

$$(4.50) \quad -d_{g1}(x) - \mu_2 \tau_2 A_{g1} \geq \lambda, \quad -d_{g2}(x) - \tau_2 A_{g2} \geq \lambda, \quad -d_{g3}(x) - \tau_2 A_{g3} \geq \lambda,$$

where we choose λ to be the same as that in (4.23). The above constraints involve the parameters $p_{71}, p_{81}, p_{91}, p_{92}, \mu, \tau_2$. The parameter p_{71} has been chosen before we compute (4.42). See the paragraph above (4.42). We choose the remaining parameters $p_{81}, p_{91}, p_{92}, \mu_2, \tau_2$ such that $p_{81} \tau_2, \tau_2 \mu_4$ are as large as possible under the above constraints. From the definitions (4.41) and (4.44), this allows us to obtain a stronger control of the solution in the far-field using the energy.

It is easy to see that $\mu_4 \tau_2 A_{g1}, \tau_2 A_{gi}$ is increasing in τ_2 . For example, in $\tau_2 A_{g2}$, we have

$$\tau_2 \varphi_{g2} |\bar{v}_x| (\varphi_3^{-1} \wedge \tau_2^{-1} \varphi_{g3}^{-1}) = \varphi_{g2} |\bar{v}_x| (\tau_2 \varphi_3^{-1} \wedge \varphi_{g3}^{-1}).$$

Moreover, for larger p_{ij} , the left hand side of (4.50) usually becomes smaller. In fact, the damping term d_i becomes smaller since the weight of the largest power $|x|^\gamma$ increases and $|x|^\gamma$ contributes less to the damping term if γ is large. See (2.27) for the computation of $|x|^\gamma$ with larger γ . Moreover, if we neglect $\tau_2^{-1} \varphi_{gi}^{-1}$ part in A_{gi} in (4.49), other quantities are increasing with respect to p_{ij} due to the weights φ_{gi} (4.41). Due to these monotonicity properties, it is not difficult to find a set of reasonable parameters (p_{ij}, μ_4) and τ_2 .

4.5.2. Weighted L^∞ estimate related to the Hölder norm. Recall from Section 2.7.4 that to control the Hölder norm of ω_1 in \mathbb{R}_+^2 , which is used to control $\|\nabla \mathbf{u}(\omega_1)\|_{C^{1/2}}$, we need to further estimate $\|\omega_1 \psi_1 x_1^{-1/2}\|_{L^\infty}$. To simplify the notation, we use $\varphi_4 = \psi_1 |x_1|^{-1/2}$ from (4.14). Using the existing estimates and derivations in Section 4.3, including (4.15), (4.19)-(4.20), we obtain

$$\partial_t(\omega_1 \varphi_4) + (\bar{c}_l x + \bar{\mathbf{u}} + \mathbf{u}) \cdot \nabla(\omega_1 \varphi_4) = -d_4(x) \omega_1 \varphi_4 + B_1(x) \varphi_4,$$

where the damping term d_4 is given below and $B_1 \varphi_4$ defined in (4.5) satisfies the following estimate

$$d_4(x) \triangleq d_1(\varphi_4) = \mathcal{T}_d(\varphi_4) + \bar{c}_\omega, \quad |B_1(x) \varphi_4| \leq \frac{\varphi_4}{\varphi_2} \|\eta_1 \varphi_2\|_\infty + \frac{\varphi_4}{\rho_{10}} \mathcal{T}_u(\bar{\omega}) \|\omega_1 \varphi_1\|_\infty.$$

The operator $\mathcal{T}_d, d_1(\cdot)$ is defined in (4.4). We want to include $\|\omega_1 \varphi_4\|_\infty$ in a new energy E_4 with

$$E_4(t) \geq \tau_1^{-1} [\omega]_{C_x^{1/2}}.$$

We have the factor τ_1^{-1} since the previous energy E_4 already controls $\tau_1^{-1} [\omega]_{C_x^{1/2}(\mathbb{R}_{++}^2)}$. In view of the estimate (2.32) and Section 2.7.4, we define

$$E_4(t) = \max(E_3(t), \tau_1^{-1} \sqrt{2} \|\omega \varphi_4\|_\infty).$$

From (2.32) and $E_3 \geq \tau_1^{-1} [\omega]_{C_x^{1/2}(\mathbb{R}_{++}^2)}$, we obtain the above inequality for $E_4(t)$. We do not use a larger weight for $\|\omega \varphi_4\|_\infty$ since it is not necessary, and it is easier to establish the condition (A.6) for $\|\omega \varphi_4\|_\infty$ with a smaller weight $\mu_i = \tau_1^{-1} \sqrt{2}$, which reads

$$(4.51) \quad -d_4 - \frac{\sqrt{2}}{\tau_1} \left(\frac{\varphi_4}{\varphi_2} + \frac{\varphi_4}{\rho_{10}} \mathcal{T}_u(\bar{\omega}) \right) \geq \lambda.$$

We choose the same λ as that in (4.23).

4.6. Estimate of some linear functionals. In the previous sections, we have performed the weighted L^∞ and $C^{1/2}$ estimates on $W_{1,i}$ for the main equations (4.1) and established the stability estimates provided that (4.23), (4.50), (4.51) hold. To close the energy estimates of (2.75), we need to further estimate the residual operators \mathcal{R} (2.74). The error part related to the approximate solution constructed numerically, e.g. $\hat{F}_i(0) - \bar{F}_i$, will be estimated in Section 6. To control \mathcal{R} , we need to control the functional $a_i(W)$ and $a_{nl,i}(W)$.

For the linear functional $a_i(W)$, we have two types. The first type is $c_\omega(\omega_1)$ from $\mathcal{K}_{1i}(\omega_1)$ (2.66). The second type is from $\mathcal{K}_{i2}(\omega_1)$ (2.68) for the approximation of $\tilde{\mathbf{u}}, \tilde{\nabla} \mathbf{u}$ (2.88), (2.82), (2.89). For $a_{nl,i}$ defined in (2.72), we need to control $c_\omega(W_1 + \hat{W}_2)$ and $\partial^2(W_1 + \hat{W}_2)(0)$. For the second type of term, we will represent it as

$$\int_{\mathbb{R}_{++}^2} \omega(y) p(y) dy$$

for some function $p(y)$ that has a fast decay, e.g. it has a decay rate faster than $|x|^{-3}$. Then we estimate it directly using the norms $\|\omega\varphi_1\|_\infty, \|\omega\varphi_{g1}\|_\infty$ in the energy. See (4.55) for an example. Next, we consider how to estimate $c_\omega(\omega_1), c_\omega(\omega_1 + \hat{\omega}_2), \partial^2(W_1 + \hat{W}_2)(0)$.

4.6.1. Controlling $c_\omega, \omega_{xy}(0)$ and $\theta_{xx}(0)$. Denote

$$(4.52) \quad \varphi_{M1}(x) \triangleq \max(\varphi_1(x), \tau_2 \mu_4 \varphi_{g1}(x)), \quad \varphi_{Mi}(x) \triangleq \max(\varphi_i(x), \tau_2 \varphi_{gi}(x)), \quad i = 2, 3.$$

From the definition of the energy (4.21), (4.44), we have the pointwise control

$$(4.53) \quad |W_{1,i}(x)| \leq \varphi_{Mi}^{-1}(x) E_3(t), \quad W_{1,1} = \omega_1, \quad W_{i,2} = \eta_1, \quad W_{i,3} = \xi_1.$$

Denote

$$(4.54) \quad f_*(y) = \frac{y_1 y_2}{|y|^4}.$$

Recall the inner product (2.5). Controlling the normalization factor (2.19)

$$c_\omega(\omega) = u_x(0) = -\frac{4}{\pi} \int_{\mathbb{R}_{++}^2} \frac{y_1 y_2}{|y|^4} \omega(y) dy = -\frac{4}{\pi} \langle \omega, f_* \rangle$$

is difficult since the integrand $\frac{y_1 y_2}{|y|^4}$ decays slowly (it is not L^1 integrable) and our weight for ω_1 is very weak in the far-field. See (4.41) and (4.44). Using (4.53) and a direct estimate, we get

$$(4.55) \quad |c_\omega(\omega_1)| \leq E_3 \frac{4}{\pi} \int_{\mathbb{R}_{++}^2} \frac{y_1 y_2}{|y|^4} \varphi_{M1}^{-1}(y) dy = C_1 E_3,$$

where C_1 is about $170 - 200$ and is very large. Although this estimate and constant only enter the energy estimates via the lower order and small terms, e.g. the residual operators and the nonlinear terms, it requires us to obtain smaller residual error in the computation. To ease the computation burden, we seek a more effective estimate based on the evolution of $c_\omega(\omega_1)$.

4.6.2. Controlling of $c_\omega(\omega_1)$. Following [12, 13], we perform the estimates based on the ODE of c_ω . Using the main equations (4.1) and dropping the nonlinear and error terms, we can derive the evolution of $\langle \omega_1, f_* \rangle, \langle \eta_1, f_* \rangle$

$$(4.56) \quad \begin{aligned} \frac{d}{dt} \langle \omega_1, f_* \rangle &= \bar{c}_\omega \langle \omega_1, f_* \rangle - \langle (\bar{c}_l x + \bar{\mathbf{u}}) \cdot \nabla \bar{\omega}, f_* \rangle - \langle \mathbf{u}_A \cdot \nabla \omega_1, f_* \rangle + \langle \eta_1, f_* \rangle, \\ \frac{d}{dt} \langle \eta_1, f_* \rangle &= 2\bar{c}_\omega \langle \eta_1, f_* \rangle - \langle (\bar{c}_l x + \bar{\mathbf{u}}) \cdot \nabla \eta_1, f_* \rangle - \langle \bar{u}_x, \eta_1 f_* \rangle - \langle \bar{v}_x, \xi_1 f_* \rangle \\ &\quad - \langle \mathbf{u}_A \cdot \nabla \bar{\theta}_x + \mathbf{u}_{x,A} \cdot \nabla \bar{\theta}, f_* \rangle, \end{aligned}$$

where $\langle \cdot, \cdot \rangle$ (2.5) is the standard inner product on \mathbb{R}_{++}^2 . Here, we derive the evolution of $\langle \eta_1, \varphi_* \rangle$ to control it in the first equation. Similar ideas have been used in [12, 13]. Using integration by parts, we get

$$-\int (\bar{c}_l y + \bar{\mathbf{u}}) \cdot \nabla g(y) f_*(y) dy = \int g(y) \nabla \cdot ((\bar{c}_l y + \bar{\mathbf{u}}) f_*(y)) dy = \int g(y) \bar{\mathbf{u}} \cdot \nabla f_*(y) dy,$$

where we have used $\nabla \cdot (y f_*(y)) = 0$, which is an algebraic property of f_* (4.54), and $\nabla \cdot (\bar{\mathbf{u}} f_*) = \bar{\mathbf{u}} \cdot \nabla f_*$.

The first terms on the right hand side are damping terms since $\bar{c}_\omega \approx -1$. The advantage of the above ODE system is that the integrands, e.g. $g(y) \bar{\mathbf{u}} \cdot \nabla f_*$, have faster decay than $g(y) \varphi_*$ since $\bar{\mathbf{u}}$ grows sublinearly.

For the nonlocal terms involving $\mathbf{u}_A, \nabla \mathbf{u}_A$, we apply the estimates (4.45). For the local terms other than $\langle \omega_1, f_* \rangle, \langle \eta_1, f_* \rangle$, we use (4.53) to estimate them. Performing energy estimates, we can estimate $\langle \omega_1, \varphi_* \rangle$ and $\langle \eta_1, \varphi_* \rangle$.

Improvement. We can further improve the above estimate by decomposing

$$\langle \omega_1, f_* \rangle = \langle \omega_1, \chi f_* \rangle + \langle \omega_1, (1 - \chi) f_* \rangle, \quad \langle \eta_1, f_* \rangle = \langle \eta_1, \chi f_* \rangle + \langle \eta_1, (1 - \chi) f_* \rangle,$$

where χ is a smooth cutoff function supported away from the origin. We derive the ODEs for $\langle \omega_1, \chi f_* \rangle, \langle \eta_1, \chi f_* \rangle$ similar to (4.56), and perform energy estimates on these terms. For the second part $\langle \omega_1, (1 - \chi) f_* \rangle$ with integrand supported near 0, we estimate it directly using (4.53)

$$|\int \omega_1 (1 - \chi) f_*| \leq E_3 \|(1 - \chi) f_* \varphi_1^{-1}\|_{L^1}.$$

The motivation for the above decomposition is that the estimate via the ODE system is more effective to the control the far-field part of the integral $\int \omega_1 f_*$ since the integrand in the ODE system has faster decay. For the integrand near 0, since our weight φ_1 is singular and large near 0, we can control it effectively using a direct estimate.

We choose $\chi(x, y) = \chi_e(\frac{x-\nu_3}{\nu_3}) \chi_e(\frac{y-\nu_3}{\nu_3})$ with a suitable support size ν_3 , where χ_e is the cutoff function defined in (F.1). Then we perform energy estimate on the above system and show that the condition (A.6) is satisfied by choosing a weight $\frac{1}{85}$ for $c_\omega(\omega_1)$.

4.6.3. Controlling $c_\omega(\omega)$. Recall that $W_1 + \hat{W}_2 = (\omega, \eta, \xi)$ is the solution to (2.65). We use similar ideas to estimate $c_\omega(\omega)$. Using (2.65) and focusing on the linear terms, we derive the ODEs for $\langle \omega, f_* \rangle, \langle \eta, f_* \rangle$

$$(4.57) \quad \begin{aligned} \frac{d}{dt} \langle \omega, f_* \rangle &= \bar{c}_\omega \langle \omega, f_* \rangle + c_\omega \langle \bar{f}_{c_\omega, 1}, f_* \rangle - \langle (\bar{c}_l x + \bar{\mathbf{u}}) \cdot \nabla \omega, f_* \rangle - \langle \bar{\mathbf{u}} \cdot \nabla \bar{\omega}, f_* \rangle + \langle \eta, f_* \rangle, \\ \frac{d}{dt} \langle \eta, f_* \rangle &= 2\bar{c}_\omega \langle \eta, f_* \rangle + c_\omega \langle \bar{f}_{c_\omega, 2}, f_* \rangle - \langle (\bar{c}_l x + \bar{\mathbf{u}}) \cdot \nabla \eta, f_* \rangle - \langle \bar{u}_x, \eta f_* \rangle - \langle \bar{v}_x, \xi f_* \rangle \\ &\quad - \langle \bar{\mathbf{u}} \cdot \nabla \bar{\theta}_x + \bar{\mathbf{u}}_x \cdot \nabla \bar{\theta}, f_* \rangle. \end{aligned}$$

Different from (4.56), the above system contains extra terms $c_\omega \langle f_{c_\omega i}, f_* \rangle, i = 1, 2$. For the ω equation, this term is an additional damping term

$$c_\omega \langle f_{c_\omega 1}, f_* \rangle = -\frac{4}{\pi} \langle \omega, f_* \rangle \cdot \langle f_{c_\omega 1}, f_* \rangle \approx -2.5 \langle \omega, f_* \rangle.$$

Thus, we have better estimate for $c_\omega(\omega)$ than $c_\omega(\omega_1)$. For the nonlocal terms in (4.57), we decompose them into three parts. For example, we have

$$\langle \bar{\mathbf{u}} \cdot \nabla \bar{\omega}, f_* \rangle = \langle (\bar{\mathbf{u}}_A(\omega_1) + \hat{\mathbf{u}}(\omega_1) + \tilde{\mathbf{u}}(\omega_2)) \cdot \nabla \bar{\omega}, f_* \rangle \triangleq I_1 + I_2 + I_3.$$

For I_1 , the estimate is similar to that in Section 4.6.2. For I_2 , we can rewrite it as an integral of ω_1 since

$$\tilde{\mathbf{u}}(\omega_1) = \sum_{1 \leq i \leq n} \langle \omega_1, f_i \rangle g_i$$

for some functions f_i, g_i and n . It follows

$$\langle \tilde{\mathbf{u}}(\omega_1), \bar{\omega}_x f_* \rangle = \sum_{1 \leq i \leq n} \langle \omega_1, f_i \rangle \cdot \langle g_i, \bar{\omega}_x f_* \rangle = \langle \omega_1, \sum_{1 \leq i \leq n} \bar{a}_i f_i \rangle, \quad \bar{a}_i = \langle g_i, \bar{\omega}_x f_* \rangle.$$

We can apply (4.53) to further estimate it. The advantage of the above estimate is that we exploit the cancellations among $\bar{a}_i f_i$ by performing an argument similar to integration by parts and rewriting an integral of the nonlocal terms to the local term. For I_3 , we use the formula of $\hat{\mathbf{u}}_A$ to obtain its sharp estimate.

For the local terms in (4.57) except for $\langle \omega, f_* \rangle, \langle \eta, f_* \rangle$, we decompose it into the integrals of (ω_1, η_1) and of $(\hat{\omega}_2, \hat{\eta}_2)$, and then use (4.53) and the formulas of $\hat{\omega}_2, \hat{\eta}_2$ (2.73) to estimate them. We refer to (2.75) in Section 2.10.4 for the decomposition of $\omega = \omega_1 + \hat{\omega}_2$ and $\eta = \eta_1 + \hat{\eta}_2$.

Using the above estimates, we can choose a weight $\frac{1}{65}$ for the $c_\omega(\omega)$.

4.6.4. Controlling $\omega_{xy}(0), \eta_{xy}(0), \xi_{xx}(0)$. To control $\omega_{xy}(0), \eta_{xy}(0), \xi_{xx}(0)$, we first note that $\eta_{xy}(0) = \xi_{xx}(0) = \theta_{xxy}(0)$ since the solution to (2.65) satisfies $\eta = \theta_x, \xi = \theta_y$ (2.20).

Recall the ODEs for $\omega_{xy}(0), \theta_{xxy}(0)$ in (2.67). Linearizing it around the approximate steady state and using the normalization conditions (2.19), (2.22), we yield the equations for the perturbations

$$(4.58) \quad \begin{aligned} \frac{d}{dt} \omega_{xy}(0) &= (-2\bar{c}_l + \bar{c}_\omega) \omega_{xy}(0) + \theta_{xxy}(0) + c_\omega \bar{\omega}_{xy}(0) + c_\omega \omega_{xy}(0) + \bar{\partial}_{xy} \mathcal{F}_1(0), \\ \frac{d}{dt} \theta_{xxy}(0) &= (-2\bar{c}_l + 2\bar{c}_\omega - \bar{u}_x(0)) \theta_{xxy}(0) + c_\omega \bar{\theta}_{xxy}(0) + c_\omega \theta_{xxy}(0) + \bar{\partial}_{xy} \mathcal{F}_2(0), \end{aligned}$$

where $\bar{\mathcal{F}}_i$ is defined in (2.2).

Note that the matrix involving $\omega_{xy}(0), \theta_{xxy}(0)$ has negative eigenvalues. After we obtain the ODE for c_ω , we can diagonalize the above ODE system and estimate $\omega_{xy}(0), \theta_{xxy}(0)$. Using the above ODEs, we can choose a weight $\frac{1}{10}$ for $\theta_{xxy}(0)$, and $\frac{1}{5}$ for $\omega_{xy}(0)$.

Then we define our final energy $E_4(t)$ to close the estimates

$$(4.59) \quad \begin{aligned} E_4(t) &\triangleq \max \left(E_3(t), \mu_5 |c_\omega(W_1)|, \mu_6 |c_\omega(\omega)|, \mu_7 |\theta_{xxy}(0)|, \mu_8 |\omega_{xy}(0)| \right), \\ \mu_5 &= \frac{1}{85}, \quad \mu_6 = \frac{1}{65}, \quad \mu_7 = \frac{1}{10}, \quad \mu_8 = \frac{1}{5}. \end{aligned}$$

where the energy E_3 is defined in (4.44). See also (4.21), (4.25).

4.7. Estimate \hat{W}_2 and the residue operator. Using the estimates in the previous section on the time dependent factor, we can control the residue error (2.74). To illustrate the ideas of the estimate, we want to control the error \mathcal{R} and estimate the solution

$$(4.60) \quad \mathcal{R} = \sum_{i=1}^n \int_0^t b_i(s) \hat{\mathcal{R}}_i(t-s) ds, \quad G = \sum_{i=1}^n \int_0^t b_i(s) \hat{G}_i(t-s) ds,$$

for some time-dependent factor $b_i(s)$ depending on W_1 and $W_1 + \hat{W}_2$, where $\hat{\mathcal{R}}_i$ is the residue error in solving a specific equation, e.g., $\hat{\mathcal{R}}_i = (\partial_t - \mathcal{L}) \hat{F}_i$ in (2.74), and \hat{G}_i is the numeric approximation of some solution, e.g. $\hat{G}_i = \hat{F}_i$ in (2.73). The difficult part is to control the time integral part in (2.73), (2.74). Thus, we focus on the above variables. The time-dependent factor $b_i(s)$ can be controlled using the energy estimate

$$|b_i(s)| \leq c_i E_4(s).$$

Since we will use a bootstrap argument to show that $E_4(s)$ is below some threshold E_* for all time, under such an assumption we further have

$$(4.61) \quad |b_i(s)| \leq c_i E_*$$

for some threshold E_* to be determined.

We remark that $\hat{\mathcal{R}}_i, \hat{G}_i$ only depend on the numeric construction. From Section 6, since we construct \hat{G}_i such that it is piecewise cubic in time, the residue $\hat{\mathcal{R}}_i(t-s)$ is also piecewise cubic in time.

4.7.1. Linearity and estimate \mathcal{R} and G . To estimate \mathcal{R}, G (4.60), we have a crucial observation that both \mathcal{R} and G are linear in the numeric solution \hat{G}_i and residue $\hat{\mathcal{R}}_i$.

To control the weighted norm of \mathcal{R}, G , we only need to control the piecewise derivatives bound. Using linearity in $\hat{G}_i, \hat{\mathcal{R}}_i$, and (4.61), for $\alpha, \beta \geq 0$, we have

$$(4.62) \quad |\partial_1^\alpha \partial_2^\beta \mathcal{R}(t, x)| = \left| \sum_{i \leq n} \int_0^t b_i(s) \partial_1^\alpha \partial_2^\beta \hat{\mathcal{R}}_i(t-s) ds \right| \leq \sum_{i \leq n} c_i E_* \int_0^t |\partial_1^\alpha \partial_2^\beta \hat{\mathcal{R}}_i(s)| ds$$

In the above summation, the integral only depends on $|\partial_1^\alpha \partial_2^\beta \mathcal{R}_i(s)|$ and $\int_0^t |\partial_1^\alpha \partial_2^\beta \mathcal{R}_i(s)| ds$ is monotone in time t . Moreover, we completely decouple the numeric solution $\hat{\mathcal{R}}_i$ and the time-depend factor $b_i(t)$. Since $\hat{\mathcal{R}}_i$ is a piecewise cubic polynomial in time, we have

$$\hat{\mathcal{R}}_i(t_m + s) = \sum_{l \leq 3} \hat{\mathcal{R}}_{i,m,j} s^j, \quad s \in [0, t_{m+1} - t_m]$$

in each time interval $I_m = [t_m, t_{m+1}]$ in our construction in Section 6 for some time-independent residue error $\hat{\mathcal{R}}_{i,m,j}$. The main term is given by $\hat{\mathcal{R}}_{i,m,0}$. Other terms have a small factor s which is bounded by the time step. Therefore, using triangle inequality, we yield

$$|\partial_1^\alpha \partial_2^\beta \mathcal{R}_i(t_m + s)| \leq \sum_{j \leq 3} |\partial_1^\alpha \partial_2^\beta \hat{\mathcal{R}}_{i,m,j}| s^j.$$

Plugging the above estimates in (4.62), we can bound $|\partial_1^\alpha \partial_2^\beta \mathcal{R}(t, x)|$ in terms of the linear combination of $|\partial_1^\alpha \partial_2^\beta \hat{\mathcal{R}}_{i,m,j}|$,

$$\int_0^{t_M} |\partial_1^\alpha \partial_2^\beta \hat{\mathcal{R}}_i(s)| ds \leq \sum_{j \leq 3} \sum_{i \leq M-1} |\partial_1^\alpha \partial_2^\beta \hat{\mathcal{R}}_{i,m,j}| \int_0^\tau s^j ds,$$

where we use uniform time step $t_{j+1} - t_j = \tau$. Therefore, to control $|\partial_1^\alpha \partial_2^\beta \mathcal{R}(t, x)|$, we only need to track the sum of the discrete residue error $|\partial_1^\alpha \partial_2^\beta \hat{\mathcal{R}}_{i,m,j}|$ over m .

As a result, once we have estimate of the piecewise derivatives bound of $\hat{\mathcal{R}}_{i,m,j}$, we can assemble them to yield the bound for \mathcal{R} . We can also control the weighted piecewise bounds of \mathcal{R} using the associated bounds for $\hat{\mathcal{R}}_{i,m,j}$. Then we can apply the methods in Section G to estimate the weighted L^∞ and $C^{1/2}$ norm of \mathcal{R} rigorously.

Then same ideas apply to estimate G in (4.60).

Remark 4.2. Using linearity and triangle inequality, we can assemble the estimates for \mathcal{R} from the estimates of each mode $\int_0^t b_i(s) \hat{\mathcal{R}}_i(t-s) ds$. In practice, this means that we can implement the above estimate for each individual mode completely in parallel.

Although we estimate G (4.60) by applying the triangle inequality and combining the estimate of different modes, such an estimate does not lead to a constant of $O(n)$ since the different solutions are large in different regions. In fact, when we construct the approximation terms for the velocity in Section 7, we apply some partition of unity. The coefficients of different approximation terms are large in different region. These coefficients are the initial condition for the approximate solution (2.73). We can exploit these properties in the above estimates and do not obtain a large constant when we combine the estimates of different modes.

The same reasoning applies to the estimate of the residue operator.

4.7.2. Estimate the nonlocal parts. In the estimate, we also need to control the nonlocal terms of G , e.g. $\mathbf{u}(\hat{W}_2)$ appears in the nonlinear terms in (2.69). The ideas and derivations in Section 4.7.1 generalizes to linear operator \mathcal{K} . We focus on the estimate of $\mathbf{u}(G)$ in (4.60). We can decompose the velocity as the numeric approximation and the error $\hat{\varepsilon}_i$,

$$(4.63) \quad \mathbf{u}(\hat{G}_i(s)) = \mathbf{u}((- \Delta) \hat{\psi}_i^N(s)) + \mathbf{u}(\hat{\varepsilon}_i), \quad \hat{\varepsilon}_i = \hat{G}_i(s) - (- \Delta) \hat{\psi}_i^N(s),$$

where $\hat{\psi}^N$ is our numeric solution for the Poisson equation $-\Delta \hat{\psi}^N = \hat{G}_i$, and $\hat{\varepsilon}_i$ is the error. Since \hat{G}_i is piecewise cubic in time, we can also construct the associated $\hat{\psi}_i^N$ cubic in time. The first part is our numeric solution for the velocity \mathbf{u} , which is local in $\hat{\psi}_i^N$

$$\mathbf{u}((- \Delta) \hat{\psi}_i^N) = \nabla^\perp \hat{\psi}_i^N.$$

Applying \mathbf{u} to (4.60) and using linearity, we yield

$$\mathbf{u}(G) = \sum_{i \leq n} \int_0^t b_i(s) \mathbf{u}(\hat{G}_i(t-s)) ds = \sum_{i \leq n} \int_0^t b_i(s) \nabla^\perp \hat{\psi}_i^N(t-s) ds + \sum_{i \leq n} \int_0^t b_i(s) \mathbf{u}(\hat{\varepsilon}_i) ds \triangleq I + II.$$

The first part is the main term, which can be estimated using the method in Section 4.7.1. To control II , using linearity, we rewrite it as follows

$$II = \mathbf{u} \left(\sum_{i \leq n} \int_0^t b_i(s) \hat{\varepsilon}_i ds \right).$$

We can estimate the velocity by applying functional inequalities

$$\|\mathbf{u}(f)\|_X \leq C_{XY} \|f\|_Y,$$

between two spaces X, Y . Thus to control II , we only need to control the error

$$\sum_{i \leq n} \int_0^t b_i(s) \hat{\varepsilon}_i ds,$$

which is small. Since $\hat{\varepsilon}_i$ depends on $\hat{G}_i, \hat{\psi}_i^N$ locally (4.63), again, we can apply the method in Section 4.7.1 to control it. This allows us to control the velocity of G effectively. We also apply these ideas to estimate the error in solving the Poisson equations in Section 6.

Using the above methods and the methods in Section 6, Appendix G, we can control the residue operator (2.74), which is much smaller than the damping factors we obtain in the weighted L^∞ and Hölder estimate. The largest term in the residue operator is associated to the term $c_\omega(W_1) \bar{f}_{c_\omega, i}, i = 1, 2, 3$ from (2.66) since we only have a poor estimate for $c_\omega(W_1)$

$$|c_\omega(W_1)| \leq 85E_4(t),$$

which leads to a large constant $c_1 = 85$ in (4.61). On the other hand, since the functions $\bar{f}_{c_\omega, i}, i = 1, 2, 3$, are smooth, we have a very small residue error $(\partial_t - \mathcal{L})\hat{F}_1$, i.e. $\hat{\mathcal{R}}_i$ in (4.60).

Remark 4.3. We remark that we only need to construct the approximate solution $\hat{G}_i(s)$ in a finite time T_1 since the solution decays over time. See Section 6.6 for more discussions.

Near 0, For a domain D near the origin, the residue operator enjoys the estimate

$$\max_{i \leq 3} \|\mathcal{R}_{l,i}(W_1) \varphi_i\|_{L^\infty(D)} \leq 0.02E_4(t).$$

where $\mathcal{R}_{l,i}$ is the i -th component of \mathcal{R}_l (2.74). Note that the damping factors in the weighted L^∞ estimate and Hölder estimate are large. See Figure 5, 7 for an illustration. The weighted estimate of the residue operator in the bulk of \mathbb{R}_2^{++} is much better since the weight is nonsingular. The nonlinear part R_{nl} (2.74) is much smaller.

4.8. Nonlinear estimates. The nonlinear stability estimate of $W_1 = (\omega_1, \eta_1, \xi_1)$ in (2.75) is relatively simple after we obtain the linear stability. Using the estimates established in Sections 4.3 and 4.5.1, including the L^∞ estimates of $\nabla \mathbf{u}, \omega_1, \eta_1, \xi_1$, we can control the nonlinear parts associated to W_1 in (2.75). For \hat{W}_2 , it depends on W_1 and can be estimated using the methods in Section 4.7. We remark that to close the nonlinear stability, we need to check the condition (A.14).

Recall the nonlinear operators \mathcal{N} from (2.1) and NF from (2.71). We focus on the estimate of the nonlinear part $\mathcal{N}_1(W_1 + \hat{W}_2) - NF_1(W_1 + \hat{W}_2)$ in the ω equation (2.75), which takes the form

$$(4.64) \quad J_0 \triangleq -\mathbf{u}(\omega) \cdot \nabla \omega + c_\omega(\omega) \omega - c_\omega \omega_{xy}(0) \bar{f}, \quad \bar{f} = \bar{f}_{c_\omega, 1}$$

where $\omega = W_{1,1} + \hat{W}_{2,1}$, and $\bar{f}_{c_\omega, i}$ is defined in (2.64). To simplify the notation, we introduce the above \bar{f} . Note that in the weighted $L^\infty(\varphi_1)$ estimate of ω_1 , the transport term $\mathbf{u}(\omega) \cdot \nabla \omega_1$ leads to a nonlinear term

$$\varphi_1^{-1}(\mathbf{u}(\omega) \cdot \nabla \varphi_1) \omega_1.$$

See (4.6) and (4.4). Note that we do not need to estimate the advection in the weighted $L^\infty(\varphi_1)$ estimate

$$\mathbf{u}(\omega) \cdot \nabla(\omega_1 \varphi_1).$$

Thus, instead of estimating J_0 , we need to estimate the following J

$$(4.65) \quad J = -\mathbf{u}(\omega) \cdot \nabla \omega_2 + c_\omega(\omega) \omega - c_\omega \omega_{xy}(0) \bar{f} + \varphi_1^{-1}(\mathbf{u}(\omega) \cdot \nabla \varphi_1) \omega_1,$$

which vanishes cubically near the origin. We have a similar term in the Hölder estimate of W_1 .

Next, we focus on the weighted L^∞ estimate. The Hölder estimate is similar but contains more terms. The constants in our estimate of the nonlinear term in the Hölder estimate are actually smaller due to the factor τ_1^{-1} in the energy E_2 (4.25). Our goal is to show that the nonlinear term can be all bounded by

$$(4.66) \quad 12000E_4^2(t),$$

in the estimate of each term in the energy E_4 (4.59), e.g. $\tau^{-1}\|\omega_1\psi_1\|_{C_{g_1}^{1/2}}$ and $\mu_5c_\omega(W_1)$ where E_4 is defined in (4.59). The above estimate of $\mathcal{N}_i(x)$ can be significantly improved in the region away from the origin. We refine the estimate in the region where the stability factors in the linear estimate is not too large.

4.8.1. The main term in the near-field. Recall from the discussion in Section 2.10.4 that $\omega = \omega_1 + \hat{\omega}_2$ and $\omega_1 = O(|x|^3)$ near 0. Therefore, we have $\omega_{xy}(0) = \partial_{xy}\hat{\omega}_{20}$. We decompose (4.65) as follows

$$\begin{aligned} J &= -\mathbf{u}(\omega) \cdot \nabla \hat{\omega}_2 + c_\omega(\omega)\omega - c_\omega\omega_{xy}(0)\bar{f} + \varphi_1^{-1}(\mathbf{u}(\omega) \cdot \nabla \varphi_1)\omega_1 \\ &= \left(-\mathbf{u}(\omega) \cdot \nabla \hat{\omega}_2 + c_\omega\hat{\omega}_2 - c_\omega\hat{\omega}_{2,xy}(0)\bar{f} \right) + \left(c_\omega\omega_1 + \varphi_1^{-1}(\mathbf{u}(\omega) \cdot \nabla \varphi_1)\omega_1 \right) \triangleq J_1 + J_2. \end{aligned}$$

The term in our estimate that has the largest constant is J_1 due to the poor estimate of $c_\omega(\omega)$ and $c_\omega(W_1)$ in terms of the energy E_4 (4.59).

$$(4.67) \quad |c_\omega(\omega)| \leq \mu_6 E_4, \quad |c_\omega(W_1)| \leq \mu_5 E_4.$$

From (4.61) and Section 4.7, in our estimate of $\hat{\omega}_2$, we need to pay a large constant $c_1 = \mu_5$. In the nonlinear estimate of $c_\omega\hat{\omega}_2$, we have a large constant $\mu_5\mu_6$, which causes the poor bound in the near field.

In comparison, for ω_1 , by definition, we have

$$\|\omega_1\varphi_1\|_{L^\infty} \leq E_4, \quad |c_\omega\omega_1\varphi_1| \leq \mu_6 E_4^2,$$

where the constant is much smaller. Similarly, the velocity with approximation \mathbf{u}_A (4.2) also has size 1. In fact, we have developed many inequalities to show that it is small.

Therefore, we should mainly focus on J_1 . Near the origin, we further decompose J_1 as follows

$$\begin{aligned} J_1 &= \tilde{\mathbf{u}}(\omega) \cdot \nabla \hat{\omega}_2 + c_\omega(\omega)(\hat{\omega}_2 - x\hat{\omega}_{2,x} + y\hat{\omega}_{2,y} - c_\omega\hat{\omega}_{2,xy}(0)\bar{f}) \\ &= \tilde{\mathbf{u}}(\omega_1) \cdot \nabla \hat{\omega}_2 + \tilde{\mathbf{u}}(\omega_2) \cdot \nabla \hat{\omega}_2 + c_\omega(\omega)(\hat{\omega}_2 - x\hat{\omega}_{2,x} + y\hat{\omega}_{2,y} - c_\omega\hat{\omega}_{2,xy}(0)\bar{f}) \triangleq J_{11} + J_{12} + J_{13}, \end{aligned}$$

where we have used the notation (2.63). The first term is small relative to the second and the third term. The term $\tilde{\mathbf{u}}(\omega_1)$ can be estimated similar to that of $\mathbf{u}_A(\omega_1)$ and the constant in the estimate of $\tilde{\mathbf{u}}(\omega_1)$ is of order 1. The reason why we have much better estimate of $\tilde{\mathbf{u}}(\omega_1)$ than $\mathbf{u}(\omega_1)$ or $c_\omega(\omega_1)$ is that the term $(c_\omega x_1, -c_\omega x_2)$ captures the slow decay part in the kernel of \mathbf{u} . See the estimate of the kernel in (4.19), (4.20). Since our weights $\varphi_1, \varphi_{1,g}$ for ω_1 is strong in the near-field and the kernel in $\tilde{\mathbf{u}}(\omega_1)$ has a fast decay, we have a much better estimate for $\tilde{\mathbf{u}}(\omega_1)$ and x in the near-field.

For the second and the third term, we can further decompose $\hat{\omega}_2$ according to different modes. The dominated term in \hat{W}_2 is generated by $c_\omega(W_1)\bar{f}_{c_\omega,i}$ in (2.66)

$$I = \int_0^t c_\omega(W_1)(s)\hat{F}_1(t-s)ds.$$

Using the method in Section 4.7, we can estimate $J_{12}(\hat{\omega}_2) + J_{13}$ for $\hat{\omega}_2$ generated by $c_\omega(W_1)\bar{f}_{c_\omega,i}$. Such term is the main term in the nonlinear estimate in the near-field. Other terms are much smaller since they do not involve the product of two large constants. In the left figure in Figure 9, we plot the piecewise bounds of $(J_{12}(\hat{\omega}_2) + J_{13})\varphi_1$. In the right figure, we plot the estimate of a similar term in the η_1 equation. In both cases, such a term is bounded by $6200E_4^2$. We have a large bound since we multiply the constants $\mu_5\mu_6$ (4.67). Since the approximate solution decays, the estimate becomes much better for large x . Other terms in the estimate are much smaller since it only involves one of these two constants. In particular, we can establish the conservative

bounds in the near field. We can obtain a uniform estimate over time since the solution decays in time and we only construct \hat{F}_i in a finite time. See Section 6.6.

For other weighted L^∞ or the Hölder estimates, the main terms in the near-field are also determined by the term generated $c_\omega(W_1)\bar{f}_{c_\omega,i}$ in \hat{W}_2 .

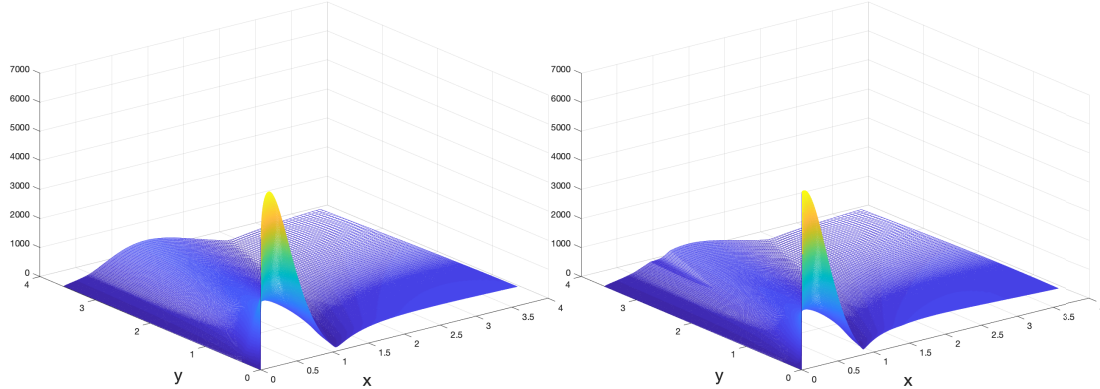


FIGURE 9. Weighted L^∞ estimate of the main terms in the near field. Left figure: estimate in the ω -equation; right figure: estimate in the η -equation.

4.8.2. The main term in the far-field. Due to the decay of \hat{W}_2 in the far-field, the nonlinear terms involving \hat{W}_2 are small. The main terms in the far-field are from W_1 . We focus on a typical term $u_x(\omega_1)\eta_1$ in the nonlinear terms in \mathcal{N}_2 (2.1). To estimate such a term, we write it as follows

$$-u_x(\omega_1)\eta_1 = -u_{x,A}(\omega_1)\eta_1 + \hat{u}_x(\omega_1)\eta_1,$$

where the approximation \hat{u}_x is constructed in (2.89), (2.82), (2.88). In the far-field, we only have $C_{f0}(x,y)u_x(\omega_1)(0)$ in the first approximation (2.82) and the second approximation term (2.88). For \hat{u}_x , the term is not large

$$\|C_{f0}(x,y)u_x(\omega_1)(0)\eta_1\varphi_2\|_\infty \leq E_4\mu_5.$$

The second approximation term involves $I_i - u_x(0)$, which is an integral of ω_1 in the near-field. It can be estimated directly using the pointwise control (4.53).

Since our weight $\varphi_{g,1}$ grows slowly $|x|^{1/16}$ and we choose a small parameter $\tau_2\mu_4$ in the energy E_3 (4.44), the leading order behavior in the upper bound (4.53) is $(\tau_2\mu_4)^{-1}|x|^{-1/16}$ with $\tau_2\mu_4)^{-1} \approx 64$. As a result, we have weak control of ω_1 and the velocity $\nabla \mathbf{u}_A$. In particular, we have the estimate

$$|u_{A,x}| < 1000E_4$$

using the estimates in Sections 4.3, 4.5.1. It follows

$$\|\varphi_1 u_{x,A}(\omega_1)\eta_1\|_\infty < \|u_{x,A}\|_\infty \cdot \|\eta_1\varphi_1\|_\infty < 1000E_4^2.$$

Such a constant is still much smaller than (4.66). We remark that in the far-field, we have much larger stability factors in the linear estimates in Sections 4.3-4.5.1 since the coefficients of the nonlocal term decay. For example, in the weighted L^∞ estimate, for large x , the stability factors for η_1 is larger than 1. Thus, controlling the nonlinear terms in the far-field are relatively simple.

4.8.3. *Estimate near the region with small stability factor.* In the weighted L^∞ estimate and the Hölder estimate, we have a stability factor with a minimum about 0.08. Notice that we have a small stability factor only in the bulk region, x away from the origin and in the near-field. We need to discuss a few cases more carefully.

In the weighted L^∞ , we can have a large constant in the nonlinear estimates, and the stability factor is not very large for $|x| \leq 0.2$, especially x around 0.1. In such a region, we have a stability factor ≥ 0.13 . We need a tighter bound for the constant in the nonlinear estimate. In particular, the nonlinear term can be bounded by $8000E_*^2$. Thus, to choose the bootstrap threshold and close the argument, we need to consider the constraint

$$8000E_*^2 < 0.13E_*$$

according to (A.14). For the threshold $E_* = 5 \cdot 10^{-6}$ we will choose, the left hand side is $0.04E_*$ and the inequality is valid.

We need to check a few cases similarly. Note that other cases enjoy similar or better estimates. We refer the discussion to the upcoming Supplementary Material.

4.8.4. *Estimate of the error terms.* Note that the residue error in the weighted norm is very small in the bulk region. In the weighted $L^\infty(\varphi_1)$, it is smaller than $2 \cdot 10^{-8}$ in the near-field and near the origin. See Figure 2. Such an error is very small compared to the damping factor. For example, for a bootstrap threshold $E_* = 5 \cot 10^{-6}$, we have $2 \cdot 10^{-8} = 0.004E_*$, which is very small compared to the stability terms, e.g. λE_* , with $\lambda = 0.08$.

Near the origin (the first 3 grid points), we have a relative large residue error, which is about $4 \cdot 10^{-7}$ in the weighted $L^\infty(\varphi_1)$ norm. See Figure 2. On the other hand, we design our weights such that we have relative large damping factors. In particular, the stability factors in the $L^\infty(\varphi_1)$ estimate of ω_1 is larger than 0.5. At the bootstrap threshold $E_* = 5 \cdot 10^{-6}$, we have

$$0.5 \cdot 5 \cdot 10^{-6} = 2.5 \cdot 10^{-6}$$

which is much larger than the weighted residue error near the origin. Similar consideration applies to the estimates of η_1, ξ_1 .

In the Hölder estimate, we have a large damping factors near the origin. Thus, it is easy to check the stability conditions (A.14).

The estimate of the nonlinear terms and the error terms in the estimate of the linear functionals in Section 4.6.3 are simpler since the functional, e.g. $c_\omega(W_1), \omega_{xy}(0)$ are constants in space.

For the error in solving the Poisson equations, i.e. the error between $\bar{\psi}^N$ and $(-\Delta)^{-1}\bar{\omega}$, where $\bar{\psi}^N$ is our numeric approximation of the stream function $(-\Delta)^{-1}\bar{\omega}$, we use the method in Section 6 to show that it is small enough.

Remark 4.4. We remark that an advantage of the stability condition in (A.14) is that it depends on the estimate locally. In our estimates, we have small stability factors in the region away from the origin, which is different from the region with large weighted residue error. We remark that we do not have the situation, where the weighted residue error is large, constants in the nonlinear estimates are large, and the stability factors are small. This allows us to close the nonlinear estimates using Lemma A.3.

4.8.5. *Nonlinear stability and finite time blowup.* To close the nonlinear estimates, we choose the threshold $E_* = 5 \cdot 10^{-6}$ for the bootstrap argument in Lemma A.3. Using Lemma A.3, we can obtain that if the initial perturbation satisfies

$$E_4(\omega_1(0), \eta_1(0), \xi_1(0)) < E_*,$$

then we

$$E_4(\omega_1(t), \eta_1(t), \xi_1(t)) < E_*$$

for all time $t > 0$. With the estimates of W_1 , we can control \bar{W}_2 using the estimates in Sections 4.6, 4.7. In particular, we can obtain

$$\|W_{1,i} + \hat{W}_{2,i}\|_\infty < 1000E_*, \quad |c_\omega(\omega)| < 100E_*.$$

Recall the normalization condition (2.19). We also have $|u_x(0)| = |c_\omega| < 100E_*$.

Moreover, since we choose 0 initial condition for \hat{W}_2 , we have $W_1 = (\omega, \eta, \xi) = (\omega, \theta_x, \theta_y)$ at the initial time. Therefore, we prove the estimates in Theorem 2. Passing from the stability analysis to finite time blowup follows standard rescaling argument [12], [14].

5. CONSTRUCTION OF AN APPROXIMATE STEADY STATE

Following our previous works with Huang on the De Gregorio model [14] and the Hou-Luo model [13], we construct the approximate steady state to the dynamic rescaling equations (2.10) with the normalization conditions (2.11) by solving (2.10) numerically for a long enough time. The residual error is estimated *a-posteriori* and incorporated in the energy estimate as a small error term. It is extremely challenging to obtain an approximate steady state with a *sufficiently* small residual error, e.g. of order 10^{-7} , since the solution is supported on the whole \mathbb{R}_+^2 with a slowly decaying tail in the far-field, e.g., $\omega(t, x) \sim |x|^{-1/3}$ for large x . See (5.1). If we solve (2.10) in a very large domain to capture the far-field behavior of the solution, we have to deal with the relatively large round-off errors in the computation. To overcome these difficulties, we follow [13] to use a combination of numerical computation and a semi-analytic construction.

5.1. Far-field asymptotics. Let (r, β) be the polar coordinate in \mathbb{R}_+^2 : $r = (x^2 + y^2)^{1/2}$, $\beta = \arctan(y/x)$. It has been observed in [13] that the approximate steady state (2.10) enjoys the following asymptotics

$$(5.1) \quad \omega(r, \beta) \sim g_1(\beta)r^\alpha, \quad \theta(r, \beta) \sim g_2(\beta)r^{1+2\alpha}, \quad \alpha = \frac{c_\omega}{c_l} < 0, \quad \alpha \approx -\frac{1}{3},$$

in the far-field for some angular profiles $g_1(\beta), g_2(\beta)$, under the mild assumption that ω decays for large $|x|$, $c_l > 0$, and $c_\omega > 0$. These conditions are satisfied by the blowup solutions [54, 55].

In fact, if ω decays for large $|x|$, the velocity $\mathbf{u} = \nabla^\perp(-\Delta)^{-1}\omega$ has a sublinear growth: $\frac{u(x)}{r} \rightarrow 0$ as $r \rightarrow \infty$. Note that $x \cdot \nabla = r\partial_r$. Passing to the polar coordinate (r, β) , $r = |x|$, $\beta = \arctan \frac{x_2}{x_1}$ and dropping the lower order terms, we yield

$$c_l r \partial_r \omega(r, \beta) = c_\omega \omega + \theta_x + l.o.t., \quad c_l r \partial_r \theta(r, \beta) = (2c_\omega + c_l)\theta + l.o.t..$$

Assume that $\omega(r, b) = r^k g_1(\beta), \theta(r, b) = r^l g_2(\beta)$. Using the above equations and matching the power, we obtain the asymptotic relation (5.1). Thus, we represent the approximate steady state as follows

$$(5.2) \quad \bar{\omega} = \bar{\omega}_1 + \bar{\omega}_2, \quad \bar{\theta} = \bar{\theta}_1 + \bar{\theta}_2, \quad \bar{\omega}_1 = \chi(r)r^\alpha g_1(\beta), \quad \bar{\theta}_1 = \chi(r)r^{1+2\alpha} g_2(\beta),$$

where $\chi(r)$ is the radial cut-off function defined in (F.4). The crucial first part is constructed semi-analytically, and it captures the far-field asymptotic behavior of the approximate steady state. The second part has a much faster decaying rate, and we construct it using numerical computation with a piecewise sixth order B-spline.

5.2. Angular profiles and the representation. Due to symmetry in x , we compute (2.10) in a domain $[0, L]^2$ with $L \approx 10^{13}$. Since $\theta(t, x, y)$ vanishes quadratically on $x = 0$, instead of using θ in our computation, we consider $\zeta(t, x, y) = \frac{1}{x}\theta(t, x, y)$. Then ζ is odd in x , and its equation can be derived by dividing the θ equation by x .

In the case without semi-analytic part, we represent the numerical solution (ω, ρ) using a piecewise 6th order B-spline in x and y , e.g.

$$(5.3) \quad \omega(t, x, y) = \sum_{i,j} a_{i,j} B_i(x) B_j(y)$$

where $B_i(x)$ is the B-spline basis (E.2). For ψ , we represent it using a piecewise B-spline with additional weight $\rho_p(y)$ vanishing on the boundary $y = 0$ to enforce the no-flow boundary condition $\psi(x, 0) = 0$. See more details about the representation in Appendix E.1. Note that similar representations based on piecewise B-splines have been used in [54]. Given the grid point values of ω , we obtain the coefficients of the variable ω by solving the linear equations

(5.3) for (x, y) on the grid and using suitable extrapolation in the far-field. After we obtain the coefficients $a_{i,j}$, we compute the derivatives of ω using the basis functions

$$\partial_x^i \partial_y^j \omega(t, x, y) = \sum_{i,j} a_{i,j} \partial_x^i B_i(x) \partial_y^j B_j(y).$$

Similar consideration applies to ζ . We solve the Poisson equations

$$(5.4) \quad -\Delta \psi = \omega$$

using B-spline based finite element method. After we obtain the B-spline coefficients for ψ , we compute its derivatives by taking derivatives on the basis functions.

In the temporal variable, we use a second order Runge-Kutta method to update the PDE.

To construct the decomposition in (5.2), firstly, we obtain the exponent α_1 and construct the angular profile and the semi-analytic part $\bar{\omega}_1, \bar{\theta}_1$ in (5.2). Then, using $\bar{\omega}_1, \bar{\theta}_1$, we refine the construction $\bar{\omega}_2, \bar{\theta}_2$ in (5.2).

5.2.1. Fitting the angular profile and the exponent. We need to find the angular profiles in the semi-analytic parts in (5.2). Firstly, we solve (2.10) numerically using the above method without the semi-analytic part, i.e. $\bar{\omega}_1 = 0, \bar{\theta}_1 = 0$, to obtain an approximate steady state $(\bar{\omega}, \bar{\zeta}), \bar{\theta} = x\bar{\zeta}$. Using the ansatz in (5.2) and fitting the angular part of the far-field of $r^{-\alpha_1} \omega_1, r^{-1-2\alpha_1} \bar{\theta} = r^{-2\alpha_1} \cos \beta \cdot \bar{\zeta}$ with exponent $\alpha_1 = \frac{\bar{e}_\omega}{\bar{e}_l}$ (5.1), we find the following approximate profiles

$$g_{10}(\beta) = \frac{a_{11}\tilde{\beta}(1 + a_{15}\tilde{\beta}^2)}{(\tilde{\beta}^2 + a_{12})^{2/3} + a_{13}\tilde{\beta}^2 + a_{14}}, \quad \tilde{\beta} = \frac{\pi}{2} - \beta, \quad g_{20}(\beta) = \frac{a_{21}\cos^2 \beta(1 + a_{25}\sin \beta)}{(\cos^2 \beta + a_{22})^{2/3} + a_{23} + a_{24}\cos^2 \beta},$$

for some parameters a_{ij} . We have the factor $\frac{\pi}{2} - \beta$ since ω is odd in x and $g_{10}(\beta)$ is odd with respect to $\beta = \pi/2$. Similarly, we add the factor $\cos^2 \beta$ in $g_{20}(\beta)$ since $\theta(x, 0) = 0$ and $\theta_x(x, 0)$ is odd in x . After we find the above analytic formulas, we further approximate the above profiles by piecewise 8th order B-splines (E.2) B_i with $k = 8$

$$g_j(\beta) = \sum_{1 \leq i \leq n} b_{ji} B_i(x), \quad j = 1, 2,$$

for some coefficients b_{ji} . We further use the B-spline to represent the angular profiles for the following reason. To verify that the approximate steady state $(\bar{\omega}, \bar{\theta})$ has a small residual error, we need to estimate the high order derivatives of $\bar{\omega}, \bar{\theta}$, e.g. 6-th order. However, the high order derivatives of the above analytic forms are very complicated, and are difficult to estimate. For solution represented by piecewise polynomials, we have a systematic approach to estimate it. In 1D, the estimate follows our previous work with Huang [13, 14]. Once we obtain $g_i(\beta)$, we construct the semi-analytic part

$$(5.5) \quad \bar{\omega}_{10} = \chi(r)r^{\bar{\alpha}_1}g_1(\beta), \quad \bar{\theta}_{10} = \chi(r)r^{1+2\bar{\alpha}_2}g_2(\beta), \quad \bar{\zeta}_{10} = \bar{\theta}_{10}x^{-1}.$$

To compute the semi-analytic part of the stream function, we follow the ideas outlined in [13]. Given the asymptotic behavior of $\bar{\omega}$ in (5.5), the far-field asymptotic behavior of $\psi = (-\Delta)^{-1}\bar{\omega}_{10}$ is $r^{2+\bar{\alpha}_1}f(\beta)$ for some profile $f(\beta)$. We construct $f(\beta)$ by solving

$$-\Delta(r^{2+\bar{\alpha}_1}f(\beta)) = r^{\bar{\alpha}_1}g_1(\beta)$$

with boundary condition $f(0) = f(\pi/2) = 0$ due to the Dirichlet boundary condition $\psi(x, 0) = 0$ and the odd symmetry for the solution ω . In the polar coordinate, the above equation is equivalent to

$$(5.6) \quad (-\partial_\beta^2 - (2 + \bar{\alpha}_1)^2)f(\beta) = g_1(\beta), \quad f(0) = f(\pi/2) = 0.$$

We represent $f(\beta)$ using a weighted 8th order B-spline and solve the above elliptic equations using the finite element method. Then, we construct the semi-analytic part for ψ as follows

$$(5.7) \quad \bar{\psi}_{10} = \chi(r)r^{2+\bar{\alpha}_1}f(\beta).$$

5.2.2. *Refinement.* We use the semi-analytic profile (5.5) to capture the far-field contribution of $\bar{\omega}, \bar{\zeta}$. Note that in this step, we do not update the angular profile nor the exponent in (5.5).

Given the grid point values of $\omega(t, x, y)$, we first update the constant $c(t)$ such that $c(t)\bar{\omega}_{10}$ best approximate $\omega(t, x, y)$ in the far-field. Then we represent $\omega_2(t, x, y) = \omega(t, x, y) - c(t)\bar{\omega}_{10}$ using the B-spline (5.3). In other words, we interpolate the grid point values using the representation $c(t)\bar{\omega}_{10} + \omega_2(t, x, y)$, where ω_2 is a piecewise polynomial in the compact domain. Similar consideration applies to ζ . To update the stream functions ψ , we use $c(t)\bar{\psi}_{10}$ to capture the far-field of ψ and then construct the near-field part by solving

$$(5.8) \quad -\Delta(\psi_2 + c(t)\bar{\psi}_{10}) = \omega_2 + c(t)\bar{\omega}_{10}, \quad \text{or} \quad -\Delta\psi_2 = \omega_2 + c(t)(\bar{\omega}_{10} + \Delta\bar{\psi}_{10}).$$

Then the stream function is represented as $\psi_2 + c(t)\bar{\psi}_{10}$.

Let us motivate the above decomposition to construct the steam function over (5.4). If we use (5.4), the source term ω has a slow decay $r^{\alpha_1} \approx r^{-1/3}$. Since the domain is very large, we have to use an adaptive mesh to discretize the domain, which leads to a poor condition number of the stiffness matrix in (5.4). Thus, solving (5.4) can have a significant round-off error. In (5.4), since the semi-analytic part $c(t)\bar{\omega}_{10}$ captures the asymptotic behavior of $\omega(t, x, y)$, ω_2 is much smaller than ω in the far-field. By definition of $\bar{\omega}_{10}, \bar{\psi}_{10}$ (5.5)-(5.7), the far-field of $\bar{\omega}_{10} + \Delta\bar{\psi}_{10}$ is about $\varepsilon r^{-1/3}$ with a small constant ε . Hence, the far-field of the source term in (5.8) is much smaller than $\omega(t, x)$, which enables us to overcome the significant round-off error. We remark that similar technique has been used in the Hou-Luo model [13] to overcome the significant round-off errors. The above decomposition is a generalization of the method in [13] to 2D. We refer to [13] for the more motivations and the difficulties caused by the round-off error.

After we obtain the steam function, we can update the PDE using the second order Runge-Kutta method. We stop the computation at time t_* if the residual error on the grid points is about the round-off error. Then we finalize the semi-analytic part in (5.2) as

$$(5.9) \quad \bar{\omega}_1 = \bar{c}_1\bar{\omega}_{10}, \quad \bar{\theta}_1 = \bar{c}_2\bar{\theta}_{10}, \quad \bar{\theta}_1 = \bar{c}_1\bar{\psi}_{10},$$

where $\bar{c}_1\bar{\omega}_{10}, \bar{c}_2\bar{\zeta}_{10}$ best approximate $\omega(t_*, x, y), \zeta(t_*, x, y)$ in the far-field, respectively. We construct $\bar{\omega}_2, \bar{\theta}_2 = x\bar{\zeta}_2$ in (5.2) by interpolating the grid point values of $\omega - \bar{\omega}_1, \theta - \bar{\theta}_1$ and applying a low-pass filter to the solution to reduce the round off error.

We refer more details of the computation to the upcoming Supplementary Materials.

In Appendix E, we estimate the derivatives of the approximate steady state rigorously, which will be used to verify the residual error.

5.3. Rigorous verification of the numerical values. In this subsection, we describe some main ideas how we use computer-assisted proofs in our stability analysis.

(1) As we discussed in the Introduction and Section 2, the most challenging and essential part in the proof is the weighted L^∞ and weighted $C^{1/2}$ linear stability analysis established in Section 4, since there is *no* small parameter and the linearized equations are complicated.

(2) The weighted L^∞ linear stability estimates can be seen as a-priori estimates on the perturbation, and we proceed to perform $C^{1/2}$ estimates in a similar manner and establish the nonlinear energy estimate for some energy $E(t)$ of the perturbation

$$(5.10) \quad \frac{d}{dt}E^2 \leq CE^3 - \lambda E^2 + \varepsilon E.$$

Here, $-\lambda E^2$ with $\lambda > 0$ comes from the linear stability, CE^3 with some constant $C(\bar{\omega}, \bar{\theta}) > 0$ controls the nonlinear terms, and ε is the weighted norm of the residual error of the approximate steady state. To close the bootstrap argument $E(t) < E^*$ with some threshold $E^* > 0$, a sufficient condition is that $\varepsilon < \varepsilon^* = \lambda^2/(4C)$, which provides an upper bound on the required accuracy of the approximate steady state.

The essential parts of the estimates in (1), (2) are established based on the grid point values of $(\bar{\omega}, \bar{\theta})$ constructed using a moderate fine mesh. These parts do not involve the lengthy rigorous verification in the Supplementary Materials. These estimates already provide a strong evidence of nonlinear stability.

A significant difference from this step and step (1) is that we have a small parameter ε . As long as ε is sufficiently small, thanks to the damping term $-\lambda E^2$ established in step (1), we can afford a large constant $C(\bar{\omega}, \bar{\theta})$ in the estimate of the nonlinear terms and close the nonlinear estimates. We can complete all the nonlinear estimates in this step.

(3) We described how to construct an approximate steady state with residual error below a required level ε^* in the previous subsections. To achieve the desired accuracy, we need to solve the dynamic rescaling equations for a sufficiently long time using a fine mesh. The difficulty of the construction depends on the target accuracy ε^* . Here, the mesh size plays a role similar to a small parameter that we can use. In practice, the profile $(\bar{\omega}_1, \bar{\theta}_1)$ constructed using a moderate fine mesh Ω_1 is close to the one (ω_2, θ_2) constructed using a finer mesh Ω_2 with higher accuracy. As a result, the constants $C(\bar{\omega}, \bar{\theta})$ and λ that we estimate in (5.10) using different approximate steady states (ω_i, θ_i) are nearly the same. This refinement procedure allows us to obtain an approximate steady state, based on which we close the nonlinear estimates (5.10). We refer more discussion of this philosophy to [14].

(4) Finally, we follow the standard procedure to perform rigorous verification on the estimates to pass from the grid point value to its continuous counterpart. In the verification step, we can evaluate the approximate steady state on a much finer mesh Ω_3 with many more grid points so that they almost capture the whole behavior of the solution. Then, we use the regularity of the solution to pass from finite grid points to the whole upper half plane. In this procedure, the mesh size in Ω_3 plays a role similar to a small parameter that we can exploit.

In summary, in steps (2)-(4), we can take advantage of a small parameter which can be either the small error or the small mesh size, while there is no small parameter in step (1). Though these three steps could be technical, they are relatively standard from the viewpoint of analysis.

We remark that the approach of computer-assisted proof has played an important role in the analysis of many PDE problems, especially in computing explicit tight bounds of complicated (singular) integrals [7, 21, 37] or bounding the norms of linear operators [4, 33]. We refer to [36] for an excellent survey on computer-assisted proofs in establishing rigorous analysis for PDEs. Our approach to establish stability analysis with computer assistance is different from existing computer-assisted approach, e.g. [6], where the stability is established by numerically tracking the spectrum of a given operator and quantifying the spectral gap. The key difference between their approach and ours is that we *do not* use direct computation to quantify the spectral gap of the linearized operator since the linearized operator in our case is not compact.

6. CONSTRUCTING AND ESTIMAING THE APPROXIMATE SOLUTION TO THE LINEARIZED EQUATIONS

Recall the decomposition of the system (2.65) in Sections 2.10.3, 2.10.4. We need to construct the approximate solutions to $e^{\mathcal{L}t}F_0$ for several initial data $\bar{F}_i, \bar{F}_{\chi,i}$. In this section, we discuss how to construct these space-time solutions numerically with the vanishing properties (2.76).

The linearizeq equations associated with \mathcal{L} (2.65) read

$$(6.1) \quad \begin{aligned} \partial_t \omega &= -(\bar{c}_l x + \bar{u}) \cdot \nabla \omega + \eta + \bar{c}_\omega \omega - \mathbf{u} \cdot \nabla \bar{\omega} + c_\omega \bar{\omega} = \mathcal{L}_1(\omega, \eta, \xi), \\ \partial_t \eta &= -(\bar{c}_l x + \bar{u}) \cdot \nabla \eta + (2\bar{c}_\omega - \bar{u}_x)\eta - \bar{v}_x \xi - \mathbf{u}_x \cdot \nabla \bar{\theta} - \mathbf{u} \cdot \nabla \bar{\theta}_x + 2c_\omega \bar{\theta}_x = \mathcal{L}_2(\omega, \eta, \xi), \\ \partial_t \xi &= -(\bar{c}_l x + \bar{u}) \cdot \nabla \xi + (2\bar{c}_\omega + \bar{u}_x)\xi - \bar{u}_y \eta - \mathbf{u}_y \cdot \nabla \bar{\theta} - \mathbf{u} \cdot \nabla \bar{\theta}_y + 2c_\omega \bar{\theta}_y = \mathcal{L}_3(\omega, \eta, \xi), \end{aligned}$$

where $c_\omega = u_x(0)$ (2.19). Although η, ξ represent θ_x, θ_y in the Boussinesq equations (2.20), we will consider initial data $(\omega_0, \eta_0, \xi_0)$ with $\partial_y \eta_0 \neq \partial_x \xi_0$. Thus, we do not have the relation $\partial_y \eta = \partial_x \xi$ and will treat η, ξ as two independent variables.

The solutions ω, η are odd, ξ is even with $\xi(0, y) = 0$. We consider initial data $(\omega_0, \eta_0, \xi_0) = O(|x|^2)$ near $x = 0$. Using an argument similar to (2.22) and a direct calculation, we obtain that these vanishing conditions are preserved

$$(6.2) \quad \omega(t, x), \eta(t, x), \xi(t, x) = O(|x|^2).$$

6.1. A posteriori error estimates: decomposition of errors. Since we cannot solve the Poisson equation exactly, for the stream function $\bar{\psi}, \psi$, we have the natural decomposition

$$\bar{\psi} = \bar{\psi}^N + \bar{\psi}^e, \quad \psi = \psi^N + \psi^e,$$

where the short hands N, e denote *numeric, error*, respectively. We use similar notations below for other nonlocal terms since we cannot construct them exactly. We will construct $\bar{\psi}^N, \psi^N$ numerically and explicitly and treat $\bar{\psi}^e, \psi^e$ as error. The reader should not confuse ψ^N with the N -th power of ψ . We will never use power of ψ throughout the paper. Similarly, we denote by $\mathbf{u}^N, \mathbf{u}^e$ the velocities corresponding to ψ^N, ψ^e . For example, we have

$$u^N = -\partial_y(-\Delta)^{-1}\psi^N, \quad u^e = -\partial_y(-\Delta)^{-1}\psi^e, \quad c_\omega^N = u_x^N(0), \quad c_\omega^e = u_x^e(0).$$

The above decomposition leads to the following decomposition of the operator \mathcal{L}

$$\begin{aligned} \mathcal{L}_1 &= \mathcal{L}_1^N + \mathcal{L}_1^e + \mathcal{L}_1^{\bar{e}}, \quad \mathcal{L}_2 = \mathcal{L}_2^N + \mathcal{L}_2^e + \mathcal{L}_2^{\bar{e}}, \quad \mathcal{L}_3 = \mathcal{L}_3^N + \mathcal{L}_3^e + \mathcal{L}_3^{\bar{e}}, \\ \mathcal{L}_1^N &= \eta + \bar{c}_\omega^N \omega - (\bar{c}_l x + \bar{\mathbf{u}}^N) \cdot \nabla \omega + c_\omega^N \bar{\omega} - \mathbf{u}^N \cdot \nabla \bar{\omega}, \\ \mathcal{L}_1^e &= c_\omega^e \bar{\omega} - \mathbf{u}^e \cdot \nabla \bar{\omega}, \quad \mathcal{L}_1^{\bar{e}} = \bar{c}_\omega^e \omega - \bar{\mathbf{u}}^e \cdot \nabla \omega, \\ (6.3) \quad \mathcal{L}_2^N &= -(\bar{c}_l x + \bar{\mathbf{u}}^N) \cdot \nabla \eta + (2\bar{c}_\omega^N - \bar{u}_x^N) \eta - \bar{v}_x^N \xi - \mathbf{u}_x^N \cdot \nabla \bar{\theta} - \mathbf{u}^N \cdot \nabla \bar{\theta}_x + 2c_\omega^N \bar{\theta}_x, \\ \mathcal{L}_2^e &= -\mathbf{u}_x^e \cdot \nabla \bar{\theta} - \mathbf{u}^e \cdot \nabla \bar{\theta}_x + 2c_\omega^e \bar{\theta}_x, \quad \mathcal{L}_2^{\bar{e}} = -\bar{\mathbf{u}}^e \cdot \nabla \eta + (2\bar{c}_\omega^e - \bar{u}_x^e) \eta - \bar{v}_x^e \xi, \\ \mathcal{L}_3^N &= -(\bar{c}_l x + \bar{\mathbf{u}}^N) \cdot \nabla \xi + (2\bar{c}_\omega^N - \bar{u}_y^N) \xi - \bar{u}_y^N \eta - \mathbf{u}_y^N \cdot \nabla \bar{\theta} - \mathbf{u}^N \cdot \nabla \bar{\theta}_y + 2c_\omega^N \bar{\theta}_y, \\ \mathcal{L}_3^e &= -\mathbf{u}_y^e \cdot \nabla \bar{\theta} - \mathbf{u}^e \cdot \nabla \bar{\theta}_y + 2c_\omega^e \bar{\theta}_y, \quad \mathcal{L}_3^{\bar{e}} = -\bar{\mathbf{u}}^e \cdot \nabla \xi + (2\bar{c}_\omega^e - \bar{u}_y^e) \xi - \bar{u}_y^e \eta, \end{aligned}$$

where $\mathcal{L}_i^e, \mathcal{L}_i^{\bar{e}}$ denote the errors from $\psi^e, \bar{\psi}^e$, respectively. These operators depend on ω, η, ξ , and we drop the dependence in (6.3) to simplify the presentation.

6.2. First correction and the construction of ψ^N . Firstly, we solve (6.1) using the numerical method outlined in Section 5 to obtain the solution $(\omega_k, \eta_k, \xi_k)$ at discrete time t_k . Since ξ is even with $\xi(0, y) = 0$, we write $\xi = x\zeta$ for an odd function ζ . Then we represent ω, η, ζ using the piecewise 6-th order B-spline (5.3). We remark that we do not add the semi-analytic part in this construction for efficiency consideration and that the far-field behaviors of the solutions are different for different initial data.

According to the normalization condition and (6.2), the solution to (6.1) satisfies $\omega_x(0, t) = \eta_x(0, t) = 0$. To obtain an approximate solution with this condition, we make the first correction

$$\omega_k \rightarrow \omega_k - \omega_{k,x}(0, 0)\chi_{11}, \quad \eta_k \rightarrow \eta_k - \eta_{k,x}(0, 0)\chi_{21},$$

where χ_{ij} are cutoff functions defined in (6.6) with $\chi_{ij} = x + O(|x|^4)$ near 0. We do not modify ξ_k since ξ_k already vanishes quadratically near $(0, 0)$. We remark that the first correction does not change the second order derivatives of the solution near 0 and c_ω since

$$\partial_{xy}\chi_{11}(0) = \partial_{xy}\chi_{21}(0) = 0, \quad c_\omega(\chi_{11}) = -\partial_{xy}\psi_1(0) = 0.$$

Here ψ_1 is defined below

$$\psi_1 = -\frac{xy^2}{2}\kappa(x)\kappa(y),$$

where $\kappa(x)$ is the cutoff function chosen in (F.5) in Appendix F.2 satisfying $\kappa(x) = 1 + O(|x|^4)$ near $x = 0$, and ψ_1 satisfies $-\Delta\psi_1 = x + O(|x|^4)$. To construct the stream function ψ^N , we first solve $-\Delta\psi_k = \omega_k$ numerically to obtain $\psi_{k,1}^N$. Then we correct it as follows

$$\psi_{k,1}^N \rightarrow \psi_{k,1}^N + \partial_{xyy}\psi_{k,1}^N(0)\psi_1 \triangleq \psi_k^N.$$

This allows us to obtain

$$\begin{aligned} (6.4) \quad \partial_x(-\Delta)\psi_k^N(0) &= -\partial_x\Delta\psi_{k,1}^N(0) + \partial_{xyy}\psi_{k,1}^N(0) = 0, \\ \Delta\psi_k^N &= O(|x|^2), \quad \omega_k - (-\Delta)\psi_k^N = O(|x|^2). \end{aligned}$$

We further extend it to Lipschitz continuous solutions $\widehat{W} \triangleq (\hat{\omega}(t), \hat{\eta}(t), \hat{\xi}(t))$ in time using a cubic spline interpolation in t . See section 6.5 for more details.

6.3. The second correction.

The error

$$(\partial_t - \mathcal{L}_i)(\hat{\omega}(t), \hat{\eta}(t), \hat{\xi}(t))$$

may not vanish to the order $O(|x|^3)$, which is a property (2.76) that we require in the energy estimate. Then we add the second correction

$$\hat{\omega}(t) \rightarrow \hat{\omega}(t) + a_1(t)\chi_{12}, \quad \hat{\eta} \rightarrow \hat{\eta} + a_2(t)\chi_{22}, \quad \hat{\xi}(t) \rightarrow \hat{\xi}(t) + a_3(t)\chi_{32}$$

so that the error satisfies

$$(6.5) \quad \varepsilon_i^{(2)} \triangleq (\partial_t - \mathcal{L}_i)(\hat{\omega}(t) + a_1(t)\chi_{12}, \hat{\eta} + a_2(t)\chi_{22}, \hat{\xi}(t) + a_3(t)\chi_{32}) = O(|x|^3)$$

near $x = 0$. We use the following functions for this correction

$$(6.6) \quad \begin{aligned} \chi_{11} &= -\Delta\psi_1, \quad \psi_1 = -\frac{xy^2}{2}\kappa(x)\kappa(y), \quad \chi_{21} = x\kappa(x)\kappa(y), \\ \chi_{12} &= -\Delta\psi_2, \quad \psi_2 = -\frac{xy^3}{6}\kappa(x)\kappa(y), \quad \chi_{22} = xy\kappa(x)\kappa(y), \quad \chi_{32} = \frac{x^2}{2}\kappa(x)\kappa(y), \end{aligned}$$

where $\kappa(x)$ is chosen in (F.5). Since $\kappa(x)$ satisfies $\kappa(x) = 1 + O(|x|^4)$ near $x = 0$, the behaviors of the above functions near $x = 0$ are given by

$$\chi_{11} = y + l.o.t., \quad \chi_{21} = x + l.o.t., \quad \chi_{12} = xy + l.o.t., \quad \chi_{22} = xy + l.o.t., \quad \chi_{32} = x^2/2 + l.o.t.$$

We choose $\chi_{1j} = -\Delta\psi_j$ so that its associated velocity $\nabla^\perp(-\Delta)^{-1}\chi_{1j}$ can be obtained explicitly.

For cutoff functions χ_1, χ_2, χ_3 with $c_\omega(\chi_1) = -\partial_{xy}(-\Delta)^{-1}\chi_1 = 0$, e.g. $\chi_i = \chi_{i2}$ chosen above, we have the following general formula of $\mathcal{L}_i(a_1(t)\chi_1, a_2(t)\chi_2, a_3(t)\chi_3)$

$$\begin{aligned} \mathcal{L}_1(a_1\chi_1, a_2\chi_2, a_3\chi_3) &= a_1(t) \left(-(\bar{c}_l x + \bar{\mathbf{u}}) \cdot \nabla \chi_1 + \bar{c}_\omega \chi_1 - \mathbf{u}(\chi_1) \cdot \nabla \bar{\omega} \right) + a_2(t)\chi_2, \\ \mathcal{L}_2(a_1\chi_1, a_2\chi_2, a_3\chi_3) &= a_2(t) \left(-(\bar{c}_l x + \bar{\mathbf{u}}) \cdot \nabla \chi_2 + (2\bar{c}_\omega - \bar{u}_x)\chi_2 \right) - a_3(t)\bar{v}_x \chi_3 - a_1(t) \left(\mathbf{u}(\chi_1) \cdot \nabla \bar{\theta} \right)_x, \\ \mathcal{L}_3(a_1\chi_1, a_2\chi_2, a_3\chi_3) &= a_3(t) \left(-(\bar{c}_l x + \bar{\mathbf{u}}) \cdot \nabla \chi_3 + (2\bar{c}_\omega + \bar{u}_x)\chi_3 \right) - a_2(t)\bar{u}_y \chi_2 - a_1(t) \left(\mathbf{u}(\chi_1) \cdot \nabla \bar{\theta} \right)_y, \end{aligned}$$

where $\mathbf{u}(\chi_1)$ is the velocity associated with χ_1 . We want to apply the above formulas to the second corrections $\chi_{i2}, i = 1, 2, 3$. We use the Hadamard product

$$(6.7) \quad (A \circ B)_i = A_i B_i,$$

to simplify the notation as follows

$$\mathcal{L}_i(a \circ \chi) = \text{Cor}_{ij}(x; \chi) a_j(t).$$

In the second correction, we use $\chi_{i2}, i = 1, 2, 3$ in (6.6). Note that Cor_{ij} involves the nonlocal term $\bar{\mathbf{u}} = \bar{\mathbf{u}}^N + \bar{\mathbf{u}}^e$. According to this decomposition, we decompose Cor_{ij} as follows

$$(6.8) \quad \text{Cor}_{ij} = \text{Cor}_{ij}^N + \text{Cor}_{ij}^{\bar{e}}.$$

Note that we do not decompose $\mathbf{u}(\chi_1)$ since we can obtain it explicitly.

Next, we derive the equations for $a(b), b(t), c(t)$. Using the condition

$$\partial_{xy}\varepsilon_1^{(2)}(0) = \partial_{xy}\varepsilon_2^{(2)}(0) = \partial_{xx}\varepsilon_3^{(2)}(0) = 0,$$

from (6.5), we obtain the following ODEs for $a(t), b(t), c(t)$

$$(6.9) \quad \begin{aligned} \dot{a}_1(t) &= (-2\bar{c}_l + \bar{c}_\omega)a_1(t) + a_2(t) - F_1(t), \\ \dot{a}_2(t) &= (-2\bar{c}_l + 2\bar{c}_\omega - \bar{u}_x(0))a_2(t) - F_2(t), \\ \dot{a}_3(t) &= (-2\bar{c}_l + 2\bar{c}_\omega - \bar{u}_x(0))a_3(t) - F_3(t), \end{aligned}$$

where $F(t) = (F_1(t), F_2(t), F_3(t))^T$ is the error associated to the second order derivatives of $(\partial_t - \mathcal{L})\hat{W}$ near 0. More precisely, we have

$$(6.10) \quad \begin{aligned} F_1(t) &= \partial_{xy}(\partial_t - \mathcal{L}_1)\hat{W} = \frac{d}{dt}\hat{\omega}_{xy}(t, 0) - (-2\bar{c}_l + \bar{c}_\omega)\hat{\omega}_{xy}(t, 0) - \hat{\eta}_{xy}(t, 0) - c_\omega(t)\bar{\omega}_{xy}(0), \\ F_2(t) &= \partial_{xy}(\partial_t - \mathcal{L}_2)\hat{W} = \frac{d}{dt}\hat{\eta}_{xy}(t, 0) - (-2\bar{c}_l + 2\bar{c}_\omega - \bar{u}_x(0))\hat{\eta}_{xy}(t, 0) - c_\omega(t)\bar{\theta}_{xxy}(0), \\ F_3(t) &= \partial_x^2(\partial_t - \mathcal{L}_3)\hat{W} = \frac{d}{dt}\hat{\xi}_{xx}(t, 0) - (-2\bar{c}_l + 2\bar{c}_\omega - \bar{u}_x(0))\hat{\xi}_{xx}(t, 0) - c_\omega(t)\bar{\theta}_{xxy}(0). \end{aligned}$$

Denote $D^2 = (\partial_{xy}, \partial_{xy}, \partial_x^2)^T$. Then we can simplify (6.10) as

$$F_i = D_i^2(\partial_t - \mathcal{L}_i)\hat{W}(0).$$

Denote by M the coefficients in (6.9)

$$(6.11) \quad M = \begin{pmatrix} -2\bar{c}_l + \bar{c}_\omega & 1 & 0 \\ 0 & -2\bar{c}_l + 2\bar{c}_\omega - \bar{u}_x(0) & 0 \\ 0 & 0 & -2\bar{c}_l + 2\bar{c}_\omega - \bar{u}_x(0) \end{pmatrix} \triangleq M^N + M^{\bar{e}},$$

where the last identity is based on the decomposition $\bar{c}_\omega = \bar{c}_\omega^N + \bar{c}_\omega^e$, $\bar{u}_x(0) = \bar{u}_x^N(0) + \bar{u}_x^e(0)$, and $M^{\bar{e}}$ only contains the contribution from $\bar{c}_\omega^e, \bar{u}_x(0)^e$. According to the normalization condition (2.19), we have $\bar{u}_x(0)^e = \bar{c}_\omega^e$. It follows

$$M^{\bar{e}} = \bar{c}_\omega^e I_3.$$

We simplify the ODE for $a = (a_1, a_2, a_3)^T$ as

$$(6.12) \quad \dot{a}_i(t) = M_{ij}a_j(t) - F_i(t), \quad \dot{a}(t) = Ma - F.$$

Recall $\chi_{\cdot 2} = (\chi_{12}, \chi_{22}, \chi_{32})$ from (6.6). The overall error for the approximate solution $\hat{W} + a(t) \circ \chi_{\cdot 2}$ is

$$\begin{aligned} (\partial_t - \mathcal{L})(\hat{W} + a(t) \circ \chi_{\cdot 2}) &= (\partial_t - \mathcal{L})\hat{W} + \partial_t a(t) \circ \chi_{\cdot 2} - \mathcal{L}(a(t) \circ \chi_{\cdot 2}) \\ &= ((\partial_t - \mathcal{L})\hat{W} - F(t) \circ \chi_{\cdot 2}) + (Ma(t) \circ \chi_{\cdot 2} - Cor(x; \chi_{\cdot 2})a) \triangleq I + II. \end{aligned}$$

To simplify the notation, we drop the dependence of $\chi_{\cdot 2}$ in Cor . Denote by e_1, e_2, e_3 the canonical basis in \mathbb{R}^3 , e.g., $e_1 = (1, 0, 0)$. For II , we have

$$(6.13) \quad II = e_i \chi_{i2} M_{ij} a_j - e_i Cor_{ij}(x) a_j = -e_i (Cor_{ij}(x) - M_{ij} \chi_{i2}) a_j.$$

Using (6.8) and (6.11), we yield

$$\tilde{Cor}_{ij}(x, \chi_{\cdot 2}) \triangleq Cor_{ij}(x) - M_{ij} \chi_{i2} = Cor_{ij}^N(x) - M_{ij}^N \chi_{i2} + Cor_{ij}^{\bar{e}}(x) - M_{ij}^{\bar{e}} \chi_{i2}.$$

It is not difficult to show that $\tilde{Cor}_{ij}(x)$ vanishes to the order $O(|x|^3)$ near $x = 0$. For example, for $i = j = 1$, we have

$$J \triangleq Cor_{11}^{\bar{e}}(x) - M_{11}^{\bar{e}} \chi_{12} = -\bar{u}^e \cdot \nabla \chi_{12} + \bar{c}_\omega^e \chi_{12} - \bar{c}_\omega^e \chi_{12} = -\bar{u}^e \cdot \nabla \chi_{12}.$$

Since $\chi_{12} = xy + O(|x|^4)$ (6.6), $\bar{u}^e = \bar{u}_x^e(0)x + O(|x|^2)$, $\bar{v}^e = -\bar{u}_x^e(0)y$ near 0, we have $J = O(|x|^3)$ near 0. For II , we estimate the weighted norm for \tilde{Cor}_{ij} and then apply the triangle inequality to further bound II .

For the I term, using (6.3) and (6.10), for each equation i , we get

$$(6.14) \quad \begin{aligned} (\partial_t - \mathcal{L}_i)\hat{W} - F_i \chi_{i2} &= (\partial_t - \mathcal{L}_i)\hat{W} - D_i^2(\partial_t - \mathcal{L}_i)\hat{W}(0)\chi_{i2} \\ &= (\partial_t - \mathcal{L}_i^N)\hat{W} - D_i^2(\partial_t - \mathcal{L}_i^N)\hat{W}(0)\chi_{i2} - (\mathcal{L}_i^e \hat{W} - D_i^2 \mathcal{L}_i^e \hat{W}(0)\chi_{i2}) \\ &\quad - (\mathcal{L}_i^{\bar{e}} \hat{W} - D_i^2 \mathcal{L}_i^{\bar{e}} \hat{W}(0)\chi_{i2}) \triangleq I_{i,N} + I_{i,e} + I_{i,\bar{e}}. \end{aligned}$$

Since $D_i^2(\partial_t - \mathcal{L}_i^N)\hat{W}(0)\chi_{i2}$ is the leading order term of $(\partial_t - \mathcal{L}_i^N)\hat{W}$ near 0, we yield $I_{i,s} = O(|x|^3)$ near 0. We estimate each term and then apply the triangle inequality to bound I_i .

In summary, to estimate the error $(\partial_t - \mathcal{L})(\hat{W} + A \circ \chi_{\cdot 2})$, we will use the triangle inequality and estimate $I_{i,N}, I_{i,e}, I_{i,\bar{e}}$ and II separately. The error II is due to the second correction, $I_{1,N}$ is from the error of solving (6.1) numerically, $I_{i,e}, I_{i,\bar{e}}$ are due to the error of solving the

Poisson equations for ω and $\widehat{\omega}$. Since we use a cubic spline interpolation to obtain the continuous function $\bar{W}(t)$, each error is a piecewise cubic polynomial in time, and we track the coefficients of these polynomials to verify that they are small.

6.4. Estimate of the solutions to the ODE. Since we need to solve the ODE (6.9) exactly to achieve the vanishing order (6.5) for all time, we cannot use a numerical method, e.g. the Runge-Kutta method, to obtain the approximate solution. Since (6.9) is a linear ODE with constant coefficients and some forcing terms, we can solve it exactly by diagonalizing the system. Introduce

$$\begin{aligned}\lambda_1 &= -2\bar{c}_l + \bar{c}_\omega, \quad \lambda_2 = \lambda_3 = -2\bar{c}_l + 2\bar{c}_\omega - \bar{u}_x(0), \\ \tilde{a}_1 &= a_1 + \frac{a_2}{\lambda_1 - \lambda_2}, \quad \tilde{F}_1 = F_1 + \frac{F_2}{\lambda_1 - \lambda_2}, \quad \tilde{a}_i = a_i, \quad \tilde{F}_i = F_i, \quad i = 2, 3.\end{aligned}$$

The approximate steady state satisfies $\lambda_1 \approx -7, \lambda_2 = \lambda_3 \approx -5.5$. We diagonalize (6.9) as follows

$$\frac{d}{dt} \tilde{a}_i = \lambda_i \tilde{a}_i - \tilde{F}_i.$$

Let a_0 be the initial data, which will be chosen to correct the vanishing order of the error $\hat{F}_i(0) - \tilde{F}_i$ in (6.2). Then the solution \tilde{a}_i is given by

$$\tilde{a}_i(t) = e^{\lambda_i t} \tilde{a}_i(0) - \int_0^t e^{\lambda_i(t-s)} \tilde{F}_i(s) ds.$$

It follows

$$|\tilde{a}_i(t)| \leq \frac{1 - e^{\lambda_i t}}{-\lambda_i} \|\tilde{F}_i(s)\|_{L^\infty(0,t)}.$$

Using the relation between a_i and \tilde{a}_i , we further obtain the estimate for a_i . With the estimate on a_i , we can estimate the error term II (6.13). For example, we have a $L^\infty(\rho)$ estimate

$$|II\rho(x)| \leq e_i \|\tilde{C}or_{ij}(\cdot, \chi)\rho\|_{L^\infty} |a_j|.$$

The norm $\|\tilde{C}or_{ij}(\cdot, \chi)\rho\|_{L^\infty}$ is time-independent and we only need to compute it once.

We remark that we do not need to track the values of $a(t)$ during the computation. Since F_i is a piecewise cubic polynomial in t , to bound $F_i(s)$ over time, we only need to track the coefficients of the cubic polynomial.

6.5. Cubic interpolation in time. Given the numerical solution with correction $\widehat{W}_n = (\widehat{\omega}_n, \widehat{\eta}_n, \widehat{\xi}_n)$, we use a piecewise cubic interpolation to construct $\widehat{W}(t, x)$ over $(t, x) \in [0, T] \times \mathbb{R}_2^+$. For $s \in [-3k/2, 3k/2]$, we construct

$$\begin{aligned}W(s + t_n + \frac{3k}{2}) &= \frac{1}{16}(-W_0 + 9W_1 + 9W_2 - W_3) + \frac{1}{24}(W_0 - 27W_1 + 27W_2 - W_3)\frac{s}{k} \\ &\quad + \frac{1}{4}(W_0 - W_1 - W_2 + W_3)(\frac{s}{k})^2 + \frac{1}{6}(-W_0 + 3W_1 - 3W_2 + W_3)(\frac{s}{k})^3 \\ &\triangleq \sum_{i \leq 3} C_i \cdot V \frac{1}{i!} (\frac{s}{k})^i, \quad V = (W_0, W_1, W_2, W_3),\end{aligned}$$

where k is the time step, $W_i = \hat{W}_{n+i}$ for $t_n = nk$, and $C_i \in \mathbb{R}^4$ is the coefficient determined by the interpolation formula. A direct calculation yields

$$\begin{aligned}\partial_t \widehat{W} - \mathcal{L} \widehat{W} &= \sum_{1 \leq i \leq 3} \frac{C_i \cdot V}{k} \frac{1}{(i-1)!} (\frac{s}{k})^{i-1} - \sum_{i \leq 3} \mathcal{L}(C_i \cdot V) \frac{1}{i!} (\frac{s}{k})^i \\ &= \sum_{i \leq 2} \left(\frac{C_{i+1} \cdot V}{k} - \mathcal{L}(C_i \cdot V) \right) \frac{1}{i!} (\frac{s}{k})^i - \mathcal{L}(C_4 \cdot V) \frac{s^3}{6k^3}.\end{aligned}$$

To estimate $\partial_t \widehat{W} - \mathcal{L} \widehat{W}$, we will use the triangle inequality and estimate $\frac{C_{i+1} \cdot V}{k} - \mathcal{L}(C_i \cdot V)$, $\mathcal{L}(C_4 \cdot V)$ rigorously using the method described in the previous sections.

Applying the triangle inequality and integrating the error over $s \in [-\frac{3k}{2}, \frac{3k}{2}]$ yield

$$\begin{aligned} \int_{|s| \leq 3k/2} |\partial_t W - \mathcal{L}W| ds &\leq \sum_{i \leq 2} \left| \frac{C_{i+1} \cdot V}{k} - \mathcal{L}(C_i \cdot V) \right| \int_{|s| \leq 3k/2} \frac{1}{i!} \left| \frac{s}{k} \right|^i + |\mathcal{L}(C_4 \cdot V)| \int_{|s| \leq 3k/2} \frac{1}{6} \left| \frac{s}{k} \right|^3 \\ &= k \sum_{i \leq 2} \left| \frac{C_{i+1} \cdot V}{k} - \mathcal{L}(C_i \cdot V) \right| C_I(i) + |\mathcal{L}(C_4 \cdot V)| C_I(3), \end{aligned}$$

where

$$C_I = [3, \frac{9}{4}, \frac{9}{8}, \frac{27}{64}].$$

6.5.1. Decomposing the time interval for parallel computing. To verify that the posterior error is small, we need to estimate the error rigorously at each time step, which takes a significant amount of time. Consider a partition of the time interval $0 = T_0 < T_1 < \dots < T_n = T$, where T is the final time of the computation. To reduce the computational time, we first solve the equations on $[0, T]$ without any rigorously verification and save the solution at T_i . Since we do not need to perform verification at this step, the running time for each time step is short. Then we solve the equations on a smaller time interval $[T_i, T_{i+1}], i = 0, 1, 2, \dots, n-1$ from the initial data $W(T_i)$ and then perform the verification in each time interval in parallel.

6.6. Stopping criterion. To construct an approximate solution, we do not need to solve the linearized equations (6.1) for all time. In fact, since the solution decays in certain norm as t increases, we stop the computation at time T if $\hat{W} - D^2\hat{W} \circ \chi$ is small in the energy norm. Then we extend $\hat{W}(t)$ trivially for $t > T$

$$\hat{W}(t) = 0, \quad t > T.$$

As a result, the error satisfies

$$\mathcal{R}_i = (\partial_t - \mathcal{L}_i)\hat{W} = (\partial_t - \mathcal{L}_i)\hat{W}\mathbf{1}_{t \leq T} - \delta_T \hat{W}_i(T).$$

Let $F = (F_1, F_2, F_3)$, $F_i = D_i^2(\partial_t - \mathcal{L}_i)\hat{W} \Big|_{x=0}$, where $D^2 = (D_{xy}, D_{xy}, D_x^2)$. Then similarly, we get

$$F = D^2(\partial_t - \mathcal{L})\hat{W}\mathbf{1}_{t \leq T} - D^2\hat{W}(T)\delta_T.$$

Recall that the coefficients of the second correction a satisfies (6.12)

$$\dot{a} = Ma - F.$$

Using the Duhamel formula, we yield

$$a(t) = e^{Mt}a_0 - \int_0^t \exp(M(t-s))F(s)ds$$

for $t < T$. For $t \geq T$, we derive

$$a(t) = e^{Mt}a_0 - \int_0^{\min(t, T)} \exp(M(t-s))F(s)ds + (\widehat{D^2W})(T)e^{M(t-T)}\mathbf{1}_{t \geq T}.$$

Although the forcing terms only have finite support in time, $a(t)$ has global support. Moreover, it is in L^∞ and piecewise smooth. Now, with the second correction, for $t > T$, the residual error for rank-one perturbation is given by

$$\begin{aligned} \mathcal{R} &= \int_0^t c(t-s)(\partial_t - \mathcal{L})(\hat{W} + a \circ \chi)ds \\ &= \int_0^T c(t-s) \left((\partial_t - \mathcal{L})\hat{W} - F(t) \circ \chi \right) ds - (\hat{W}(T) - D^2\hat{W}(t) \circ \chi)c(t-T) \\ &\quad + \int_0^t c(t-s)(Ma \circ \chi - Cor(x; \chi)a)(s)ds. \end{aligned}$$

Note that the last part is a linear combination of $(a_1(t), a_2(t), a_3(t))$. We will apply the previous method to estimate it. The above formula can be generalized straightforward to the finite rank perturbation.

In practice, we construct the numeric solution up to time $T = 12$. At that time, the solution is very small.

6.7. Ideas of estimating the norm of the error. In this section, we discuss how to estimate the error derived in the previous section, e.g. $(\partial_t - \mathcal{L}_i)\widehat{W} - F_i\chi_{i2}$ (6.14), a-posteriori. The general idea is to first evaluate f on some grid points and estimate the higher order derivatives of f in a domain D . Then we can construct an approximation \hat{f} of f by interpolating the values of f at different points. The approximation error $f - \hat{f}$ can be bounded by $C_k\|f\|_{C^k}h^k$, where h measures the size of the domain. For example, we have the simple second order estimate (E.5) in 1D. If the mesh h is sufficiently small and we partition $[a, b]$ into many small sub-intervals with size h , applying (E.5), we obtain sharp estimate of $\|f\|_{L^\infty[a, b]}$.

To estimate the derivatives of f in the error term $C_k\|f\|_{C^k}h^k$, we can use a rough estimate. Since we have the small factor h^k , the overall estimate will be small. The estimate of $\|f\|_{C^k}$ for f being the numeric solution or residual error can be established using the estimates in Appendix E for piecewise polynomials or semi-analytic solutions.

In order to develop efficient method for rigorous estimates, we have the following considerations. Firstly, we should evaluate as a small number of points as possible so that the method is efficient. Secondly, most functions f in the verification are complicated and it is difficult to obtain the sharp bound of the higher derivatives. We observe that, for a product $f = pq$, e.g. $f = u_x\bar{\omega}_x$, the estimates of its higher order derivatives can be established by the triangle inequality, the Leibniz rule, and the estimates of the derivatives of p and q . This approach allows us to reduce estimating some complicated functions to estimating several simpler functions. Yet, in general, this approach overestimates the derivatives significantly. To compensate the overestimates of the derivatives, we use higher order interpolations and estimates, which provide the small factor h^k . We develop three estimates based on different interpolations: the Newton interpolation, the Lagrangian interpolation, and the Hermite interpolation. We generalize these interpolations to 2D and develop the estimates in Appendix G.

Each estimate has its own advantages and we will apply them in different situations. We note that the approximation errors in these estimates are bounded by Ch^k for $k = 4$ or 5. We want to estimate the constant C as sharp as possible to reduce the computational cost and improve the efficiency. In fact, when $k = 4$, if we can obtain an interpolation method and reduce the constant C to $\frac{C}{16}$, to achieve the same level of error, we can increase h to $2h$. In this verification step, since the domain is 2D, it means that we can evaluate only $\frac{1}{4}$ of the grid point values of f , which is much faster.

Based on these L^∞ estimates of f , we can obtain sharp estimate of the derivatives of f . Using the method in Section G.5, we can further estimate the weighted norm of f with singular weight near 0. This allows us to verify the smallness of the residual error in some weighted L^∞ norm. Using these L^∞ estimates of f and its derivatives, we can further develop Hölder estimate for f . See Section G.6. We remark that the numeric solutions are regular, e.g. the approximate steady state and the solutions to the linearized equations are C^3 ,

6.8. Posteriori estimates of the velocity. In our estimate of the error for the linearized equations, we need to verify the error between the computed stream function ψ^N , its related velocity $\mathbf{u}^N = \nabla^\perp\psi^N$ and the ground true stream function $(-\Delta)^{-1}\omega$ and velocity $\nabla^\perp(-\Delta)^{-1}\omega$ for the given vorticity. We observe that

$$\nabla^\perp(-\Delta)^{-1}\omega - \nabla^\perp\psi^N = \nabla^\perp(-\Delta)^{-1}(\omega - (-\Delta)\psi^N),$$

and the error $\omega - \Delta\psi^N$ depends on the numerical solution ω, ψ^N locally. Since ψ^N is the numerical solution to the Poisson equations $-\Delta\psi = \omega$, we expect that the error $\omega - \Delta\psi^N$ is very small. The norm of $\omega - (-\Delta)\psi^N$ can be estimated using the method in Appendix G. For this reason, we use functional inequalities to estimate the operator $\mathbf{u}(F) = \nabla^\perp(-\Delta)^{-1}F, \nabla\mathbf{u}(F) = \nabla\nabla^\perp(-\Delta)^{-1}F$, where $F = \omega - (-\Delta)\psi^N$ is the error. If the error F is small in the energy norm. Then we can show that $\mathbf{u}(F)$ and $\nabla\mathbf{u}(F)$ are small.

Due to the round off error in solving the elliptic equation numerically, the error $\partial_x F(x, y)$ is large for small x and large y , e.g. $x \leq 1, y \geq 10^7$, and $\partial_y F(x, y)$ is large for small y and large x ,

e.g. $y \leq 1, x \geq 10^7$. To obtain a sharp estimate of $\mathbf{u}(F)$ and its derivatives, we avoid using the pointwise value of these quantities.

6.8.1. Estimates of \mathbf{u} and $\nabla \mathbf{u}$. The simplest way to estimate the nonlocal term $\mathbf{u}(f)$ is to use some embedding inequality that bounds the weighted L^∞ norm of $\mathbf{u}(f)$ by the weighted L^∞ norm of f . To estimate $\nabla \mathbf{u}(\omega)$, firstly, we rewrite them as the velocity of some function f .

Let $\chi : \mathbb{R}_+ \rightarrow [0, 1]$ be some cutoff function such that $\chi(y) = 1$ for small y and $\chi = 0$ for large y . Denote $\chi_1(y) = \chi(y), \chi_2(y) = 1 - \chi(y)$. We decompose F as $F\chi_1 + F\chi_2$. The first part is supported in the region with small y . Since ∂_x commutes with $(-\Delta)^{-1}$, we have

$$\partial_x \mathbf{u}(F\chi_1) = \mathbf{u}(F_x \chi_1), \quad u_y(F\chi_1) = F\chi_1 + v(F_x \chi_1), \quad v_y(F\chi_1) = -u_x(F\chi_1) = -u(F_x \chi_1),$$

where we have used $u_y(g) - v_x(g) = g$.

Denote $\bar{y} = (y_1, -y_2)$. For the second part, using the definition of u_x and integration by parts in y direction, we yield

$$\begin{aligned} u_x(F\chi_2) &= \frac{1}{2\pi} \int_{\mathbb{R}_+^2} \left(\frac{-2(x_1 - y_1)(x_2 - y_2)}{|x - y|^4} + \frac{2(x_1 - y_1)(x_2 + y_2)}{|x - \bar{y}|^4} \right) F(y) \chi_2(y) dy \\ &= \frac{1}{2\pi} \int_{\mathbb{R}_+^2} \left(-\partial_{y_2} \frac{x_1 - y_1}{|x - y|^4} - \partial_{y_2} \frac{x_1 - y_1}{|x - \bar{y}|^4} \right) F(y) \chi_2(y) dy \\ &= \frac{1}{2\pi} \int \left(\frac{x_1 - y_1}{|x - y|^2} + \frac{x_1 - y_1}{|x - \bar{y}|^2} \right) \partial_{y_2} (F(y) \chi_2(y)) dy \triangleq -v^e((F\chi_2)_y), \end{aligned}$$

where the boundary term vanishes since $\chi_2(y_2) \Big|_{y_2=0} = 0$ and e in the superscript means even function. Similarly, for u_y and $x_2 \geq 0$, we have

$$u_y(F\chi_2) = \frac{1}{2\pi} \int_{\mathbb{R}_+^2} \left(-\partial_{y_2} \frac{x_2 - y_2}{|x - y|^2} - \partial_{y_2} \frac{x_2 + y_2}{|x - \bar{y}|^2} \right) F\chi_2 dy,$$

where ∂_{y_2} is the distributional derivatives. Using integration by parts, we derive

$$u_y(F\chi_2) = \frac{1}{2\pi} \int_{\mathbb{R}_+^2} \left(\frac{x_2 - y_2}{|x - y|^2} + \frac{x_2 + y_2}{|x - \bar{y}|^2} \right) \partial_{y_2} (F\chi_2) dy \triangleq u^e(\partial_y(F\chi_2)).$$

For v_x, v_y , we get

$$v_x(F\chi_2) = u_y(F\chi_2) - F\chi_2 = u^e((F\chi_2)_y) - F\chi_2, \quad v_y(F\chi_2) = -u_x(F\chi_2) = v^e(F\chi_2).$$

Therefore, we obtain

$$\begin{aligned} u_x(F) &= u(F_x \chi_1) - v^e((F\chi_2)_y), \quad u_y(F) = F\chi_1 + v(F_x \chi_1) + u^e((F\chi_2)_y) \\ v_x(F) &= v(F_x \chi_1) + u^e((F\chi_2)_y) - F\chi_2, \quad v_y(F) = -u_x(F). \end{aligned}$$

Thus, to estimate the error $\nabla \mathbf{u}(F)$ and $\mathbf{u}(F)$, we can use the above decomposition and estimate the weighted norm of F , which depends on two local terms ω, ψ^N . Then we develop functional inequalities for the nonlocal operator using the methods in Section 7.

6.8.2. Estimate near 0 and estimates of $\nabla^2 \mathbf{u}$. Denote by F the error in the elliptic equation $F = \omega - (-\Delta)\psi^N$ after correction on ω, ψ^N . We have $F = O(|x|^2)$ near $x = 0$ (6.4). Denote $\tilde{u} = u - u_x(0)x, \tilde{v} = v - v_y(0)y$. We need to estimate

$$\frac{1}{|x|^3} \tilde{u}(F), \quad \frac{1}{|x|^3} \tilde{v}(F).$$

See Section 6.8.3.

Note that in general, the operator \tilde{u} does not map $L^\infty(|x|^{-2})$ to $L^\infty(|x|^{-3})$. We use the regularity of $u(F)$ and estimate $\nabla^2 u(F)$ near 0. Firstly, we solve another Poisson equation to obtain ψ_2

$$(6.15) \quad (-\Delta)\psi_2 = \omega_{xx}.$$

Denote $\psi_1 = \psi^N$. Then we perform the decomposition

$$\begin{aligned}\partial_{xx}\tilde{u}(F) &= \partial_{xx}u(F) = u(F_{xx}) = u(\omega_{xx} - (-\Delta)\psi_{1,xx}) \\ &= u(\omega_{xx} - (-\Delta)\psi_2 + (-\Delta)\psi_2 - (-\Delta)\psi_{1,xx}) = u(\omega_{xx} - (-\Delta)\psi_2) + \psi_{1,xxx} - \psi_{2,y}.\end{aligned}$$

Similarly, we obtain

$$\begin{aligned}\partial_{xx}\tilde{v}(F) &= v(\omega_{xx} - (-\Delta)\psi_2) - \psi_{1,xxx} + \psi_{2,x}, \\ \partial_{xy}\tilde{u}(F) &= \partial_{xy}u(F) = \partial_x(F + v_x(F)) = F_x + v_{xx}(F) \\ &= \partial_x(\omega - (-\Delta)\psi_1) + v(\omega_{xx} - (-\Delta)\psi_2) - \psi_{1,xxx} + \psi_{2,x}, \\ &= \partial_x(\omega + \psi_{1,yyy} + \psi_2) + v(\omega_{xx} - (-\Delta)\psi_2), \\ \partial_{yy}\tilde{u}(F) &= \partial_{yy}u(F) = \partial_y(F + v_x(F)) = F_y + v_{xy}(F) = F_y - u_{xx}(F) = F_y - u(F_{xx}) \\ &= \partial_y(\omega - (-\Delta)\psi_1) - u(\omega_{xx} - (-\Delta)\psi_2) - \psi_{1,xy} + \psi_{2,y} \\ &= \partial_y(\omega + \psi_{1,yy} + \psi_2) - u(\omega_{xx} - (-\Delta)\psi_2).\end{aligned}$$

The important reason we introduce ψ_2 is that the error $\omega_{xx} - (-\Delta)\psi_{1,xx}$ is not small. In fact, suppose that the numerical scheme of solving the Poisson equation has order k . Then, formally, the error $\omega_{xx} - (-\Delta)\psi_{1,xx}$ is of order h^{k-4} , which is not small. Moreover, due to the slow decay of ω and large round off error, ψ_1 is not accurate for large $|x|$. Thus, if we use functional inequality and some weighted norm of $\omega_{xx} - (-\Delta)\psi_{1,xx}$ to estimate $u(\omega_{xx} - (-\Delta)\psi_{1,xx})$, the resulting estimate is not small. The error $\omega_{xx} - (-\Delta)\psi_2$ related to solving (6.15) is much smaller since it only involves second order derivative of the numerical solution and the source term ω_{xx} decays much faster. To estimate the nonlocal terms in the above decomposition, we estimate the weighted L^∞ norm of $\omega_{xx} - (-\Delta)\psi_2$ and use functional inequalities for u, v developed in Section 7.

6.8.3. Estimate weighted norm of \tilde{u} using $\nabla^k\tilde{u}$. In the previous Section, we discuss the estimate of ∇^2u . Based on these estimates, we can develop the weighted estimate of \tilde{u} with singular weights. Recall $\tilde{u} = u - u_x(0)x$, $\tilde{v} = v - v_y(0)y = v + u_x(0)y$. We show how to estimate $|x|^{-k}\tilde{u}$ using the estimate of $|x|^{-l}\nabla^k\tilde{u}$.

Basic operators. Define the average operators

$$E_1F(x, y) = \frac{1}{x} \int_0^x F(z, y) dz, \quad E_2F(x, y) = \frac{1}{y} \int_0^y F(x, z) dz.$$

For $i + j = 3$, define

$$C_{i,j}(x, y) \triangleq \left(\frac{1}{xy} \int_0^x \int_0^y \frac{1}{|x|^2} |\partial_x^i \partial_y^j \tilde{\psi}(x, y)|^2 dx dy \right)^{1/2}$$

where $\tilde{\psi}$ is the modified stream function $\tilde{\psi} = \psi - \psi_{xy}(0)xy$.

Estimate of $\tilde{u}/|x|^3$. Since \tilde{u} is odd in x , to estimate $\tilde{u}/|x|^3$ using $\nabla^2\tilde{u}/|x|$, we use the following estimates

$$\begin{aligned}\left| \frac{1}{|x|^3} \tilde{u} \right| &= \left| \frac{1}{|x|^3} \left(\int_0^x \int_0^y \partial_{xy}\tilde{u} + \int_0^x \partial_{xx}\tilde{u}(a, 0)(x-a) da \right) \right| \\ &\leq \frac{1}{|x|^3} \left(\left(\frac{1}{xy} \int_0^x \int_0^y \frac{(\tilde{u}_{xy})^2}{|x|} dx dy \right)^{1/2} \frac{xy|x|}{\sqrt{3}} + \frac{x^3}{\sqrt{30}} \left(\frac{1}{x} \int_0^x (\tilde{u}_{xx})^2 dx \right)^{1/2} \right) \\ &= \frac{1}{|x|^3} \left(\frac{xy|x|}{\sqrt{3}} C_{1,2}(x, y) + \frac{x^3}{\sqrt{30}} C_{2,1}(x, 0) \right).\end{aligned}$$

Similarly, for \tilde{v} , we yield

$$\left| \frac{1}{|x|^3} \tilde{v} \right| = \left| \frac{1}{|x|^3} \left(\int_0^x \int_0^y \partial_{xy}\tilde{v} + \int_0^y \partial_{yy}\tilde{v}(y-a) da \right) \right| \leq \frac{1}{|x|^3} \left(\frac{xy|x|}{\sqrt{3}} C_{2,1}(x, y) + \frac{y^3}{\sqrt{30}} C_{1,2}(0, y) \right).$$

Next, we estimate $\nabla \tilde{u}$. We have

$$\begin{aligned} \left| \frac{\tilde{u}_x}{|x|^2} \right| &= \frac{1}{|x|^2} \left(\int_0^y \partial_{xy} \tilde{u} dy + \int_0^x \tilde{u}_{xx}(z, 0) dz \right) \\ &\leq \frac{1}{|x|^2} \left((E_2((\frac{\partial_{xy} \tilde{u}}{|x|})^2))^{1/2} y \sqrt{x^2 + \frac{y^2}{3}} + E_1((\frac{\tilde{u}_{xx}}{x})^2)^{1/2} \frac{x^2}{\sqrt{3}} \right). \end{aligned}$$

Using the incompressibility condition, we obtain the estimate for $\tilde{v}_y = -\tilde{u}_x$.

For $\tilde{v}_x = v_x$, we have

$$\left| \frac{v_x}{|x|^2} \right| = \frac{1}{|x|^2} \left| \int_0^x v_{xx}(z, y) dz \right| \leq \frac{1}{|x|^2} \left(E_1 \left(\frac{v_{xx}^2}{|x|^2} \right) \right)^{1/2} x \sqrt{\frac{x^2}{3} + y^2}.$$

For $\tilde{u}_y = u_y$, there are two different estimates. The first one is to use $u_y = v_x + \omega$ and the above estimate. The second one is the following

$$\left| \frac{u_y}{|x|^2} \right| = \frac{1}{|x|^2} \int_0^x u_{xy}(z, y) dz \leq \frac{1}{|x|^2} \left(E_1 \left(\frac{u_{xy}^2}{|x|^2} \right) \right)^{1/2} x \sqrt{\frac{x^2}{3} + y^2}.$$

Using these estimates, we obtain the weighted estimate for $\tilde{u}, \nabla \tilde{u}$ near $x = 0$.

6.9. Estimate the velocity based on the sharp functional inequalities. Another way to estimate the weighted L^∞ and $C^{1/2}$ norm of $\mathbf{u}(F), \nabla \mathbf{u}(F)$ is to use the sharp nonlocal estimate that we develop in Sections 4, 7. Since such inequalities for $\mathbf{u}_A, \nabla \mathbf{u}_A$ only involve the norm $\|\omega_1 \varphi_1\|_\infty$ and $\|\omega_1 \psi\|_{C_g^{1/2}}$, we only need to estimate these norms for F . Yet, since F does not vanish to $O(|x|^3)$ in general, we decompose F as follows

$$F = (F - F_{xy}(0)\chi_F) + F_{xy}(0)\chi_F \triangleq F_1 + F_2,$$

where $\chi_F(x, y)$ is some cutoff function with $\chi_F(x, y) = xy$ for x, y near 0. Then we can decompose the velocity as follows

$$\mathbf{u}(F) = \mathbf{u}(F_2) + \mathbf{u}(F_1) = \mathbf{u}(F_2) + \mathbf{u}_A(F_1) + \hat{\mathbf{u}}(F_1).$$

where $\hat{\mathbf{u}}$ is the approximation term for \mathbf{u} (2.89). Similarly, we perform a decomposition for $\nabla \mathbf{u}$. We can further require $\chi_F = -\Delta \chi_{F,2}$ for another cutoff function. For example, we can choose

$$\chi_{F,2} = -\frac{x^3 y}{2} \chi_{F,3}$$

for some cutoff function $\chi_{F,3}$ with $\chi_{F,3} = 1 + O(|x|^4)$ near 0. In this case, we have

$$\mathbf{u}(F_2) = F_{xy}(0)\mathbf{u}(\chi_F) = F_{xy}(0)\mathbf{u}(-\Delta \chi_{F,2}) = F_{xy}(0)\nabla^\perp \chi_{F,2},$$

which depends on $\chi_{F,2}$ locally. For $\hat{\mathbf{u}}(F_1)$, we can write it as

$$\hat{\mathbf{u}}(F_1) = \sum_{i=1}^n a_i(F_1) \bar{g}_i(x), \quad a_i(F_1) = \int_{\mathbb{R}_2^{++}} F_1(y) q_i(y) dy$$

for some functions $\bar{g}_i(x)$ and $q_i(y)$. We can estimate $\partial_x^i \partial_y^j F_1$ in each piecewise small domain $[a, b] \times [c, d]$. Gluing them together, we can estimate the weighted norm of F_1 and the above integrals on F_1 .

7. ESTIMATE THE L^∞ AND HÖLDER NORM OF THE VELOCITY IN THE REGULAR CASE

In the energy estimate in Section 4, we need to estimate the weighted L^∞ and Hölder norm of $\mathbf{u}_A, \nabla \mathbf{u}_A$ (4.2). The most singular part in these estimates can be obtained using the sharp Hölder estimates in Section 3. In Section 4.2, we outline some ideas of obtaining sharp weighted estimates of the nonlocal terms with computer assistance. In this section, we discuss in details how to estimate them. We will use the scaling symmetries of the singular integral in a crucial way. See the discussions in Section 4.2.1.

Difficulties in the computations. In addition to the difficulties discussed in Section 4.2.1, the singular integral introduces several technical difficulties in our estimates. To address these difficulties, we need to consider different scenarios and decompose the domain of the integrals carefully in our computer assisted estimates. Given $\omega\varphi \in L^\infty$, the velocity \mathbf{u} and the commutator (2.34) for $\nabla\mathbf{u}$ is only log-Lipschitz. The logarithm singularity introduces several difficulties. For example, if \mathbf{u} is Lipschitz, a natural approach to estimate its Hölder norm in terms of $\|\omega\varphi\|_\infty$ is to estimate the piecewise bound of \mathbf{u} and $\partial\mathbf{u}$, which are local, and then use the method in Section G.6. However, since \mathbf{u} is only log-Lipschitz, we need to perform a decomposition of \mathbf{u} into the regular part and the singular part carefully. For different parts, we will apply different estimates. For $\nabla\mathbf{u}$, the estimates are more involved since it is more singular.

Another difficulty is that the odd extension W of ω from \mathbb{R}_+^2 to \mathbb{R}^2 (3.3) is not Hölder continuous in y near the boundary. The specific quantity W to be considered is relevant since $f = K_f(s) * W$ for $f = u, v, u_x$ etc (3.4). To overcome this difficulty and estimate $\nabla\mathbf{u}(x)$ for x near the boundary effectively, we need to perform careful decomposition of the kernels with the singular region adapted to the distance between x and the boundary.

7.1. Several strategies. Recall the discussion of scaling symmetry in Section 4.2.1.

7.1.1. Integral with approximation. In our computation of $\mathbf{u}_A = \mathbf{u} - \hat{\mathbf{u}}, \nabla\mathbf{u}_A = \nabla\mathbf{u} - \widehat{\nabla\mathbf{u}_A}$, where the approximation terms are defined in (2.82), (2.88), (2.89), the rescaling argument still applies. We consider one approximation term $c(x) \int \mathbf{1}_{y \notin S} K(x_1, y) \omega(y) dy$ for $\int K(x, y) \omega(y) dy$ to illustrate the ideas, where S is the singular region associated with x_1 . Such an approximation term relates to (2.82). Suppose that K is -2 -homogeneous. We want to estimate

$$I = \rho(x) \int_{\mathbb{R}^2} (K(x, y) - c(x)K(x_1, y)\mathbf{1}_{y \notin S}) W(y) dy,$$

where W is the odd extension of ω from \mathbb{R}_+^2 to \mathbb{R}^2 . Denote

$$(7.1) \quad f_\lambda(x) \triangleq f(\lambda x).$$

We choose $\lambda \asymp |x|$ and denote $x = \lambda\hat{x}, y = \lambda\hat{y}, x_1 = \lambda\hat{x}_1$. Then we have

$$(7.2) \quad \begin{aligned} I &= \rho_\lambda(\hat{x}) \int_{\mathbb{R}^2} \left(K(\lambda\hat{x}, \lambda\hat{y}) - c(\lambda\hat{x})\mathbf{1}_{\lambda\hat{y} \notin S} K(\lambda\hat{x}_1, \lambda\hat{y}) \right) W(\lambda\hat{y}) \lambda^2 d\hat{y} \\ &= \rho_\lambda(\hat{x}) \int_{\mathbb{R}^2} \left(K(\hat{x}, \hat{y}) - c(\lambda\hat{x})\mathbf{1}_{\hat{y} \notin S/\lambda} K(\hat{x}_1, \hat{y}) \right) W_\lambda(\hat{y}) d\hat{y}. \end{aligned}$$

The singular region becomes S/λ and close to $x_1/\lambda = \hat{x}_1$. For example, if $S = \{y : \max|y_i - x_{1,i}| \leq a\}$, we have $S/\lambda = \{y : \max|y_i - x_{1,i}| \leq a/\lambda\}$. For the above integral, we can still symmetrize the kernel and then estimate it similar to that in Section 4.2.1.

The bulk and approximation. To take advantage of the scaling symmetry and overcome the singularity, in our computation for x away from the origin and not too large, we choose several dyadic rescaling parameters $\lambda = 2^i, i \in I$, e.g. $I = \{-4, -3, \dots, 10\}$. Then for any x with $\max(x_1, x_2) \in [2^i x_c, 2^{i+1} x_c]$, we can choose $\lambda = 2^i$ so that the rescaled $\hat{x} = \frac{x}{\lambda}$ satisfies

$$(7.3) \quad \hat{x} \in \begin{cases} [x_c, 2x_c] \times [0, 2x_c], & \text{if } x_2 \leq x_1, \\ [0, x_c] \times [x_c, 2x_c], & \text{if } x_2 > x_1. \end{cases}$$

We also choose the x_i and the size of the singular region t_i for the approximation term (2.82) such that x_i/λ is on the grid point of the mesh and the boundary of the singular region $\{y : |x_i - y_1| \vee |y_2| \geq t_i/\lambda\}$ aligns with one of the edges of a mesh cell. For example, this can be done by choosing the following y mesh in the near-field to discretize the y -integral, x_i , and t_i

$$y_{1,i} = ih, \quad y_{2,i} = ih, \quad x_i = 2^{n_i} h, \quad t_i = 2^{m_i} h.$$

Then when we discretize the rescaled integral in y , e.g. (7.2), the singular region is the union of several mesh cells. For large y , it is away from the singularity \hat{x} . Then we can use an adaptive mesh in y_1, y_2 to discretize the integral.

We remark that in (7.2), if $x_1 \neq 0$ and x_1/λ is too large or too small, since $c(x)$ is supported near x_i (see (2.82)), $c(\lambda\hat{x})$ will be 0. This means that when we compute $\mathbf{u}_A(x), \widehat{\nabla \mathbf{u}_A}$, if the coefficient of an approximation term with center x_i and parameter t_i is nonzero, e.g., $c(x) \neq 0$, then λ is comparable to x_1 when we rescale the integral by λ . Thus $\hat{x}_1 = x_1/\lambda$ is on the grid. We also choose t_i such that t_i/λ is a multiple of mesh size h for λ comparable to x_i .

Remark 7.1. Using the scaling symmetry and rescaling the integral by dyadic scales, we can compute the integral for $x \in [0, D]^2 \setminus [0, d]^2$ with roughly $O(\log(D/d))$ computational cost.

The near-field and the far-field. If x is sufficiently small, i.e. $\max(x_1, x_2) < \min_{i \in I} 2^i x_c$, we choose $\lambda = \max(x_1, x_2)/x_c$ so that the rescaled $\hat{x} = \frac{x}{\lambda}$ is on the line $x_1 = x_c$ or $x_2 = x_c$. Assuming $\varphi(x) \geq |x|^{-\beta_1} |x_1|^{-\beta_2}$, $\rho \sim |x|^{-\alpha}$ near $x = 0$, and K is $-l$ -homogeneous, then we get

$$(7.4) \quad \begin{aligned} |\rho(x) \int_{\mathbb{R}_2^{++}} K(x, y) \omega(y) dy| &\leq \|\omega_\lambda \varphi_\lambda\|_{L^\infty} \rho_\lambda(\hat{x}) \int_{\mathbb{R}_2^{++}} |K(\hat{x}, \hat{y})| \varphi_\lambda(\hat{y})^{-1} \lambda^{2-l} d\hat{y} \\ &\leq \|\omega_\lambda \varphi_\lambda\|_{L^\infty} \lambda^{\beta_1 + \beta_2 + 2-l} \rho_\lambda(\hat{x}) \int_{\mathbb{R}_2^{++}} |K(\hat{x}, \hat{y})| |\hat{y}|^{\beta_1} \hat{y}_1^{\beta_2} d\hat{y}. \end{aligned}$$

As $x \rightarrow 0$, $\lambda \rightarrow 0$. The factor $\lambda^{\beta_1 + \beta_2 + 2-l}$ absorbs the large factor $\lambda^{-\alpha}$ in $\psi_\lambda(\hat{x})$. In our estimate of $\mathbf{u}_A, \nabla \mathbf{u}_A$, we have $\beta_1 + \beta_2 = 3$ for φ_1 (4.14), $l = 2$, $\alpha = 2$ for ψ_1 (C.1), and $\beta_1 + \beta_2 + 2 - l - 2 = 1 > 0$.

In general, the above integral may not be integrable due to the growing weight $|y|^{\beta_1} y_1^{\beta_2}$. For $\mathbf{u}_A, \nabla \mathbf{u}_A$ with small x , it takes the form (2.84), (2.81)

$$(7.5) \quad f(x) - C_{f0}(x)u_x(0) - C_f(x)\mathcal{K}_{00} = \int_{\mathbb{R}_2^{++}} (K_f^{sym} + C_{f0}(x) \frac{4}{\pi} \frac{y_1 y_2}{|y|^4} - C_f(x)K_{00}(y)) \omega(y) dy,$$

where C_{f0}, C_f are defined in (2.80), and $f = u, v, u_x, v_x, u_y, v_y$. In particular, the associated kernel has a much faster decay rate $|y|^{-6}$, which will be shown in (D.16), (D.17). Thus, the integral is integrable.

Since $\lambda = \max(x_1, x_2)/x_c$ is very small, $\rho_\lambda(\hat{x})$ can be well approximated by the most singular power $c\lambda^{-\alpha}|x|^{-\alpha}$ for some $c > 0$, which can be estimated effectively after factorizing out $\lambda^{-\alpha}$.

Similarly, if x is sufficiently large, i.e. $\max(x_1, x_2) > \max_{i \in I} 2^{i+1} x_c$, we choose $\lambda = \frac{\max(x_1, x_2)}{x_c}$ so that the rescaled $\hat{x} = x/\lambda$ is on the line $x_1 = x_c$ or $x_2 = x_c$. Since λ is sufficiently large, we can estimate the weight $\rho_\lambda, \varphi_\lambda$ based on their asymptotic behavior.

7.1.2. The scaling relations. We discuss several scaling relations, which will be useful in later computation. For a $-d$ -homogeneous kernel K , i.e., $K(\lambda x) = \lambda^{-d} K(x)$, we have

$$I(x) = \rho(x) \int K(x, y) \omega(y) dy = \rho_\lambda(\hat{x}) \int K(\hat{x}, \hat{y}) \omega_\lambda(\hat{y}) \lambda^{2-d} d\hat{y} \triangleq \lambda^{2-d} I_\lambda(\hat{x}),$$

where $x = \lambda\hat{x}, y = \lambda\hat{y}$. To compute the derivative of $I(x)$, using the chain rule, we have

$$\partial_{x_i} I(x) = \lambda^{2-d} \frac{d\hat{x}_i}{dx_i} \partial_{\hat{x}_i} I_\lambda(\hat{x}) = \lambda^{1-d} \partial_{\hat{x}_i} I_\lambda(\hat{x}).$$

For the L^∞ part, clearly, we get $|I(x)| = |I_\lambda(\hat{x})|$. To compute the Hölder norm, we use the following relation $|x - z| = \lambda|\hat{x} - \hat{z}|$ and

$$\frac{|I(x) - I(z)|}{|x - z|^{1/2}} = \lambda^{-1/2} \frac{|I_\lambda(\hat{x}) - I_\lambda(\hat{z})|}{|\hat{x} - \hat{z}|^{1/2}}.$$

In particular, we have

$$(7.6) \quad \|\omega_\lambda \varphi_\lambda\|_\infty = \|\omega \varphi\|_\infty, \quad [\omega_\lambda \psi_\lambda]_{C_{x_i}^{1/2}} = \lambda^{1/2} [\omega \psi]_{C_{x_i}^{1/2}}, \quad i = 1, 2.$$

Using these scaling relations, we can perform the estimate in a rescaled domain with any $\lambda > 0$.

7.1.3. *Mesh and the Trapezoidal rule.* After rescaling the integral with suitable scaling factor λ , we can restrict the rescaled singularity $\hat{x} \in [0, 2x_c]^2 \setminus [0, x_c]^2$ (7.2), (7.3).

If a domain Q is away from the singularity \hat{x} of the kernel, applying (7.6), we get

$$(7.7) \quad \int_Q |K(\hat{x}, y)| |\omega_\lambda(y)| dy \leq \|\omega_\lambda \varphi_\lambda\|_\infty \int_Q |K(\hat{x}, y)| \varphi_\lambda^{-1}(y) dy = \|\omega \varphi\|_\infty \int_Q |K(\hat{x}, y)| \varphi_\lambda^{-1}(y) dy.$$

Then, it suffices to estimate the integral of an explicit function $|K(\hat{x}, y)| \varphi_\lambda^{-1}(y)$. If in addition, the region Q is small, e.g. Q is the grid $[y_i, y_{i+1}] \times [y_j, y_{j+1}]$ introduced below, we further apply

$$\int_Q |K(\hat{x}, y)| |\omega_\lambda(y)| dy \leq \|\omega \varphi\|_\infty \|\varphi_\lambda^{-1}\|_{L^\infty(Q)} \int_Q |K(\hat{x}, y)| dy.$$

Since the domain Q is small, the estimate is sharp. We use the following method to estimate $\int |K(\hat{x}_i, y)| dy$ for a suitable kernel K and \hat{x}_i on the grid points.

We consider the estimate of the L^1 norm of some function f in \mathbb{R}_{++}^2 , e.g. $f = K(\hat{x}_i, y)$ mentioned above. To discretize the integral, we design uniform mesh in the domain $[0, b]^2$ covering Ω_1 and Ω_2 with mesh size h and adaptive mesh in the larger domain $[0, D]^2$

$$(7.8) \quad 0 = y_0 < y_1 < \dots < y_n = D, \quad y_i = ih, \quad i \leq b/h.$$

The finer mesh in the near field $[0, b]^2$ allows us to estimate the integral with higher accuracy. We choose sparser mesh in the far-field since y is away from the singularity \hat{x} and the kernel decays in y . We partition the integral as follows

$$(7.9) \quad \int_{\mathbb{R}_{++}^2} |f(y)| dy = \sum_{0 \leq i, j \leq n-1} \int_{[y_i, y_{i+1}] \times [y_j, y_{j+1}]} |f(y)| dy + \int_{y \notin D} |f(y)| dy.$$

We focus on how to estimate the first part for nonsingular f . In Section 7.4, we estimate the integral beyond $[0, D]^2$ using the decay of the integral. We will discuss how to estimate the integral near the singularity of the kernel in a later section.

Denote $Q = [a, b] \times [d, c], h_1 = b - a, h_2 = d - c$. We use the Trapezoidal rule

$$\int_{[a, b] \times [c, d]} |f(y)| dy \leq T(|f|, Q) + Err(f),$$

where

$$T(f, Q) \triangleq \frac{(b-a)(d-c)}{4} (f(a, c) + f(a, d) + f(b, c) + f(b, d)).$$

The error estimate of the above Trapezoidal rule is not obvious due to the absolute sign. In fact, even if f is smooth, $|f|$ is only Lipschitz near the zeros of f . Since the set of zeros is hard to characterize and that $|f|$ can have low regularity, we do not pursue higher order quadrature rule. We have the following error estimate.

Lemma 7.2 (Trapezoidal rule for the L^1 integral). *For $f \in C^2(Q)$, we have*

$$\int_Q |f(y)| dy \leq T(|f|, Q) + \frac{|Q|}{12} (h_1^2 \|f_{xx}\|_{L^\infty(Q)} + h_2^2 \|f_{yy}\|_{L^\infty(Q)}).$$

Remark 7.3. The above estimate shows that the Trapezoidal rule remains second order accurate from the above. In particular, this error estimate is comparable to the case without taking the absolute value.

Proof. Define the linear interpolation of f in Q

$$L(f) = \sum_{i=1}^4 \lambda_i(x) f_i, \quad E(f) = f - L(f),$$

where $\lambda_i(x)$ is linear and satisfies $\sum \lambda_i(x) = 1$ and $\lambda_i(x) \geq 0$ for $x \in Q$. Using the triangle inequality, we obtain

$$\int_Q |f| dy \leq \int_Q |E(f)| dy + \int_Q \lambda_i(x) |f_i| dy = T(|f|, Q) + \int_Q |E(f)| dy.$$

We have the standard error bound for $E(f)$

$$(7.10) \quad |E(f)| \leq \frac{\|f_{xx}\|_{L^\infty(Q)}}{2}|(x-a)(x-b)| + \frac{\|f_{yy}\|_{L^\infty(Q)}}{2}|(y-c)(y-d)|.$$

It can also be established using the error estimate for the 2D Lagrangian interpolation with $k = 2$ (G.11) in Section G.2. Integrating the above estimate in x, y and using $\frac{1}{2} \int_0^1 t(1-t)dt = \frac{1}{12}$ conclude the proof. \square

To estimate the integral $\int |K(x, y)|$ for all $\hat{x} \in \Omega_1, \Omega_2$ (7.3), we discretize $[0, 2a]^2$ using uniform mesh with mesh size $h_x = h/2$. We use the above method to estimate $\int |K(\hat{x}_i, y)|dy$ for x_i on the grid points. After we estimate the derivatives of the kernel, we use the following Lemma to estimate the integral for any x in a domain.

Lemma 7.4. *Suppose that $K(x, y) \in C^2(P \times D)$, $P = [a_1, b_1] \times [a_2, b_2]$, $h_i = b_i - a_i, i = 1, 2$, and $Q = [a, b] \times [c, d]$. Let $L(K)(x, y) = \sum_{i,j=1,2} \lambda_{ij}(x)K((a_i, b_j), y)$ be the linear interpolation of $K(x, y)$ in x using $K((a_i, b_j), y), i, j = 1, 2$. Then for any $x \in P$, we have*

$$\int_Q |K(x, y)|dy \leq \sum_{i,j=1,2} \lambda_{ij}(x) \int_Q |K((a_i, b_j), y)|dy + \left(\frac{h_1^2}{8} \|K_{xx}\|_{L^\infty(P \times Q)} + \frac{h_2^2}{8} \|K_{yy}\|_{L^\infty(P \times Q)} \right) |Q|.$$

The proof follows from (7.10), the triangle inequality and $\frac{1}{2}|t(1-t)| \leq \frac{1}{8}$ for $t \in [0, 1]$. We will apply the above Lemma and sum Q over all the near-field domains $Q_{ij} = [y_i, y_{i+1}] \times [y_j, y_{j+1}]$ (7.8). Since $\sum_{ij} \lambda_{ij}(x) = 1$, we can simplify the first term as follows

$$\sum_{i,j=1,2} \lambda_{ij}(x) \sum_{k,l \leq n} \int_{Q_{kl}} |K((a_i, b_j), y)|dy \leq \max_{i,j} \sum_{k,l \leq n} \int_{Q_{kl}} |K((a_i, b_j), y)|dy.$$

Therefore, it suffices to estimate the integral for x on the grid points and the piecewise derivative bounds of the kernel.

We apply Lemmas 7.2, 7.4 to estimate the weighted integral related to the velocity. The integrands take the form (7.24), (7.25), (7.18). To estimate the error in the above integrals, we need to obtain piecewise L^∞ estimate of the derivatives of the integrands in P, Q . We estimate the derivatives of the weights in Appendix C.3, the kernel in Appendix D.

Parameters for the integrals. In our computation, we choose

$$(7.11) \quad h_x = 13 \cdot 2^{-12}, \quad h = 13 \cdot 2^{-11}, \quad x_c = 13 \cdot 2^{-5},$$

which can be represented exactly in binary system, to reduce the round off error. The approximate values of the above parameters are $h_x \approx 0.0032, h \approx 0.0064, x_c \approx 0.4$. For $x \in [0, 2x_c]^2 \setminus [0, x_c]^2$ (7.3), we have

$$(7.12) \quad \max(x_1, x_2) \geq x_c = 64h = 128h_x.$$

In our decomposition of the integral, e.g. (7.18), (7.34), (7.37), we impose a constraint on the size of the singular region to satisfy $kh < x_c$ such that the region does not cover the origin.

7.1.4. Decomposition, commutators and the Lipschitz norm. The most difficult part of the computation is to estimate the Hölder norm of $\nabla \mathbf{u}$, and we discuss several strategies. In this computation, we cannot first estimate the local Lipschitz norm of ∇u and then obtain the local Hölder norm due to the difficulties discussed at the beginning of Section 7. We need to decompose the integral related to ∇u into several parts according to the distance between y and the singularity and use different estimates for different parts.

We focus on the integral related to u_x without subtracting any approximation term and assume that $x \in [0, 2x_c]^2 \setminus [0, x_c]^2$. The approximation term $\widehat{\nabla \mathbf{u}}_A$ is nonsingular and can be estimated using the method in Section 7.1.3. Let h be the mesh size in the discretization of the integral in y . Suppose that $x \in [ih, (i+1)h] \times [jh, (j+1)h]$. Denote by $R(x, k)$ the rectangle covering x

$$(7.13) \quad R(x, k) \triangleq [(i-k)h, (i+1+k)h] \times [(j-k)h, (j+1+k)h]$$

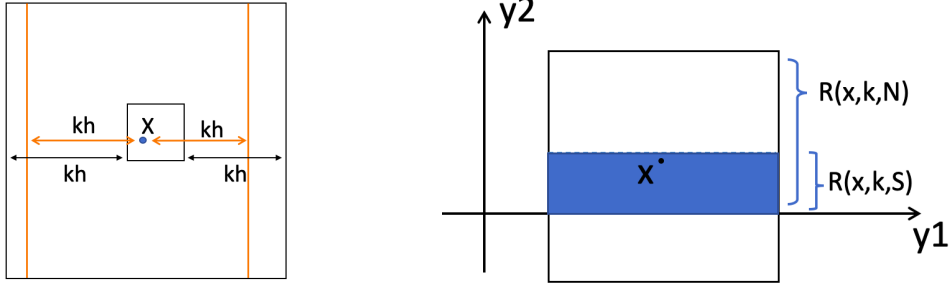


FIGURE 10. Left: The large box is $R(x, k)$ and the red box is $R_{s,1}(x, k)$. The small box containing x has size $h \times h$. Right: The upper box is $R(x, k, N)$, and the shaded box is $R(x, k, S)$, the reflection of the region below the y -axis.

for any $k > 0$. If $k \in \mathbb{Z}^+$, the boundary of $R(x, k)$ is along with the mesh grid and is at least kh away from x . Denote by $R_s, R_{s,1}, R_{s,2}$ different symmetric rectangles with respect to x

$$(7.14) \quad \begin{aligned} R_s(x, k) &\triangleq [x_1 - kh, x_1 + kh] \times [x_2 - kh, x_2 + kh], \\ R_{s,1}(x, k) &\triangleq [x_1 - kh, x_1 + kh] \times [(j - k)h, (j + 1 + k)h], \\ R_{s,2}(x, k) &\triangleq [(i - k)h, (i + 1 + k)h] \times [x_2 - kh, x_2 + kh]. \end{aligned}$$

Clearly, we have $R_s(x, k) \subset R_{s,1}(x, k), R_{s,2}(x, k) \subset R(x, k)$. We introduce the upper and lower parts of the rectangle

$$(7.15) \quad R^+(x, k) \triangleq R(x, k) \cap \{y : y_2 \geq x_2\}, \quad R^-(x, k) \triangleq R(x, k) \cap \{y : y_2 \leq x_2\}.$$

We use similar notations for $R_s(x, k), R_{s,1}(x, k), R_{s,2}(x, k)$. We further introduce the intersection of the rectangle and four half planes with reflection

$$(7.16) \quad \begin{aligned} R(x, k, N) &= R(x, k) \cap \{y : y_2 \geq 0\}, \quad R(x, k, S) = \mathcal{R}_2(R(x, k) \cap \{y : y_2 \leq 0\}), \\ R(x, k, E) &= R(x, k) \cap \{y : y_1 \geq 0\}, \quad R(x, k, W) = \mathcal{R}_1(R(x, k) \cap \{y : y_1 \leq 0\}), \end{aligned}$$

where N, E, S, W are short for *north, east, south, west*, respectively and the reflection operators $\mathcal{R}_1, \mathcal{R}_2$ are given by

$$\mathcal{R}_1(y_1, y_2) = (-y_1, y_2), \quad \mathcal{R}_2(y_1, y_2) = (y_1, -y_2).$$

It is clear that $R(x, k, S) \subset \mathbb{R}_2^{++}, R(x, k, W) \subset \{y : y_1 \geq 0\}$. An illustration of these domains is given in Figure 10. If $x, y \in \mathbb{R}_2^{++}$, we have the equivalence

$$(7.17) \quad (y_1, -y_2) \notin R(x, k) \iff (y_1, -y_2) \notin R(x, k) \cap \{y : y_2 \leq 0\} \iff y \notin R(x, k, S).$$

The above notations will be very useful in our later decomposition of the symmetrized kernel.

Recall the odd extension W of ω in \mathbb{R}^2 (3.3). For simplicity, we drop the x variable in the R notation. For $k > k_2, k, k_2 \in \mathbb{Z}^+$, we decompose the weighted $u_x(x)$ integral as follows

$$(7.18) \quad \begin{aligned} \psi(x) \int K_1(x - y)W(y)dy &= \psi(x) \int_{R(k)^c} K_1(x - y)W(y)dy + \int_{R_{s,1}(k)} K_1(x - y)\psi(y)W(y)dy \\ &+ \int_{R(k) \setminus R_{s,1}(k)} K_1(x - y)\psi(y)W(y)dy + \int_{R(k) \setminus R(k_2)} K_1(x - y)(\psi(x) - \psi(y))W(y)dy \\ &+ \int_{R(k_2)} K_1(x - y)(\psi(x) - \psi(y))W(y)dy \\ &\triangleq I_1(x, k) + I_2(x, k) + I_3(x, k) + I_4(x, k, k_2) + I_5(x, k_2), \end{aligned}$$

where $K_1(s)$ is defined in (3.1), and we have dropped the constant $-\frac{1}{\pi}$ in $u_x(x)$ at this moment to simplify the notation. For the regular part, we use numerical computation in Section 7.1.3 to estimate the derivatives. For the singular part, we will use a change of variables $y = x + s$ to localize our estimate to the singularity.

7.1.5. *Symmetrization.* After we obtain the decomposition, we use the odd symmetry of W in y_1, y_2 to symmetrize the integral and reduce the integral over \mathbb{R}_2 to the first quadrant \mathbb{R}_2^{++} . This enables us to exploit the cancellation in the integral and obtain a sharper estimate. In our computation, we symmetrize the integrals in $I_1(x, k)$ and $I_4(x, k, k_2)$, which are more regular. For a given kernel $K(x, y)$, we denote by K^{sym} the symmetrization of K

$$(7.19) \quad K^{sym}(x, y) \triangleq K(x, y) - K(x, -y_1, y_2) - K(x, y_1, -y_2) + K(x, -y).$$

We show how to symmetrize $I_1(x, k)$ as an example. Suppose that

$$(7.20) \quad x \in \mathbb{R}_2^{++}, \quad x_2 \leq x_1, \quad x \in B_{i_1, j_1}(h_x) \subset B_{ij}(h), \quad j \leq i,$$

where $h_x = h/2$ and $B_{lm}(r)$ is defined as

$$(7.21) \quad B_{lm}(r) = [lr, (l+1)r] \times [mr, (m+1)r].$$

Recall the notations in (7.16). We choose $k < i$ so that $R(x, k) \subset \{y : y_1 > 0\}$ and $R(x, k, W) = \emptyset$. By definition (7.13), the domains $R(x, k), R(x, k, N), R^+(x, k)$ etc are the same for all $x \in B_{i_1, j_1}(h_x)$. Yet, $R(x, k)$ may cross the boundary $y_2 = 0$, i.e. $R(x, k, S) \neq \emptyset$. See the right figure in Figure 10 for a possible configuration. Using the equivalence (7.17) and the property that W is odd in y_1 and y_2 , we can symmetrize $I_1(x, k)$ as follows

$$\begin{aligned} I_1(x, k) = \psi(x) \int_{\mathbb{R}_2^{++}} & \left(K_1(x - y) \mathbf{1}_{y \in R(k)^c} - K_1(x_1 - y_1, x_2 + y_2) \mathbf{1}_{y \notin R(k, S)} \right. \\ & \left. - K_1(x_1 + y_1, x_2 - y_2) + K_1(x + y) \right) \omega(y) dy. \end{aligned}$$

For x in a general location, the symmetrization of I_1 reads

$$(7.22) \quad \begin{aligned} I_1(x, k) = \psi(x) \int_{\mathbb{R}_2^{++}} & \left(K_1(x - y) \mathbf{1}_{y \in R(k)^c} - K_1(x_1 - y_1, x_2 + y_2) \mathbf{1}_{y \notin R(k, S)} \right. \\ & \left. - K_1(x_1 + y_1, x_2 - y_2) \mathbf{1}_{y \notin R(k, W)} + K_1(x + y) \right) \omega(y) dy. \end{aligned}$$

For $I_4(x)$ (7.18), we will choose weight $\psi(y)$ that is even in y_1, y_2 . Thus, the symmetrization of I_4 is

$$(7.23) \quad \begin{aligned} I_4(x, k, k_2) = \int_{\mathbb{R}_2^{++}} & \left(K_1(x - y) \mathbf{1}_{y \in R(k) \setminus R(k_2)} - K_1(x_1 - y_1, x_2 + y_2) \mathbf{1}_{y \in R(k, S) \setminus R(k_2, S)} \right. \\ & \left. - K_1(x_1 + y_1, x_2 - y_2) \mathbf{1}_{y \in R(k, W) \setminus R(k_2, S)} \right) (\psi(x) - \psi(y)) W(y) dy. \end{aligned}$$

In the above formula, we do not have the term $K_1(x + y)$ since for $y \in \mathbb{R}_2^{++}$, $x + y \notin R(k)$. Thus after symmetrizing the kernel in I_4 , we do not have such a term.

Though the symmetrized kernel is complicated, since these regions $R(k), R(k, \alpha), \alpha = N, E$ (7.13), (7.16) can be decomposed into the union of the mesh girds $[y_i, y_{i+1}] \times [y_j, y_{j+1}]$, in each grid, the indicator functions are constants. See also Remark 7.6. In particular, in each grid $y \in [y_i, y_{i+1}] \times [y_j, y_{j+1}]$, we can write the integrand in $I_1 + I_4$ as

$$(7.24) \quad J = K^{NC}(x, y) \cdot \psi(x) + K^C(x, y) \cdot (\psi(x) - \psi(y))$$

where NC, C are short for *non-commutator*, *commutator*, respectively, and K^{NC}, K^C can be determined by the distance between $[y_i, y_{i+1}] \times [y_j, y_{j+1}]$ and $B_{i_1 j_1}(h_x)$. For y away from x , e.g. $|y_1| \vee |y_2| \geq 4x_c$ in our computation, we have

$$(7.25) \quad J = K^{sym}(x, y) \psi(x).$$

7.1.6. *Integral in domains depending on x .* In the computation, we need to estimate several integrals in the domains depending on x , e.g. I_3 in (7.18). We use the L^∞ estimate of I_3 to illustrate the ideas. A direct estimate yields

$$|I_3(x)| \leq \|W\varphi\|_\infty \int_{R(k) \setminus R_{s,1}(k)} |K_1(x - y)| \psi(y) \varphi^{-1}(y) dy.$$

We cannot apply the method in Section 7.1.3 to first estimate $I_3(x)$ for x on the grid points and then estimate $\partial^2 I_3(x)$ for the error since the kernel is singular and the error part associated with $\partial^2 I_3(x)$ is more singular (see Lemma 7.4).

Denote $f = \psi\varphi^{-1}$. We consider a change of variable $y = x + s$ to center our analysis around the singularity x . The domain for s is

$$(7.26) \quad \{y \in R(k) \setminus R_{s,1}(k)\} = \{s \in R(k) - x\} \cap \{|s_1| \geq kh\} \triangleq D(x, k).$$

It suffices to estimate

$$(7.27) \quad J = \int_{s \in D(x, k)} |K_1(-s)|f(x + s)dy$$

for all $x \in B_{i_1,j_1}(x)$ (7.20). We want to further simplify the above domain so that it does not depend on x . Recall the location of x (7.20). To obtain a sharp estimate, we further partition the location of $x \in B_{i_1,j_1}(h_x)$ as follows

$$(7.28) \quad A_a = [i_1 h_x + ah_x/m, i_1 h_x + (a+1)h_x/m], \quad B_b \triangleq [j_1 h_x + bh_x/m, j_1 h_x + (b+1)h_x/m],$$

for some $m \in \mathbb{Z}^+$ and $0 \leq a, b \leq m-1$. Clearly, $A_a \times B_b$ is a partition of $B_{i_1,j_1}(h_x)$. Recall (7.20) and (7.13). We have

$$R(x, k) = [(i-k)h, (i+1+k)h] \times [(j-k)h, (j+1+k)h].$$

Now, for $x \in A_a \times B_b$, since $|s_1| \geq kh$, we have

$$(7.29) \quad \begin{aligned} s_1 = y_1 - x_1 &\in [(i-k)h - i_1 h_x - (a+1)h_x/m, -kh] \cup [kh, (i+1+k)h - i_1 h_x - ah_x/m] \\ &\triangleq X_{l,a} \cup X_{r,a}, \end{aligned}$$

where the subscripts l, r are short for left, right, respectively. Similarly, for s_2 , we have

$$(7.30) \quad \begin{aligned} s_2 = y_2 - x_2 &\in [(j-k)h - j_1 h_x - (b+1)h_x/m, (j+k)h - j_1 h_x - bh_x/m] \\ &\triangleq [(j-k)h - j_1 h_x - (b+1)h_x/m, -kh] \cup [-kh, kh] \cup [kh, (j+1+k)h - j_1 h_x - bh_x/m] \\ &\triangleq Y_{d,b} \cup Y_{m,b} \cup Y_{u,b} \end{aligned}$$

where the subscripts d, m, u are short for down, middle, upper, respectively. Note that the intervals X, Y do not depend on x . We have

$$(7.31) \quad D(x, k) \subset (X_{l,a} \cup X_{r,a}) \times (Y_{d,b} \cup Y_{m,b} \cup Y_{u,b}).$$

Now, we can decompose J (7.27) as follows

$$J \leq \sum_{\alpha=l,r, \beta=d,m,u} J_{\alpha,\beta}, \quad J_{\alpha,\beta} \triangleq \int_{X_{\alpha,a} \times Y_{\beta,b}} |K_1(-s)|f(s+x)dy, \quad \alpha = l, r, \quad \beta = d, m, u.$$

See the left figure in Figure 11 for different domains in the above decomposition. From the definitions of X, Y , the total width of the left and the right domains $X_{\alpha,a} \times (Y_{d,b} \cup Y_{m,b} \cup Y_{u,b})$, $\alpha = l, u$ is

$$|X_{l,a}| + |X_{r,a}| = h + h_x/m.$$

For a fixed x , from the definition (7.13), the width of $R(k) \setminus R_{s,1}(k)$ is h . We choose a large m and further partition the location of x so that we do not overestimate the region too much.

For a small domain $Q = [a, b] \times [c, d]$, we can estimate the integral as follows

$$(7.32) \quad \int_Q |K_1(-s)|f(x + s)ds \leq \int_Q |K_1(-s)|ds \|f\|_{L^\infty(B_{i_1,j_1}(h_x) + Q)}.$$

Since Q is given, $K_1(s)$ is explicit and has scaling symmetries, we can estimate the integral of $|K_1(s)|$ easily. For example, if $Q = [ah, bh]^2$, we can use the scaling symmetries of $K_1(s)$ to obtain $\int_Q |K_1(-s)| = h^\beta \int_{[a,b]^2} |K_1(-s)|$ for some β . Moreover, for many kernels in our computations, e.g. $K(s) = \frac{s_1 s_2}{|s|^4}$, we have explicit formulas for the integral.

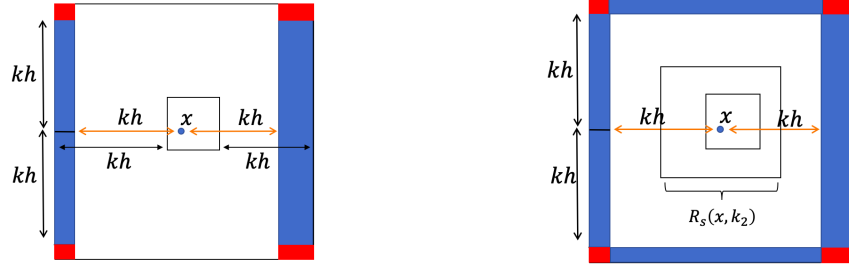


FIGURE 11. The largest box is $R(x, k)$. Left: The left and right blue regions are $X_{l,a} \times Y_{m,b}, X_{r,a} \times Y_{m,b}$. The four red regions correspond to $X_{\alpha,a} \times Y_{\beta,b}, \alpha = l, u, \beta = d, u$. Right: Illustration of $R(x, k) \setminus R_s(x, k)$ and $R_s(x, k_2)$. $R(x, k) \setminus R_s(x, k)$ consists of the blue and the red regions.

We apply the above method to estimate the integral in $X_{\alpha,a} \times Y_{\beta,b}, \alpha = l, r, \beta = d, u$ (red region in Figure 11). Since $Y_{m,b} = [-kh, kh]$, for the integral in $X_{\alpha,a} \times Y_{m,b}$ (blue region), we further decompose it

$$(7.33) \quad J_{\alpha,m} = \sum_{-k \leq t \leq k-1} \int_{X_{\alpha,a} \times [th, (t+1)h]} |K_1(-s)| f(s+x) dy,$$

and then apply the above method to estimate it.

Next, we further simplify $\|f\|_{L^\infty(B_{i_1 j_1}(h_x) + Q)}$ in the above estimate. Firstly, from (7.20), we get

$$ih \leq i_1 h_x < (i_1 + 1)h_x \leq (i + 1)h, \quad jh \leq j_1 h_x < (j_1 + 1)h_x \leq (j + 1)h.$$

For $X_{l,a}$ (7.29) with $0 \leq a \leq m-1$, we have the lower bound for the endpoint

$$(i-k)h - i_1 h_x - (a+1)h_x/m \geq (i-k)h - i_1 h_x - h_x \geq (i-k)h - ((i+1)h - h_x) - h_x = -kh - h.$$

Similarly, we can cover the intervals of X, Y (7.29), (7.30) uniformly for $0 \leq a, b \leq m-1$ and obtain

$$\begin{aligned} X_{l,a} &\subset [(i-k)h - i_1 h_x - h_x, -kh] \subset [-(k+1)h, -kh], \\ X_{u,a} &\subset [kh, (i+1+k)h - i_1 h_x] \subset [kh, (k+1)h], \\ Y_{d,b} &\subset [-(k+1)h, -kh], \quad Y_{d,u} \subset [kh, (k+1)h]. \end{aligned}$$

Thus, we only need to estimate the L^∞ norm of f in

$$Q_{i_1 j_1}(h_x) + [\alpha h, (\alpha+1)h] \times [\beta h, (\beta+1)h], \quad \alpha = -k-1, k, \quad \beta = -(k+1), -k, \dots, k.$$

These estimates are independent of the choice of m, a, b . Since the size of each domain is at most $2h \times 2h$, the above estimates based on (7.32) are sharp. We will estimate the piecewise bound of the weights ψ, φ in later sections.

Using the above decomposition and estimates, we obtain the estimate of J (7.27) for $x \in A_a \times B_b$ (7.28). Similarly, we can estimate J for any $0 \leq a, b \leq m-1$. Taking the maximum of these m^2 estimates, we obtain the estimate of J and $I_3(x)$ for all $x \in B_{i_1 j_1}(h_x)$.

7.1.7. First generalization: the boundary terms. We generalize the above ideas to estimate integrals in other domains depending on x . The first generalization is to estimate the boundary term. We estimate the x_1 -derivative of $I_3(x)$ (7.18) to illustrate the ideas. In the estimate of the x -derivative, we have an extra boundary term I_{32}

$$\partial_1 I_3(x) = \int_{R(k) \setminus R_{s,1}(k)} \partial_{x_1} K_1(x-y) (W\psi)(y) dy - \int_{(j-k)h}^{(j+1+k)h} K_1(x-y) (W\psi)(y) \Big|_{y_1=x_1-kh}^{x_1+kh} dy_2 \triangleq I_{31} + I_{32},$$

where we have used the doamin for $R(x, k)$ (7.13).

For I_{31} , we apply the previous method to estimate it. Denote $\Gamma_k \triangleq [j-k)h, (j+1+k)h]$. Using a change of variable $y = x + s$, we can rewrite I_{32} as follows

$$I_{32} = - \int_{s_2 \in \Gamma_k - x_2} \left(K_1(-kh, -s_2)(W\psi)(x_1 + kh, x_2 + s_2) - K_1(kh, -s_2)(W\psi)(x_1 - kh, x_2 + s_2) \right) ds_2.$$

We partition the location of x and assume $x \in A_a \times B_b \subset B_{i_1, j_1}(h_x)$ (7.28). From (7.30), we have

$$s_2 \in \Gamma_k - x_2 \subset Y_{d,b} \cup Y_{m,b} \cup Y_{u,b}.$$

Using the above decomposition and $|W\psi(x)| \leq \|W\varphi\|_\infty f(x)$, $f = \psi\varphi^{-1}$, we obtain

$$|I_{32}| \leq \|W\varphi\|_\infty \sum_{\alpha=\pm, \beta=d, m, u} M_{\alpha, \beta}, \quad M_{\alpha, \beta} \triangleq \int_{Y_{\beta, b}} |K_1(-\alpha kh, -s_2)| \cdot |f(x_1 + \alpha kh, x_2 + s_2)| ds_2,$$

for $\alpha = \pm, \beta = u, m, d$. For $\beta = u, d$, the domain $Y_{\beta, b}$ is small $|Y_{\beta, b}| \leq h$. We apply the method in (7.32) to estimate $M_{\alpha, \beta}$. The only difference is that we need consider a 1D integral here

$$\int_Q |K_1(-\alpha kh, -s_2)| ds_2$$

for some interval Q , rather than a 2D integral in (7.32). For $M_{\alpha, m}$, we decompose the domain $Y_{m, b}$ into small intervals with length h similar to (7.33) and then apply the method in (7.32).

We combine these estimates to bound I_{32} for $x \in A_a \times B_b$. Then, we maximize the estimates over $0 \leq a, b \leq m-1$ to bound I_{32} for $x \in B_{i_1, j_1}(h_x)$.

7.1.8. Second generalization. In some of the computations, we need to estimate

$$J = \int_{R(k) \setminus R_s(k_2)} |K(x - y)| f(y) dy$$

for some $k_2 < k$ with $2k_2, k \in \mathbb{Z}^+$, where $R_s(k)$ is defined in (7.14). Similarly, we introduce $y = x + s$ and use

$$R_s(k_2) \subset R_s(k) \subset R(k), \quad R(k) \setminus R_s(k_2) = R(k) \setminus R_s(k) \cup R_s(k) \setminus R_s(k_2),$$

to obtain

$$J = \left(\int_{s \in R(k) - x, |s_1| \vee |s_2| \geq kh} + \int_{k_2 h \leq |s_1| \vee |s_2| \leq kh} \right) K(-s) f(x + s) dy \triangleq J_1 + J_2.$$

The estimate of J_1 is similar to J in (7.27). See the right figure in Figure 11 for different regions. Compared to $R(k) \setminus R_{s,1}(k)$, the domain $R(k) \setminus R_s(k)$ contains two more parts

$$X_{m,a} \triangleq [-kh, kh], \quad X_{m,a} \times Y_{u,b}, \quad X_{m,a} \times Y_{d,b},$$

i.e., the upper and lower blue regions in the right figure in Figure 11. The estimate of the integral in these regions is similar to that in $X_{\alpha,a} \times Y_{m,b}$ in (7.31).

For J_2 , the domain is simpler. Since $2k_2 \in \mathbb{Z}^+$, we partition the domain into $h_x \times h_x$ grids

$$J_2 = \sum_{(c,d) \in S_k \setminus S_{k_2}} \int_{[ch_x, (c+1)h_x] \times [dh_x, (d+1)h_x]} |K(-s)| f(s+x) ds, \quad S_l \triangleq \{-k \leq c < k, -k \leq d < k\}.$$

For each integral, we estimate it using the method in (7.32). The remaining steps are the same as those of J in (7.27) studied previously.

Remark 7.5. In the estimates in Section 7.1.6-7.1.8, we use the important property that the weights are locally smooth to move them outside the integral. Moreover, we use the fact that the singular region depend on x smoothly and monotonously so that we can cover it effectively. Note that the integral $\int_Q |K_1(s)| dy$ for different Q, a, b in the above estimates does not depend on x . We can first compute these integrals once and store them. Then use them in the estimate of different x .

7.1.9. *Hölder estimate of log-Lipschitz function.* In some computation, we need to perform $C^{1/2}$ estimate of some log-Lipschitz function. We consider a simple example to illustrate the ideas

$$F(x) = \int_{\max_i |x_i - y_i| \leq b} K(x, y) f(y) dy, \quad |K(x, y)| \leq C_1 |x - y|^{-1}, \quad |\partial K(x, y)| \leq C_2 |x - y|^{-2},$$

for some constant C_1, C_2 . Given $f \in L^\infty$, F is log-Lipschitz. To estimate $[f]_{C_x^{1/2}}$, we cannot first estimate the piecewise values of f and $\partial_x f$ and then combine them to obtain the $C_x^{1/2}$ estimate. Instead, given x, z , for a to be determined, we decompose F into the smooth part and the singular part

$$F_1(x) \triangleq \int_{a \leq \max_i |x_i - y_i| \leq b} K(x, y) f(y) dy, \quad F_2(x) \triangleq \int_{\max_i |x_i - y_i| \leq a} K(x, y) f(y) dy,$$

Using the assumptions of the kernel, we have

$$|\partial_{x_1} F_1(x)| \leq C_3 \log \frac{b}{a} \|f\|_\infty, \quad |F_2(x)| \leq C_4 |a| \cdot \|f\|_\infty,$$

where the constants C_3, C_4 depend on b, C_1, C_2 . Applying the above estimates, we obtain

$$\frac{|F(x) - F(z)|}{|x_1 - z_1|^{1/2}} \leq \frac{|F_1(x) - F_1(z)| + |F_2(x) - F_2(z)|}{|x_1 - z_1|^{1/2}} \leq \left(C_3 \log \frac{b}{a} \cdot |x_1 - z_1|^{1/2} + 2C_4 |a| |x_1 - z_1|^{-1/2} \right) \|f\|_\infty.$$

We optimizing the estimates by choosing $a = C_5 |x_1 - z_1|$ for some constant C_5 depending on C_3, C_4 . Then we establish the estimate. The above simple estimates show that the choice of a depends on $|x - z|$. Thus, in our later Hölder estimates, we perform decomposition guided by the above estimates and optimize the choice of size of the singular region $[-a, a]^2$. On the other hand, since for different $|x - z|$, we need to choose different a , it increases the technicality of the computer-assisted estimates.

7.2. L^∞ estimate. Let $\hat{u}_{x,A}$ be the approximation term of u_x (2.89). We focus on the estimate of the piecewise L^∞ norm of $u_{x,A} = u_x - \hat{u}_{x,A}$ (4.2), which is a representative case. For simplicity, we assume the rescaling factor $\lambda = 1$. We assume that x satisfies (7.20) without loss of generality. We want to estimate $u_{x,A}$ for all $x \in B_{i_1 j_1}(h_x)$.

We can write $u_{x,A} = u_x - \hat{u}_x$ as follows

$$u_{x,A} = \int (K(x - y) - \hat{K}(x, y)) W(y) dy, \quad K_A \triangleq K(x - y) - \hat{K}(x, y),$$

where $\hat{K}(x, y)$ is the kernel for the approximation term. From (2.82), (2.88), it is nonsingular. Given x with (7.20), similar to (7.18), for $k \geq k_2$, we perform the following decomposition

$$(7.34) \quad \begin{aligned} u_{x,A} &= \left(\int_{R(k)^c} + \int_{R(k) \setminus R_s(k_2)} + \int_{R_s(k_2)} \right) K(x - y) W(y) dy - \int \hat{K}(x, y) W(y) dy \\ &\triangleq I_1 + I_2 + I_3 + I_4. \end{aligned}$$

where $R_s(k)$ is the symmetric singular region (7.14). See Section 7.2.4 for the choice of k .

Since $I_1 + I_4$ is nonsingular, we use the ideas in Section 7.1.5 to symmetrize the kernels in $I_1 + I_4$. Then we use the method in Section 7.1.3 to estimate it.

Remark 7.6. In our computation, the domain $[0, D]^2 \cap R(k)^c$ can be decomposed into the union of small grids $[y_i, y_{i+1}] \times [y_j, y_{j+1}]$ (7.8) since the boundary of $R(x, k)$ aligns with the mesh (7.13). In particular, in each grid, the indicator function is constant, and the integrand is smooth in y .

Next we consider I_2 . The domain of the integral is close to the singularity. If we use the method in Section 7.1.3 to estimate it, the error will be quite large since $\partial^2 K(x - y)$ is very singular. We want to estimate I_2 using $\|W\varphi\|_\infty$ and the singular part I_3 using $[W\psi]_{C_x^{1/2}}$. Since $K(z)$ is singular of order -2 , we expect an estimate

$$|I_2| + |I_3| \lesssim \log \frac{k}{k_2} \varphi^{-1}(x) \|W\varphi\|_{L^\infty[R(k)]} + \psi^{-1}(x) k_2^{1/2} [W\psi]_{C_x^{1/2}}.$$

Note that the weights φ, ψ have a different order of singularity for small x and a different rate of decay. Moreover, we need to control the right hand side using the energy, e.g. $E_1(t)$ (4.21), which assigns different weights to two norms (seminorms). Thus, to obtain a sharp estimate, we need to optimize the choice of k_2 .

Firstly, we consider $k_2 = 2, 2 + \frac{1}{2}, \dots, k$, we use the method in Section 7.1.6 to estimate I_2 . We also consider very small $k_2 < 2$. In this case, we further decompose I_2 as follows

$$I_2 = \left(\int_{R(k) \setminus R_s(2)} + \int_{R_s(2) \setminus R_s(k_2)} \right) K(x - y) W(y) dy \triangleq I_{21} + I_{22}.$$

For I_{21} , we apply the method in Section 7.1.6. For I_{22} , we use a change of variables $y = x + sh$

$$|I_{22}| = \left| \int_{k_2 \leq |s_1| \vee |s_2| \leq 2} K(-sh) W(x + sh) h^2 ds \right|.$$

Since the region is very small, $x + sh \in B_{i_1 j_1}(h_x) + [-2h, 2h]$, and $K_1(hs) = h^{-2} K_1(s)$, we get

$$|I_{22}| \leq \|W\varphi\|_\infty \|\varphi^{-1}\|_{L^\infty(B_{i_1 j_1}(h_x) + [-2h, 2h])} \int_{k_2 \leq |s_1| \vee |s_2| \leq 2} |K(s)| ds.$$

The integral can be computed explicitly and has the order $\log \frac{2}{k_2}$.

It remains to estimate the most singular part I_3 for different k_2 . Using a change of variables $y = x + sh$, the scaling symmetries, and the above derivations, we get

$$I_3 = \int_{[-k_2, k_2]^2} K(-s) W(x + sh) ds.$$

To use the Hölder norm of $W\psi$, we decompose it as follows

$$I_3 = \int_{[-k_2, k_2]^2} K(-s)(W\psi)(x + sh) \left(\frac{1}{\psi(x + sh)} - \frac{1}{\psi(x)} \right) + K(-s) \frac{(W\psi)(x + sh)}{\psi(x)} ds \triangleq I_{31} + I_{32}.$$

For I_{32} , using the Hölder seminorm, the odd symmetry of $K(s) = c \frac{s_1 s_2}{|s|^4}$ in s_1 , and $|(W\psi)(x + sh) - (W\psi)(x - sh)| \leq \sqrt{2s_1 h}$, we get

$$|I_{32}| \leq \frac{h^{1/2}}{\psi(x)} [W\psi]_{C_x^{1/2}} \int_{[0, k_2] \times [-k_2, k_2]} |K(s) \sqrt{2s_1} ds = \frac{2k_2^{1/2} h^{1/2}}{\psi(x)} [W\psi]_{C_x^{1/2}} \int_{[0, 1]^2} |K(s) \sqrt{2s_1} ds,$$

where we used the scaling symmetry of K and a change of variables $s \rightarrow k_2 s$ in the last equality.

7.2.1. The commutator. For I_{31} , we apply the simple Taylor expansion to $f = \psi^{-1}$

$$(7.35) \quad |f(x + sh) - f(x)| \leq |f_x(x) h s_1 + f_y(x) h s_2| + h^2 \left(\frac{m_{20} s_1^2}{2} + m_{11} s_1 s_2 + \frac{m_{02} s_2^2}{2} \right).$$

where m_{ij} is the bound for the second derivatives of ψ^{-1}

$$m_{ij}(s) = \max_{B_{i_1 j_1}(h) + I(\text{sgn}(s_1)) \times I(\text{sgn}(s_2))} \|\partial_x^i \partial_y^j (\psi^{-1})\|_{L^\infty}, \quad I(1) = [0, k_2 h], \quad I(-1) = [-k_2 h, 0].$$

Note that m_{ij} is constant in each quadrant of $[-k_2, k_2]^2$. We plug in the expansion (7.35) to estimate I_{31} . We only discuss a typical term $m_{20} s_1^2 h_1^2$

$$I_{31,02} \triangleq h^2 \int_{[-k_2, k_2]^2} |K(-s)(W\psi)(x + sh)| m_{20}(s) \frac{s_1^2}{2} ds.$$

If $k_2 \geq 2$, we can further partition $[-k_2, k_2]^2$ it into $B_{2p,2q}(1/2) = [p, p + 1/2] \times [q, q + 1/2]$, $-k_2 \leq p, q \leq k_2 - 1/2$, where we use the notation (7.21). For each grid $B_{2p,2q}(1/2)$, the sign of s and $m_{20}(s)$ are fixed, and we have

$$\int_{B_{2p,2q}(\frac{1}{2})} |K(-s)|(W\psi)(x + sh) m_{20}(s) \frac{s_1^2}{2} ds \leq m_{20} \|W\varphi\|_\infty \int_{B_{2p,2q}(\frac{1}{2})} \frac{|K(s)| s_1^2}{2} \left(\frac{\psi}{\varphi} \right) (x + sh) ds.$$

The last integral can be estimated using the method in (7.27). Combining the estimate of integral in different regions $B_{p,q}(1/2)$, we obtain the estimate of $I_{31,02}$. Similarly, we can estimate the contributions of other terms in (7.35) to I_{31} .

For small $k_2 \leq 2$, we do not partition the domain. We denote $D(k_2) = B_{i_1, j_1}(h_x) + [-k_2 h, k_2 h]^2$. For $s \in [-k_2, k_2]$, we use $x + sh \subset D(k_2) \subset D(2)$ to get

$$(7.36) \quad |f(x+sh) - f(x)| \leq \|f_x\|_{L^\infty(D(k_2))} s_1 h + \|f_y\|_{L^\infty(D(k_2))} s_2 h. \quad |W\psi(x+sh)| \leq \|W\varphi\|_\infty \|\frac{\psi}{\varphi}\|_{L^\infty(D(2))}.$$

Plugging the above estimate into I_{31} , we get

$$I_{31} \leq \sum_{(i,j)=(1,0),(0,1)} h \|\partial_x^i \partial_y^j (\psi^{-1})\|_{L^\infty(D(k_2))} \|W\varphi\|_\infty \|\frac{\psi}{\varphi}\|_{L^\infty(D(2))} \int_{[-k_2, k_2]^2} |K(s) s_1^i s_2^j| ds.$$

Using the scaling symmetry, we can reduce the last integral to $k_2^{i+j} \int_{[-1,1]^2} |K(s) s_1^i s_2^j| ds$.

We apply the above estimates to a list of k_2 . Then by optimizing the k_2 , we obtain the sharp estimate of $u_{x,A}$.

Remark 7.7. In (7.35), we do not bound $f(x+sh) - f(x)$ directly using the estimate (7.36) since s is large. Thus, we perform a higher order expansion.

7.2.2. Estimate of u_y, v_x . The estimates of u_y, v_x follow similar ideas and estimates. Since $v_x(x, y)$ vanishes near $y = 0$, to exploit this smallness, we need more careful estimates when (x, y) is close to the boundary. We refer the details to the upcoming Supplementary Materials.

7.2.3. Estimate of \mathbf{u}_A . The estimate of \mathbf{u}_A is much simpler since it is more regular. Let K and \hat{K} be the kernel of u, v and its approximation term, respectively. For $f = u$ or v , we perform a decomposition similar to (7.34)

$$(7.37) \quad f_A = \left(\int_{R(k)^c} + \int_{R(k) \setminus R_s(k)} + \int_{R_s(k)} \right) K(x - y) W(y) dy - \int \hat{K}(x, y) W(y) dy \triangleq I_1 + I_2 + I_3 + I_4.$$

The estimates of $I_1 + I_4$ follow the method for $u_{x,A}$. For I_2 , we use the method in Section 7.1.6. For I_3 , since K has a singularity of order $|x|^{-1}$, which is locally integrable, we use a change of variable $y = x + sh$ to obtain

$$I_3 = h \int_{[-k, k]^2} K(-s) W(x + sh) ds.$$

Then we partition $[-k, k]^2$ into small grids, and use the method in (7.32) to estimate the integral in each grid. Here, we get a factor h in the change of variables since $K(\lambda s) = \lambda^{-1} K(s)$.

7.2.4. Choice of parameters. Recall the choice of several parameters a, h, h_x from (7.11). We choose $3 \leq k \leq 10$. We choose k for the size of the singular region kh (7.34), (7.37) not so small such that the error $h^2 \partial^2 K$ in Lemma 7.2, which has the order $h^2 |x - y|^{-\alpha-2}$ near the singularity, is smaller than the main term K , which has the order $|x - y|^{-\alpha}$, $\alpha = 1, 2$. Since we will estimate $I_1 + I_4, I_2, I_3$ in the decomposition separately using the triangle inequality, we do not choose k to be too large so that we can exploit the cancellation in $I_1 + I_4$.

7.3. Hölder estimates. We want to estimate $\frac{|f(x) - f(z)|}{|x - z|^{1/2}}$ for any $x, z \in \mathbb{R}_2^{++}$ with $x_1 = z_1$ or $x_2 = z_2$ and some function f , e.g. $f = u_{x,A}$. Without loss of generality, we assume $|z| > |x|$. Then in the $C_x^{1/2}$ estimate, we have $x_1 < z_1, x_2 = z_2$; in the $C_y^{1/2}$ estimate, we have $x_1 = z_1, x_2 < z_2$. Applying the rescaling argument in Section 7.1, we can restrict $\hat{x} = \frac{x}{\lambda}$ to $\hat{x} \in [0, 2a]^2 \setminus [0, a]^2$. For this reason, we assume $\lambda = 1$ for simplicity. We will only estimate the Hölder difference for comparable x, z : $|x| \asymp |z|$. If $|z| \gg |x|$, we simply apply L^∞ estimate to $f(x), f(z)$ and use the triangle inequality.

We focus on the Hölder estimate of $u_{x,A}$, which is representative and the most important nonlocal term to estimate in our energy estimate. See (2.23), (2.39).

7.3.1. $C_x^{1/2}$ estimate. Recall I_i from the decomposition (7.18) and $K_1(s) = \frac{s_1 s_2}{|s|^4}$. We apply the same decomposition to $u_{x,A}(z)$. We assume that the approximation term \hat{u}_x (2.89) takes the following form

$$(7.38) \quad \hat{u}_x(x) = \int \hat{K}_1(x, y) W(y) dy, \quad I_6(x) \triangleq \psi(x) \hat{u}_x(x) = \psi(x) \int \hat{K}_1(x, y) W(y) dy,$$

with a nonsingular kernel \hat{K}_1 . We first discuss how to estimate the regular part I_1, I_3, I_4 in (7.18) and I_6 , which are Lipschitz. We will apply Lemmas 3.1-3.5 to estimate the most singular part I_2 . The most technical part is to estimate I_5 , which is log-Lipschitz since the kernel $K_1(x-y)(\psi(x) - \psi(y))$ has a singularity of order -1 . We assemble the estimates of different parts to estimate $[u_{x,A}]_{C_x^{1/2}}$ in Section 7.6.

7.3.2. *Estimates of the regular terms I_1, I_3, I_4, I_6 .* Recall I_1, I_3, I_4 from (7.18) and I_6 from (7.38). Since the integrands in I_1, I_3, I_4 are supported at least $k_2 h$ away from the singularity x , if W is in some suitable weighted L^∞ space, we can show that I_1, I_3, I_4 are Lipschitz and their derivatives can be bounded by $\|W\varphi\|_{\infty(\mathbb{R}_2^{++})} = \|\omega\varphi\|_\infty$. In fact, I_1 and I_4 are piecewise smooth. Their derivatives jump when $R(x, k), R(x, k_2)$ change, or equivalently, x moves from one grid to another. For $x \in B_{i_1, j_1}(h_x)$ (7.20), these rectangle domains are the same, and these functions are smooth. The approximation term I_6 (7.38) is smooth in x . To exploit the cancellation, we combine the estimates of I_1, I_4, I_6 together. We symmetrize the kernel in $I_1(x) + I_4(x) - I_6(x)$ and use the method in Section 7.1.3 to estimate the derivatives of $I_1(x) + I_4(x) - I_6(x)$. See also (7.24), (7.25) for the form of the symmetrized integrands in these integrals.

We estimate both the L^∞ and Lipschitz norm of I_3 using the method in Sections 7.1.6, 7.1.7. We will optimize two estimates to obtain a sharper Hölder norm of I_3 .

We choose integer k, k_2 in the decomposition (7.18). Then in each grid $[y_i, y_{i+1}] \times [y_j, y_{j+1}]$, the indicator functions in $I_1 + I_4 - I_6$, e.g. $\mathbf{1}_{R(k)^c}, \mathbf{1}_{R(k) \setminus R(k_2)}$, are constant. See Remark 7.6.

7.3.3. $C_x^{1/2}$ estimate of I_2 . We first estimate the second term I_2 in (7.18). Recall $R(x, k), R_s(x, k)$ from (7.13), (7.14) and the location of x (7.20). We have

$$x_2 - (j-k)h \leq (j+1)h - (j-k)h = (k+1)h, \quad (j+1+kh) - x_2 \leq (j+1+kh) - jh = (k+1)h.$$

Since $x_2 = z_2$, using Lemma 3.1 with $(a, b_1, b_2) = (kh, x_2 - (j-k)h, (j+1+k)h - x_2)$ and $|b_1|, |b_2| \leq (k+1)h$, we obtain

$$\frac{1}{|x-z|^{1/2}} |I_2(x, k) - I_2(z, k)| \leq C_1 \left(\frac{(k+1)h}{|x-z|} \right) [W\psi]_{C_x^{1/2}} = C_1 \left(\frac{(k+1)h}{|x-z|} \right) [\omega\psi]_{C_x^{1/2}}.$$

For $I_2(x, k)$ associated with other terms u, v, u_y, v_x , we can estimate it using similar ideas and Lemmas 3.1-3.5. The $C_y^{1/2}$ estimate of $I_2(x, k)$ is completely similar. See Section 7.3.8 for more details.

7.3.4. $C_x^{1/2}$ estimate of I_5 . For I_5 (7.18), $K_1(x-y)(\psi(x) - \psi(y))$ is singular of order -1 near $y = x$. Given $W \in L^\infty(\varphi)$, I_5 is log-Lipschitz and thus in $C^{1/2}$. There are several approaches to estimate its Hölder norm. One approach is the following. We use part of the $C_x^{1/2}$ norm of ω to get a better estimate. We further decompose I_5 as follows

$$\begin{aligned} I_5(x, k_2) &= \int_{R(k_2) \setminus R_{s,1}(k_2)} K_1(x-y)(\psi(x) - \psi(y)) W(y) dy \\ &+ \int_{R_{s,1}(k_2)} K_1(x-y)(\psi(x) - \psi(y)) W(y) dy \triangleq I_{5,1}(x, k_2) + I_{5,2}(x, k_2). \end{aligned}$$

The estimate of $I_{5,1}$ is similar to that of I_3 . We estimate its L^∞ and x -derivative using the method in Sections 7.1.6, 7.1.7.

For $I_{5,2}$, we want to estimate it using a method similar to that of I_2 . See the left figure in Figure 12 for the domains of the integrals in $I_{5,2}(x), I_{5,2}(z)$. The integrand satisfies

$$\begin{aligned} K_1(x-y)(\psi(x)-\psi(y))W(y) &= \psi(x)K_1(x-y)(\psi^{-1}(y)-\psi^{-1}(x))(W\psi)(y) \\ &\approx \psi(x)\partial_i(\psi^{-1}(x)) \cdot K_1(x-y)(y_i-x_i)(W\psi)(y). \end{aligned}$$

Thus, $I_{5,2}(x)$ can be seen as a weighted version of I_2 (7.18) with a weight $\psi(x)\partial_i(\psi^{-1}(x))$, a more regular kernel $K_1(x-y)(y_i-x_i)$, and a smaller domain $R_s(k_2)$. Since the kernel is more regular and the domain is smaller, our estimate for $I_{5,2}$ is much smaller than that of I_2 .

Now, we justify this approach. Using a change of variables $y = x + s, s \in R_{s,1}(k_2) - x$ and the above identity, we yield

$$I_{5,2}(x, k_2) = \psi(x) \int_{R_{s,1}(k_2)-x} K_1(-s)(\psi^{-1}(x+s) - \psi^{-1}(x))(W\psi)(x+s) ds.$$

Using Newton's formula $f(1) = f(0) + f'(0) + \int_0^1 (1-t)f'(t)dt$, we get

$$\begin{aligned} \psi^{-1}(x+s) - \psi^{-1}(x) &= s \cdot \nabla \psi^{-1}(x) + \int_0^1 (1-t) \left(s \cdot (\nabla^2 \psi^{-1})(x+ts) \cdot s \right) dt \\ &= \sum_{i=1,2} s_i \partial_i(\psi^{-1})(x) + \sum_{0 \leq i \leq 2} \binom{2}{i} s_1^i s_2^{2-i} \int_0^1 (1-t) \partial_1^i \partial_2^{2-i}(\psi^{-1})(x+ts) dt. \end{aligned}$$

Denote

$$\begin{aligned} Q_{ij}(x) &= \psi(x) \int_0^1 (1-t) \partial_1^i \partial_2^j (\psi^{-1})(x+ts) dt, \quad i+j=2, \quad D(x) = R_{s,1}(x, k_2) - x, \\ Q_{ij}(x) &= \psi(x) \cdot \partial_1^i \partial_2^j (\psi^{-1})(x) = -\frac{\partial_1^i \partial_2^j \psi(x)}{\psi(x)}, \quad i+j=1, \quad P_{ij}(x) = \int_{D(x)} K_1(-s) s_1^i s_2^j (W\psi)(x+s) ds. \end{aligned}$$

Using the above expansion and notations, we get

$$I_{5,2}(x, k_2) = \sum_{i+j=1} P_{ij} Q_{ij} + \sum_{i+j=2} \binom{2}{i} P_{ij} Q_{ij}.$$

Next, we use the above decomposition to estimate $I_{5,2}(x, k_2) - I_{5,2}(z, k_2)$. The leading order terms are $P_{ij} Q_{ij}$ with $i+j=1$. We observe that if $x_2 = z_2$, we have

$$D(x) = R_{s,1}(x, k_2) - x = R_{s,1}(z, k_2) - z = D(z).$$

Suppose that $x_1 < z_1$. We perform a decomposition

$$\begin{aligned} (7.39) \quad |P_{ij}(x)Q_{ij}(x) - P_{ij}(z)Q_{ij}(z)| &\leq J_1 + J_2, \\ J_1 &\triangleq |Q_{ij}(z)(P_{ij}(x) - P_{ij}(z))|, \quad J_2 \triangleq |P_{ij}(x)(Q_{ij}(x) - Q_{ij}(z))|. \end{aligned}$$

Using $D(x) = D(z)$, we bound J_1 as follows

$$\begin{aligned} |J_1| &\leq |Q_{ij}(z)| \left| \int_{D(x)} K_1(-s) s_1^i s_2^j ((W\psi)(x+s) - (W\psi)(z+s)) ds \right| \\ &\leq |Q_{ij}(z)| \cdot |x-z|^{1/2} \|\omega\psi\|_{C_x^{1/2}} \int_{s \in D(x)} |K_1(s) s_1^i s_2^j| ds. \end{aligned}$$

The term Q_{ij} only depends on the weight and is smoother than P_{ij} . We can estimate $Q_{ij}(x) - Q_{ij}(z)$ by bounding $\partial_1 Q_{ij}$ since Q_{ij} is locally smooth. For P_{ij} in J_2 , we use the method in (7.32) to bound it by $C\|\omega\varphi\|_\infty$ with some constant C . Then we obtain the estimate

$$|J_2| \leq C_2 |x-z| \cdot \|\omega\varphi\|_{L^\infty}$$

for some constant C_2 . Note that the second order term $P_{ij}Q_{ij}, i+j=2$ is much smaller than the leading order terms. For $|x-z|$ not too small, we can estimate its contribution trivially

$$\frac{1}{|x-z|^{1/2}} |P_{ij}(x)Q_{ij}(x) - P_{ij}(z)Q_{ij}(z)| \leq \frac{1}{|x-z|^{1/2}} (|P_{ij}(x)Q_{ij}(x)| + |P_{ij}(z)Q_{ij}(z)|).$$

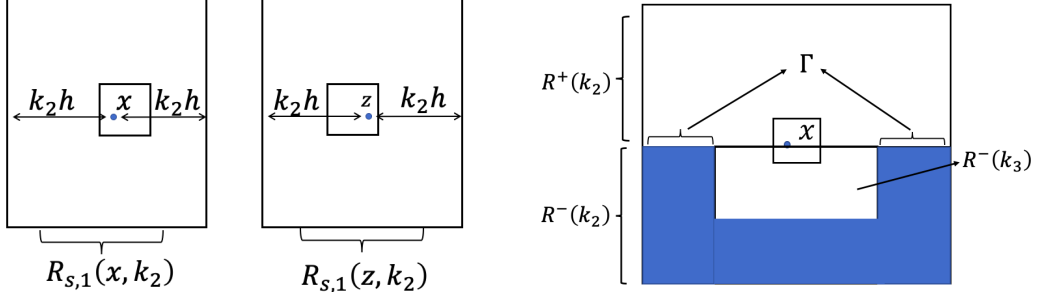


FIGURE 12. Left: $R_{s,1}(x, k_2)$ and $R_{s,1}(z, k_2)$ with $x_2 = z_2$. The small square is a mesh grid containing x or z . x, z can have different locations relative to the grids. Right: The large rectangle is $R(k_2)$, the upper part is $R^+(k_2)$, and the lower part is $R^-(k_2)$. The blue region is $R^-(k_2) \setminus R^-(k_3)$. Γ is part of its boundary.

In summary, to obtain the above estimates, we need to estimate piecewise bound for $|Q_{ij}(x)|$, $P_{ij}(x), |\partial_k Q_{ij}(x)|$, and the integrals $\int_{D(x)} |K_1(s)s_1^i s_2^j| ds$, $i + j = 1, 2$.

The above estimate of $I_5(x, k_2)$ can be generalized to the $C_x^{1/2}$ estimate of u, v, v_x, u_y . Yet, it does not apply to the $C_y^{1/2}$ estimate of $\mathbf{u}, \nabla \mathbf{u}$ since it requires the estimate of $(W\psi)(x+s) - (W\psi)(z+s)$ for s in some rectangle $R = D(x) = D(z)$. However, since W is discontinuous across the boundary $y = 0$, $W\psi \notin C_y^{1/2}(R)$ if $x+s, z+s$ are not in the same half plane. If $x_1 < x_2$, then the rectangles $R(x, k_2), R(z, k_2)$ will not intersect the boundary and the previous estimate holds true. If $x_1 > x_2$, we consider two modifications for different kernels in the following subsections.

7.3.5. Ideas of the $C_y^{1/2}$ estimates of I_5 . The main idea in the following $C_y^{1/2}$ estimates is to use a combination of the estimates for the log-Lipschitz function in Section 7.1.9 and the estimate in Section 7.3.4. The latter provides better estimates, and we try to use this method *as much as possible*. Following the ideas in Section 7.1.9, we decompose $I_5(x)$ into the singular part and nonsingular part with different size k_3 of the singular region

$$I_5(x) = I_{5,S}(x, k_3) + I_{5,NS}(x, k_3).$$

Although we cannot apply the second method to the whole $I_5(x)$, our observation is that we can apply it to the integrals in the upper part of the regions, e.g. $R^+(k_2), R^+(k_3)$ (7.15), since these integrals only involve $W\psi$ in \mathbb{R}_2^+ and we have $W\psi \in C^{1/2}$. Thus, we will further decompose some of the regions into the upper part and the lower part, and then apply the first method to the lower part, and the second method to the upper part.

7.3.6. $C_y^{1/2}$ estimate of the velocity with a kernel of the first type. The kernels

$$(7.40) \quad K = \frac{y_1 y_2}{|y|^4}, \quad \frac{y_2}{|y|^2}$$

associated with $u_x = -\partial_{xy}(-\Delta)^{-1}\omega, u = -\partial_y(-\Delta)^{-1}\omega$ vanish when $y_2 = 0$. We call them the first type kernel.

Let K be a kernel of the first type. We use the following decomposition

$$\begin{aligned} I_5(x, k_2) &= \int_{R^+(k_2)} K(x-y)(\psi(x) - \psi(y))W(y)dy \\ &+ \int_{R^-(k_2)} K(x-y)(\psi(x) - \psi(y))W(y)dy \triangleq I_5^+(x, k_2) + I_5^-(x, k_2) \end{aligned}$$

See the right figure in Figure 12 for $R^\pm(k_2)$. Since $R^+(k_2)(x, k_2)$ is in \mathbb{R}_2^+ , we can apply the same argument as that in Section 7.3.4 to obtain the desired estimates by restricting all the derivations in $R^+(x, k_2), R^+(z, k_2)$.

For the lower part $I_5^-(x, k_2)$, it is log-Lipschitz if $W \in L^\infty(\varphi)$. We cannot bound its derivative using $\|W\varphi\|_\infty$. We face the difficulty discussed at the beginning of Section 7.

Alternatively, we follow the ideas in Section 7.1.9. The kernel $K(x-y)(\psi(x)-\psi(y))$ satisfies the assumptions in Section 7.1.9, at least for x, y in some region. We decompose it into the smooth part and rough part. We introduce $0 < k_3 < k_2$ and consider the following decomposition

$$(7.41) \quad \begin{aligned} I_5^-(x, k_2) &= \int_{R^-(k_2) \setminus R^-(k_3)} K(x-y)(\psi(x)-\psi(y))W(y)dy \\ &+ \int_{R^-(k_3)} K(x-y)(\psi(x)-\psi(y))W(y)dy \triangleq I_{5,1}^-(x, k_2) + I_{5,2}^-(x, k_2). \end{aligned}$$

See the right figure in Figure 12 for an illustration of different domains. Recall that $k_2 \in Z_+$. We choose $k_3 = k_2 - \frac{i}{2}, i = 0, 1, 2, \dots, 2k_2 - 4$. Since the integrand in $I_{5,1}^-$ supports at least $k_3 h$ away from the singularity, $I_{5,1}^-(x, k_2)$ is Lipschitz. We can estimate the derivative of $I_{5,1}^-(x, k)$ in the y direction. The domain $R^-(k_2) \setminus R^-(k_3)$ is not piecewise constant since the upper part of its boundary, i.e.

$$\Gamma = \{(y_1, x_2) : y_1 \in [(i-k_2)h, (i+1+k_2)h] \setminus [(i-k_3)h, (i+1+k_3)h]\},$$

depends on x_2 . See Figure 12 for an illustration of Γ . Taking x_2 derivative on $I_{5,1}^-$, we get

$$\begin{aligned} |\partial_{x_2} I_{5,1}^-(x, k_2)| &\leq \left| \int_{R^-(k_2) \setminus R^-(k_3)} \partial_{x_2} (K(x-y)(\psi(x)-\psi(y)))W(y)dy \right| \\ &+ \left| \int_{y \in \Gamma} K(x-y)(\psi(x)-\psi(y))W(y)dy_1 \right|. \end{aligned}$$

Since $y \in \Gamma \subset \{y : y_2 = x_2\}$ and that $K(y_1, 0) \equiv 0$, the second term vanishes. The first term can be estimated using a change of variables $y = x + s$ and the method in Section 7.1.6, 7.1.7, since its support is at least $k_3 h$ away from the singularity.

For $I_{5,2}^-$, the kernel satisfies $K(x-y)(\psi(x)-\psi(y)) \sim |x-y|^{-1}$ for small $|x-y|$ and is locally integrable. We estimate its piecewise L^∞ bound using the method in Section 7.2.1 for the commutator.

The above decomposition can be applied to estimate

$$\frac{|I_5^-(x, k_2) - I_5^-(z, k_2)|}{|x-z|^{1/2}} \leq \min_{k_3=k_2-\frac{i}{2}} \frac{|I_{5,1}^-(x, k_3) - I_{5,1}^-(z, k_3)|}{|x-z|^{1/2}} + \frac{|I_{5,2}^-(x, k_3)| + |I_{5,2}^-(z, k_3)|}{|x-z|^{1/2}}$$

for $|x-z|$ not too small, e.g. $|x-z| \geq d_s = \frac{h}{10}$. When $|x-z|$ is sufficiently small, the second term in the above estimate can be very large.

According to the analysis in Section 7.1.9, for $|x-z|$ very small, we need to choose $k_2 h \sim |x-z|$ to get the sharp estimate. Thus, we consider one more decomposition for $a \leq 1$

$$(7.42) \quad \begin{aligned} I_5^-(x, k_2) &= \int_{R^-(k_2) \setminus R_s^-(a)} K(x-y)(\psi(x)-\psi(y))W(y)dy \\ &+ \int_{R_s^-(a)} K(x-y)(\psi(x)-\psi(y))W(y)dy \triangleq I_{5,3}^-(x, a) + I_{5,4}^-(x, a). \end{aligned}$$

The above decomposition is slightly different from (7.41). We choose $R_s^-(a)$ rather than $R^-(k_3)$, since we need to choose the singular region with size going to 0 as $|x-z| \rightarrow 0$. Yet, $R^-(k_3)$ (7.13) does not satisfy this requirement for $k_3 \rightarrow 0$. We can estimate the derivative of $I_{5,3}^-(x, a)$ following Sections 7.1.6, 7.1.7, and the L^∞ norm of $I_{5,4}^-(x, a)$ following Section 7.2.1. Again, in the computation of $\partial_{x_2} I_{5,3}^-(x, a)$, the boundary term vanishes due to $K(y_1, 0) \equiv 0$. In summary, we can obtain the following estimate

$$(7.43) \quad |\partial_{x_2} I_{5,3}^-(x, a)| \leq A(x) + B(x) \log(1/a), \quad |I_{5,4}^-(x, a)| \leq C(x)ah,$$

for any $a \leq 1$, where $A(x), B(x)$ can be estimated following the method in Appendix D.5.1, and the estimate of $C(x)$ follows the method in Section 7.2.1. Using the above estimates and the

ideas in Section 7.1.9, we can estimate $d_y(I_5^-(\cdot, k_2), x, z)$ for small $|x - z|$ by optimizing a , where d_y is defined below

$$(7.44) \quad d_y(f, x, z) = |f(x) - f(z)| |x - z|^{-1/2}.$$

We will assemble these estimates in Section 7.6.

7.3.7. $C_y^{1/2}$ estimate of the velocity with a kernel of the second type. For the kernels $K_2 = \frac{y_1^2 - y_2^2}{|y|^4}$ and $\frac{y_1}{|y|^2}$, they do not vanish on $y_2 = 0$ in general. We call them the second type kernel. If we use the strategies in the previous subsection, the boundary term in the computation of $\partial_{x_2} I_{5,1}^-(x, k_3)$ or $\partial_{x_2} I_{5,3}^-(x, k_3)$ does not vanish and can be large.

To avoid picking up a boundary term and apply the ideas in Section 7.3.5, we consider another estimate on $I_5(x, k_2)$. For $k_3 = k_2 - \frac{i}{2}$, $i = 0, 1, \dots, 2k_2 - 4$, we perform the following decomposition

$$\begin{aligned} I_5(x, k_2) &= \int_{R(k_2) \setminus R(k_3)} K(x - y)(\psi(x) - \psi(y))W(y)dy + \int_{R^+(k_3)} K(x - y)(\psi(x) - \psi(y))W(y)dy \\ &\quad + \int_{R^-(k_3)} K(x - y)(\psi(x) - \psi(y))W(y)dy \triangleq I_{5,1} + I_{5,2} + I_{5,3}. \end{aligned}$$

Following the ideas in Section 7.1.9, we estimate the derivative of the regular part and then the L^∞ norm of the singular part. Indeed, we can estimate the y -derivative of $I_{5,1}$ using the method in Section 7.1.3, and the L^∞ norm of $I_{5,3}$ following Section 7.2.1. The estimate of $I_{5,1}$ is similar to that of I_4 in Section 7.3.2. For $I_{5,2}$, since $R^+(k_3)$ is in \mathbb{R}_2^+ , we can obtain a better estimate following the method in the estimate of $I_{5,2}$ in Section 7.3.4.

After we estimate these quantities, we can estimate $d_y(I_5, x, z)$ (7.44) for $|x - z|$ not too small by optimizing k_3 . To estimate $d_y(I_5, x, z)$ (7.44) for sufficiently small $|x - z|$, following (7.42), we use the following decomposition

$$(7.45) \quad \begin{aligned} I_5(x, k_2) &= \int_{R(k_2) \setminus R_s(a)} K(x - y)(\psi(x) - \psi(y))W(y)dy + \int_{R_s^+(a)} K(x - y)(\psi(x) - \psi(y))W(y)dy \\ &\quad + \int_{R_s^-(a)} K(x - y)(\psi(x) - \psi(y))W(y)dy \triangleq I_{5,4} + I_{5,5} + I_{5,6}. \end{aligned}$$

Then we estimate the derivative of $I_{5,4}$ and the L^∞ norm of $I_{5,6}$ as follows

$$(7.46) \quad |\partial_{x_2} I_{5,4}| \leq A(x) + B(x) \log(1/a), \quad |I_{5,6}| \leq C(x)ah,$$

where the estimates of A, B are given in Appendix D.5.1, and the estimate of C follows the method in Section 7.2.1. The Hölder estimate of $I_{5,5}$ follows the method in the estimate of $I_{5,2}$ in Section 7.3.4. With these estimates, we can further bound $d_y(I_5, x, z)$ (see (3.5)) for sufficiently small $|x - z|$ by optimizing a . See Section 7.6.

Remark 7.8. We do not use the later decomposition on I_5 , i.e. $I_5 = I_{5,4} + I_{5,5} + I_{5,6}$, to estimate $d_y(f, x, z)$ when $|x - z|$ is not too small since the domain of the integral in $I_{5,4}$ is not piecewise constant. As a result, we need to bound the boundary term in the computation of $\partial_{x_2} I_{5,4}$. The resulting estimate is worse than the estimate using the decomposition $I_5 = I_{5,1} + I_{5,2} + I_{5,3}$.

We do not apply the above computation with smaller window $[-ah, ah]^2$ in the $C_x^{1/2}$ estimate, since it leads to a worse estimate. See also the discussions in Section 7.3.5.

7.3.8. Hölder estimate of u, v, u_y, v_x . The ideas of the Hölder estimate for other terms are similar. For a kernel K associated with $\mathbf{u}, \nabla \mathbf{u}$, we perform another decomposition similar to (7.18)

$$(7.47) \quad \begin{aligned} \psi(x) \int K(x - y)W(y)dy &= \int \left(\psi(x) \mathbf{1}_{R(k)^c} + \mathbf{1}_{R_s(k)} \psi(y) + \mathbf{1}_{R(k) \setminus R_s(k)} \psi(y) \right. \\ &\quad \left. + \mathbf{1}_{R(k) \setminus R(k_2)} (\psi(x) - \psi(y)) + \mathbf{1}_{R(k_2)} (\psi(x) - \psi(y)) \right) K(x - y)W(y)dy \\ &\triangleq I_1(x, k) + I_2(x, k) + I_3(x, k) + I_4(x, k, k_2) + I_5(x, k_2), \end{aligned}$$

Here, we use $R_s(x, k)$ (7.14), which is symmetric with respect to both x_1 and x_2 , rather than $R_{s,1}(x, k)$. Denote by $I_{f6}(x, k_2)$ the approximation term for $f = u_x, u_y, v_x, u, v$. It takes the form similar to (7.38).

We consider two cases of $\hat{x} \in [0, 2x_c]^2 \setminus [0, x_c]^2$. In the first case, we consider $\hat{x} \in [x_c, 2x_c] \times [0, 2x_c] \triangleq D_{X1}$, where we have $\hat{x}_1 \geq c\hat{x}_2$ for some constant $c > 0$. In the second case, we consider $\hat{x} \in [0, x_c] \times [x_c, 2x_c] \triangleq D_{X2}$, where we have $\hat{x}_1 \leq c\hat{x}_2$. We distinguish these two cases since in the second case, the singular region does not touch the boundary, we can apply the method in Section 7.3.4.

$C_x^{1/2}$ estimate of u_y, v_x . In the $C_x^{1/2}$ estimate of u_y, v_x , we follow Section 7.3.2 to estimate the regular part $I_1 + I_4 - I_6$ and I_3 . We follow Section 7.3.3 and use Lemma 3.4 to estimate I_2 . For I_5 , we follow Section 7.3.4.

$C_y^{1/2}$ estimate of u_x . In the $C_y^{1/2}$ estimate of u_x , we perform the decomposition (7.47) rather than (7.18). The estimates of $I_1 + I_4 - I_6$, I_3 follow Section 7.3.2. For I_2 , we use Lemma 3.3. We follow Section 7.3.6 to estimate I_5 if $\hat{x} \in D_{X1}$, and Section 7.3.4 if $\hat{x} \in D_{X2}$.

We remark that we use the decomposition (7.47) rather than (7.18) since in Lemma 3.3, we need to assume that the singular region around x is symmetric in both x_1 and x_2 .

$C_x^{1/2}$ and $C_y^{1/2}$ estimate of u, v . The Hölder estimates of u, v are substantially easier since u, v are more regular. We perform $C_x^{1/2}, C_y^{1/2}$ of $\rho \mathbf{u}_A$ for another weight ρ . We decompose the integral as follows

$$(7.48) \quad \rho(x) \int K(x - y)W(y)dy = \int \left(\mathbf{1}_{R(k)^c} \rho(x) + \mathbf{1}_{R(k)} \rho(x) \right) K(x - y)W(y)dy \triangleq I_1(x, k) + I_2(x, k).$$

We follow Section 7.3.2 to estimate $I_1 - I_6$. For I_2 , we follow the ideas in Sections 7.1.9, 7.3.6, 7.3.7 to estimate the log-Lipschitz function. We choose a list of k_2 and associated region $S(k_2)$ and decompose I_2 as follows

$$I_2(x, k) \triangleq \int_{R(k) \setminus S(k_2)} \rho(x)K(x - y)W(y)dy + \int_{S(k_2)} \rho(x)K(x - y)W(y)dy \triangleq I_{21}(x, k_2) + I_{22}(x, k_2).$$

For large k_2 , we choose $k_2 = k, k - 1/2, \dots, 2$ with $S(k_2) = R(k_2)$. For $k_2 < 2$, we choose $S(k_2) = R_s(k_2)$. For $I_{21}(x, k_2)$, we estimate its derivatives following the estimate of I_{51} when $k_2 \geq 2$, and the estimate of I_{54} when $k_2 < 2$ in Section 7.3.7. For $I_{22}(x, k_2)$, we estimate its L^∞ norm following the estimate of I_{53} when $k_2 \geq 2$, and the estimate of I_{56} when $k_2 < 2$ in Section 7.3.7. The estimate is simpler since the above kernel is much simpler than $K(x - y)(\psi(x) - \psi(y))$ in Section 7.3.7.

7.3.9. Special case: $C_y^{1/2}$ estimate of u_y, v_x . In this case, we want to apply Lemma 3.5 to estimate the most singular part. Since in Lemma 3.5, we do not localize the integral, we perform the following decomposition

$$(7.49) \quad \psi(x) \int K(x - y)W(y)dy = \int \left(\psi(y) + \mathbf{1}_{R(k_2)^c}(\psi(x) - \psi(y)) + \mathbf{1}_{R(k_2)}(\psi(x) - \psi(y)) \right) K(x - y)W(y)dy \\ \triangleq I_1(x, k) + I_2(x, k) + I_3(x, k).$$

For I_1 , we apply Lemma 3.5. We follow Section 7.3.7 to estimate I_5 if $\hat{x} \in D_{X1}$, and Section 7.3.4 if $\hat{x} \in D_{X2}$.

We follow Section 7.3.2 to estimate $I_2 - I_6$. There are additional difficulties since the weight $\psi(y)$ and the symmetrized integrand $J = K(x, y)(\psi(x) - \psi(y))$ (see similar derivations in (7.24), (7.25)) are singular near 0.

Estimate the integral near 0. To estimate the $D_1 = \partial_{x_2}$ derivative, we use

$$|D_1 I| = |D_1 K(\psi(x) - \psi(y)) + K \cdot D_1 \psi(x)| \leq |D_1 K \cdot \psi(x) + K \cdot D_1 \psi(x)| + |D_1 K \cdot \psi(y)|.$$

Note that for y close to 0, $\psi(y)$ is much larger than $\psi(x)$ and $K(x, y)$ is not singular. The main term in $D_1 I$ is given by $D_1 K \psi(y)$, and we expect that the above estimate is sharp. It follows

$$\int_Q |D_1 I \cdot W(y)| dy \leq \|W\varphi\|_\infty \left(\|\varphi^{-1}\|_{L^\infty(Q)} \int_Q |D_1 K \psi(x) + K \cdot D_1 \psi(x)| dy + \left\| \frac{\psi}{\varphi} \right\|_{L^\infty(Q)} \int_Q |D_1 K| dy \right),$$

where Q is some grid near the origin. The integrands in both integrals do not involve the singular weight, and we can compute them using the previous methods.

Estimate in the far-field. For the tail part in this case, we have improvement if $\lambda \rightarrow 0$ due to the approximation term near 0 (2.84)

$$\hat{f} = C_{f0}(x, y) u_x(0) + C_f(x, y) \mathcal{K}_{00} = C_f(x, y) \mathcal{K}_{00},$$

where $f = u_y, v_x$ and we have used $C_{f0}(x, y) = 0$ (2.80). Its associated integrand is given by

$$K_{app} \triangleq \pi^{-1} C_f(x, y) \mathcal{K}_{00}(y),$$

where \mathcal{K}_{00} is defined in (2.79). To estimate it, we use the following decomposition

$$D_1(J - \psi(x) K_{app}) = D_1((K - K_{app}) \cdot \psi(x)) - D_1 K \cdot \psi(y) \triangleq P_1 + P_2.$$

The first part P_1 is estimated using the method in Section 7.4. Due to the approximation, $(K - K_{app})$ has a much faster decay for large y beyond $[0, D]^2$. For P_2 , we have

$$\int_{\Omega^c} |P_2| |W(y)| dy \leq \|W\varphi\|_\infty \|\psi(y)\|_{L^\infty(\Omega^c)} \int_{\Omega^c} |D_1 K| \varphi^{-1}(y) dy,$$

where $\Omega = [0, D]^2$ with large D . The last integral is computed using the method in Section 7.4.

7.4. Estimate the integrals near 0 and in the far field. In the computation of the L^1 type integral, we use a combination of uniform mesh and adaptive mesh to compute the integral in a finite domain $[0, D]^2$, e.g. $D = 1000$. See Section 7.1.3. Since the kernel decays and the singularity is in the near-field, the integral beyond this domain is small, and we estimate it directly. In addition, for y near 0, we estimate the integrals related to $|y|^{-2}$ or $|y|^{-4}$ directly, which come from the approximation terms $u_x(0), \mathcal{K}_{00}$ (7.5).

For simplicity, we consider $\lambda = 1$. The estimates can be generalized to other scales λ . To estimate $\int_D k(y) \omega(y) dy$ for D near 0 or D in the far-field, following (7.7), we only need to estimate $\int_D |k(y)| \varphi^{-1}(y) dy$. Since $|y|$ is either very small or very large, we can use the asymptotics of φ in these estimates.

7.4.1. Near-field estimate. Firstly, we estimate $\int_{[0, R_1]^2} |k(y)| \varphi^{-1}(y) dy$ for $k(y) = \frac{y_1 y_2}{|y|^4}, \frac{y_1 y_2 (y_1^2 - y_2^2)}{|y|^8}$ related to $u_x(0), \mathcal{K}_{00}$ (2.79). We partition $[0, R_1]$ into

$$0 = z_0 < z_1 < \dots < z_n = R_1$$

with z_1 much smaller than R_1 . Denote $Q_{ij} = [z_{i-1}, z_i] \times [z_{j-1}, z_j]$. Clearly, we have

$$\int_{[0, R_1]^2} |k(y)| \varphi^{-1}(y) dy \leq \sum_{1 \leq i, j \leq n} I_{ij}, \quad I_{ij} \triangleq \int_{Q_{ij}} |k(y)| \varphi^{-1}(y) dy.$$

For $I_{ij}, (i, j) \neq (1, 1)$, we apply a trivial bound

$$(7.50) \quad I_{ij} \leq |Q_{ij}| \cdot \|k\|_{L^\infty(Q_{ij})} \|\varphi^{-1}\|_{L^\infty(Q_{ij})}.$$

For $k(y) = \frac{y_1 y_2}{|y|^4}, \frac{y_1 y_2 (y_1^2 - y_2^2)}{|y|^8}$, the estimate of $\|k\|_{L^\infty(Q_{ij})}$ is established in Appendix D. It remains to estimate the first term I_{11} . Denote $r = y_1$. Suppose that

$$\varphi(x) \geq q|x|^a (\cos \beta)^b, \quad b \leq 0,$$

If $k(y) = \frac{y_1 y_2}{|y|^4}$, we yield

$$\begin{aligned} I_{11} &\leq q^{-1} \int_0^{\sqrt{2}r} \int_0^{\pi/2} \frac{\sin \beta \cos \beta}{r^2} r^{-a} (\cos \beta)^{-\beta} r dr d\beta = q^{-1} \int_0^{\sqrt{2}r} r^{-a-1} dr \int_0^{\pi/2} \sin \beta (\cos \beta)^{-b+1} d\beta \\ &= q^{-1} \frac{(\sqrt{2}r)^{-a}}{-a} \int_0^1 t^{-b+1} dt = q^{-1} \frac{(\sqrt{2}r)^{-a}}{-a} \frac{1}{2-b}. \end{aligned}$$

If $k(y) = \frac{y_1 y_2 (y_1^2 - y_2^2)}{|y|^8}$, we yield $|k(y)| \leq \frac{1}{4} \frac{\sin 4\beta}{r^4}$. Since $b \leq 0$, we get $\varphi \geq qr^a$ and

$$\begin{aligned} I_{11} &\leq q^{-1} \int_0^{\sqrt{2}r} \int_0^{\pi/2} \frac{1}{4} \frac{|\sin 4\beta|}{s^4} s^{-a} s ds d\beta = \frac{1}{4q} \int_0^{\sqrt{2}r} s^{-a-3} ds \frac{1}{4} \int_0^{2\pi} |\sin \beta| d\beta \\ &= \frac{1}{4q} \frac{(\sqrt{2}r)^{-a-2}}{-2-a} \int_0^{\pi/2} \sin \beta d\beta = \frac{1}{4q} \frac{(\sqrt{2}r)^{-a-2}}{-2-a}. \end{aligned}$$

7.4.2. Far-field estimate. Denote $a \vee b = \max(a, b)$. To estimate the far field integral $I \triangleq \int_{y_1 \vee y_2 \geq R_0} |k(y)| \varphi^{-1}(y) dy$, we first pick sufficient large R , and then partition the domain

$$0 = z_0 < z_1 < \dots < z_m = R_0 < z_{m+1} < \dots < z_n = R_1 < +\infty.$$

Denote $Q_{ij} = [z_{i-1}, z_i] \times [z_{j-1}, z_j]$. Clearly, we have

$$I = \sum_{m+1 \leq \max(i, j) \leq n} I_{ij} + J, \quad I_{ij} \triangleq \int_{Q_{ij}} |k(y)| \varphi^{-1}(y) dy, \quad J = \int_{y_1 \vee y_2 \geq R_1} |k(y)| \varphi^{-1}(y) dy.$$

For I_{ij} , we apply the trivial estimate (7.50). Suppose that

$$\varphi \geq qr^a (\cos \beta)^b, \quad |k(y)| \leq |y|^{-p}, \quad \beta \leq 0.$$

We get

$$J \leq \frac{1}{q} \int_{R_1}^{\infty} \int_0^{\pi/2} r^{-p-a} (\cos \beta)^{-b} r dr d\beta = \frac{1}{q} \frac{R_1^{-p-a+2}}{|p+a-2|} \int_0^{\pi/2} (\cos \beta)^{-b} d\beta.$$

Using Holder's inequality, we get

$$\int_0^{\pi/2} (\cos \beta)^{-b} d\beta \leq \left(\int_0^{\pi/2} \cos \beta d\beta \right)^{-b} \left(\int_0^{\pi/2} 1 \right)^{1+b} = (\pi/2)^{1+b}.$$

It follows

$$J \leq \frac{1}{q} \frac{R_1^{-p-a+2}}{|p+a-2|} (\pi/2)^{1+b}.$$

Application. We apply the above calculations to estimate the integral and its derivatives beyond the mesh $[0, D]^2$ (7.9). Since the domain is far away from the singularity, the integrand is the symmetrized kernel (3.2), e.g., (7.25). From (D.16), (D.17), and Lemma D.2 in Appendix D, for $\mathbf{u}_A, \nabla \mathbf{u}_A, \partial_i(\rho \mathbf{u}_A), \partial_i(\psi \nabla \mathbf{u}_A)$, the integrand in the far-field (y is large) satisfies

$$|K(x, y)| \leq C(x) \text{Den}^{-k}$$

with some $k \geq 2$ and coefficients $C(x)$, where Den is defined in (D.15).

In our computation, we rescale x and restrict it to the near-field $[0, b]^2$ with $b < 2$. Note that $y \notin [0, D]^2$ and $D \gg b$. From (D.15), we get

$$\text{Den} \geq \max_{|z_1| \leq x_1, |z_2| \leq x_2} |y - z|^2 \geq \max_{|z_1| \leq x_1, |z_2| \leq x_2} (|y| - |z|)^2 \geq (|y| - |x|)^2 = |y|^2 \left(1 - \frac{|x|}{|y|}\right)^2$$

Since $\frac{|x|}{|y|} \leq \sqrt{2}b/D$, we yield

$$\text{Den} \geq (1 - C_s)^2 |y|^2, \quad C_s = \sqrt{2}b/D.$$

It follows

$$\int_{y \notin [0, D]^2} |K(x, y)| \varphi^{-1}(y) dy \leq (1 - C_s)^{-2k} C(x) \int_{y \notin [0, D]^2} |y|^{-2k} \varphi^{-1}(y) dy.$$

Using the method in Section 7.4.2, we can estimate the above integral.

7.5. Estimate for very small or large x . The rescaling argument and the methods in previous sections apply to the estimate of $\mathbf{u}_A(x), \nabla \mathbf{u}_A(x)$ for $x \in [0, x_M]^2 \setminus [0, x_m]^2, 0 < x_m < x_M$. For very small or large x , we cannot use a finite number of dyadic scales $\lambda = 2^i$ to rescale x such that $x/\lambda \in [0, 2x_c]^2 \setminus [0, x_c]^2$. Instead, we choose $\lambda = \frac{\max(x_1, x_2)}{x_c}$. We want to estimate the rescaled integral with a $-d$ -homogeneous kernel K

$$p(x) \int K(x - y) W(y) dy = p_\lambda(x) \int K(\hat{x} - \hat{y}) \lambda^{2-d} W_\lambda(\hat{y}) dy,$$

uniformly for all small $\lambda \ll 1$ or large $\lambda \gg 1$, where p is some weight and p_λ is defined in (7.1). The rescaled singularity $\hat{x} = x/\lambda$ satisfies $\max \hat{x}_i = x_c$. We simplify \hat{x}, \hat{y} as x, y .

Our observation is that in the rescaled integral with scaling λ , we can use the asymptotic of the weights in our computation, see e.g. (7.4). The new difficulty is that the estimate involves the rescaled weight $p_\lambda(y)$. Since λ is not fixed and depends on x that tends to 0 or ∞ , we cannot evaluate $p_\lambda(y)$ and the integrand directly. In the following derivation, λ is comparable to $|x|$, which is either very small or very large.

For y away from the singular region, the integrand of the regular part is given by $J = K(x, y) \cdot p_\lambda(x)$ (7.25). Here we use p for the weight. We use the following decomposition to compute $D_1 J$ with $D_1 = \partial_{x_i}$

$$\begin{aligned} |D_1 J| &= |D_1(K(x, y) \cdot p_\lambda(x))| = |D_1 K(x, y) \cdot p_\lambda(x) + K(x, y) \cdot D_1 p_\lambda(x)| \\ &= \left| p_\lambda(x) \left\{ D_1 K(x, y) + R_{lim} K(x, y) + \left(\frac{D_1 p_\lambda(x)}{p_\lambda(x)} - R_{lim} \right) K(x, y) \right\} \right|, \end{aligned}$$

where R_{lim} is given by

$$R_{lim} \triangleq \lim_{x \rightarrow A} \frac{D_1 p_\lambda(x)}{p_\lambda(x)},$$

with $A = 0$ or ∞ . Since we consider very small λ or very large λ , the error term $\frac{D_1 p_\lambda(x)}{p_\lambda(x)} - R_{lim}$ is small. Hence, we use a triangle inequality to bound $D_1 J$

$$|D_1 J| \leq p_\lambda(x) \left| D_1 K(x, y) + R_{lim} K(x, y) \right| + p_\lambda(x) \left| \left(\frac{D_1 p_\lambda(x)}{p_\lambda(x)} - R_{lim} \right) K(x, y) \right|.$$

The advantage of the above decomposition is that the main term $D_1 K(x, y) + R_{lim} K(x, y)$ does not depend on λ so that we can estimate it using previous methods.

Since the estimate of derivative of u, v does not involve the commutator, see, e.g. (7.48), we can apply the above method to compute the integral of $D_1 u$ for small x or large x .

For y near the singular region, from (7.24), the symmetrized integrand is given by

$$J = K^C(p_\lambda(x) - p_\lambda(y)) + K^{NC} p_\lambda(x),$$

where we use p for the weight. Firstly, we have

$$|D_1 J| = |D_1 K^C(p_\lambda(x) - p_\lambda(y)) + D_1 K^{NC} p_\lambda(x) + (K^C + K^{NC}) D_1 p_\lambda(x)|$$

Denote $K = K^C + K^{NC}$. We use the following method to bound $D_1 J$

$$\begin{aligned} |D_1 J| &\leq p_\lambda(x) \left| D_1 K^C \cdot \left(1 - \frac{p_\lambda(y)}{p_\lambda(x)} \right) + D_1 K^{NC} + K \cdot \frac{D_1 p_\lambda}{p_\lambda} \right| \\ &\leq p_\lambda(x) \left\{ \left| D_1 K^C \cdot \left(1 - \frac{p_{lim}(y)}{p_{lim}(x)} \right) + D_1 K^{NC} + K \cdot \frac{D_1 p_{lim}}{p_{lim}} \right| \right. \\ &\quad \left. + \left| D_1 K^C \left(\frac{p_\lambda(y)}{p_\lambda(x)} - \frac{p_{lim}(y)}{p_{lim}(x)} \right) \right| + K \left| \frac{D_1 p_{lim}}{p_{lim}} - \frac{D_1 p_\lambda}{p_\lambda} \right| \right\}. \end{aligned}$$

The second and the third term on the right hand side can be seen as an error term. The main term $\left| D_1 K^C \cdot \left(1 - \frac{p_{lim}(y)}{p_{lim}(x)} \right) + D_1 K^{NC} + K \cdot \frac{D_1 p_{lim}}{p_{lim}} \right|$ does not depend on λ , and the singularity x is in the near-field and away from 0. We can apply all the delicate decompositions developed in previous sections to estimate $D_1 J$.

In the Hölder estimates, we need various bounds for the weights p_λ . Using the asymptotics of $p(x)$, we can estimate the derivatives of p_λ for very small λ or very large λ uniformly. See

Appendix C.3. Once we obtain the estimates of ψ_λ , and the weight φ_λ in the L^∞ norm $\|\omega_\lambda \varphi_\lambda\|_\infty$, we can use the methods in previous sections and the scaling relations in Section 7.1.2 to perform the Hölder estimates.

The L^∞ estimate follows similar ideas and is much easier. We refer more details to the upcoming Supplementary Materials.

7.6. Assemble the Hölder estimates. In Section 7.3, we decompose the velocity in several parts and estimate them separately. In this section, we assemble these estimates and estimate

$$\delta(f, x, z) \triangleq \frac{|f(x) - f(z)|}{|x - z|^{1/2}},$$

for $f = \rho \mathbf{u}_A, \psi \nabla \mathbf{u}_A$ with suitable weights. One way to combine the estimates of different terms is to use the triangle inequality. To obtain better estimates, we combine some of the estimates.

To illustrate the ideas, we focus on the $C_x^{1/2}$ estimate, $x \in [x_c, 2x_c] \times [0, 2x_c]$, i.e. x_1 is large relative to x_2 , $z_1 \geq x_1$, and $x_2 = z_2$. For general pairs (x, z) , we can rescale (x, z) to $(\lambda x, \lambda z)$ such that $\lambda x \in [0, 2x_c]^2 \setminus [0, x_c]^2$. Using the scaling relations in (7.1.2), we can estimate the rescaled version of $\delta(f, x, z)$. See also the discussion at the beginning of Section 7.3.

We assume that $z_1 \in [x_c, 2(1+\nu)x_c]$ with $\nu < 1$. For $z_1 \geq 2(1+\nu)x_c$, we have $z_1 > (1+\nu)x_1$. Since z_1, x_1 are large relative to z_2, x_2 , respectively, we have

$$|x - z| = |z_1 - x_1| \asymp |z_1| \gtrsim |x|, |z|.$$

Then, we can use the L^∞ estimate and triangle inequality to estimate $\delta(f, x, z)$. Note that we can estimate the piecewise L^∞ norm of $|x|^{-1/2} \rho(x) \mathbf{u}_A(x)$ and $|x|^{-1/2} \psi \nabla \mathbf{u}_A$ following Section 7.2, where ρ, ψ are the weights in the Hölder estimate of $\rho \mathbf{u}_A, \psi \nabla \mathbf{u}_A$.

We focus on $f = \psi u_{x,A}$. We partition the domain $D_\nu = [x_c, 2(1+\nu)x_c] \times [0, 2x_c]$ into $h_x \times h_x$ grids D_{ij} , $1 \leq i \leq 2(1+\nu)x_c/h_x$, $1 \leq j \leq 2x_c/h_x$. We apply the decomposition (7.48) with the same parameters k, k_2 to x in different grids D_{ij} . For $x \in D_{ij}$, using the method in Section 7.3, we obtain the estimate

$$(7.51) \quad \begin{aligned} f(x) &= I_1(x) + I_2(x) + I_3(x) + I_4(x) + I_5(x) - I_6(x), \quad I_5 = I_{5,1} + I_{5,2} \\ |\partial_x(I_1 + I_4 - I_6)| &\leq a_{ij,1} \|\omega \varphi\|_\infty, \quad |\partial_x I_3| \leq a_{ij,2} \|\omega \varphi\|_\infty, |I_3| \leq b_{ij,2} \|\omega \varphi\|_\infty, \\ |\partial_x I_{5,1}| &\leq a_{ij,3} \|\omega \varphi\|_\infty, \quad |I_{5,1}| \leq b_{ij,3} \|\omega \varphi\|_\infty, \end{aligned}$$

for some constants $a_{ij,l}, b_{ij} \geq 0$, where $I_{5,1}, I_{5,2}$ are defined and estimated in Section 7.3.4.

For $x, z \in D_\nu$ with $x_2 = z_2, z_1 \leq x_1$, we have $x \in D_{i_1,j}, z \in D_{i_2,j}$ for some $i_1 \leq i_2$. We apply the method in Section 7.3.3 to estimate $\delta(I_2, x, z)$ and the method in Section 7.3.4 to estimate J_1 related to $\delta(I_{5,2}, x, z)$ (7.39). These estimates contribute to the bound $C[\omega \psi]_{C_x^{1/2}}$ for some $C > 0$, which can be computed.

By averaging the piecewise derivative bounds and using the estimates in Appendix D.5.2, for $x \in D_{i_1,j}, z \in D_{i_2,j}$, we can obtain

$$|(I_1 + I_4 - I_6)(x) - (I_1 + I_4 - I_6)(z)| \leq C|x_1 - z_1| \cdot \|\omega \varphi\|_\infty$$

for constant C depending only on $\{a_{kl,1}\}_{k,l \geq 1}$ and the mesh h_x explicitly. From the above discussions, for the remaining terms in f not estimated using the seminorm $[\omega \psi]_{C_x^{1/2}}$, e.g. $I_1 + I_3 + I_4 + I_{5,1} - I_6$ and J_2 related to $I_{5,2}$ (7.39), they satisfy

$$f_R(x) = \sum_{1 \leq l \leq N} f_l(x), \quad |f_l(x) - f_l(z)| \leq \min(p_l|x_1 - z_1|, q_l) \cdot \|\omega \varphi\|_\infty$$

for some N , where we can choose $q_l = \infty$ if we do not have L^∞ estimate for $f_l(x)$. Similar consideration applies to p_l . In our problem, there are only a few terms and $N < 10$. Now, for $x \in D_{i_1,j}, z \in D_{i_2,j}$, we have

$$(7.52) \quad \begin{aligned} \frac{|f_R(x) - f_R(z)|}{|z_1 - x_1|^{1/2}} &\leq \sum_{1 \leq l \leq N} \min(p_l \delta^{1/2}, q_l \delta^{-1/2}) \|\omega \varphi\|_\infty, \\ \delta &= z_1 - x_1 \in [\max(i_2 - i_1 - 1, 0)h_x, (i_2 - i_1 + 1)h_x], \end{aligned}$$

The upper bound can be obtained explicitly by partitioning the range of $z_1 - x_1$ into finite many subintervals M_l according to the threshold $\delta_l = q_l/p_l$. In each subinterval M_l , the bound reduces to

$$P\delta^{1/2} + Q\delta^{-1/2}$$

for some constants P, Q . It is convex in $\delta^{1/2}$ and can be optimized easily and explicitly in any interval $[\delta_l, \delta_u], \delta_l > 0$.

Remark 7.9. We combine the estimates of different parts in (7.51) using (7.52) to obtain a sharp estimate. If one estimate different parts separately, the distance $\delta = z_1 - x_1$ for the optimizer may not be achieved for the same value, which leads to an overestimate. We remark that for small distance $|z_1 - x_1|$, such an overestimate can be significant since the ratio between the endpoints $|i_2 - i_1 + 1|/\max(i_2 - i_1 - 1, 0)$ varies a lot.

In some estimates, e.g. the $C_y^{1/2}$ estimate of u_x in Section 7.3.6, we need to decompose I_5 using different size of small singular region k_3 . In such a case, we have a list of estimates associated to different k_3 for the part f_R not estimated by $[\omega\psi]_{C_x^{1/2}}$ or $[\omega\psi]_{C_y^{1/2}}$:

$$\frac{|f_R(x) - f_R(z)|}{|z_1 - x_1|^{1/2}} \leq \sum_{1 \leq l \leq N} \min(p_{l,k_3}\delta^{1/2}, q_{l,k_3}\delta^{-1/2}) \|\omega\varphi\|_\infty.$$

For $|x_1 - z_1|$ bounded away from 0, e.g. $|x_1 - z_1| \geq \frac{1}{10}h_x$, we can still partition the range of $|x_1 - z_1|$ and optimizing the above estimates first over δ and then k_3 .

7.6.1. Hölder estimate for small distance. In some Hölder estimates, e.g. the $C_y^{1/2}$ estimate in Sections 7.3.6, 7.3.7, when $|x - z|$ is very small, e.g. $|x - z| \leq ch_x$ with $c < 1$, we need to choose a singular region with size a to be arbitrary small. See also Section 7.1.9 for the estimates of a log-Lipschitz function. In these estimates, we can decompose $f_R(x)$ that is not estimated using the Hölder norm of $\omega\psi$ as follows

$$f_R(x) = f_1(x, a, b) + f_2(x, a),$$

for $a < b$ and b is fixed. We can estimate the derivative of f_1 , and the L^∞ norm for f_2

$$|\partial_x f_1(x, a, b)| \leq (A_i + B_i \log \frac{b}{a}) \|\omega\varphi\|_\infty, \quad |f_2| \leq \frac{C_i a}{2} \|\omega\varphi\|_\infty$$

in each grid D_{ij} for any $a \leq b$, see e.g., (7.43) and (7.51). We drop j since we consider x, z with $x_2 = z_2$. For $t = |x - z| \leq h_x$, we get

$$(7.53) \quad \frac{|f(x) - f(z)|}{|x - z|^{1/2}} \leq (A + B \log \frac{b}{a}) \sqrt{t} + \frac{C a}{\sqrt{t}} \triangleq F(a, t)$$

where $A = \max(A_i, A_{i+1})$, $B = \max(B_i, B_{i+1})$, $C = \max(C_i, C_{i+1})$. For each $t \leq ch_x$, we can optimize the above estimate over $a \leq b$ explicitly. We refer the derivations to Appendix D.5.3.

APPENDIX A. SOME LEMMAS FOR STABILITY ESTIMATES

Lemma A.1. *Suppose that $F_i(t) \geq 0, i = 1, 2, \dots, n$, is Lipschitz in t and satisfies the following estimates*

$$\frac{d}{dt} F_i(t) \leq -a_{ii} F_i(t) + \sum_{j \neq i} a_{ij} F_j(t), \quad a_{ii} > 0.$$

If there exists $\mu_i > 0$ such that

$$(A.1) \quad a_{ii} \mu_i^{-1} - \sum_{j \neq i} |a_{ij}| \mu_j^{-1} \geq \lambda \mu_i^{-1}$$

for some $\lambda > 0$. Then for $E(t) \triangleq \max_i(\mu_i F_i(t))$, which is Lipschitz, we have

$$\frac{d}{dt} E(t) \leq -\lambda E(t),$$

for t almost everywhere. We can do integration to estimate $E(t)$ since $E(t)$ is Lipschitz. In particular, when $n = 2$, condition (A.1) is equivalent to

$$(A.2) \quad a_{11}a_{22} - |a_{12}a_{21}| > 0,$$

and we can choose $\mu_1 = 1, \mu_2 = \sqrt{\frac{a_{22}|a_{12}|}{a_{11}|a_{21}|}}$.

Proof. A direct calculation yields

$$(A.3) \quad \begin{aligned} \frac{d}{dt} \mu_i F_i(t) &\leq -a_{ii}(\mu_i F_i) + \mu_i \sum_{j \neq i} a_{ij} F_j(t) \leq -a_{ii}\mu_i F_i + \mu_i \sum_{j \neq i} |a_{ij}| \mu_j^{-1} E \\ &\leq -a_{ii}\mu_i F_i + \mu_i(a_{ii}\mu_i^{-1} - \lambda\mu_i^{-1})E = -\lambda\mu_i F_i + (a_{ii} - \lambda)(E - \mu_i F_i). \end{aligned}$$

Let Ω be the domain where F_i, E are differentiable. Since F_i, E are Lipschitz, Ω is almost everywhere. For $t \in \Omega$, we assume $E(t) = \mu_j F_j(t)$ for some j . Then for any $s > 0$, we have

$$E(t) - E(t-s) = \mu_j F_j(t) - \max_i \mu_i F_i(t-s) \leq \mu_j(F_j(t) - F_j(t-s)).$$

Dividing s on both sides and then taking $s \rightarrow 0$, we get

$$\frac{d}{dt} E(t) \leq \mu_j \frac{d}{dt} F_j(t) \leq -\lambda\mu_j F_j + (a_{jj} - \lambda\mu_j)(E - \mu_j F_j) = -\lambda E(t),$$

where we have used (A.3) and $E(t) = \mu_j F_j(t)$ in the second inequality. The desired estimate follows. When $n = 2$, obtaining $a_{11}a_{22} - |a_{12}a_{21}| > 0$ from (A.1) is trivial. For the other direction, we choose $\mu_1 = 1, \mu_2 = \sqrt{\frac{a_{22}|a_{12}|}{a_{11}|a_{21}|}}$ to obtain (A.1) for some $\lambda > 0$. \square

We can generalize the above ODE Lemma to the L^∞ estimates.

Lemma A.2. Suppose that $f_i(x, z, t) : \mathbb{R}_{++}^2 \times \mathbb{R}_{++}^2 \times [0, T] \rightarrow \mathbb{R}, 1 \leq i \leq n$, satisfies

$$(A.4) \quad \partial_t f_i + v_i(x, z) \cdot \nabla_{x,z} f_i = -a_{ii}(x, z, t) f_i + B_i(x, z, t),$$

where $v_i(x, z, t)$ are some vector fields Lipschitz in x, z with $v_i|_{x_1=0} = 0, v_i|_{z_1=0} = 0$, and B_i satisfies the following estimate

$$(A.5) \quad |B_i(x, z, t)| \leq \sum_{j \neq i} |a_{ij}(x, z, t)| \cdot \|f_j\|_{L^\infty}.$$

If there exists some constants $M, \lambda, \mu_i > 0$ such that for all (x, z) , we have

$$(A.6) \quad a_{ii}(x, z, t) - \sum_{j \neq i} |a_{ij}| \mu_i \mu_j^{-1} \geq \lambda, \quad \sum_{j \neq i} \mu_i \mu_j^{-1} |a_{ij}| \leq M.$$

Then for $E(t) = \max_i (\mu_i \|f_i(t)\|_\infty)$, which is Lipschitz, and $0 \leq t_0 < t \leq T$, we have

$$E(t) \leq e^{-\lambda(t-t_0)} E_0, \quad E_0 = E(t_0).$$

The condition (A.5) means that the damping term is stronger than the bad terms, which further leads to the stability. We apply $f(x, z, t) = ((S_i \psi_i)(x) - (S_i \psi_i)(z))g_i(x, z)$ in the weighted Hölder estimate, and $f_i(x, z, t) = (S_i \varphi_i)(x)$ in the weighted L^∞ estimate, $S_1 = \omega, S_2 = \eta, S_3 = \xi$. In the weighted L^∞ estimate, we do not need the extra variable z and f_i is constant in z . For the Boussinesq equations (4.1), we choose

$$b(x, t) = \bar{c}_l x + \bar{\mathbf{u}}(x) + \mathbf{u}(\omega)(x, t), \quad v_i(x, t) = b(x, t), \quad \text{or} \quad v_i(x, z, t) = (b(x, t), b(z, t)).$$

We will also perform energy estimates on some scalars $a_i(t)$ and choose $f_i(x, z, t) = a_i(t)$ in the above Lemma. In this case, advection term is 0, and a_{ii}, a_{ij}, B_i only depend on t .

Proof. For simplicity, we assume that the condition (A.6) holds for $\mu_i = 1$. Otherwise, we can estimate the variables $\mu_i f_i$ and introduce $\tilde{a}_{ij} = a_{ij} \mu_i \mu_j^{-1}$. Then the equations and estimates (A.4), (A.5) become

$$\begin{aligned} \partial_t \mu_i f_i + v_i(x, z) \cdot \nabla_{x,z} (\mu_i f_i) &= -a_{ii}(\mu_i f_i) + \mu_i B_i(x, z, t) \\ \mu_i |B_i(x, z, t)| &\leq \sum_{j \neq i} \mu_i \mu_j^{-1} a_{ij}(x, z, t) \cdot \mu_j \|f_j\|_{L^\infty} = \sum_{j \neq i} \tilde{a}_{ij}(x, z, t) \cdot \mu_j \|f_j\|_{L^\infty}. \end{aligned}$$

In this case, then the condition (A.6) for a_{ij} becomes the condition for \tilde{a}_{ij} with equal weights. Thus, it suffices to consider the case $\mu_i = 1, i = 1, 2, \dots, n$.

Formally, we can apply the L^∞ estimate on both sides of (A.4) and then evaluate (A.4) at the maximizer to obtain the desired result. To justify it rigorously, we use the characteristics, Duhamel's principle, and a bootstrap argument. We define the characteristics associated with v_i

$$(A.7) \quad \frac{d}{dt}(X_i(t), Z_i(t)) = v_i(X_i, Z_i, t), \quad X_i(0) = x_0, \quad Z_i(0) = z_0, \quad F_i(t) = f_i(X_i(t), Z_i(t), t)$$

To simplify the notation, we drop x_0, z_0 . Denote

$$(A.8) \quad A_i(t) = a_{ii}(X_i(t), Z_i(t)), \quad C_i(t) \triangleq \sum_{j \neq i} |a_{ij}(X_i(t), Z_i(t), t)|.$$

It suffices to prove that for small $\varepsilon > 0$, we have

$$(A.9) \quad E(t) \leq (1 + c(M)\varepsilon)e^{-\lambda_\varepsilon(t-t_0)}E_0, \quad \lambda_\varepsilon = \lambda - \varepsilon, \quad c(M) = \frac{2}{M},$$

where M is the upper bound in (A.6). Then taking $\varepsilon \rightarrow 0$ completes the proof.

We want to use a bootstrap argument to prove (A.9). Firstly, since $E(0) = E_0$ and $E(t)$ is Lipschitz, the above condition holds for $t \in [t_0, t_0 + T_1]$ with some $T_1 > 0$. Now, we want to show that under (A.9), we can obtain

$$(A.10) \quad E(t) \leq (1 + c(M)\varepsilon/2)e^{-\lambda_\varepsilon(t-t_0)}E_0.$$

By definition, along the characteristics, we get

$$\frac{d}{dt}F_i(t) = -A_i(t)F_i(t) + B_i(X_i(t), Z_i(t), t),$$

Using the estimates (A.5) and definition (A.8), we yield

$$|B_i(X_i(t), Z_i(t), t)| \leq \sum_{j \neq i} |a_{ij}|E(t) \leq C_i(t)E(t).$$

Using the Duhamel principle and the above estimate, we obtain

$$(A.11) \quad \begin{aligned} F_i(t) &= e^{\int_{t_0}^t -A_i(s)ds}F_i(t_0) + \int_{t_0}^t B_i(X_i(s), Z_i(s), s)e^{\int_s^t -A_i(\tau)d\tau}ds \\ |F_i(t)| &\leq e^{\int_{t_0}^t -A_i(s)ds}F_i(t_0) + \int_{t_0}^t C_i(s)E(s)e^{\int_s^t -A_i(\tau)d\tau}ds \triangleq I + II. \end{aligned}$$

For the second term, using the bootstrap assumptions (A.9), we yield

$$|II| \leq \int_{t_0}^t C_i(s)(1 + c(M)\varepsilon)e^{-\lambda_\varepsilon(s-t_0)}E_0e^{-\lambda_\varepsilon(t-s)-\int_s^t (A_i(s)-\lambda_\varepsilon)ds}$$

Using $C_i(s) \leq M, C_i(s) \leq A_i(s) - \lambda$ (A.6) and the definition of $c(M)$ (A.9), we get

$$\frac{C_i(s)}{C_i(s) + \varepsilon} \leq \frac{M}{M + \varepsilon} \leq \frac{1 + \varepsilon/M}{1 + 2\varepsilon/M} = \frac{1 + c(M)\varepsilon/2}{1 + c(M)\varepsilon}, \quad C_i(s) + \varepsilon \leq A_i(s) - \lambda + \varepsilon = A_i(s) - \lambda_\varepsilon,$$

which implies

$$C_i(s)(1 + c(M)\varepsilon) \leq (C_i(s) + \varepsilon)(1 + c(M)\varepsilon/2) \leq (A_i(s) - \lambda_\varepsilon)(1 + c(M)\varepsilon/2).$$

Note that we choose $c(M)$ in (A.9) small enough such that the above inequality holds. Hence, we can simplify the bound of II as follows

$$\begin{aligned} |II| &\leq (1 + c(M)\varepsilon/2)e^{-\lambda_\varepsilon(t-t_0)}E_0 \int_{t_0}^t (A_i(s) - \lambda_\varepsilon)e^{-\int_s^t (A_i(\tau)-\lambda_\varepsilon)d\tau}ds \\ &= (1 + c(M)\varepsilon/2)e^{-\lambda_\varepsilon(t-t_0)}E_0(1 - e^{-\int_{t_0}^t (A_i(\tau)-\lambda_\varepsilon)d\tau}). \end{aligned}$$

The estimate of I is trivial. Since $|F_i(0)| \leq E_0$, we have

$$|I| = |F_i(t_0)|e^{-\lambda_\varepsilon(t-t_0)}e^{-\int_{t_0}^t (A_i(\tau)-\lambda_\varepsilon)d\tau} \leq E_0e^{-\lambda_\varepsilon(t-t_0)}e^{-\int_{t_0}^t (A_i(\tau)-\lambda_\varepsilon)d\tau},$$

which along with the estimate of II yields

$$|F_i(t)| \leq |I| + |II| \leq (1 + c(M)\varepsilon/2)e^{-\lambda_\varepsilon(t-t_0)}E_0.$$

Since the above estimate holds for any initial data x_0, z_0 and i , taking the supremum, we prove (A.10). Then the standard bootstrap argument implies the desired estimate (A.9). \square

We can generalize the previous linear stability Lemma to the nonlinear stability estimates.

Lemma A.3. *Suppose that $f_i(x, z, t) : \mathbb{R}_{++}^2 \times \mathbb{R}_{++}^2 \times [0, T] \rightarrow \mathbb{R}, 1 \leq i \leq n$, satisfies*

$$(A.12) \quad \partial_t f_i + v_i(x, z) \cdot \nabla_{x,z} f_i = -a_{ii}(x, z, t)f_i + B_i(x, z, t) + N_i(x, z, t) + \bar{\varepsilon}_i,$$

where $v_i(x, z, t)$ are some vector fields Lipschitz in x, z with $v_i|_{x_1=0} = 0, v_i|_{z_1=0} = 0$. For some $\mu_i > 0$, we define the energy

$$E(t) = \max_{1 \leq i \leq n} (\mu_i \|f_i\|_{L^\infty}).$$

Suppose that B_i, N_i and $\bar{\varepsilon}_i$ satisfy the following estimate

(A.13)

$$|B_i(x, z, t)| + |N_i(x, z, t)| + |\bar{\varepsilon}_i| \leq \sum_{j \neq i} (|a_{ij}(x, z, t)|E(t) + |a_{ij,2}(x, z, t)|E^2(t) + |a_{ij,3}(x, z, t)|).$$

If there exists some $E_*, \varepsilon_0, M > 0$ such that

$$(A.14) \quad \begin{aligned} a_{ii}(x, z, t)E_* - \sum_{j \neq i} (|a_{ij}|E_* + |a_{ij,2}|E_*^2 + |a_{ij,3}(x, z, t)|) &> \varepsilon_0, \\ \sum_{j \neq i} (|a_{ij}|E_* + |a_{ij,2}|E_*^2 + |a_{ij,3}(x, z, t)|) &< M, \end{aligned}$$

for all x, z and $t \in [0, T]$. Then for $E(0) < E_*$, we have $E(t) < E_*$ for $t \in [0, T]$.

We remark that the second inequality in (A.14) is only qualitative.

Proof. The proof is very similar to that of Lemma A.2. We fix $E(0)$. It suffices to prove that under the bootstrap assumption

$$(A.15) \quad E(t) < E_*,$$

on $[0, T_1]$, there exists ε that depends on $E_0, \varepsilon_0, M, E_*$, such that we can obtain

$$(A.16) \quad E(t) \leq (1 - \varepsilon)E_*, \quad t \in [0, T_1].$$

Since $E(0) < E_*$ and $E(t)$ is Lipschitz, we know that the bootstrap assumption holds for some short time T_1 .

We adopt most notations from the proof of Lemma A.2 but use

$$C_i(t) \triangleq \sum_{j \neq i} (|a_{ij}(X_i(t), Z_i(t), t)|E(t) + |a_{ij,2}(X_i(t), Z_i(t), t)|E^2(t) + |a_{ij,3}(X_i(t), Z_i(t), t)|).$$

Using these notations, derivations and estimates similar to those in the proof of Lemma A.2, we obtain

$$|F_i(t)| \leq e^{-\int_0^t -A_i(s)ds} F_i(0) + \int_0^t C_i(s) e^{-\int_s^t A_i(\tau)d\tau} ds.$$

Using the bootstrap assumption and (A.14), we obtain

$$C_i(s) < \min(M, A_i(t)E_* - \varepsilon_0) < (1 - \delta)A_i(t)E_*,$$

for some small δ depending on ε_0, M, E_* . Note that if $A_i(t)E_* < 2M$, we pick δ such that $A_i(t)E_* - \varepsilon_0 < (1 - \delta)A_i(t)E_*$. If $A_i(t)E_* > 2M$, we require $\delta < 1/2$. Now, we obtain

$$\begin{aligned} |F_i(t)| &\leq e^{-\int_0^t -A_i(s)ds} |F_i(0)| + \int_0^t (A_i(s)E_* - \varepsilon_0) e^{-\int_s^t A_i(\tau)d\tau} ds \\ &\leq e^{-\int_0^t -A_i(s)ds} |F_i(0)| + (1 - \delta) \int_0^t A_i(s)E_* e^{-\int_s^t A_i(\tau)d\tau} ds \\ &= e^{-\int_0^t -A_i(s)ds} |F_i(0)| + (1 - \delta)E_* (1 - e^{-\int_0^t -A_i(s)ds}) \\ &\leq \max(|F_i(0)|, (1 - \delta)E_*) \leq \max(|E(0)|, (1 - \delta)E_*). \end{aligned}$$

Taking the supremum over the initial data of the trajectory and i , we get

$$E(t) \leq \max(|E(0)|, (1 - \delta)E_*).$$

Since we fix $E(0)$ and $E(0) < E_*$, we can pick small δ to obtain

$$(1 - \delta)E_* > E(0), \quad E(t) < (1 - \delta)E_*,$$

which is (A.16). Using the bootstrap argument, we complete the proof. \square

A.1. Proof of Lemma 2.2. In this section, we prove Lemma 2.2 related to the Hölder estimates.

Proof. Using (2.29), we first derive the equation for $f\varphi$

$$\partial_t(f\varphi) + b(x) \cdot \nabla(f\varphi) = c(x)f\varphi + (b \cdot \nabla\varphi)f + \mathcal{R}\varphi = d(x)f\varphi + \mathcal{R}\varphi,$$

where $d(x) = c(x) + \frac{b \cdot \nabla\varphi}{\varphi}$ is defined in Lemma 2.2. For $x, z \in \mathbb{R}_2^+$, we derive the equation of $\delta(f\varphi)(x, z) = f\varphi(x) - f\varphi(z)$:

$$\partial_t\delta(x, z, t) + b(x) \cdot \nabla_x(f\varphi)(x) - b(z) \cdot \nabla_z(f\varphi)(z) = (df\varphi)(x) - (d\eta\varphi)(z) + \delta(\mathcal{R}\psi).$$

Since

$$\nabla_x(f\varphi)(x) = \nabla_x((f\varphi)(x) - (f\varphi)(z)) = \nabla_x\delta(f\varphi), \quad \nabla_z(f\varphi)(z) = -\nabla_z(\delta(f\varphi)),$$

$$df\varphi(x) - df\varphi(z) = d(x)(f\varphi(x) - f\varphi(z)) + (d(x) - d(z))f\varphi(z) = d(x)\delta(f\varphi)(x, z) + (d(x) - d(z))f\varphi(z),$$

we obtain

$$(A.17) \quad \partial_t\delta(f\varphi) + (b(x) \cdot \nabla_x + b(z) \cdot \nabla_z)\delta(f\varphi) = d(x)\delta(f\varphi)(x, z) + (d(x) - d(z))(f\varphi)(z) + \delta(\mathcal{R}\varphi).$$

Since $g(h)$ is even in h_1, h_2 , $\partial_i g$ is odd in h_i and we have

$$\begin{aligned} & (b(x) \cdot \nabla_x + b(z) \cdot \nabla_z)(\delta(f\varphi)g(x - z)) \\ &= g(x - z) \cdot (b(x) \cdot \nabla_x + b(z) \cdot \nabla_z)\delta(f\varphi) + \delta(f\varphi) \cdot (b(x) \cdot \nabla_x + b(z) \cdot \nabla_z)g(x - z) \\ &= g(x - z) \cdot (b(x) \cdot \nabla_x + b(z) \cdot \nabla_z)\delta(f\varphi) + \delta(f\varphi) \cdot (b(x) - b(z)) \cdot (\nabla g)(x - z). \end{aligned}$$

We further multiply both sides of (A.17) by $g(x - z)$ and use $F(x, z, t) = \delta(f\varphi)(x, z)g(x - z)$ and the above identity to yield

$$\partial_t F + (b(x) \cdot \nabla_x + b(z) \cdot \nabla_z)F = (d(x) + \frac{(b(x) - b(z)) \cdot (\nabla g)(x - z)}{g(x - z)})F + ((d(x) - d(z))(f\varphi)(z) + \delta(\mathcal{R}\varphi))g(x - z),$$

which concludes the proof of (2.30). \square

APPENDIX B. PROOF OF SHARP HÖLDER ESTIMATES

In this Appendix, we prove the sharp Hölder estimates in Section 3, and discuss the properties of the transport map and rigorous estimate of the sharp constant. Note that we have proved Lemmas 3.1, 3.3 in Section 3. We will discuss the properties of the map related to u_x and estimate the constant in Section B.3.

B.1. $C_x^{1/2}$ estimate of v_x and u_y . We follow the ideas in Section 3.2 and argument in Section to estimate the Hölder seminorm of u_y, v_x . Recall the kernel $K_2 = \frac{1}{2} \frac{y_1^2 - y_2^2}{|y|^4}$ for u_y, v_x . Firstly, we need the following Lemma for the principle value of the integral.

Lemma B.1. *Suppose that $f \in L^\infty$, is Hölder continuous near 0. For $0 < a, b < \infty$ and $Q = [0, a] \times [0, b], [0, a] \times [-b, 0], [-a, 0] \times [0, b]$, or $[-a, 0] \times [-b, 0]$, we have*

$$P.V. \int_Q K_2(y)f(y)dy = \lim_{\varepsilon \rightarrow 0} \int_{Q \cap |y_1| \geq \varepsilon} K_2(y)f(y)dy - \frac{\pi}{8}f(0) = \lim_{\varepsilon \rightarrow 0} \int_{Q \cap |y_2| \geq \varepsilon} K_2(y)f(y)dy + \frac{\pi}{8}f(0).$$

In the strip $|y_1| \leq \varepsilon$, $K_2(y) < 0$ if $|y_2| > \varepsilon$. It contributes to $-\frac{\pi}{8}f(0)$ in the first identity. In the strip $|y_2| \leq \varepsilon$, $K_2(y) > 0$ if $|y_1| > \varepsilon$. It contributes to $\frac{\pi}{8}f(0)$ in the second identity.

Proof. Since K_2 is even in y_1, y_2 , we focus on $Q = [0, a] \times [0, b]$ without loss of generality. By definition, we have

$$P.V. \int_Q K_2(y)f(y)dy = \lim_{\varepsilon \rightarrow 0} \left(\int_{-\varepsilon}^a \int_0^b + \int_0^{\varepsilon} \int_{-\varepsilon}^b \right) K_2(y)f(y)dy \triangleq \lim_{\varepsilon \rightarrow 0} (I_\varepsilon + II_\varepsilon)$$

We just need to compute II_ε . Since f is Hölder continuous near 0, we get

$$\lim_{\varepsilon \rightarrow 0} \int_0^{\varepsilon} \int_{-\varepsilon}^b K_2(y)(f(y) - f(0))dy = 0.$$

The first identity follows from

$$\lim_{\varepsilon \rightarrow 0} \int_0^{\varepsilon} \int_{-\varepsilon}^b K_2(y)f(0)dy = f(0) \lim_{\varepsilon \rightarrow 0} \int_0^{\varepsilon} \frac{1}{2} \frac{y_2}{y_2^2 + y_1^2} \Big|_{-\varepsilon}^b dy_1 = \frac{f(0)}{2} \lim_{\varepsilon \rightarrow 0} \int_0^{\varepsilon} \left(\frac{b}{b^2 + y_1^2} - \frac{\varepsilon}{\varepsilon^2 + y_1^2} \right) dy_1 = -\frac{\pi}{8} f(0).$$

The second identity follows from the same argument. \square

Next, we perform the sharp Hölder estimate for u_y, v_x . Without loss of generality, we assume $z_1 = -1, x_1 = 1$ and $z_2 = x_2 > 0$. We are going to estimate

$$(B.1) \quad v_x(z) - v_x(x) = \frac{1}{\pi} \left(\int (K_{2,B}(y_1 + 1, y_2) - K_{2,B}(y_1 - 1, y_2)) W(y_1, x_2 - y_2) dy_2 - \frac{1}{2} \pi (\omega(z) - \omega(x)) \right).$$

To simplify the notation, we denote

$$A = \min(B, x_2), \quad K^+ \triangleq K_{2,B}(y_1 + 1, y_2), \quad K^- \triangleq K_{2,B}(y_1 - 1, y_2), \quad \Delta(y) = K^+ - K^-.$$

We focus on $B \geq 2$. It is easy to see that Δ is odd in y_1 . Since the transportation cost in y direction is cheaper, we shall use the Y -transportation as much as possible to obtain a sharp estimate. Due to the presence of the boundary and the discontinuity of W across the boundary, we partition the domain into the inner part and the outer part

$$\Omega_{in} \triangleq \{y_2 \in [-A, A]\}, \quad \Omega_{out} \triangleq \{y_2 \notin [-A, A]\}.$$

Then we have $\omega(\cdot, x_2 - \cdot) \in C^{1/2}(\Omega_{in})$. We add the parameter A in these domains due to the localization of the kernel. Define

$$\Delta_{1D}(y_1) = \int_{-A}^A \Delta(y_1, y_2) dy_2.$$

Remark that for fixed y_1 , $\Delta(y_1, y_2)$ may not have a fixed sign over y_2 .

The estimates consist of three steps. In the first two steps, we estimate the integral in Ω_{in} . In the first step, we fix y_1 and consider the 1D transportation problem on the vertical line

$$vl_{y_1} \triangleq \{(y_1, y_2) : y_2 \in \mathbb{R}\}$$

by moving the positive part of Δ to its negative part. If $|y_1| \leq 9$, we move the remaining part with total mass Δ_{1D} to the horizontal line

$$hl_{x_2} \triangleq \{(y_1, x_2) : y_1 \in \mathbb{R}\}.$$

Here, vl , hl are short for vertical line, horizontal line, respectively. In this step, the estimate is bounded by $C[\omega]_{C_y^{1/2}}$.

In the second step, we study the transportation problem on hl_{x_2} . We also move the remaining part with total mass $\Delta_{1D}(y_1)$ for $|y_1| \geq 9$ in the first step horizontally. The estimate will be bounded by $C[\omega]_{C_x^{1/2}}$ for some constant C .

In the third step, we estimate the integral in the outer domain Ω_{out} . The estimate will be bounded by $C[\omega]_{C_y^{1/2}}$ for some constant C .

We focus on $|y_2 - x_2| \leq B$ since otherwise $\Delta = 0$. We assume $x_2 > 0$. The case $x_2 = 0$ can be obtained by taking limit $x_2 \rightarrow 0$.

B.1.1. *Sign of Δ and Δ_{1D} .* Due to odd symmetry of $\Delta(y_1, y_2)$ in y_1 . We focus on $y_1 \geq 0$. Solving $K_2(y_1 + 1, y_2) - K_2(y_1 - 1, y_2) = 0$, we get $y_2 = s_c(y_1)$ (B.42). It is easy to show that

$$(B.2) \quad \begin{aligned} K_2(y_1 + 1, y_2) - K_2(y_1 - 1, y_2) &\geq 0, |y_2| \geq s_c(y_1), \\ K_2(y_1 + 1, y_2) - K_2(y_1 - 1, y_2) &\leq 0, |y_2| \leq s_c(y_1). \end{aligned}$$

For $|y_1| \leq B - 1$, we get

$$(B.3) \quad \Delta(y) = K_2(y_1 + 1, y_2) - K_2(y_1 - 1, y_2).$$

The sign of $\Delta(y_1, \cdot)$ is given above. For $|y_1| \in [B - 1, B + 1]$, we have

$$(B.4) \quad \Delta(y) = -K_2(y_1 - 1, y_2) = -\frac{1}{2} \frac{(y_1 - 1)^2 - y_2^2}{((y_1 - 1)^2 + y_2^2)^2}.$$

Since $B - 1 \geq 1$, it satisfies

$$(B.5) \quad \Delta(y) \geq 0, |y_2| \geq s_c(y_1) \triangleq |y_1| + 1, \quad \Delta(y) \leq 0, |y_2| \leq s_c(y_1) = |y_1| + 1.$$

For $y_1 \geq B + 1$, we have $\Delta(y) = 0$. Next, we compute Δ_{1D} . Since Δ is singular at $y = (\pm 1, 0)$ and $B > 2$, the singularity is in $[-9, 9] \triangleq J_1$. In the inner part, we have

$$(B.6) \quad S_{in} \triangleq \int_{\Omega_{in}} \Delta(y_1, y_2) W(y_1, x_2 - y_2) dy = \left(\int_{y_1 \in J_1} + \int_{y_1 \notin J_1} \right) \Delta(y_1, y_2) W(y_1, x_2 - y_2) dy \triangleq S_1 + S_2.$$

By definition, we yield

$$(B.7) \quad S_1 = \int_{y_1 \in J_1} \Delta(y_1, y_2) (W(y_1, x_2 - y_2) - W(y_1, x_2)) dy + \int_{y_1 \in J_1} \Delta(y_1, y_2) W(y_1, x_2) dy \triangleq S_{11} + S_{12}.$$

For S_{11} , since $|W(y_1, x_2 - y_2) - W(y_1, x_2)| \lesssim y_2^{1/2}$, the integrand is locally integrable. We will estimate S_{12} and S_2 in Section B.1.2.

We should pay attention to the principle value in the singular integral in S_{12} near the singularity $(\pm 1, 0)$. Since $\Delta(y) = K_2(y_1 + 1, y_2) - K_2(y_1 - 1, y_2)$ near $y_1 = 1$, applying Lemma B.1 four times to $-K_2(y_1 - 1, y_2)$, we yield

$$(B.8) \quad \begin{aligned} S_{12}^+ &\triangleq \int_{y_1 \in J_1 \cap \mathbb{R}_+} \Delta(y_1, y_2) W(y_1, x_2) dy \\ &= \frac{\pi}{2} W(1, x_2) + \lim_{\varepsilon \rightarrow 0} \int_{y_1 \in J_1 \cap \mathbb{R}_+ \setminus [1 - \varepsilon, 1 + \varepsilon]} \Delta(y_1, y_2) W(y_1, x_2) dy. \end{aligned}$$

Recall definition of Δ from (3.1), (B.3), (B.4). Denote

$$(B.9) \quad g_b(y) = \frac{b}{y^2 + b^2}, \quad \Delta_{1D}(y_1) = \frac{A}{(y_1 + 1)^2 + A^2} \mathbf{1}_{|y_1+1| \leq B} - \frac{A}{(y_1 - 1)^2 + A^2} \mathbf{1}_{|y_1-1| \leq B}.$$

For $y_1 \notin [1 - \varepsilon, 1 + \varepsilon]$, a direct computation yields

$$\int_{-A}^A \Delta(y_1, y_2) dy_2 = \frac{1}{2} \left(\frac{y_2}{(y_1 + 1)^2 + y_2^2} - \frac{y_2}{(y_1 - 1)^2 + y_2^2} \right) \Big|_{-A}^A = g_A(y_1 + 1) - g_A(y_1 - 1) = \Delta_{1D}(y_1)$$

for $|y_1| \leq B - 1$, and

$$\int_{-A}^A \Delta(y_1, y_2) dy_2 = -\frac{1}{2} \frac{y_2}{(y_1 - 1)^2 + y_2^2} \Big|_{-A}^A = -g_A(y_1 - 1) = \Delta_{1D}(y_1)$$

for $|y_1| \in [B - 1, B + 1]$. Plugging the above computation to the P.V. integral yields

$$S_{12}^+ = \int_{J_1 \cap \mathbb{R}_+} \Delta_{1D}(y_1) W(y_1, x_2) dy_1 + \frac{\pi}{2} \omega(1, x_2).$$

The computation of the integral over \mathbb{R}_- is similar due to symmetry. We yield

$$(B.10) \quad S_{12} = \int_{J_1} \Delta_{1D}(y_1) W(y_1, x_2) dy_1 + \frac{\pi}{2} (\omega(1, x_2) - \omega(-1, x_2)).$$

B.1.2. *First step.* We are in a position to estimate S_2 (B.6) and S_{11} (B.7). Recall the sign of Δ from (B.2), (B.5)

$$\Delta(y) \geq 0, |y_2| \geq s_c(y_1), \quad \Delta(y) \leq 0, |y_2| \leq s_c(y_1).$$

Since Δ is even in y_2 in Ω_{in} and odd in y_1 , we focus on the first quadrant.

For a fixed $y_1 \geq 0$, we transport the positive part of Δ to its negative part on the line vl_{y_1} in the first quadrant. We construct the transportation map $T(y) > 0$ by solving

$$\int_{T(y)}^{y_2} \Delta(y_1, s_2) ds_2 = 0.$$

For $y_1 \leq B - 1$, $\Delta = K_2(y_1 + 1, y_2) - K_2(y_1 - 1, y_2)$. The map T can be obtained from the cubic equation (B.44). For $y_1 \in [B - 1, B + 1]$, $D = -K_2(y_1 - 1, y_2)$ and we get

$$0 = \int_{T(y)}^{y_2} K_2(y_1 - 1, s_2) ds_2 = \frac{1}{2} \frac{s_2}{(y_1 - 1)^2 + s_2^2} \Big|_T^{y_2}, \quad T(y) = \frac{(y_1 - 1)^2}{y_2}.$$

Denote

$$\tilde{W}(y) = W(y_1, x_2 - y_2) - W(y_1, x_2), J_1^+ \triangleq J_1 \cap \mathbb{R}_+.$$

Using the above map,

$$|\tilde{W}(y_1, y_2) - \tilde{W}(y_1, T(y))| = |W(y_1, y_2) - W(y_1, T(y))| \leq |y_2 - T(y)|^{1/2} [\omega]_{C_y^{1/2}}, \quad |\tilde{W}(y_1, y_2)| \leq |y_2|^{1/2} [\omega]_{C_y^{1/2}},$$

and applying Lemma 3.6 to the integral on $[T(y_1, A), A]$, we yield

$$\begin{aligned} \left| \int_0^A \Delta(y) \tilde{W}(y) dy \right| &= \left| \left(\int_{T(y_1, A)}^A + \int_0^{T(y_1, A)} \right) \Delta(y) \tilde{W}(y) dy_2 \right| \\ &\leq \left(\int_{s_c(y_1)}^A |\Delta(y)| |y_2 - T(y)|^{1/2} dy_2 + \int_0^{T(y_1, A)} |\Delta(y)| |y_2|^{1/2} dy_2 \right) [\omega]_{C_y^{1/2}}. \end{aligned}$$

Due to symmetry of Δ in y_1, y_2 , we can estimate S_{11} (B.7) as follows

$$S_{11} \leq 4 \int_{J_1} \left(\int_{s_c(y_1)}^A |y_2 - T(y)|^{1/2} dy_2 + \int_0^{T(y_1, A)} |y_2|^{1/2} dy_2 \right) dy_1 [\omega]_{C_y^{1/2}}.$$

The factor 4 is due to the fact that we have 4 quadrants.

The estimate of S_2 (B.6) is similar except that we do not further transport the remaining negative part of Δ to the location (y_1, x_2)

$$(B.11) \quad S_2 = \int_{y_1 \notin J_1} \left(\int_{T(y_1, A) \leq |y_2| \leq A} + \int_{|y_2| \leq T(y_1, A)} \right) \Delta(y) W(y) dy \triangleq I + II.$$

For I , we obtain

$$|I| \leq 2 \int_{y_1 \notin J_1} \int_{s_c(y_1)}^A |T(y) - y_2|^{1/2} dy = 4 \int_{y_1 \notin J_1, y_1 \geq 0} \int_{s_c(y_1)}^A |T(y) - y_2|^{1/2} dy$$

For II , we use the odd symmetry of $\Delta(y_1, y_2)$ in y_1

$$\begin{aligned} (B.12) \quad |II| &\leq \left| \int_{y_1 \notin J_1, y_1 \geq 0} \int_{|y_2| \leq T(y_1, A)} \Delta(y) (W(y) - W(-y_1, y_2)) dy \right| \\ &\leq \int_{y_1 \notin J_1, y_1 \geq 0} \int_{|y_2| \leq T(y_1, A)} \sqrt{2y_1} |\Delta(y)| dy [\omega]_{C_x^{1/2}} = \int_{y_1 \notin J_1, y_1 \geq 0} \sqrt{2y_1} |\Delta_{1D}(y_1)| dy_1 [\omega]_{C_x^{1/2}}, \end{aligned}$$

where we have used $\int_{T(y_1, A)}^A \Delta(y) dy_2 = 0$, and for $s_c(y_1) < A$,

$$\int_{|y_2| \leq T(y_1, A)} |\Delta(y)| dy_2 = \int_{|y_2| \leq T(y_1, A)} -\Delta(y) dy_2 = \int_{|y_2| \leq A} -\Delta(y) dy_2 = -\Delta_{1D}(y_1).$$

The reason why we do not transport the negative part $\Delta(y_1, y_2)$ for $|y_2| \leq T(y_1, A)$, $|y_1| \geq 9$ down to (y_1, x_2) will be clear after we estimate S_{12} (B.10). See remark B.2

B.1.3. *Second step: Estimate S_{12} .* We combine the estimate of S_{12} (B.10) and the local part of v_x , e.g. $-\frac{\pi}{2}(\omega(z) - \omega(x))$. For v_x , since $\omega(z) - \omega(x) = -\omega(1, x_2) + \omega(-1, x_2)$, we obtain

$$(B.13) \quad I \triangleq S_{12} - \frac{\pi}{2}(\omega(z) - \omega(x)) = \int_{J_1} \Delta_{1D}(y_1) W(y_1, x_2) + \pi(\omega(1, x_2) - \omega(-1, x_2)).$$

Recall the definition of $\Delta_{1D}(y_1)$ (B.9). Clearly, Δ_{1D} is odd and $\Delta_{1D} < 0$ for $y_1 > 0$. Note that

$$P(k) \triangleq \int_0^k \Delta_{1D} dy_1 \geq \int_{\mathbb{R}_+} \Delta_{1D} dy_1 = - \int_{-1}^1 \frac{A}{y_1^2 + A^2} dy_1 = -2 \arctan\left(\frac{1}{A}\right) \geq -\pi.$$

We transport all the negative part of Δ_{1D} on $[0, \infty]$ to $(1, x_2)$. Similarly, we transport all the positive part of Δ_{1D} on $(-\infty, 0]$ to $(-1, x_2)$. We derive the following estimate

$$(B.14) \quad \begin{aligned} |I| &= \left| \int_{J_1 \cap \mathbb{R}_+} \Delta_{1D}(y_1)(W(y_1, x_2) - W(1, x_2)) dy_1 \right. \\ &\quad \left. + \int_{J_1 \cap \mathbb{R}_-} \Delta_{1D}(y_1)(W(y_1, x_2) - W(-1, x_2)) dy_1 + (\pi + P(9))(W(1, x_2) - W(-1, x_2)) \right| \\ &\leq \left(2 \int_{J_1 \cap \mathbb{R}_+} |\Delta_{1D}|y_1 - 1|^{1/2} dy_1 + (\pi + P(9))\sqrt{2} \right) [\omega]_{C_x^{1/2}}, \end{aligned}$$

where we have used the symmetry of Δ_{1D} to get the factor 2.

Remark B.2. Suppose that we further transport the negative part in II in S_2 (B.11) to (y_1, x_2) . Then we get

$$II = \int_{y_1 \notin J_1} \int_{|y_2| \leq T(y_1, A)} \Delta(y)(W(y) - W(y_1, x_2)) dy + \int_{y_1 \notin J_1} \Delta_{1D}(y_1) W(y_1, x_2) dy \triangleq II_1 + II_2.$$

For II_2 , we need to incorporate it into the estimate of S_{12}, I (B.13)

$$\begin{aligned} C &\triangleq II_2 + S_{12} - \frac{\pi}{2}(\omega(z) - \omega(x)) = \int_{\mathbb{R}} \Delta_{1D}(y_1) W(y_1, x_2) dy_1 + \pi(\omega(1, x_2) - \omega(-1, x_2)) \\ &= \int_{\mathbb{R}^+} \Delta_{1D}(W(y_1, x_2) - W(-y_1, x_2) - W(1, x_2) + W(-1, x_2)) + (\pi + P(\infty))(\omega(1, x_2) - \omega(-1, x_2)), \end{aligned}$$

for $-\pi \leq P(\infty) < 0$. For the integrand, we have two estimates

$$|W(y_1, x_2) - W(-y_1, x_2) - W(1, x_2) + W(-1, x_2)| \leq \min(\sqrt{2y_1} + \sqrt{2}, 2\sqrt{|y_1 - 1|}) \|W\|_{C_x^{1/2}}.$$

Note that for $|y_1| \geq 9$, the estimate $(\sqrt{2y_1} + \sqrt{2}) \|W\|_{C_x^{1/2}}$ is sharper. Then we yield

$$|C| \leq \left(\int_0^9 |\Delta_{1D}|2\sqrt{|y_1 - 1|} dy_1 + \int_9^\infty |\Delta_{1D}|(\sqrt{2} + \sqrt{2y_1}) dy_1 + (\pi + P(\infty))\sqrt{2} \right) [\omega]_{C_x^{1/2}}.$$

Since

$$\int_9^\infty |\Delta_{1D}| \sqrt{2} dy_1 + P(\infty)\sqrt{2} = \sqrt{2} \left(\int_0^\infty - \int_9^\infty \right) \Delta_{1D} dy_1 = \sqrt{2} P(9),$$

we further obtain

$$|C| \leq \left(\int_0^9 |\Delta_{1D}|2\sqrt{|y_1 - 1|} dy_1 + \int_9^\infty |\Delta_{1D}| \sqrt{2y_1} dy_1 + (\pi + P(9))\sqrt{2} \right) [\omega]_{C_x^{1/2}}.$$

We remark that the above constant of $[\omega]_{C_x^{1/2}}$ is the same as the sum of those in (B.12) and (B.14). Moreover, we need to further bound II_1 in the above. Therefore, the overall estimate in this approach is worse. It is due to the inequality $2|y_1 - 1|^{1/2} \geq \sqrt{2} + \sqrt{2y_1}$ for $y_1 \geq 9$.

B.1.4. *Third step.* In this step, we estimate the integral in the outer part, which is much easier. If $B < x_2$, since $\Delta(y_1, y_2)$ is localized to $|y_2| \leq B = A$, the contribution from outer part $|y_2| > B$ is 0. If $B > x_2 = A$, using the odd symmetry of W and the even symmetry of Δ in y_2 , we yields

$$\begin{aligned} S_{out} &= \int_{\Omega_{out}} \Delta(y) W(y_1, x_2 - y_2) dy = \int_{\mathbb{R}} \int_{x_2}^B \Delta(y) W(y_1, x_2 - y_2) dy + \int_{\mathbb{R}} \int_{-B}^{-x_2} \Delta(y) W(y_1, x_2 - y_2) dy \\ &= - \int_{\mathbb{R}} \int_{x_2}^B \Delta(y) \omega(y_1, y_2 - x_2) dy + \int_{\mathbb{R}} \int_{x_2}^B \Delta(y) \omega(y_1, x_2 + y_2) dy. \end{aligned}$$

It follows

$$(B.15) \quad |S_{out}| \leq \int_{\mathbb{R}} \int_{x_2}^B |\Delta(y)| \cdot |\omega(y_1, x_2 + y_2) - \omega(y_1, y_2 - x_2)| dy \leq \sqrt{2x_2} \int_{\mathbb{R}} \int_{x_2}^B |\Delta(y)| dy [\omega]_{C_y^{1/2}}.$$

B.1.5. $C_x^{1/2}$ Estimate of u_y . The estimates of u_y in step 1 and 2 are similar to that of v_x except that we do not transport the negative part of $\Delta(y_1, y_2)$ with $|y_2| \leq T(y_1, A)$ for any $y_1 > 0$. The reason is similar to that in Remark B.2 and will be clear later. See Remark. The estimate of the outer part in the third step is the same as that of v_x in Section B.1.4.

Denote $J_\varepsilon = [-1 - \varepsilon, -1 + \varepsilon] \cup [1 - \varepsilon, 1 + \varepsilon]$. Note that $\Delta = K_2(y_1 + 1, y_2) - K_2(y_1 - 1, y_2)$ has singularities at $(\pm 1, 0)$. Applying Lemma B.1 four times to $K_2(y_1 + 1, y_2)$ and $-K_2(y_1 - 1, y_2)$, respectively, we can rewrite S_{in} (B.6) as follows

$$\begin{aligned} (B.16) \quad S_{in} &\triangleq \int_{\mathbb{R}} \int_{-A}^A \Delta(y) W(y_1, x_2 - y_2) dy \\ &= \frac{\pi}{2} (\omega(1, x_2) - \omega(-1, x_2)) + \lim_{\varepsilon \rightarrow 0} \int_{J_\varepsilon^c} \int_{-A}^A \Delta(y) W(y_1, x_2 - y_2) dy \triangleq I + \lim_{\varepsilon \rightarrow 0} II_\varepsilon. \end{aligned}$$

For $y_1 \notin J_\varepsilon$, we perform a decomposition

$$\begin{aligned} f(y_1) &\triangleq \int_{-A}^A \Delta(y) W(y_1, x_2 - y_2) dy_2 \\ &= \left(\int_{T(y_1, A) < |y_2| \leq A} + \int_{|y_2| \leq T(y_1, A)} \right) \Delta(y) W(y_1, x_2 - y_2) dy_2 \triangleq f_1(y_1) + f_2(y_1). \end{aligned}$$

For $f_1(y_1)$, we estimate it using Lemma 3.6

$$(B.17) \quad |f_1(y_1)| \leq 2 \int_{s_c(y_1)}^A |\Delta(y)| |y_2 - T(y)|^{1/2} dy [\omega]_{C_y^{1/2}}$$

The part $f_2(y_1)$ denotes the purely negative part. If $T(y_1, A) < A$, we get $T(y_1, A) < s_c(y_1) < A$ and $\Delta(y) < 0$. It follows

$$\int_{|y_2| < T(y_1, A)} |\Delta(y)| dy_2 = \int_{|y_2| < T(y_1, A)} -\Delta(y) dy_2 = \int_{|y_2| \leq A} -\Delta(y) dy_2 = -\Delta_{1D}(y_1) = |\Delta_{1D}(y_1)|.$$

Using this estimate and the fact that Δ is odd in y_1 , we get

$$\begin{aligned} (B.18) \quad |f_2(y_1) + f_2(-y_1)| &= \left| \int_{|y_2| \leq T(y_1, A)} \Delta(y) (W(y_1, x_2 - y_2) - W(-y_1, x_2 - y_2)) dy_2 \right| \\ &\leq \int_{|y_2| \leq T(y_1, A)} \sqrt{2y_1} |\Delta(y)| dy_2 [\omega]_{C_x^{1/2}} = |\Delta_{1D}(y_1)| \sqrt{2y_1} [\omega]_{C_x^{1/2}}. \end{aligned}$$

Integrating (B.17), (B.18) over $y_1 \notin J_\varepsilon$, we establish

$$|II_\varepsilon| \leq 4 \int_{J_\varepsilon^c \cap \mathbb{R}_+} \int_{s_c(y_1)}^A |\Delta(y)| |y_2 - T|^{1/2} dy [\omega]_{C_y^{1/2}} + \int_{J_\varepsilon^c \cap \mathbb{R}_+} |\Delta_{1D}(y_1)| \sqrt{2y_1} [\omega]_{C_x^{1/2}}.$$

Notice that near the singularity $(1, 0)$ of $\Delta(y)$, $|y_2 - T|^{1/2} \lesssim |y_2|^{1/2} + |y_1 - 1|^{1/2}$. Thus, the integrand in the first integral is locally integrable. Plugging the the above estimate in (B.16),

we derive

$$(B.19) \quad \begin{aligned} |S_{in} - \frac{\pi}{2}(\omega(1, x_2) - \omega(-1, x_2))| &\leq \limsup_{\varepsilon \rightarrow 0} |I_\varepsilon - \frac{\pi}{2}(\omega(1, x_2) - \omega(-1, x_2))| + II_\varepsilon \\ &\leq 4 \int_{\mathbb{R}_+} \int_{s_c(y_1)}^A |\Delta(y)| |y_2 - T|^{1/2} dy [\omega]_{C_y^{1/2}} + \int_{\mathbb{R}_+} |\Delta_{1D}(y_1)| \sqrt{2y_1} [\omega]_{C_x^{1/2}}. \end{aligned}$$

Recall the definition of localized u_y (3.1). Combining the above estimate and the estimate of S_{out} in (B.15), we prove the estimate of u_y .

Remark B.3. For a fixed y_1 , if we transport $\Delta(y_1, y_2)$ for $|y_2| \leq A$ to the line hl_{x_2} , we need to estimate the 1D integral

$$S \triangleq \left(\int_{\mathbb{R}} \Delta_{1D}(y) W(y_1, x_2) + \frac{\pi}{2}(\omega(1, x_2) - \omega(-1, x_2)) \right) - \frac{\pi}{2}(\omega(1, x_2) - \omega(-1, x_2))$$

The first part is derived similar to (B.10), and the second part is from the local term in u_y (3.1). Since the local terms are exactly canceled, and $\Delta_{1D} < 0$ for $y_1 > 0$ and $\Delta_{1D} > 0$ for $y_1 < 0$, the sharp estimate of S is trivial

$$|S| = \left| \int_{\mathbb{R}_+} D_{1D}(y) (W(y_1, x_2) - W(-y_1, x_2)) dy_1 \right| \leq \int_{\mathbb{R}_+} |D_{1D}(y)| \sqrt{2y_1} dy_1 [\omega]_{C_x^{1/2}}$$

The constant of $[\omega]_{C_x^{1/2}}$ is exactly the same as that in (B.19).

B.2. $C_y^{1/2}$ estimate of v_x . Since W is not continuous across the boundary $y_2 = 0$, the localized v_x or u_y is no longer Hölder continuous. Therefore, we study the estimate without localization. Without loss of generality, we assume $z_2 = m + 1, x_2 = m - 1, x_1 = z_1 = 0$ with $m > 1$. The case $m = 1$ can be obtained by taking limit. The difference $v_x(z) - v_x(x)$ or $u_y(z) - u_y(x)$ is given by

$$I \triangleq \frac{1}{\pi} \int K_2(y_1, 1 + y_2) - K_2(y_1, y_2 - 1) W(y_1, m - y_2) dy + s(\omega(z) - \omega(x)),$$

where $s = \frac{1}{2}$ for u_y and $s = -\frac{1}{2}$ for v_x . Denote

$$(B.20) \quad \eta(y_1, y_2) = W(y_2, y_1), \quad \eta_m(y_1, y_2) = \eta(m - y_1, y_2).$$

By definition, η is odd in y_1 , is discontinuous across y_1 , and satisfies

$$(B.21) \quad [\eta]_{C_x^{1/2}(\Omega)} = [\omega]_{C_y^{1/2}(\Omega)}, \quad [\eta]_{C_y^{1/2}(\Omega)} = [\omega]_{C_x^{1/2}},$$

for $\Omega = \{y : y_1 \geq 0\}$ or $\Omega = \{y : y_1 \leq 0\}$.

Swapping the dummy variables y_1, y_2 and then using $K_2(y_1, y_2) = -K_2(y_2, y_1)$, $\eta_m(y) = \eta(m - y_1, y_2) = W(y_2, m - y_1)$, we yield

$$(B.22) \quad \begin{aligned} I &= -\frac{1}{\pi} \int (K_2(y_1 + 1, y_2) - K_2(y_1 - 1, y_2)) \eta(m - y_1, y_2) dy + s(\omega(z) - \omega(x)) \\ &= -\frac{1}{\pi} \int \Delta(y) \eta_m(y) dy + s(\eta_m(-1, 0) - \eta_m(1, 0)), \quad s = -\frac{1}{2} \text{ for } v_x, \quad s = \frac{1}{2} \text{ for } u_y. \end{aligned}$$

We perform the above reformulation so that we can adopt the analysis of

$$\Delta(y) = K_2(y_1 + 1, y_2) - K_2(y_1 - 1, y_2)$$

in (B.2) and Section B.1.1. Since η is discontinuous across $y_1 = 0$, which relates to $y_1 = m$ in the integral in (B.22), and the singularity of Δ is at $y = (\pm 1, 0)$, we decompose the integral into the inner region, middle region, and outer region

$$(B.23) \quad \begin{aligned} \Omega_{in} &\triangleq \{y : |y_1| \leq 1\}, \quad \Omega_{mid} \triangleq \{y : |y_1| \in [1, m]\}, \quad \Omega_{out} \triangleq \{y : |y_1| > m\}, \\ S_\alpha &\triangleq \int_{\Omega_\alpha} \Delta(y) \eta_m(y) dy, \quad \alpha \in \{in, mid, out\}. \end{aligned}$$

In each region, η_m is Hölder continuous. Since we can obtain a small factor from $[\omega]_{C_y^{1/2}}$ and we have (B.21), to obtain a sharp estimate of (B.22), we should use X transportation as much as possible.

Firstly, we analyze the sign of $\Delta(y)$. Since Δ is odd in y_1 and even in y_2 , we can focus on the $y_1, y_2 \geq 0$. For fixed y_2 , we have

$$(B.24) \quad \begin{aligned} \Delta(y) < 0, \quad y_1 < h_c^-(y_2) \leq 1, \quad \Delta(y) > 0, \quad y_1 \in (h_c^-(y_2), 1), \quad y_2 \leq y_c \triangleq 3^{-1/2}, \\ \Delta(y) < 0, \quad y_1 > h_c^+(y_2) \geq 1, \quad \Delta(y) > 0, \quad y_1 \in (1, h_c^+(y_2)), \end{aligned}$$

where $h_c^\pm(y_2)$ solves $\Delta(h_c^\omega(y_2), y_2) = 0$ and is given explicitly in (B.42). Denote $Q_\varepsilon = [1 - \varepsilon, 1 + \varepsilon] \times [-\varepsilon, \varepsilon]$ and Q_i is the four quadrants with center at $(1, 0)$, e.g. $Q_1 = \{y_1 \geq 1, y_2 \geq 0\}$. For the P.V. integral, since the kernel $\frac{y_1^2 - y_2^2}{|y|^4}$ has mean 0 in each quadrant $\mathbb{R}^\pm \times \mathbb{R}^\pm$, it is not difficult to show that

$$\lim_{\varepsilon \rightarrow 0} \int_{Q_\varepsilon^c} \Delta(y) \eta(m - y_1, y_2) \mathbf{1}_{y_1 \geq 0} dy = \sum_{i=1}^4 \lim_{\varepsilon_i \rightarrow 0} \int_{Q_\varepsilon^c \cap Q_i} \Delta(y) \eta(m - y_1, y_2) \mathbf{1}_{y_1 \geq 0} dy.$$

That is, we can compute the P.V. integral separately in each Q_i .

In the following subsections, we estimate the integral in each region.

B.2.1. Inner region Ω_{in} . In this region, we have $|y_1| \leq 1$. Denote $y_c = 3^{-1/2}$. Note that $\Delta = K_2(y_1 + 1, y_2) - K_2(y_1 - 1, y_2)$ is singular at $(1, 0)$. Applying Lemma B.1 to $-K_2(y_1 - 1, y_2)$ yields

$$(B.25) \quad \int_0^1 \int_0^{y_c} \Delta(y) \eta_m(y) dy = \lim_{\varepsilon \rightarrow 0} \int_0^1 \int_\varepsilon^{y_c} \Delta(y) \eta_m(y) dy - \frac{\pi}{8} \eta_m(1, 0) \triangleq \lim_{\varepsilon \rightarrow 0} I_\varepsilon - \frac{\pi}{8} \eta_m(1, 0).$$

Let $T_1(y) \geq 0$ be the map that solves

$$\int_{y_1}^{T_1(y)} \Delta(s, y_2) ds = 0,$$

which is given in (B.45). Using the sign inequality (B.24) and applying Lemma 3.6 in the y_1 direction, we yield

$$\left| \int_\varepsilon^{y_c} dy_2 \int_0^{T_1(0, y_2)} \Delta(y) \eta_m(y) dy_1 \right| \leq \int_\varepsilon^{y_c} dy_2 \int_0^{h_c^-(y_2)} |\Delta(y)| |y_1 - T_1(y)|^{1/2} dy_1 [\eta]_{C_x^{1/2}}.$$

Using symmetry of Δ in y_1, y_2 , we obtain

$$\left| \int_{\varepsilon \leq |y_2| \leq y_c} \int_{|y_1| \leq T_1(0, |y_2|)} \Delta(y) \eta_m(y) dy \right| \leq 4 \int_\varepsilon^{y_c} dy_2 \int_0^{h_c^-(y_2)} |\Delta(y)| |y_1 - T_1(y)|^{1/2} dy_1 [\eta]_{C_x^{1/2}}.$$

The remaining part of the integral in Ω_{in} is in the following region

$$(B.26) \quad \begin{aligned} R_{in, \varepsilon} &\triangleq \{|y_1| \leq 1, |y_2| \geq y_c\} \cup \{T_1(0, |y_2|) \leq y_1 \leq 1, \varepsilon \leq |y_2| \leq y_c\}, \\ R_{in, \varepsilon}^+ &= R_{in, \varepsilon} \cap [0, 1] \times \mathbb{R}, \quad R_{in, \varepsilon}^{++} = R_{in, \varepsilon} \cap [0, 1] \times \mathbb{R}^+. \end{aligned}$$

Since $\Delta > 0$ in $\mathbb{R}_{in, \varepsilon}^+$, we use the odd symmetry of Δ in y_1 and even symmetry in y_2 to obtain

$$\left| \int_{R_{in, \varepsilon}} \Delta(y) \eta_m(y) dy \right| = \left| \int_{R_{in, \varepsilon}^+} \Delta(y) (\eta_m(y_1, y_2) - \eta_m(-y_1, y_2)) dy \right| \leq 2 \int_{R_{in, \varepsilon}^{++}} |\Delta(y)| \sqrt{2y_1} dy [\eta]_{C_x^{1/2}},$$

where we have the factor 2 since the estimates in $y_2 \geq 0$ and $y_2 \leq 0$ are the same.

Plugging the above estimate in (B.25) and using the symmetry of Δ in y_1, y_2 , we derive

$$(B.27) \quad \begin{aligned} &\left| \int_{\Omega_{in}} \Delta(y) \eta_m(y) + \frac{\pi}{4} (\eta_m(1, 0) - \eta_m(-1, 0)) \right| \\ &\leq \left(4 \int_0^{y_c} dy_2 \int_0^{h_c^-(y_2)} |\Delta(y)| |y_1 - T_1(y)|^{1/2} dy_1 + 2 \int_{R_{in, 0}^{++}} |\Delta(y)| \sqrt{2y_1} dy \right) [\eta]_{C_x^{1/2}} \triangleq C_{in} [\eta]_{C_x^{1/2}}. \end{aligned}$$

B.2.2. Estimate in Ω_{mid} . We develop two estimates for the integral (B.23)

$$S_{mid} \triangleq \int_{\Omega_{mid}} \Delta(y) \eta_m(y) dy.$$

First estimate. The first estimate is similar to that in Section B.2.1. Notice that the singularities of Δ are $(\pm 1, 0)$. We first rewrite S_{mid} as follows using Lemma B.1 twice with $Q = [1, m] \times [0, 1]$ and $Q = [1, m] \times [-1, 0]$

$$(B.28) \quad S_{mid} = \lim_{\varepsilon \rightarrow 0} \int_{\Omega_{mid} \cap |y_2| \geq \varepsilon} \Delta(y) \eta_m(y) dy - \frac{\pi}{4} (\eta_m(1, 0) - \eta_m(-1, 0)).$$

To estimate the integral, we first study the sign of $\Delta(y)$. For $y_1 \in [1, m]$, we have

$$\Delta(y) > 0, |y_2| > s_c(m)$$

where s_c is given in (B.42). For $|y_2| < s_c(m)$, the sign of $\Delta(y)$ is given in (B.24). Denote

$$(B.29) \quad \begin{aligned} R_{out} &\triangleq \{|y_1| \in [1, m], |y_2| \geq s_c(m)\} \cup \{|y_2| < s_c(m), 1 \leq |y_1| \leq T(m, |y_2|)\}, \\ R_{out}^+ &\triangleq R_{out} \cap \{y_1 \geq 0\}, \quad R_{out}^{++} \triangleq R_{out} \cap \mathbb{R}_2^{++}. \end{aligned}$$

In $\Omega_{out} \setminus R_{out}$, using the sign properties of Δ (B.24) and applying Lemma 3.6 in the y_1 direction, we yield

$$\left| \int_{\varepsilon}^{s_c(m)} \int_{T(m, y_2)}^m \Delta(y) \eta_m(y) dy \right| \leq \int_{\varepsilon}^{s_c(m)} dy_2 \int_{h_c^+(y_2)}^m |\Delta(y)| |y_1 - T_1(y)|^{1/2} dy,$$

where T_1 is given in (B.45). For the integral in R_{out} , $\Delta(y)$ is positive if $y_1 > 0$. We use the odd symmetry of Δ and

$$|\eta_m(y_1, y_2) - \eta(-y_1, y_2)| \leq \sqrt{2y_1} [\eta]_{C_x^{1/2}}.$$

In particular, we obtain estimate similar to (B.27)

$$(B.30) \quad \begin{aligned} |S_{mid} + \frac{\pi}{4} (\eta_m(1, 0) - \eta_m(-1, 0))| &\leq \left(4 \int_0^{s_c(m)} dy_2 \int_{h_c^+(y_2)}^m |\Delta(y)| |y_1 - T_1(y)|^{1/2} dy_1 \right. \\ &\quad \left. + 2 \int_{R_{mid}^{++}} |\Delta(y)| \sqrt{2y_1} dy \right) [\eta]_{C_x^{1/2}} \triangleq C_{mid,1}(m) [\eta]_{C_x^{1/2}}. \end{aligned}$$

Second estimate. In the second estimate, instead of using transportation in the y_1 direction, we use transportation in y_2 direction. This estimate will be very useful for v_x with small m . Firstly, applying Lemma B.1 twice to $K_2(y_1 + 1, y_2)$ and $-K_2(y_1 - 1, y_2)$, respectively, we yield

$$S_{mid} = \frac{\pi}{4} (\eta_m(1, 0) - \eta_m(-1, 0)) + \lim_{\varepsilon \rightarrow 0} \int_{\Omega_{mid} \cap |y_1| - 1 \geq \varepsilon} \Delta(y) \eta_m(y) dy \triangleq I + \lim_{\varepsilon \rightarrow 0} II_{\varepsilon}.$$

We remark that the above decomposition and the sign of $(\eta_m(1) - \eta_m(-1))$ are different from those in (B.28). Here, we restrict y_1 ε away from ± 1 in the limit, while in (B.28), we restrict y_2 ε away from 0. Recall that Δ satisfies the sign condition (B.3). Note that

$$(B.31) \quad \int_0^{\infty} \Delta(y_1, y_2) dy_2 = \frac{y_2}{y_2^2 + (y_1 + 1)^2} - \frac{y_2}{y_2^2 + (y_1 - 1)^2} \Big|_0^{\infty} = 0,$$

and Δ is even in y_2 and odd in y_1 . Applying Lemma 3.6 in the y_2 direction, we obtain

$$(B.32) \quad II_{\varepsilon} \leq 4 \int_{1+\varepsilon}^m dy_1 \int_{s_c(y_1)}^{\infty} |\Delta(y)| |y_2 - T(y)|^{1/2} dy_2 [\eta]_{C_y^{1/2}}$$

We have a factor 4 since the same estimate apply to integral in each quadrant. It follows

$$(B.33) \quad \begin{aligned} |S_{mid} - \frac{\pi}{4} (\eta_m(1, 0) - \eta_m(-1, 0))| &\leq 4 \int_1^m dy_1 \int_{s_c(y_1)}^{\infty} |\Delta(y)| |y_2 - T(y)|^{1/2} dy_2 [\eta]_{C_y^{1/2}} \\ &\triangleq C_{mid,2}(m) [\eta]_{C_y^{1/2}}. \end{aligned}$$

When we combine different estimates to estimate $[v_x]_{C_y^{1/2}}$, the factor $-\frac{\pi}{4} (\eta_m(1) - \eta_m(-1))$ allows us to cancel the local term in v_x . The factor $\frac{\pi}{4} (\eta_m(1) - \eta_m(-1))$ in (B.30) has the opposite sign and does not offer such cancellation.

B.2.3. *Estimate in the outer region.* We also develop two estimates for the integral (B.23)

$$S_{out} \triangleq \int_{\Omega_{out}} \Delta(y) \eta_m(y) dy.$$

In Ω_{out} , we note that $\eta_m \in C^{1/2}([m, \infty) \times \mathbb{R})$ and $\eta_m \in C^{1/2}((-\infty, m] \times \mathbb{R})$. We will apply the same estimate to the integral in $\Omega_{out} \cap \{y_1 \geq m\}$ and in $\Omega_{out} \cap \{y_1 \leq -m\}$. Thus, we focus on the estimate in the region with $y_1 \geq m$.

First estimate. The first estimate is similar to that in the second estimate of S_{mid} in Section B.2.2. Following the argument in (B.31), (B.32), we obtain

$$(B.34) \quad |S_{out}| \leq 4 \int_m^\infty \int_{s_c(y_2)}^\infty |\Delta(y)| |y_2 - T(y)|^{1/2} dy [\eta]_{C_y^{1/2}} \triangleq C_{out,1}(m) [\eta]_{C_y^{1/2}}.$$

Second estimate. In the second estimate, we use the horizontal transportation as much as possible. Recall the function g from (B.9). Denote

$$\begin{aligned} \Delta_m(y_2) &\triangleq \int_{y_1 \geq m} \Delta(y_1, y_2) dy_1 = \frac{1}{2} \left(-\frac{y_1 + 1}{(y_1 + 1)^2 + y_2^2} + \frac{y_1 - 1}{(y_1 - 1)^2 + y_2^2} \Big|_m^\infty \right) \\ &= \frac{1}{2} \left(\frac{m + 1}{(m + 1)^2 + y_2^2} - \frac{m - 1}{(m - 1)^2 + y_2^2} \right) = \frac{1}{2} (g_{m+1}(y_2) - g_{m-1}(y_2)), \\ J_m(y_2) &\triangleq \int_{y_1 \geq m} \Delta(y) \eta_m(y) dy_1, \quad E_m(y_2) \triangleq J_m(y_2) - \Delta_m(y_2) \eta_m(m, y_2). \end{aligned}$$

It is easy to obtain that

$$(B.35) \quad \Delta_m(y_2) < 0, \quad |y_2| < y_m \triangleq \sqrt{m^2 - 1}, \quad \Delta_m(y_2) > 0, \quad |y_2| > y_m.$$

For a fixed y_2 , our idea is to apply Lemma 3.6 to estimate the integral on the line $[m, \infty) \times \{y_2\}$, and then transport the remaining positive or negative part with total mass $\Delta_{1D}(y_2)$ to (m, y_2) . Then, we study the transportation problem on the line $\{m\} \times \mathbb{R}$.

Firstly, we estimate $E_m(y_2)$. For $y_2 \in [0, s_c(m)]$, we have $\Delta(y) < 0$ for $y_1 \geq m$ and estimate $E_m(y_2)$ as follows

$$|E_m(y_2)| = \left| \int_{y_1 \geq m} \Delta(y) (\eta_m(y) - \eta_m(m, y_2)) dy_1 \right| \leq \int_{y_1 \geq m} |\Delta(y)| |y_1 - m|^{1/2} dy [\eta]_{C_x^{1/2}}.$$

It is not difficult to show that $s_c(m) < y_m = (m^2 - 1)^{1/2}$ from (B.42). From the sign property (B.24) and (B.35), for $y_2 \in [s_c(m), y_m]$, we get

$$\int_m^{T(m, y_2)} \Delta(y) dy_1 = 0, \quad \text{for some } T(m, y_1) \in (h_c^+(y_2), \infty),$$

for $y_2 \in (y_m, \infty)$, we get

$$\int_{T(\infty, y_2)}^\infty \Delta(y) dy_1 = 0, \quad T(\infty, y_2) = (y_2^2 - 1)^{1/2} \in (m, s_c(y_2)).$$

Therefore, for $y_2 \in [s_c(m), y_m]$, we have the following estimate

$$\begin{aligned} |E_m(y_2)| &= \left| \int_m^{T(m, y_2)} \Delta(y) \eta_m(y) dy_1 + \int_{T(m, y_2)}^\infty \Delta(y) (\eta_m(y) - \eta_m(m, y_2)) dy_1 \right| \\ &\leq \left(\int_m^{h_c^+(y_2)} |\Delta(y)| |y_1 - T(y)|^{1/2} dy_1 + \int_{T(m, y_2)}^\infty |\Delta(y)| |y_1 - m|^{1/2} dy_1 \right) [\eta]_{C_x^{1/2}}. \end{aligned}$$

For $y_2 \in [y_m, \infty)$, we yield

$$\begin{aligned} |E_m(y_2)| &= \left| \int_{T(\infty, y_2)}^\infty \Delta(y) \eta_m(y) dy_1 + \int_m^{T(\infty, y_2)} \Delta(y) (\eta_m(y) - \eta_m(m, y_2)) dy_1 \right| \\ &\leq \left(\left| \int_{h_c^+(y_1)}^\infty |\Delta(y)| |y_1 - T(y)|^{1/2} dy_1 \right| + \int_m^{T(\infty, y_2)} |\Delta(y)| |y_1 - m|^{1/2} dy_1 \right) [\eta]_{C_x^{1/2}}. \end{aligned}$$

The estimate of $E_m(y_2)$ with $y_2 < 0$ is the same since $\Delta(y)$ is even in y_2 .

Now it remains to estimate the transportation on $m \times \mathbb{R}$

$$II = \int \Delta_m(y_2) \eta_m(m, y_2) dy_2.$$

From the sign properties (B.35), we construct the 1D map as follows

$$\int_{y_2}^{T(y_2)} \Delta_m(s) ds = 0, \quad T_m(y_2) = \frac{m^2 - 1}{y_2}.$$

Note that $\int_0^\infty \Delta_m(s) ds = 0$. Applying Lemma 3.6, we establish

$$|II| \leq 2 \int_{y_m}^\infty |\Delta_m(y_2)| |y_2 - \frac{m^2 - 1}{y_2}|^{1/2} dy_2 [\eta]_{C_y^{1/2}}.$$

We can apply the above estimates to estimate the integral in $\Omega_{out} \cap \{y_1 \leq -m\}$, which leads to an additional factor 2 in (B.36). Denote

$$\begin{aligned} R_{out,1} &\triangleq \{y_2 \in [s_c(m), y_m], m \leq y_1 \leq h_c^+(y_2)\} \cup \{y_2 \geq y_m, y_1 \geq h_c^+(y_2)\}, \\ R_{out,2} &\triangleq [m, \infty] \times [0, s_c(m)] \cup \{y_2 \in [s_c(m), y_m], y_1 \geq T(m, y_2)\} \cup \{y_2 \geq y_m, m \leq y_1 \leq T(\infty, y_2)\}. \end{aligned}$$

Combining the above estimates, we prove

$$\begin{aligned} (B.36) \quad |S_{out}| &\leq 4 \int_{y_m}^\infty |\Delta_m(y_2)| |y_2 - \frac{m^2 - 1}{y_2}|^{1/2} dy_2 [\eta]_{C_y^{1/2}} \\ &\quad + 4 \left(\int_{R_{out,1}} |\Delta(y)| |y_1 - T(y)|^{1/2} dy + \int_{R_{out,2}} |\Delta(y)| |y_1 - m|^{1/2} dy \right) [\eta]_{C_x^{1/2}} \\ &\triangleq C_{out,2y}(m) [\eta]_{C_y^{1/2}} + C_{out,2x}(m) [\eta]_{C_x^{1/2}}. \end{aligned}$$

B.2.4. Summarize the estimates. Recall from (B.22)

$$\begin{aligned} v_x(z) - v_x(x) &= -\frac{1}{\pi} \int \Delta(y) \eta_m dy - \frac{1}{2} (\eta_m(-1, 0) - \eta_m(1, 0)) \\ &= -\frac{1}{\pi} (S_{in} + S_{mid} + S_{out} - \frac{\pi}{2} (\eta_m(1, 0) - \eta_m(-1, 0))) \\ u_y(z) - u_y(x) &= -\frac{1}{\pi} (S_{in} + S_{mid} + S_{out} + \frac{\pi}{2} (\eta_m(1, 0) - \eta_m(-1, 0))). \end{aligned}$$

Note that $|(\eta_m(1, 0) - \eta_m(-1, 0))| \leq \sqrt{2} [\eta]_{C_x^{1/2}}$. Combining the estimates (B.27), (B.30), (B.33), (B.34), (B.36), we prove

$$\begin{aligned} \pi |u_y(z) - u_y(x)| &\leq (C_{in} + C_{mid,1}) [\eta]_{C_x^{1/2}} + \min(C_{out,1} [\eta]_{C_y^{1/2}}, C_{out,2x} [\eta]_{C_x^{1/2}} + C_{out,2y} [\eta]_{C_y^{1/2}}), \\ \pi |v_x(z) - v_x(x)| &\leq C_{in} [\eta]_{C_x^{1/2}} + \min(C_{mid,1} [\eta]_{C_x^{1/2}} + \pi \sqrt{2} [\eta]_{C_x^{1/2}}, C_{mid,2} [\eta]_{C_y^{1/2}} + \frac{\pi}{2} \sqrt{2} [\eta]_{C_x^{1/2}}) \\ &\quad + \min(C_{out,1} [\eta]_{C_y^{1/2}}, C_{out,2x} [\eta]_{C_x^{1/2}} + C_{out,2y} [\eta]_{C_y^{1/2}}). \end{aligned}$$

Using the relation (B.21), we can rewrite the upper bound in terms of $[\omega]_{C_x^{1/2}}, [\omega]_{C_y^{1/2}}$.

B.3. Estimate of the sharp constants for u_x . Recall that the map $T(s_1, s_2)$ solves the cubic equation (3.15)

$$(B.37) \quad 0 = -1 - 8Ts_1 + 16Ts_1(T^2 + Ts_1 + s_1^2) - 8s_2^2(1 - 4s_1T + 2s_2^2).$$

Firstly, for fixed s_2 and $s_1 > 0$, we show that it has a unique solution on $[0, \infty)$. Then, we study the properties of $T(s_1, s_2)$ so that we can estimate $C_1(b)$ in Lemma 3.1 effectively.

Note that the above identity is symmetric in T and s_1 and is a cubic equation in T . For $s_1 > 0$, dividing s_1 on both side yields

$$(B.38) \quad g(T) \triangleq T^3 + T^2 s_1 + T(s_1^2 - \frac{1}{2} + 2s_2^2) - \frac{(4s_2^2 + 1)^2}{16s_1} = 0.$$

Since $g(0) < 0$ and $g(\infty) > 0$, the above equation has at least one real root on \mathbb{R}_+ . We introduce $Z = T + \frac{s_1}{3}$ and can rewrite the above equation in terms of Z

$$\begin{aligned} 0 &= (T + \frac{s_1}{3})^3 - \frac{s_1^3}{27} + T(\frac{2}{3}s_1^2 - \frac{1}{2} + 2s_2^2) - \frac{(4s_2^2 + 1)^2}{16s_1} \\ (B.39) \quad &= Z^3 + Z(\frac{2}{3}s_1^2 - \frac{1}{2} + 2s_2^2) - \left(\frac{(4s_2^2 + 1)^2}{16s_1} + \frac{7}{27}s_1^3 + \frac{s_1}{3}(2s_2^2 - \frac{1}{2})\right) \\ &\triangleq Z^3 + p(s_1, s_2)Z + q(s_1, s_2). \end{aligned}$$

The discriminant is given by

$$\Delta_Z(s_1, s_2) = -(27q(s_1, s_2)^2 + 4p(s_1, s_2)^3).$$

Note that

$$-q \geq \frac{7}{27}s_1^3 - \frac{s_1}{6} + \frac{1}{16s_1} \geq (2\sqrt{\frac{7}{27} \cdot \frac{1}{16}} - \frac{1}{6})s_1 \geq 0,$$

and $-q, p$ are increasing in s_2 . We yield

$$-\Delta_Z(s_1, s_2) \geq -D_Z(s_1, 0) = C \frac{(1 - 4s_1^2)^2(27 - 56s_1^2 + 48s_1^4)}{256s_1^2} \geq 0.$$

Using the solution formula for a cubic equation, we obtain that the cubic equation for T or Z has a unique real root given by

$$(B.40) \quad Z = r_1 - \frac{p}{3r_1}, \quad r_1 = \left(\frac{-q + \sqrt{q^2 + \frac{4}{27}p^3}}{2}\right)^{1/3}, \quad T = Z - \frac{s_1}{3},$$

where p, q are defined in (B.39).

We have the following basic properties for the map T and the threshold $f(s_2)$ (3.11).

Lemma B.4. *The map $T(s_1, s_2)$ is increasing in s_2 and decreasing in s_1 . Moreover, we have $f(s_2) \geq \frac{1}{2}$ and*

$$(B.41) \quad \begin{aligned} 4s_2^2 + 1 &\geq \max(4s_1 T(s_1, s_2), 1), \quad T^2 + Ts_1 + s_1^2 + 2s_2^2 \geq \frac{3}{4}, \quad \text{for } s_1 \geq 0, \\ |T(s_1, s_2) - s_1| &\leq \max_{x \in [f(s_2), s_1]} (|T_x(x, s_2)| + 1)|s_1 - \frac{1}{2}|, \quad s_1 \geq f(s_2). \end{aligned}$$

Proof. The estimate $f(s_1) \geq \frac{1}{2}$ follows from (3.11). Denote $P = 4s_1 T, Q = 4s_2^2 + 1$. Using (B.37), we get

$$\begin{aligned} Q^2 &= (4s_2^2 + 1)^2 = 16Ts_1(T^2 + Ts_1 + s_1^2) + 32s_2^2s_1T - 8Ts_1 \\ &\geq 16Ts_1 \cdot 3Ts_1 + 2(Q - 1)P - 2P = 3P^2 + 2PQ - 4P. \end{aligned}$$

If $P \leq 1$, we derive $Q \geq 1 \geq P$. If $P > 1$, solving the quadratic equation in Q , we yield

$$Q \geq P + \sqrt{4P^2 - 4P}, \quad \text{or } Q \leq P - \sqrt{4P^2 - 4P}.$$

Note that for $P > 1$, we have $P - \sqrt{4P^2 - 4P} < 1$. Thus, we must have

$$Q \geq P + \sqrt{4P^2 - 4P} \geq P.$$

It follows the first inequality in (B.41). Using (B.37) again, we derive

$$T^2 + Ts_1 + s_1^2 + 2s_2^2 = \frac{1}{16Ts_1}(8Ts_1 + (4s_2^2 + 1)^2) \geq \frac{1}{16Ts_1}(8Ts_1 + 4Ts_1) = \frac{3}{4},$$

where we have used the first inequality in (B.41) that we just proved.

The last inequality follows directly from $f(s_2) \geq \frac{1}{2}$ and the mean value theorem.

Since (B.37) is symmetric in T and s_1 , and its has a unique positive real root for any $s_1 > 0$, we get $T(T(s_1, s_2), s_2) = s_1$, or $T \circ T = Id$. Using (3.14), we get

$$K(s_1, s_2) = T_x(s_1, s_2)K(T(s_1, s_2), s_2).$$

Since $K(s_1, s_2)$ and $K(T(s_1, s_2), s_2)$ has opposite sign, it follows $T_x \leq 0$.

Taking s_2 derivative on both sides of (B.38), we yield

$$\frac{dT}{ds_2}(3T^2 + 2Ts_1 + s_1^2 - \frac{1}{2} + 2s_2^2) + s_2(4T - \frac{(4s_2^2 + 1)^2}{s_1}) = 0.$$

Using the first and the second inequality in (B.41), we prove $\frac{dT}{ds_2} \geq 0$. \square

B.4. Some functions related to the computation of the sharp constant. Here, we list some functions that will be used to compute the sharp constant. Recall

$$K_1 = \frac{y_1 y_2}{|y|^4}, \quad K_2 = \frac{1}{2} \frac{y_1^2 - y_2^2}{|y|^4}.$$

B.4.1. Sign functions. Solving $K_1(y_1 + 1/2, y_2) - K_1(y_1 - 1/2, y_2) = 0$ for $y_1 \geq 0$, we yield

$$y_1 = \left(\frac{1/2 - 2y_2^2 + \sqrt{16y_2^4 + 4y_2^2 + 1}}{6} \right)^{1/2}.$$

See also (3.11).

Solving $K_2(y_1 + 1, y_2) - K_2(y_1 - 1, y_2) = 0$ for $y_2 \geq 0$, we yield

$$(B.42) \quad \begin{aligned} y_1 &= h_c^\pm(y_2) \triangleq \left(y_2^2 + 1 \pm 2y_2 \sqrt{y_2^2 + 1} \right)^{1/2}, \\ y_2 &= s_c(y_1) \triangleq \left(\frac{-(y_1^2 + 1) + 2(y_1^4 - y_1^2 + 1)^{1/2}}{3} \right)^{1/2}. \end{aligned}$$

B.4.2. Transportation maps.

Map for u_x . For a fixed s_2 , solving

$$\int_{T(s)}^{s_1} (K_1(s_1 + 1/2, s_2) - K_1(s_1 - 1/2, s_2)) ds_1 = 0,$$

yields

$$(B.43) \quad T^3 + T^2 s_1 + T(s_1^2 - \frac{1}{2} + 2s_2^2) - \frac{(4s_2^2 + 1)^2}{16s_1} = 0,$$

or equivalently

$$Z^3 + Z(\frac{2}{3}s_1^2 - \frac{1}{2} + 2s_2^2) - \left(\frac{(4s_2^2 + 1)^2}{16s_1} + \frac{7}{27}s_1^3 + \frac{s_1}{3}(2s_2^2 - \frac{1}{2}) \right) = 0,$$

for $Z = T + \frac{s_1}{3}$. It has a unique real root that can be obtained explicitly. See (B.37)-(B.39).

Map for $[u_y]_{C_x^{1/2}}$. For fixed $y_1 \geq 0$, solving

$$\int_{T(y)}^{y_2} (K_2(y_1 + 1, y_2) - K_2(y_1 - 1, y_2)) dy_2 = 0,$$

yields

$$(B.44) \quad T^3 + T^2 y_2 + T(y_2^2 + 2 + 2y_1^2) - \frac{(y_1^2 - 1)^2}{y_2} = 0,$$

or equivalently

$$W^3 + W(\frac{2y_2^2}{3} + 2 + 2y_1^2) - \left(\frac{(y_1^2 - 1)^2}{y_2} + \frac{y_2^3}{27} + \frac{y_2}{3}(\frac{2y_2^2}{3} + 2 + 2y_1) \right) = 0,$$

where $W = T + \frac{y_2}{3}$. It has a unique real root that can be obtained explicitly.

Map for $[u_y]_{C_y^{1/2}}$. For fixed $y_1, y_2 \geq 0$, solving

$$\int_{T(y)}^{y_2} (K_2(y_1 + 1, y_2) - K_2(y_1 - 1, y_2)) dy_1 = 0,$$

yields

$$1 - T^2 - y_1^2 + T^2 y_1^2 - 2y_2^2 - T^2 y_2^2 - y_1^2 y_2^2 - 3y_2^4 = 0,$$

or equivalently

$$(B.45) \quad T^2 = \frac{y_1^2 + 2y_2^2 + y_1^2 y_2^2 + 3y_2^4 - 1}{y_1^2 - y_2^2 - 1}.$$

We remark that we apply the above map to two regions

$$y_1 \in [0, 1], \quad y_1 \leq h_{c-}(y_2), \quad y_1 \in [1, \infty], \quad y_1 \geq h_{c+}(y_2)$$

separately.

B.5. Some Lemmas for the computation of the constants. We have the following Lemma to estimate the integral near the singular region.

Lemma B.5. *For $0 \leq a < b$ and $f \in C_y^{1/2}([a, b] \times [0, \infty])$, we have*

$$\left| \int_a^b \int_0^\infty K_2(y) f(y) dy \right| \leq |b^{1/2} - a^{1/2}| \int_1^\infty \frac{s^2 - 1}{(s^2 + 1)^2} |s - \frac{1}{s}|^{1/2} ds [f]_{C_y^{1/2}}.$$

Proof. For fixed y_1 , note that $K_2(y) > 0$ if $y_2 < y_1$, $K_2(y) < 0$ if $y_2 > y_1$ and

$$\int_{y_1^2/y_2^2}^{y_2} K_2(y_1, s) ds = 0.$$

Applying Lemma 3.6 in the y_2 direction, we obtain

$$I \triangleq \left| \int_a^b \int_0^\infty K_2(y) f(y) dy \right| \leq \int_a^b \int_{y_1}^\infty |K_2(y)| |y_2 - \frac{y_1^2}{y_2}|^{1/2} dy [f]_{C_y^{1/2}}.$$

Using change of variable $y_2 = sy_1$, $K_2(y_1, y_2) = y_1^{-2} K_2(1, s)$, we prove

$$I \leq \int_a^b y_1^{1/2} \int_1^\infty |K_2(1, s)| |s - s^{-1}|^{1/2} ds [f]_{C_y^{1/2}} = |b^{1/2} - a^{1/2}| \int_1^\infty \frac{s^2 - 1}{(s^2 + 1)^2} |s - s^{-1}|^{1/2} ds [f]_{C_y^{1/2}}.$$

□

APPENDIX C. WEIGHTS AND PARAMETERS

C.1. Parameters for the weights. In our energy estimates and the estimate of the nonlocal terms, we need various weights. For the Hölder estimates, we use the following weights

$$(C.1) \quad \begin{aligned} \psi_1 &= |x|^{-2} + 0.6|x|^{-1} + 0.3|x|^{-1/6}, \\ \psi_2 &= p_{2,1}|x|^{-5/2} + p_{2,2}|x|^{-1} + p_{2,3}|x|^{-1/2} + p_{2,4}|x|^{1/6}, \\ \psi_3 &= \psi_2, \quad \vec{p}_{2,.} = (0.46, 0.245, 0.3, 0.112) \\ g_i(h) &= g_{i0}(h)g_{i0}(1, 0)^{-1}, \quad g_{i0}(h) = (\sqrt{h_1 + q_{i2}h_2} + q_{i3}\sqrt{h_2 + q_{i4}h_1})^{-1}, \\ \vec{q}_1 &= (0.12, 0.01, 0.25), \quad \vec{q}_2 = (0.14, 0.005, 0.27), \quad \vec{q}_3 = \vec{q}_{2,.}. \end{aligned}$$

For the weighted L^∞ estimates with decaying weights, we use the following weights

$$(C.2) \quad \begin{aligned} \varphi_1 &= x^{-1/2}(|x|^{-2.4} + 0.6|x|^{-1/2}) + 0.3|x|^{-1/6}, \\ \varphi_2 &= x^{-1/2}(p_{5,1}|x|^{-5/2} + p_{5,2}|x|^{-3/2} + p_{5,3}|x|^{-1/6}) + p_{5,4}|x|^{-1/4} + p_{5,5}|x|^{1/7}, \\ \varphi_3 &= x^{-1/2}(p_{6,1}|x|^{-5/2} + p_{6,2}|x|^{-3/2} + p_{6,3}|x|^{-1/6}) + p_{6,4}|x|^{-1/4} + p_{6,5}|x|^{1/7}, \\ p_{5,.} &= (0.3851, 0.1238, 0.1981, 0.1669, 0.0328), \\ p_{6,.} &= (0.9628, 0.3590, 0.6170, 0.3021, 0.0890). \end{aligned}$$

For the weighted L^∞ estimates with the growing weights, we use the following weights

$$(C.3) \quad \begin{aligned} \varphi_{g1} &= \varphi_1 + p_{71}|x|^{1/16}, \quad \varphi_{g2} = \varphi_2 + p_{81}|x|^{1/4}, \\ \varphi_{g3} &= (p_{31}|x|^{-5/2} + p_{32}|x|^{-3/2} + p_{33}|x|^{-1/6})x^{-1/2} + p_{34}|x|^{-1/4} + p_{91}|x|^{1/7} + p_{92}|x|^{1/4}, \\ p_{71} &= 1, \quad p_{81} = 0.071, \quad p_{9,1} = 0.1046, \quad p_{9,2} = 0.1540. \end{aligned}$$

Parameters in the energy. We choose the following parameters in our energy (4.21), (4.25)

$$(C.4) \quad \tau_1 = 5, \quad \mu_1 = 0.668, \quad \mu_2 = 1.336, \quad \mu_4 = 0.065, \quad \tau_2 = 0.24.$$

C.2. Parameters for approximating the velocity. We choose the following parameters x_i, t_i in the first approximation of velocity u, u_x in (2.82), (2.89) in Section 2.11,

$$\begin{aligned} u_x : x &= (1, 2, 3, 4, 6, 8, 11, 16, 22, 32, 48) \cdot 64h_x, \quad t = (16, 16, 20, 24, 32, 40, 56, 72, 96, 128, 256)h, \\ u : x &= (1, 2, 4, 8, 12, 16, 22, 32, 64) \cdot 64h_x, \quad t = (8, 8, 24, 40, 56, 72, 96, 128, 256)h, \end{aligned}$$

where h_x, h are chosen in (7.11).

For u, v, u_x , we need the second approximation (2.88). We choose the following parameters R_i in (2.88)

$$R = (8, 16, 32, 64, 128, 256, 512, 1024) \cdot 64h_x.$$

C.3. Estimate of the weights. In our energy estimates and the estimate of the nonlocal terms, we need various estimates of the weights and their derivatives. From (C.1), (C.2), (C.3), we have two types of weights. The first one is the radial weights

$$\rho(x, y) = \sum_i p_i r^{a_i}, \quad r = (x^2 + y^2)^{1/2},$$

where a_i is increasing and $p_i \geq 0$. We use these weights for the Hölder estimate. See e.g. (C.1).

The second type of weights is the following

$$\rho(x, y) = \rho_1(r)x^{-\alpha} + \rho_2(r),$$

where ρ_1, ρ_2 are the radial weights.

We use f_l, f_u to denote the lower and upper bound of f . We have the following simple inequalities

$$(C.5) \quad \begin{aligned} (f - g)_l &= f_l - g_u, \quad (f - g)_u = f_u - g_l, \quad (f + g)_\gamma = f_\gamma + g_\gamma, \\ (fg)_l &= \min(f_l g_l, f_u g_l, f_l g_u, f_u g_u), \quad (fg)_u = \max(f_l g_l, f_u g_l, f_l g_u, f_u g_u). \end{aligned}$$

where $\gamma = l, u$. If $g \geq 0$, we can simplify the formula for the product

$$(C.6) \quad (fg)_l = \min(f_l g_l, f_l g_u), \quad (fg)_u = \max(f_u g_l, f_u g_u).$$

C.4. Radial weights. The advantages of radial weights are that we can estimate them easily.

C.4.1. Bounds for the derivatives. We can easily derive the derivatives and their upper and lower bound as follows. Firstly, we have

$$(\partial_x^i \partial_y^j \rho(x, y))_\gamma = \sum_{1 \leq k \leq n} p_k (\partial_x^i \partial_y^j r^{a_k})_\gamma,$$

where $\gamma = l, u$. Using induction, we any α, i, j , we can obtain

$$\partial_x^i \partial_y^j r^\alpha = \sum_{k \leq i, l \leq \min(j, 1)} C_{i,j,k,l}(\alpha) x^k y^l r^{\alpha-i-j-k-l} = \sum_{k \leq i, l \leq \min(j, 1)} (C_{i,j,k,l}^+(\alpha) - C_{i,j,k,l}^-(\alpha)) x^k y^l r^{\alpha-i-j-k-l}.$$

The bounds for $C_{i,j,k,l}^\pm(\alpha) x^k y^l r^{\alpha-i-j-k-l}$ are simple:

$$(C_{i,j,k,l}^\pm(\alpha) x^k y^l r^{\alpha-i-j-k-l})_\gamma = C_{i,j,k,l}^\pm(\alpha) x_\gamma^k y_\gamma^l r_\gamma^{\alpha-i-j-k-l}.$$

Using (C.5), the above identities, and linearity, we can obtain the upper and lower bounds for $\partial_x^i \partial_y^j \rho$.

C.4.2. *Leading order behavior of $\partial\rho/\rho$.* In our verification, we need to bound $\partial\rho(\lambda x)/\rho(\lambda x)$ as $\lambda \rightarrow 0$ or $\lambda \rightarrow \infty$ uniformly. A direct calculation yields

$$\frac{\partial_{x_i}\rho}{\rho} = \frac{x_i}{|x|^2} \frac{\sum_i p_i a_i r^{a_i}}{\sum_i p_i r^{a_i}} \triangleq \frac{x_i}{|x|^2} S(x), \quad S(x) \triangleq \frac{\sum_i p_i a_i r^{a_i}}{\sum_i p_i r^{a_i}}.$$

For x close to 0, we introduce $b = a - a_1$. Clearly, we get $b_i \geq 0$ and

$$S(x) = a_1 + \frac{\sum_i p_i b_i r^{a_i}}{\sum_i p_i r^{a_i}} = a_1 + \frac{\sum_i p_i b_i r^{b_i}}{\sum_i p_i r^{b_i}} \triangleq a_1 + \frac{A(r)}{B(r)}.$$

Using $b_i \geq 0$ and the Cauchy-Schwarz inequalities, we yield

$$(C.7) \quad A'B - AB' = r^{-1} \left(\left(\sum p_i b_i^2 r^{b_i} \right) \left(\sum p_i r^{b_i} \right) - \left(\sum p_i b_i r^{b_i} \right)^2 \right) = r^{-1} \frac{1}{2} \sum_{ij} p_i p_j (b_i - b_j)^2 r^{b_i + b_j} \geq 0,$$

which implies that A/B is increasing. Thus for $\lambda \leq \lambda_*$, $r \in [r_l, r_u]$, we get the uniform bound for $S(\lambda x)$

$$a_1 \leq S(\lambda x) \leq a_1 + \frac{A(\lambda_* r_u)}{B(\lambda_* r_u)}.$$

For $\lambda = 1$, we simply obtain

$$a_1 + \frac{A(r_l)}{B(r_l)} \leq S(x) \leq a_1 + \frac{A(r_u)}{B(r_u)}.$$

Similarly, for $\lambda \geq \lambda_*$, $r \in [r_l, r_u]$, we get

$$a_n + \frac{A(\lambda_* r_l)}{B(\lambda_* r_l)} \leq S(\lambda x) \leq a_n, \quad \frac{A(r)}{B(r)} = \frac{\sum_i p_i b_i r^{b_i}}{\sum_i p_i r^{b_i}},$$

where $b = a - a_n \leq 0$. Here, we have used that $A(r)/B(r)$ is decreasing.

From the above estimates, we yield

$$\begin{aligned} \lim_{\lambda \rightarrow 0} \frac{\partial_{x_i}\rho}{\rho} &= \frac{x_i}{|x|^2} a_1 \triangleq R_0(x), \quad \left| \frac{\partial_{x_i}\rho}{\rho}(\lambda x) - R_0(\lambda x) \right| \leq \lambda^{-1} \frac{x_i}{|x|^2} \frac{|A(\lambda_* x)|}{|B(\lambda_* x)|}, \quad \lambda \leq \lambda_*, \\ \lim_{\lambda \rightarrow 0} \frac{\partial_{x_i}\rho}{\rho} &= \frac{x_i}{|x|^2} a_n \triangleq R_\infty(x), \quad \left| \frac{\partial_{x_i}\rho}{\rho}(\lambda x) - R_\infty(\lambda x) \right| \leq \lambda^{-1} \frac{x_i}{|x|^2} \frac{|A(\lambda_* x)|}{|B(\lambda_* x)|}, \quad \lambda \geq \lambda_*. \end{aligned}$$

Using (C.7), we can estimate the Lipschitz coefficient of S

$$\frac{|S(\lambda x) - S(\lambda z)|}{||x| - |z||} \leq \max_{r \in [|x|, |z|]} \left| \partial_r \frac{A(\lambda r)}{B(\lambda r)} \right| \leq \frac{\frac{1}{2} \sum_{ij} p_i p_j (b_i - b_j)^2 r^{b_i + b_j - 1} \lambda^{b_i + b_j}}{B_l(\lambda r)^2}$$

Note that we have $b_i \geq 0$ for $\lambda \rightarrow 0$ and $b_i \leq 0$ for $\lambda \rightarrow \infty$. We can derive the upper and lower bounds for the denominator and the numerator.

We use the above estimates to bound the integrals for $\partial_x(\partial^2 \psi \rho)$, where ψ is the stream functions.

C.4.3. *Bounds for the derivatives of $1/\rho$.* The bounds for $d_x^i d_y^j \rho^{-1}$ is more complicated since ρ^{-1} is not linear in the summand $p_i r^{a_i}$. We need such estimates in the estimate of the velocity. Firstly, using the bounds in Section C.4.1 and (C.6), we can obtain the upper and the lower bounds for R_{ij}

$$R_{ij} = \frac{\partial_x^i \partial_y^j \rho}{\rho}.$$

For $i + j = 1$ and $k = 2, 3$, we use the estimate in Section C.4.1 to obtain the bounds for

$$R_{10} = \frac{x}{|x|^2} S(x), \quad R_{0,1} = \frac{y}{|x|^2} S(x), \quad (R_{ij})^k.$$

In our verification, we need $\partial_x^i \partial_y^j \rho^{-1}$ for $i + j \leq 3$. A direct calculation yields

$$\begin{aligned}\partial_x \rho^{-1} &= -\frac{\rho_x}{\rho^2} = -\frac{R_{10}}{\rho}, \quad \partial_{xx} \rho^{-1} = -\frac{\rho_{xx}}{\rho^2} + 2\frac{\rho_x^2}{\rho^3} = \rho^{-1}(-R_{20} + 2R_{10}^2), \\ \partial_{xy} \rho^{-1} &= -\frac{\rho_{xy}}{\rho} + \frac{2\rho_x \rho_y}{\rho^3} = \rho^{-1}(-R_{11} + 2R_{10}R_{01}), \\ \partial_{xxx} \rho^{-1} &= -\frac{\rho_{xxx}}{\rho^2} + \frac{6\rho_{xx} \rho_x}{\rho^3} - \frac{6\rho_x^3}{\rho^4} = \rho^{-1}(-R_{30} + 6R_{20}R_{10} - 6R_{10}^3), \\ \partial_{xxy} \rho^{-1} &= -\frac{\rho_{xxy}}{\rho^2} + \frac{2\rho_{xx} \rho_y}{\rho^3} + \frac{4\rho_x \rho_{xy}}{\rho^3} = \rho^{-1}(-R_{21} + 2R_{20}R_{01} + 4R_{10}R_{11} - 6R_{10}^2R_{01}).\end{aligned}$$

Next, we estimate the $\partial_x^i \partial_y^j (\partial_{x_i} \rho / \rho)$ for $i \leq 2, j = 0$ or $i = 0, j \leq 2$. Denote $f = \partial_{x_i} \rho$. Using a direct computation, for $D_2 = \partial_x^{i_2} \partial_y^{j_2}$ with $i_2 + j_2 = 1$, we yield

$$D_2 \frac{f}{\rho} = \frac{D_2 f}{\rho} - \frac{f D_2 \rho}{\rho^2} = \rho^{-1} (D_2 f - f R_{i_2, j_2}).$$

For $(i_2, j_2) = (2, 0), (0, 2)$, denote $i_3 = i_2/2, j_3 = j_2/2, D_3 = \partial_x^{i_3} \partial_y^{j_3}$.

We yield

$$\begin{aligned}D_3^2 \frac{f}{\rho} &= \frac{D_3^2 f}{\rho} - \frac{2D_3 f \cdot D_3 \rho}{\rho^2} + f D_3^2 \left(\frac{1}{\rho}\right) = \frac{D_3^2 f}{\rho} - \frac{2D_3 f \cdot D_3 \rho}{\rho^2} + f \left(-\frac{D_3^2 \rho}{\rho^2} + \frac{2(D_3 \rho)^2}{\rho^3}\right) \\ &= \rho^{-1} (D_3^2 f - 2D_3 f R_{i_3, j_3} - f R_{i_2, j_2} + 2f R_{i_3, j_3}^2).\end{aligned}$$

where we have used $D_3^2 \frac{1}{\rho} = D_3 \left(-\frac{D_3 \rho}{\rho^2}\right) = -\frac{D_3^2 \rho}{\rho^2} + \frac{2(D_3 \rho)^2}{\rho^3}$.

Since we have estimated $\partial_x^i \partial_y^j \rho$ and R_{ij} , we can bound these derivatives of $D_1 \rho / \rho$ using (C.5).

C.4.4. Improved estimates for ρ^{-1} near $x = 0$. For the special case $a_1 = -2$, we can write

$$\rho(x) = r^{-2} \sum_i p_i r^{a_i+2} = r^{-2} \tilde{\rho}(x), \quad \rho^{-1} = (x^2 + y^2) \tilde{\rho}(x)^{-1}$$

To obtain better estimate of ρ^{-1} , we use the fact that $x^2 + y^2$ is a polynomial. Firstly, we can obtain the bounds for $\partial_x^i \partial_y^j \tilde{\rho}^{-1}$. The bounds for $S_0 = x^2 + y^2$ is trivial, e.g.,

$$(\partial_x S_0)_\gamma = 2x_\gamma, \quad \partial_{xy} S_0 = 0, \quad \partial_{xx} S_0 = \partial_{yy} S_0 = 2.$$

Then using (C.5)-(C.6), we can bound ρ^{-1} .

C.5. The mixed weight. For the second type of weights $W = \rho_1(r)x^{-1/2} + \rho_2(r)$, we can compute its derivatives and its upper and lower bounds using linearity and the Leibniz rule. For example, we have

$$W_l = \rho_{1,l} x_u^{-1/2} + \rho_{2,l}, \quad (W^{-1})_u = (W_l)^{-1}, \quad W_x = \partial_x \rho_1 x^{-1/2} - \frac{1}{2} \rho_1 x^{-3/2} + \partial_x \rho_2.$$

To obtain the upper bound for $\partial_x^i \partial_y^j W$, we use the Leibniz rule:

$$|\partial_x^i \partial_y^j W| \leq \sum_{k \leq i} \binom{i}{k} |\partial_x^{i-k} \partial_y^j \rho_1| \frac{(2k-1)!!}{2^k} x^{-1/2-k} + |\partial_x^i \partial_y^j \rho_2|.$$

We need to bound $\rho(r)/W(x, y)$ in the estimate of the integrals. Suppose that the leading and the last powers of ρ is a_1, a_n . The leading and the last terms of W are given by $p_i r^{b_i} \cos(\beta)^{-\alpha_i}, \alpha_i \geq 0$.

$$W \geq p_1 r^{b_1}, \quad W \geq p_n r^{b_n}.$$

We estimate

$$\frac{\rho}{W} \leq C_1 r^{a_1 - b_1}, \quad \frac{\rho}{W} \leq C_2 r^{a_n - b_n},$$

for all $x, y \in \mathbb{R}_2^+$. We apply the above estimates for x near 0 or x sufficiently large.

APPENDIX D. ESTIMATE THE DERIVATIVES OF THE VELOCITY KERNEL AND INTEGRANDS

In this appendix, we estimate the derivatives of the kernel $-\frac{1}{2\pi} \log |x|$ associated to the velocity $\mathbf{u} = \nabla^\perp(-\Delta)^{-1}\omega$ and its symmetrization (3.2). These estimates are used to estimate the error terms in Lemmas 7.2, 7.4. We will perform an additional estimate for the u with weight $\varphi(x)$ singular along $x_1 = 0$ in Section D.4. Some additional derivations related to the estimate of the velocity are given in Appendix D.5.

D.1. Estimate the symmetrized kernel. In this section, we estimate the symmetrized kernel. We develop several symmetrized estimates for harmonic functions. Before we introduce the estimates, we have a simple 1D estimate, which is useful for later estimates.

Lemma D.1. *We have*

$$|f(x) + f(-x) - 2f(0)| \leq x^2 \|f_{xx}\|_{L^\infty[-x,x]}, \quad |f(x) + f(-x) - 2f(0) - x^2 f_{xx}(0)| \leq \frac{x^4}{12} \|\partial_x^4 f\|_{L^\infty[-x,x]},$$

Proof. Denote $G(x) = f(x) + f(-x)$. Clearly, G is even and

$$(D.1) \quad G(0) = 2f(0), \quad G'(0) = 0, \quad \partial_x^2 G(0) = 2f_{xx}(0), \quad \partial_x^3 G(0) = 0.$$

Using Taylor expansion, we obtain

$$G(x) = G(0) + G'(0)x + \frac{\partial_x^2 G(0)x^2}{2} + \frac{\partial_x^3 G(0)x^3}{6} + \frac{\partial_x^4 G(\xi)x^4}{24}$$

for some $\xi \in [0, x]$. Using (D.1), we get

$$|G(x) - G(0) - G''(x)\frac{x^2}{2}| \leq \|\partial_x^4 G\|_{L^\infty[0,x]} \frac{x^4}{24} \leq \|\partial_x^2 f\|_{L^\infty[-x,x]} \frac{x^4}{12}.$$

Plugging the identity (D.1) into the above estimate proves the second estimate in Lemma D.1. The first estimate is simpler. \square

The following lemma is useful for estimating the symmetrized kernel (3.2) and its derivatives.

Lemma D.2. *Suppose that $Q_x = [-x_1, x_1] \times [-x_2, x_2]$ and $f \in C^4(Q_x)$ is harmonic. Denote*

$$(D.2) \quad \begin{aligned} G_1(1, x) &\triangleq f(x_1, x_2) + f(-x_1, x_2) + f(x_1, -x_2) + f(-x_1, -x_2) - 4f(0, 0), \\ G_2(1, x) &\triangleq f(x_1, x_2) - f(-x_1, x_2) - f(x_1, -x_2) + f(-x_1, -x_2), \\ \hat{G}_1(x) &\triangleq 2x_1^2 f_{xx}(0, 0) + 2x_2^2 f_{yy}(0, 0), \quad \hat{G}_2(x) \triangleq 4x_1 x_2 f_{xy}(0, 0). \end{aligned}$$

We have

$$(D.3) \quad |G_1(1, x)| \leq 2|x|^2 \|f_{xx}\|_{L^\infty(Q_x)}, \quad |\partial_{x_i} G_1(1, x)| \leq 4|x_i| \cdot \|f_{xx}\|_{L^\infty(Q_x)},$$

$$(D.4) \quad |G_1(1, x) - \hat{G}_1(x)| \leq \frac{(x_1^4 + 6x_1^2 x_2^2 + x_2^4)}{6} \|\partial^4 f\|_{L^\infty(Q_x)} \leq \frac{|x|^4}{3} \|\partial^4 f\|_{L^\infty(Q_x)}$$

$$(D.5) \quad |G_1(1, x_1, 0) - \hat{G}_1(x_1, 0)| \leq \frac{1}{6} x_1^4 \|\partial^4 f\|_{L^\infty(Q_x)},$$

$$(D.6) \quad |\partial_{x_i}(G_1(1, x) - \hat{G}_1(x))| \leq \frac{2}{3} (3x_{3-i}^2 x_i + x_i^3) \|\partial^4 f\|_{L^\infty(Q_x)} \leq \frac{2\sqrt{2}}{3} |x|^3 \|\partial^4 f\|_{L^\infty(Q_x)},$$

where $\|\partial^4 f\|_{L^\infty} = \max_{0 \leq i \leq 4} \|\partial_x^i \partial_y^j f\|_{L^\infty(Q_x)}$. For G_2 , we have the following estimate

$$(D.7) \quad |G_2(1, x)| \leq 4x_1 x_2 \|f_{xy}\|_{L^\infty(Q_x)}, \quad |\partial_{x_i} G_2(1, x)| \leq 4|x_{3-i}| \cdot \|f_{xy}\|_{L^\infty(Q_x)},$$

$$(D.8) \quad |G_2(1, x) - \hat{G}_2(x)| \leq \frac{2x_1 x_2 |x|^2}{3} \|\partial^4 f\|_{L^\infty(Q_x)},$$

$$(D.9) \quad |\partial_{x_i}(G_2(1, x) - \hat{G}_2(x))| \leq \frac{2}{3} (3x_i^2 x_{3-i} + x_{3-i}^3) \|\partial^4 f\|_{L^\infty(Q_x)} \leq \frac{2\sqrt{2}}{3} |x|^3 \|\partial^4 f\|_{L^\infty(Q_x)}.$$

Proof. Recall $Q_x = [-x_1, x_1] \times [-x_2, x_2]$. Denote

$$M_{ij}(x) = \|\partial_x^i \partial_y^j f\|_{L^\infty(Q_x)}.$$

Using Lemma D.1, for any $t \in [0, 1]$, we obtain

$$|f(tx_1, x_2) + f(tx_1, -x_2) - 2f(tx_1, 0)| \leq M_{02} x_2^2, \quad |f(x_1, 0) + f(-x_1, 0) - 2f(0, 0)| \leq M_{20} x_1^2,$$

Since f is harmonic function, we have $\partial_x^{i+2}\partial_y^j f = -\partial_x^i\partial_y^{j+2} f$ and obtain $A_{i+2,j} = A_{i,j+2}$. Taking $t = \pm 1$ in the above estimate and using triangle inequality, we prove

$$|G(1, x)| \leq 2A_{20}(x)x_1^2 + 2A_{02}x_2^2 = 2A_{20}(x_1^2 + x_2^2) = 2A_{20}|x|^2,$$

which is the first estimate in (D.3).

The second estimate in (D.3) is simple. We consider $i = 1$ without loss of generality. We get $|\partial_{x_1}G_1(1, x)| = |(\partial_1 f)(x_1, x_2) - (\partial_1 f)(-x_1, x_2) + (\partial_1 f)(x_1, -x_2) - (\partial_1 f)(-x_1, -x_2)| \leq 4x_1 A_{20}(x)$.

For (D.4), using Lemma D.1, we yield

$$\begin{aligned} |f(tx_1, x_2) + f(tx_1, -x_2) - 2f(tx_1, 0) - x_2^2(\partial_2^2 f)(tx_1, 0)| &\leq A_{04}(x) \frac{x_2^4}{12} \\ (D.10) \quad |\partial_2^2 f(x_1, 0) + \partial_2^2 f(-x_1, 0) - 2\partial_2^2 f(0, 0)| &\leq x_1^2 A_{2,2}(x), \\ |f(x_1, 0) + f(-x_1, 0) - 2f(0) - x_1^2 \partial_1^2 f(0)| &\leq A_{40} \frac{x_1^4}{12}. \end{aligned}$$

for $t = \pm 1$. Combining the above estimates and using the triangle inequality and $A_{40} = A_{22} = A_{04}$, we prove the first estimate in (D.4). The second estimate follows from $2|x|^4 - x_1^4 - 6x_1^2 x_2^2 - x_2^4 = (x_1^2 - x_2^2)^2 \geq 0$.

Estimate (D.5) follows from (D.4) by taking $x_2 = 0$.

For (D.6), we consider the estimate of ∂_{x_1} . The other case is similar. Using

$$\partial_1 f(x_1, s) - (\partial_1 f)(-x_1, s) = \int_0^{x_1} (\partial_1^2 f)(t, s) + (\partial_1^2 f)(-t, s) dt,$$

we obtain

$$\begin{aligned} \partial_1(G(1, x) - \hat{G}_1(x)) &= \partial_1 f(x_1, x_2) - (\partial_1 f)(-x_1, x_2) + \partial_1 f(x_1, -x_2) - (\partial_1 f)(-x_1, -x_2) - 4x_1 \partial_1^2 f(0) \\ &= \int_0^{x_1} \left((\partial_1^2 f)(z, x_2) + (\partial_1^2 f)(-z, x_2) + \partial_1^2 f(z, -x_2) + (\partial_1^2 f)(-z, -x_2) - 4\partial_1^2 f(0) \right) dz. \end{aligned}$$

Applying (D.3), we yield

$$|\partial_1(G(1, x) - \hat{G}_1(x))| \leq \int_0^{x_1} 2(z^2 + x_2^2) dz A_{4,0}(x) = \left(\frac{2}{3} x_1^3 + 2x_1 x_2^2 \right) A_{4,0}(x),$$

and complete the proof of the first estimate in (D.6). For the second estimate, we use the AM-GM inequality to yield

$$(D.11) \quad (3x_2^2 x_1 + x_1^3)^2 = (3x_2^2 + x_1^2)^2 x_1^2 = \frac{1}{4} (3x_2^2 + x_1^2)^2 4x_1^2 \leq \frac{1}{4} \left(\frac{2(3x_2^2 + x_1^2) + 4x_1^2}{3} \right)^3 = 2|x|^4.$$

Taking a square root completes the estimate.

To estimate G_2 in (D.2), we rewrite it as follows

$$\begin{aligned} G_2(1, x) - c\hat{G}_2(x) &= \int_{-x_1}^{x_1} \int_{-x_2}^{x_2} \partial_{12} f(y_1, y_2) - c\partial_{12} f(0) dy \\ &= \int_0^{x_1} \int_0^{x_2} (\partial_{12} f)(y_1, y_2) + (\partial_{12} f)(-y_1, y_2) + (\partial_{12} f)(y_1, -y_2) + (\partial_{12} f)(-y_1, -y_2) - 4c(\partial_{12} f)(0) dy \end{aligned}$$

for $c = 0, 1$. The integrand has the same form as G_1 in (D.2). For $c = 0$, using the above decomposition, we prove

$$|G_2(1, x)| \leq 4x_1 x_2 A_{11}.$$

When $c = 1$, using (D.6), we yield

$$|G_2(1, x) - \hat{G}_2(x)| \leq A_{40} 2 \int_0^{x_1} \int_0^{x_2} |y|^2 dy = A_{40} \frac{2}{3} (x_1^3 x_2 + x_1 x_2^3) = A_{40} \frac{2}{3} x_1 x_2 |x|^2.$$

To estimate the derivatives, we focus on ∂_{x_1} . Using the above representation, we obtain

$$\partial_{x_1} G_2(1, x) - c\hat{G}_2(x) = \int_0^{x_2} (\partial_{12} f)(x_1, y_2) + (\partial_{12} f)(-x_1, y_2) + (\partial_{12} f)(x_1, -y_2) + (\partial_{12} f)(-x_1, -y_2) - 4c(\partial_{12} f)(0) dy.$$

We apply the same estimates to the integrands with $c = 0, 1$ and yield

$$|\partial_{x_1} G_2(1, x)| \leq 4x_2 A_{11}, \quad |G_2(1, x) - \hat{G}_2(x)| \leq A_{40} 2 \int_0^{x_2} (x_1^2 + y_2^2) dy_2 = A_{40} (2x_1^2 x_2 + \frac{2}{3} x_2^3).$$

The second inequality in (D.9) follows from (D.11). The above estimates imply (D.7)-(D.9). \square

Recall the kernels associated with $\nabla \mathbf{u}, \mathbf{u}$ in (3.1). These kernels are the derivatives of the Green function $-\frac{1}{2\pi} \log |x|$ and are harmonic away from 0. We have the following estimate for their derivatives.

Lemma D.3. *Denote $r = (x^2 + y^2)^{1/2}$ and $f(x, y) = \log r$. For any $i, j \geq 0$ with $i + j \geq 1$, we have*

$$|\partial_x^i \partial_y^j f(x, y)| \leq (i + j - 1)! \cdot r^{-i-j}.$$

As a result, for $K_1(y) = -\frac{1}{2} \partial_{12} f(y), K_2(y) = -\frac{1}{2} \partial_1^2 f(y)$, we have

$$|K_i| \leq \frac{1}{2|y|^2}, \quad |\partial_{y_1}^j \partial_{y_2}^{2-j} K_i| \leq \frac{3}{|y|^4}, \quad |\partial_{y_1}^j \partial_{y_2}^{4-j} K_i| \leq \frac{60}{|y|^6}, \quad |\partial_{y_1}^j \partial_{y_2}^{6-j} K_i| \leq \frac{2520}{|y|^8}.$$

Proof. Consider the polar coordinate $\beta = \arctan(y/x), r = (x^2 + y^2)^{1/2}$. We use induction on $n = i + j$ to prove

$$(D.12) \quad \partial_x^i \partial_y^j f = (n - 1)! \cos(n\beta - \beta_{ij}) r^{-n}$$

for some constant β_{ij} . Denote $\beta = \arctan \frac{y}{x}, r = \sqrt{x^2 + y^2}$. We have the formula

$$(D.13) \quad \partial_x g = (\cos \beta \partial_r - \frac{\sin \beta}{r} \partial_\beta) g, \quad \partial_y g = (\sin \beta \partial_r + \frac{\cos \beta}{r} \partial_\beta) g.$$

Firstly, for $n = 1$, a direct calculation yields

$$\partial_x f = \frac{x}{r^2} = \frac{\cos \beta}{r}, \quad \partial_y f = \frac{y}{r^2} = \frac{\sin \beta}{r} = \frac{\cos(\beta - \pi/2)}{r}.$$

Suppose that (D.12) holds for any i, j with $i + j = n$ and $n \geq 1$. Now, since

$$\begin{aligned} \partial_x \partial_x^i \partial_y^j f &= (n - 1)! \partial_x (\cos(n\beta - \beta_{ij}) r^{-n}) \\ &= (n - 1)! (-n \cos \beta \cos(n\beta - \beta_{ij}) r^{-n-1} + n \sin \beta \sin(n\beta - \beta_{ij}) r^{-n-1}) \\ &= n! (-\cos(n\beta - \beta_{ij} + \beta) r^{-n-1}) = n! \cos((n + 1)\beta - \beta_{ij} - \pi) r^{-n-1}. \end{aligned}$$

Using a similar computation and $\sin(x) = \cos(x - \pi/2)$, we can obtain that $\partial_y \partial_x^i \partial_y^j f$ has the form (D.12). Using induction, we prove (D.12). The desired estimate follows from (D.12). \square

Using the above two Lemmas, we can estimate the error in the discretization of the kernels $K(x, y)$ in both x and y direction.

Estimate the kernels in the far field. Recall the symmetrized kernel in (3.2). The integrals in u_x, u_y can be written as

$$u_x(x) = -\frac{1}{\pi} \int_{\mathbb{R}_2^{++}} K_{1,s}(x, y) \omega(y) dy, \quad u_y = \frac{1}{\pi} \int_{\mathbb{R}_2^{++}} K_{2,s}(x, y) \omega(y) dy.$$

Denote $Q_x = [-x_1, x_1] \times [-x_2, x_2]$ and

$$(D.14) \quad f(x_1, x_2) = K_1(x_1 - y_1, x_2 - y_2), \quad \text{Den}(x, y) = \min_{z \in Q_x} |y - z|^2.$$

It is not difficult to obtain that for $x, y \in \mathbb{R}_2^{++}$, we have

$$(D.15) \quad \text{Den}(x, y) = \sum_{i=1,2} \min_{|z_i| \leq x_i} |y_i - z_i|^2 = \sum_{i=1,2} (\max(y_i - x_i, 0))^2$$

Since $K_1(y_1, y_2)$ is odd in y_1, y_2 , we have $K_{1,s} = f(x_1, x_2) + f(-x_1, x_2) + f(x_1, -x_2) + f(-x_1, -x_2)$. A direct computation yields the following formulas

$$f(0, 0) = K_1(-y_1, -y_2) = \frac{y_1 y_2}{|y|^4}, \quad f_{xx}(0, 0) = \partial_{y_1^2} K_1(y) = \frac{12 y_1 y_2 (y_1^2 - y_2^2)}{|y|^8}.$$

Using the fact that K_1 is harmonic function and then applying Lemmas D.2 and D.3 with the above f , we obtain

$$\begin{aligned}
 |K_{1,s}(x, y) - \frac{4y_1 y_2}{|y|^4}| &\leq \frac{6|x|^2}{\text{Den}^2(x, y)}, \quad |\partial_{x_1} K_{1,s}(x, y)| \leq \frac{12x_1}{\text{Den}^2(x, y)}, \\
 |K_{1,s}(x, y) - \frac{4y_1 y_2}{|y|^4} - 2(x_1^2 - x_2^2)\partial_{y_1}^2 K_1(y)| &\leq \frac{10\sqrt{2}|x|^4}{\text{Den}^3(x, y)}, \\
 |\partial_{x_1} \left(K_{1,s}(x, y) - \frac{4y_1 y_2}{|y|^4} - 2(x_1^2 - x_2^2)\partial_{y_1}^2 K_1(y) \right)| &\leq \frac{40\sqrt{2}|x|^3}{\text{Den}^3(x, y)}, \\
 |K_{1,s}(x_1, 0, y) - \frac{4y_1 y_2}{|y|^4} - 2x_1^2 \partial_{y_1}^2 K_1(y)| &\leq \frac{10x_1^4}{\text{Den}^3(x, y)}.
 \end{aligned} \tag{D.16}$$

We use the following two formulas to estimate the discretization error

$$\begin{aligned}
 \left| \partial_{y_i}^2 \left(K_{1,s}(x, y) - \frac{4y_1 y_2}{|y|^4} - 2(x_1^2 - x_2^2)\partial_{y_1}^2 K_1(y) \right) \right| &\leq \frac{\sqrt{2}}{6} |x|^4 |\partial_y^6 K| \leq \frac{\sqrt{2}}{6} \cdot \frac{2520|x|^4}{\text{Den}^4(x, y)}, \\
 \left| \partial_{x_i} \partial_{y_i}^2 \left(K_{1,s}(x, y) - \frac{4y_1 y_2}{|y|^4} - 2(x_1^2 - x_2^2)\partial_{y_1}^2 K_1(y) \right) \right| &\leq \frac{2\sqrt{2}}{3} |x|^3 |\partial_y^6 K| \leq \frac{2\sqrt{2}}{3} \cdot \frac{2520|x|^3}{\text{Den}^4(x, y)}.
 \end{aligned}$$

Similarly, we can obtain the following estimates for $K_{2,s}$

$$\begin{aligned}
 |K_{2,s}| &\leq \frac{12x_1 x_2}{\text{Den}^2(x, y)}, \quad |\partial_{x_i} K_{2,s}(x, y)| \leq \frac{12x_{3-i}}{\text{Den}^2(x, y)}, \\
 \left| K_{2,s} - 4x_1 x_2 \cdot \frac{12y_1 y_2 (y_1^2 - y_2^2)}{|y|^8} \right| &\leq \frac{40x_1 x_2 |x|^2}{\text{Den}^3(x, y)}, \\
 \left| \partial_{x_i} \left(K_{2,s} - 4x_1 x_2 \cdot \frac{12y_1 y_2 (y_1^2 - y_2^2)}{|y|^8} \right) \right| &\leq \frac{40\sqrt{2}|x|^3}{\text{Den}^3(x, y)}.
 \end{aligned} \tag{D.17}$$

The decay estimates of the symmetrized kernel for \mathbf{u} , $\frac{y_1}{|y|^2}$, $\frac{y_2}{|y|^2}$ can be established similarly.

D.2. Piecewise L^∞ estimate of derivatives of the Green function. In this section, we develop sharp L^∞ estimate of derivatives of the Green function $G(x) = -\frac{1}{2\pi} \log|x|$ and their linear combinations in a small domain $[a, b] \times [c, d]$. It will be used in Lemmas 7.2, 7.4 to estimate the error, especially near the singularity of the kernel. We remark that the linear combinations of $\partial_1^i \partial_2^j G$ can be quite complicated. If we simply use triangle inequality to estimate it, we can overestimate some terms with cancellation significantly, especially near the singularity of G . These sharp estimates are useful for reducing the estimate of the error term in Lemmas 7.2, 7.4 without choosing very small mesh, which can lead to large computational cost.

D.2.1. Coefficients of the derivatives of the Green function. To simplify the notation, we drop $\frac{1}{\pi}$ from G and denote $f_p = -\frac{1}{2} \log|x|$. Firstly, we derive the formulas of $\partial_1^i \partial_2^j f_p$. Due to homogeneity, we assume

$$\partial_{x_1}^k \partial_{x_2}^l f_p = \frac{\sum_{i+j=k+l} c_{ij} x_1^i x_2^j}{|x|^{2(k+l)}}.$$

Next, we derive the recursive formula for c_{ij} . Using induction, we can obtain

$$\begin{aligned}
 \partial_{x_1}^{k+1} \partial_{x_2}^l f_p &= \frac{\sum_{i+j=k+l} c_{ij} i x_1^{i+1} x_2^j}{|x|^{2(k+l)}} - \frac{2(k+l)x_1}{|x|^{2(k+l+1)}} \sum_{i+j=k+l} c_{ij} x_1^i x_2^j \\
 &= \frac{1}{|x|^{2(k+l+1)}} \left(\sum_{i+j=k+l} c_{ij} i x_1^{i+1} x_2^j + c_{ij} i x_1^{i-1} x_2^{j+2} - 2(k+l)c_{ij} x_1^{i+1} x_2^j \right) \\
 &= \frac{1}{|x|^{2(k+l+1)}} \left(\sum_{i+j=k+l} (c_{ij} i + c_{i+2,j-2}(i+2) - 2(k+l)c_{ij}) x_1^{i+1} x_2^j \right).
 \end{aligned}$$

Therefore, we obtain the recursive formula

$$c_{i+1,j} = ic_{ij} + (i+2)c_{i+2,j-2} - 2(k+l)c_{ij}$$

for all $i+j = k+l$, or equivalently,

$$c_{i,j} = (i-1)c_{i-1,j} - 2(k+l)c_{i-1,j} + (i+1)c_{i+1,j-2}$$

for all $i+j = k+l+1$. Similarly, for ∂_{x_2} , we yield

$$c_{i,j} = (j-1)c_{i,j-1} - 2(k+l)c_{i,j-1} + (j+1)c_{i-2,j+1}$$

for all $i+j = k+l+1$.

D.2.2. Estimates of rational functions. We use the above formulas to develop sharp estimates of the derivatives of f_p and their linear combinations in a small grid $[y_{1l}, y_{1u}] \times [y_{2l}, y_{2u}]$. For $k_1 < k_2$ and $S \subset \{(i, j) : i+j = k\}$, we estimate

$$I_S \triangleq \frac{\sum_{(i,j) \in S} c_{ij} y_1^i y_2^j}{|y|^{k_2}}.$$

Denote $i_1 = \min_{i \in S} i, j_1 = \min_{j \in S} j$. We yield

$$I_S = \frac{y_1^{i_1} y_2^{j_1}}{|y|^{i_1+j_1}} \frac{\sum_{(i,j) \in S} c_{ij} y_1^{i-i_1} y_2^{j-j_1}}{|y|^{k_2-i_1-j_1}}.$$

We further introduce

$$P \triangleq \sum_{(i,j) \in S} c_{ij}^+ y_1^{i-i_1} y_2^{j-j_1}, \quad Q \triangleq \sum_{(i,j) \in S} c_{ij}^- y_1^{i-i_1} y_2^{j-j_1}.$$

Clearly, P and Q are monotone increasing in $y_1 \geq 0$ and $y_2 \geq 0$. As a result, on $D = [y_{1l}, y_{1u}] \times [y_{2l}, y_{2u}] \subset \mathbb{R}_2^{++}$, we yield

$$\begin{aligned} |I| &\leq \frac{\max(P_u - Q_l, Q_u - P_l)}{|y|_l^{k_2-i_1-j_1}} \max_{y \in \Omega} \frac{y_1^{i_1} y_2^{j_1}}{|y|^{i_1+j_1}} \\ &= \frac{\max(P_u - Q_l, Q_u - P_l)}{|y|_l^{k_2-i_1-j_1}} \left(\frac{y_{1u}}{|y_{1u}^2 + y_{2l}^2|^{1/2}} \right)^{i_1} \left(\frac{y_{2u}}{|y_{1l}^2 + y_{2u}^2|^{1/2}} \right)^{j_1}, \end{aligned}$$

where we have used the fact that $y_i/|y|$ is increasing in y_i to obtain its upper bound.

D.3. Improved estimate of the higher order derivatives of the integrands. In the Hölder estimate, we need to estimate the derivatives of the integrands (7.24), (7.25), (7.18), which take the form

$$K^C(x, y)(p(x) - p(y)) + K^{NC}p(x)$$

for some weight p and kernels K^C, K^{NC} . Using the estimates of the kernels in Sections D.1, D.2 and the weights in Section C.3, the Leibniz rule, and the triangle inequality, we can estimate the derivative of the integrands. However, such an estimate can lead to significant overestimates near the singularity of the integrand. We use the estimates in (D.2) to handle the cancellations among different terms and obtain improved estimates for the integrand and its derivatives near the singularity:

$$(D.18) \quad T_{00}(x, y) \triangleq K(y - x)(p(x) - p(y)), \quad \partial_{x_i} T_{00}(x, y)$$

We choose weight $p(x)$ that is even in x and y . The basic idea is to do Taylor expansion on $p(x) - p(y)$ and obtain the factor $|x - y|$, which cancel one order of singularity from $K(x, y)$. We use the formulas in Section D.2 to collect the terms with the same singularity and exploit the cancellation.

D.3.1. *Y-discretization.* In the Y-discretization of the integral, we need to estimate the y -derivatives of the integrand (D.18). For $a, b = 1, 2$, denote

$$(D.19) \quad D_1 = \partial_a, \quad D_2 = \partial_b, \quad x_m = \frac{x+y}{2}.$$

Next, we compute $\partial_{y_b}^j \partial_{x_a}^i T_{00}$. The reader should be careful about the sign. Note that

$$\partial_{x_a}(K(y-x)) = -(\partial_a K)(y-x) = -D_1 K(y-x).$$

Using the Leibniz rule, we get

$$\begin{aligned} \partial_{y_b}^2 \partial_{x_a} T_{00} &= \partial_{y_b}^2 (-D_1 K(p(x) - p(y)) + K \cdot D_1 p(x)) = \partial_{y_b}^2 (D_1 K \cdot (p(y) - p(x)) + K \cdot D_1 p(x)) \\ &= D_2^2 D_1 K \cdot (p(y) - p(x)) + 2D_2 D_1 K \cdot D_2 p(y) + D_1 K \cdot D_2^2 p(y) + D_2^2 K \cdot D_1 p(x). \end{aligned}$$

We use Talyor expansion at $x = x_m$ and write

$$(D.20) \quad p(y) - p(x) = (y-x) \cdot \nabla p(x_m) + p_{m,2,err}, \quad \partial_i p(z) = \partial_i p(x_m) + (\partial_i p(z) - \partial_i p(x_m)), \quad z = x, y.$$

and then combine the terms involving ∇p to get

$$\begin{aligned} (D.21) \quad \partial_{y_b}^2 \partial_{x_a} T_{00} &= \sum_{i=1,2} \left(D_2^2 D_1 K \cdot (y_i - x_i) + \mathbf{1}_{D_2=\partial_i} 2D_2 D_1 K + \mathbf{1}_{D_1=\partial_i} D_2^2 K \right) \cdot \partial_{x_i} p(x_m) + D_2^2 D_1 K \cdot p_{m,2,err} \\ &\quad + 2D_2 D_1 K \cdot (D_2 p(y) - D_2 p(x_m)) + D_2^2 K \cdot (D_1 p(x) - D_1 p(x_m)) + D_1 K \cdot D_2^2 p(y) \\ &\triangleq \left(\sum_{i=1,2} I_i \cdot \partial_{x_i} p(x_m) \right) + II, \\ I_i &\triangleq D_2^2 D_1 K \cdot (y_i - x_i) + \mathbf{1}_{D_2=\partial_i} 2D_2 D_1 K + \mathbf{1}_{D_1=\partial_i} D_2^2 K, \end{aligned}$$

where $\partial_1^i \partial_2^j K$ is evaluated at $y-x$, and II consists of the last four terms in the second equation. The first term is the most singular term. We combine the most singular terms to exploit the cancellation and improve the estimates. We estimate the kernels

$$(D.22) \quad K_{mix}(D_1, D_2, i, s)(z_1, z_2) \triangleq D_2^2 D_1 K(z) z_i + \mathbf{1}_{D_2=\partial_i} 2D_2 D_1 K(z) + s \mathbf{1}_{D_1=\partial_i} D_2^2 K(z),$$

with $s = \pm 1$ and $D_1, D_2 \in \{\partial_1, \partial_2\}$. Then we can bound $\partial_{y_b}^2 \partial_{x_a} T_{00}$ using triangle inequality.

D.3.2. *The second singular term.* For $x = (x_1, x_2)$ close to the y -axis or the x -axis, since we have symmetrized the integral, we have another singular term in the integrand

$$T_{01} \triangleq K(y_1 - x_1, y_2 + x_2)(p(x) - p(y)), \text{ or } T_{10} \triangleq K(y_1 + x_1, y_2 - x_2)(p(x) - p(y)).$$

We have the first term if $x_2 < x_1$ and x_2 close to 0, and the second term if $x_1 < x_2$ and x_1 close to 0. We label the former case with *side* = 1 and the latter *side* = 2. See the right figure in Figure 10 for an illustration of the first case. The T_{01} term is supported in the blue region $R(x, k, S)$. Denote

$$(D.23) \quad (s_1, s_2) = (1, -1) \text{ if } \text{side} = 1, \quad (s_1, s_2) = (-1, 1) \text{ if } \text{side} = 2.$$

Case I. If $(D_1, \text{side}) = (\partial_1, 1)$ or $(\partial_2, 2)$, we obtain

$$\partial_{x_j} K(y_1 - s_1 x_1, y_2 - s_2 x_2) = -\partial_{y_j} K(y_1 - s_1 x_1, y_2 - s_2 x_2)$$

for $(j, s_1, s_2) = (1, 1, -1)$ or $(2, -1, 1)$. The computations for $\partial_{y_b}^2 \partial_{x_1} T_{01}$, $\partial_{y_b}^2 \partial_{x_2} T_{10}$ are the same as (D.21) with K and its derivatives evaluating at $z = (y_1 - s_1 x_1, y_2 - s_2 x_2)$.

We estimate II in (D.21) directly using triangle inequality and the bounds for $\partial_1^i \partial_2^j K$ in Section D.1, D.2 and p in Section C.3. For I_i in (D.21) in the most singular term, if $i = \text{side}$, from definition (D.23), we get

$$s_i = 1, \quad s_{3-i} = -1, \quad z_i = y_i - s_i x_i = y_i - x_i, \quad z_{3-i} = y_{3-i} + x_{3-i}.$$

Therefore, it follows

$$I_i = D_2^2 D_1 K(z) \cdot (y_i - x_i) + \mathbf{1}_{D_2=\partial_i} 2D_2 D_1 K(z) + \mathbf{1}_{D_1=\partial_i} D_2^2 K(z) = K_{mix}(D_1, D_2, i, 1)(z).$$

where K_{mix} is defined in (D.22). If $i \neq \text{side}$, we have $z_i = y_i + x_i \geq |y_i - x_i|$, $z_{3-i} = y_{3-i} - x_{3-i}$. We simply bound the summand using triangle inequality

$$|I_i| \leq |D_2^2 D_1 K(z)| \cdot |y_i - x_i| + \mathbf{1}_{D_2=\partial_i} 2|D_2 D_1 K(z)| + \mathbf{1}_{D_1=\partial_i} |D_2^2 K(z)|.$$

Case II. If $(D_1, \text{side}) = (\partial_1, 2)$ or $(\partial_2, 1)$, we obtain

$$\partial_{x_j} K(y_1 - s_1 x_1, y_2 - s_2 x_2) = (\partial_{y_j} K)(y_1 - s_1 x_1, y_2 - s_2 x_2)$$

for $(j, s_1, s_2) = (1, -1, 1)$ or $(2, 1, -1)$. Recall the definitions of D_1, D_2 (D.19). Using the above identity, we yield

$$\partial_{y_b}^2 \partial_{x_a} T = \partial_{y_b}^2 (D_1 K \cdot (p(x) - p(y)) + K \cdot D_1 p) = -(\partial_{y_b}^2 (D_1 K \cdot (p(y) - p(x)) - K \cdot D_1 p))$$

for $T = T_{01}$ or T_{10} . Using an expansion similar to that in (D.21), (D.20), we get

(D.24)

$$\begin{aligned} -\partial_{y_b}^2 \partial_{x_a} T &= \sum_{i=1,2} (D_2^2 D_1 K \cdot (y_i - x_i) + \mathbf{1}_{D_2=\partial_i} 2D_2 D_1 K - \mathbf{1}_{D_1=\partial_i} D_2^2 K) \cdot \partial_{x_i} p(x_m) + D_2^2 D_1 K \cdot p_{m,2,err} \\ &\quad + 2D_2 D_1 K \cdot (D_2 p(y) - D_2 p(x_m)) - D_2^2 K \cdot (D_1 p(x) - D_1 p(x_m)) + D_1 K \cdot D_2^2 p(y) \\ &\triangleq \left(\sum_{i=1,2} I_i \cdot \partial_{x_i} p(x_m) \right) + II, \\ I_i &\triangleq D_2^2 D_1 K \cdot (y_i - x_i) + \mathbf{1}_{D_2=\partial_i} 2D_2 D_1 K - \mathbf{1}_{D_1=\partial_i} D_2^2 K, \end{aligned}$$

where $\partial_1^i \partial_2^j K$ is evaluated at $z = (y_1 - s_1 x_1, y_2 - s_2 x_2)$. We bound II using triangle inequality and the bounds for K , its derivatives, and p in Sections D.1, D.2, and C.3.

For I_i , if $i = \text{side}$, from (D.23), we get $s_i = 1$ and $z_i = y_i - s_i x_i = y_i - x_i$. Hence, we get

$$I_i = D_2^2 D_1 K \cdot (y_i - x_i) + \mathbf{1}_{D_2=\partial_i} 2D_2 D_1 K - \mathbf{1}_{D_1=\partial_i} D_2^2 K = K_{mix}(D_1, D_2, i, -1)(z),$$

where K_{mix} is defined in (D.22).

If $i \neq \text{side}$ and $D_1 = D_2 = \partial_i$, we have $z_i = y_i - s_i x_i = y_i + x_i$ and get a cancellation between $D_2 D_1 K$ and $D_2^2 K$ and yield

$$|I_i| = |D_2^2 D_1 K \cdot (y_i - x_i) + D_2 D_1 K| \leq |D_2^2 D_1 K| \cdot |y_i - x_i| + |D_2 D_1 K|$$

Otherwise, we simply bound each term in I_i using triangle inequality.

D.3.3. *X-discretization.* For $K(s) = c \frac{s_1 s_2}{|s|^4}, c \frac{s_1^2 - s_2^2}{|s|^4}$, we have $K(s) = K(-s)$. Denote

$$T = K(y - x)(p(x) - p(y)) = K(x - y)(p(x) - p(y)).$$

In this section, we compute $\partial_{x_b}^i \partial_{x_a}^j T$. Using Taylor expansion at x

$$p(x) - p(y) = (x - y) \cdot \nabla p(x) + p_{x,2,err}$$

and calculations similar to those in Section D.3.1, we get

(D.25)

$$\begin{aligned} \partial_{x_b}^2 \partial_{x_a} T &= \partial_{x_b}^2 (D_1 K \cdot (p(x) - p(y)) + K D_1 p(x)) = D_2^2 D_1 K \cdot (p(x) - p(y)) + 2D_1 D_2 K \cdot D_2 p(x) \\ &\quad + D_1 K \cdot D_2^2 p(x) + D_2^2 K \cdot D_1 p(x) + 2D_2 K \cdot D_1 D_2 p(x) + K \cdot D_1 D_2^2 p(x) \\ &= \sum_{i=1,2} (D_2^2 D_1 K \cdot (x_i - y_i) + \mathbf{1}_{D_2=\partial_i} 2D_1 D_2 K + \mathbf{1}_{D_1=\partial_i} D_2^2 K) \partial_i p(x) + D_2^2 D_1 K \cdot p_{x,2,err} \\ &\quad + D_1 K \cdot D_2^2 p(x) + 2D_2 K \cdot D_1 D_2 p(x) + K \cdot D_1 D_2^2 p(x) \triangleq \left(\sum_{i=1,2} I_i \cdot \partial_i p(x) \right) + II, \\ I_i &\triangleq D_2^2 D_1 K \cdot (x_i - y_i) + \mathbf{1}_{D_2=\partial_i} 2D_1 D_2 K + \mathbf{1}_{D_1=\partial_i} D_2^2 K, \end{aligned}$$

where II consists of the last four terms in the third equation and K and its derivatives are evaluated at $x - y$. Since $D_1, D_2 = \partial_{x_i}$, we get

$$I_i = D_2^2 D_1 K \cdot (x_i - y_i) + \mathbf{1}_{D_2=\partial_i} 2D_1 D_2 K + \mathbf{1}_{D_1=\partial_i} D_2^2 K = K_{mix}(D_1, D_2, i, 1)(x - y),$$

where K_{mix} is defined in (D.22). We use the bound for K_{mix} , $\partial_1^i \partial_2^j K$ and p to estimate $D_2^2 D_1 T$.

D.3.4. *The second singular term.* Similar to Section D.3.2, we have the second singular term for x close to the x -axis or y -axis

$$T_{01} \triangleq K(x_1 - y_1, x_2 + y_2)(p(x) - p(y)), \quad T_{10} \triangleq K(x_1 + y_1, x_2 - y_2)(p(x) - p(y)).$$

We have the former if $x_2 < x_1$ and x_2 close to 0, and the latter if $x_1 < x_2$ and x_1 close to 0. Using the definition of *side*, s_1, s_2 from Section D.3.2 and (D.23), we get

$$\partial_{x_a} K(x_1 - y_1 s_1, x_2 - y_2 s_2) = (D_1 K)(x_1 - y_1 s_1, x_2 - y_2 s_2).$$

Then the computations of $D_2^2 D_1 T$ is the same as those in (D.25) with $\partial_1^i \partial_2^j K$ evaluating at $z = (x_1 - s_1 y_1, x_2 - s_2 y_2)$. We bound II in (D.25) directly using triangle inequality and the bounds for $\partial_1^i \partial_2^j K$ and p . For I_i in (D.25), if $i = \text{side}$, from (D.23), we get s_i and $z_i = x_i - s_i y_i = x_i - y_i$. It follows

$$I_i = D_2^2 D_1 K \cdot z_i + \mathbf{1}_{D_2 = \partial_i} 2 D_1 D_2 K + \mathbf{1}_{D_1 = \partial_i} D_2^2 K = K_{mix}(D_1, D_2, i, 1)(z).$$

If $i \neq \text{side}$, we have $z_i = x_i + y_i > |x_i - y_i|$. We bound each term in I_i separately. It follows the previous argument.

D.4. Estimate of $u(x)$ for small x_1 . In the energy estimate, we need to estimate $u(x)\varphi(x)$ with weight φ singular along the line $x_1 = 0$. We use the property that u vanishes on $x_1 = 0$ to establish such estimate.

By definition and symmetrizing the kernel using the odd symmetry of ω , we have

$$u(x, y) = \frac{1}{2\pi} \int_{y_1 \geq 0} \left(\frac{x_2 - y_2}{|x - y|^2} - \frac{x_2 - y_2}{(x_1 + y_1)^2 + (x_2 - y_2)^2} \right) \omega(y) dy = \frac{1}{\pi} \int_{y_1 \geq 0} K(x, y) dy,$$

where

$$(D.26) \quad K = \frac{1}{2} \left(\frac{x_2 - y_2}{|x - y|^2} - \frac{x_2 - y_2}{(x_1 + y_1)^2 + (x_2 - y_2)^2} \right) = x_1 \cdot \frac{2(x_2 - y_2)y_1}{|x - y|^2((x_1 + y_1)^2 + (x_2 - y_2)^2)} \triangleq x_1 K_{du}.$$

Using a rescaling argument, for $x = \lambda \hat{x}, y = \lambda \hat{y}$, we have

$$u = \frac{\lambda}{\pi} \int_{y_1 \geq 0} K(\hat{x}, \hat{y}) \omega_\lambda(\hat{y}) d\hat{y} = \frac{\lambda}{\pi} \left(\int_{y_1 \geq 0, y \notin S} + \int_{y_1 \geq 0, y \in S} \right) K(\hat{x}, \hat{y}) \omega_\lambda(\hat{y}) d\hat{y} \triangleq I + II,$$

where S is the singular region adapted to \hat{x} . For I , we further rewrite it and estimate it as follows

$$|I| = \frac{\lambda}{\pi} \hat{x}_1 \left| \int_{y_1 \geq 0, y \notin S} K_{dx}(\hat{x}, \hat{y}) \omega_\lambda(\hat{y}) dy \right| \leq \frac{\lambda}{\pi} \hat{x}_1 \|\omega_\lambda\|_{L^\infty} \int_{y_1 \geq 0, y \notin S} |K_{dx}(\hat{x}, \hat{y})| \varphi_\lambda^{-1}(\hat{y}) d\hat{y}.$$

Since the integral is not singular, we can use the previous method to discretize the integral and obtain its tight bound.

Large \hat{x}_1 . For the second part, if $\hat{x}_1 \geq x_l > 0$ away from 0, we have

$$K_{du}(\hat{x}, \hat{y}) \lesssim \frac{1}{x_l} \frac{1}{|\hat{x} - \hat{y}|},$$

which is integrable near the singularity \hat{x} . We can apply the similar method to estimate the singular integral

$$|II| \leq \frac{\lambda}{\pi} \hat{x}_1 \int_{y_1 \geq 0, y \in S} |K_{du}(\hat{x}, \hat{y})| \varphi_\lambda^{-1}(\hat{y}) d\hat{y}.$$

Small \hat{x}_1 . The difficulty is to estimate II for small x . It is not difficult to obtain that

$$(D.27) \quad |II| \lesssim \frac{\lambda}{\pi} \|\omega_\lambda\|_{L^\infty(S)} \hat{x}_1 |\log(\hat{x}_1)|.$$

Thus we cannot bound II by $C \hat{x}_1$ for some constant C uniformly for small \hat{x}_1 . Denote by

$$(D.28) \quad S_{sym} = [0, \hat{x}_1 + kh] \times [\hat{x}_2 - kh, \hat{x}_2 + kh], \quad \hat{y} = \hat{x} + \hat{x}_1 s.$$

Then $\hat{y} \in S_{sym}$ is equivalent to

$$s \in x_1^{-1}(S_{sym} - \hat{x}) = x_1^{-1}([-\hat{x}_1, kh] \times [-kh, kh]) = [-1, B^{-1}] \times [B^{-1}, B^{-1}] \triangleq R_B, \quad B = \frac{\hat{x}_1}{kh}.$$

We further decompose II as follows

$$II = \frac{\lambda}{\pi} \left(\int_{y_1 \geq 0, y \in S \setminus S_{sym}} + \int_{y_1 \geq 0, S \in S_{sym}} \right) K_{du}(\hat{x}, \hat{y}) \triangleq \frac{\lambda}{\pi} (II_1 + II_2).$$

For II_1 , the integral is not singular and we apply previous L^∞ estimate. For II_2 , using a change of variable (D.28), we derive

$$II_2 = \int_{s \in R_B} K_{du}(\hat{x}, \hat{x} + \hat{x}_1 s) \hat{x}_1^2 \omega_\lambda(\hat{x} + \hat{x}_1 s) ds.$$

Note that

$$\hat{y} - \hat{x} = \hat{x}_1 s, \quad \hat{y} + \hat{x} = \hat{x}_1(2 + s_1, s_2).$$

By definition (D.26), we get

$$K_{du}(\hat{x}, \hat{x} + \hat{x}_1 s) \hat{x}_1^2 = -\frac{2\hat{x}_1 s_2 \cdot (\hat{x}_1 + \hat{x}_1 s_1)}{\hat{x}_1^2 |s|^2 \cdot \hat{x}_1^2 ((s_1 + 2)^2 + s_2^2)} \hat{x}_1^2 = -\frac{2(s_1 + 1)s_2}{|s|^2 ((s_1 + 2)^2 + s_2^2)} \triangleq -K_s(s).$$

It follows

$$II_2 = - \int_{R_B} K_s(s) \omega_\lambda(\hat{x} + \hat{x}_1 s) ds.$$

Since $K_s(s)$ is symmetric in s_2 , we derive

$$\begin{aligned} |II_2| \leq & \|\omega\varphi\|_\infty \left\{ \left(\max_{z \in [-\hat{x}_1, 0] \times [0, kh]} \varphi_\lambda^{-1}(\hat{x} + z) + \max_{z \in [-\hat{x}_1, 0] \times [-kh, 0]} \varphi_\lambda^{-1} \right) J_1(B) \right. \\ & \left. + \left(\max_{z \in [0, kh] \times [0, kh]} \varphi_\lambda^{-1} + \max_{s \in [0, kh] \times [-kh, 0]} |\varphi_\lambda^{-1}| \right) J_2(B) \right\}, \end{aligned}$$

where

$$J_1(B) = \left| \int_{[-1, 0] \times [0, 1/B]} K_s(s) ds \right| = \int_{[0, 1] \times [0, 1/B]} K_s(s) ds, \quad J_2(B) = \int_{[0, 1/B]^2} K_s(s) ds.$$

The explicit formula of J_i can be obtained, and obviously J_i is decreasing in B . Note that $J_1(B)$ is bounded, but $J_2(B) \lesssim 1 + \log(B) \lesssim 1 + |\log \hat{x}_1|$, which relates to the estimate (D.27).

D.5. Additional derivations.

D.5.1. Estimate of the log-Lipschitz integral. In this section, we derive the coefficient in the estimate of $\partial_{x_2} I_{5,4}(x)$ (7.45), (7.46). For $I_{5,4}$, we further decompose it as follows

$$I_{5,4} = \left(\int_{R(k_2) \setminus R_s(k_2)} + \int_{R_s(k_2) \setminus R_s(a)} \right) K(x - y)(\psi(x) - \psi(y)) W(y) dy \triangleq I_{5,4,1} + I_{5,4,2}.$$

The first term is nonsingular and its derivative can be estimated using the method in Sections 7.1.6-7.1.8. For $I_{5,4,2}$, using the second order Taylor expansion to $\psi(x) - \psi(y)$ centered at x , we have

$$\begin{aligned} \partial_{x_2} (K(x - y)\psi(x) - \psi(y)) &= (\partial_2 K)(x - y)\psi(x) - \psi(y)) + K(x - y)\partial_2 \psi(x) \\ &= (\partial_2 K(x - y)(x_2 - y_2) + K(x - y))\partial_2 \psi(x) + \partial_2 K(x - y)(x_1 - y_1)\partial_1 \psi(x) + \mathcal{R}_K, \end{aligned}$$

where the remainder \mathcal{R}_K coming from the higher order term in the Taylor expansion satisfies

$$|\mathcal{R}_K| \leq \sum_{i+j=2} \|\partial_x^i \partial_y^j \psi\|_{L^\infty(Q)} |x_1 - y_1|^i |x_2 - y_2|^j c_{ij}$$

where $Q = B_{i_1 j_1}(h_x) + [-k_2 h, k_2 h]^2$ and $c_{20} = c_{02} = \frac{1}{2}, c_{11} = 1$. It follows

$$|\partial_{x_2} I_{5,4,2}| \leq \|\omega\varphi\|_\infty \sum_{0 \leq i \leq 1, 0 \leq j \leq i+1} S_{coe_{ij}}(x) \cdot f_{ij}(a, b),$$

where the coefficients $S_{coe_{ij}}(x)$ depend on the weight ψ, φ , and $f_{ij}(a, b)$ is the upper bound of the integral

$$(D.29) \quad \int_{[-k_2, k_2]^2 \setminus [-a, a]^2} |\partial_2 K(y) \cdot y_1^i y_2^j + \mathbf{1}_{(i,j)=(0,1)} K(y)| dy \leq f_{ij}(a, b).$$

For example, $Scoe_{01}$ comes from the following estimate for $I_{5,4,2}$

$$\begin{aligned} & \int_{R_s(k_2) \setminus R_s(a)} |(\partial_2 K(x-y)(x_2-y_2) + K(x-y))\partial_2 \psi(x)|\omega(y)dy \\ & \leq \|\omega\varphi\|_\infty \|\varphi^{-1}\|_{L^\infty(Q)} \cdot |\partial_2 \psi(x)| \int_{[-k_2, k_2]^2 \setminus [-a, a]^2} |\partial_2 K(s)s_2 + K(s)|ds. \end{aligned}$$

The function $f_{ij}(a, b)$ satisfies the following estimates

$$f_{1j}(a, b) \leq A_{1j} + B_{1j} \log(b/a), \quad j = 1, 2,$$

with some constant A_{1j}, B_{1j} . We will provide the formulas and estimates of f_{ij} in the upcoming Supplementary Materials.

D.5.2. Piecewise derivative bounds. In this section, we discuss how to obtain the sharp bound of $\frac{|p(b)-p(a)|}{|b-a|}$ using piecewise derivative bounds of p .

Suppose that $|p'(y)| \leq C_i, y \in I_i = [y_i, y_{i+1}]$. For any $a \in I_k, b \in I_l, a < b$, we have the bound

$$\begin{aligned} & |p(b) - p(a)| \leq \int_a^{y_2} |p'(y)|dy \leq |y_{k+1} - a|C_k + |b - y_l|C_l + \sum_{k+1 \leq m \leq l-1} C_m(y_{m+1} - y_m) \\ & = (y_{k+1} - a)C_k + (b - y_l)C_l + M_{kl}(y_l - y_{k+1})\mathbf{1}_{l \geq k+1}, \quad M_{kl} = |y_l - y_{k+1}|^{-1} \left(\sum_{k+1 \leq m \leq l-1} C_m|y_{m+1} - y_m| \right). \end{aligned}$$

Next, we want to bound $\frac{|p(b)-p(a)|}{|b-a|}$. If $l - k \leq 1$, we get

$$|p(b) - p(a)| \leq (b - a) \max(C_k, C_l).$$

Otherwise, if $l \geq k+2$, we have

$$(p(b) - p(a)) \leq (y_{k+1} - a)(C_k - M_{kl}) + (b - y_l)(C_l - M_{kl}) + M_{kl}(b - a).$$

Since $\frac{y_{k+1}-a}{b-a}$ is decreasing in a and b , $\frac{b-y_l}{b-a}$ is increasing in b and a , we get

$$0 \leq \frac{y_{k+1} - a}{b - a} \leq \frac{y_{k+1} - y_k}{y_l - y_k}, \quad 0 \leq \frac{b - y_l}{b - a} \leq \frac{y_{l+1} - y_l}{y_{l+1} - y_{k+1}}.$$

Using the above estimates, for $a \in I_k, b \in I_l$, we obtain

$$\frac{|p(b) - p(a)|}{|b - a|} \leq \max(C_k - M_{kl}, 0) \frac{y_{k+1} - y_k}{y_l - y_k} + \max(C_l - M_{kl}, 0) \frac{y_{l+1} - y_l}{y_{l+1} - y_{k+1}} + M_{kl}.$$

For uniform mesh, i.e. $y_{i+1} - y_i = h$, we can simplify the above estimate as follows

$$\frac{|p(b) - p(a)|}{|b - a|} \leq \frac{(\max(C_k - M_{kl}, 0) + \max(C_l - M_{kl}, 0))}{l - k} + M_{kl}, \quad M_{kl} = \frac{1}{l - k - 1} \sum_{k+1 \leq m \leq l-1} C_m.$$

D.5.3. Optimization in the Hölder estimate. For each $t = ch$, we minimize the function

$$F(a, t) = (A + B \log \frac{b}{a})\sqrt{t} + \frac{Ca}{\sqrt{t}}$$

in the upper bound in (7.53) over $a \leq b$. We assume that A, B, C, b, c, h, h_x are given. Denote

$$t_u = ch_x, \quad t_1 = \frac{Cb}{B}.$$

For fixed t , since $\partial_a^2 F < 0, \partial_a F(0, t) < 0$ and $\partial_a F(a, t) = 0$ if $a = \frac{Bt}{C}$, we choose $a = \min(b, \frac{Bt}{C})$. For $t \leq \frac{Cb}{B} = t_1$, we get

$$\min_{a \leq b} F(a, t) \leq F\left(\frac{Bt}{C}, t\right) = (A + B \log \frac{bC}{B} + B)\sqrt{t} - B\sqrt{t} \log t.$$

The right hand side can be further estimated by studying the concave function on $s \leq s_u$

$$f(p, q, s) = (p - q \log s)s \leq f(p, q, \min(s_u, \exp(\frac{p-q}{q}))),$$

with $p = A + B \log bCB + B, q = 2B, s_u = \min(t_u^{1/2}, t_1^{1/2})$.

If $\frac{C^b}{B} \leq t \leq t_u$, we choose $a = b$ and get

$$\min_{a \leq b} F(a, t) \leq F(b, t) = A\sqrt{t} + \frac{C^b}{\sqrt{t}},$$

which is convex in $t^{1/2}$. Thus its maximum is achieved at the endpoints.

APPENDIX E. REPRESENTATIONS AND ESTIMATES OF THE SOLUTIONS

Recall from Section 5 that we represent the approximate steady state as follows

$$\bar{\omega} = \bar{\omega}_1 + \bar{\omega}_2, \quad \bar{\theta} = \bar{\theta}_1 + \bar{\theta}_2, \quad \bar{\omega}_1 = \chi(r)r^\alpha g_1(\beta), \quad \bar{\theta}_1 = \chi(r)r^{1+2\alpha}g_2(\beta),$$

where $\bar{\omega}_2, \bar{\theta}_2$ have compact supports and are represented as piecewise polynomials. We also represent the approximation of the stream function in a similar form. We have discussed how to find the semi-analytic part in Section 5. We will discuss how to estimate the semi-analytic part in Section E.3. In the following sections, we discuss more details about the representations and establish rigorous estimate of the derivatives of $\bar{\omega}_2, \bar{\theta}_2$.

E.1. Representations. In the near field, we use piecewise polynomials to represent the solution. Let $D = [0, L] \times [0, L]$ be the computational domain. Given mesh points $0 = x_0 < x_1 < \dots < x_n = L < \dots < x_{n+m}, 0 = y_0 < y_1 < \dots < y_n = L < \dots < y_{n+m}$, we define

$$x_{-i} = -ih_1, \quad y_{-i} = -ih_2, \quad h_1 = x_1 - x_0 = x_1, \quad h_2 = y_1 - y_0 = y_1.$$

Then, we construct

$$(E.1) \quad \bar{\omega}_2(x, y) = \sum_{0 \leq i, j \leq n-1} a_{ij} B_{1,i}(x) B_j(y),$$

where $a_{ij} \in \mathbb{R}$ is the coefficient, $B_i(x), B_j(y)$ are constructed from the 6-th order B-spline

$$(E.2) \quad B_i(x) = C_i \sum_{0 \leq j \leq k} k \frac{(s_{ij} - x)_+^{k-1}}{d_j}, \quad d_j = \prod_{0 \leq l \leq k, l \neq j} (s_{ij} - s_{il}),$$

with $k = 6$. The constant C_i will be chosen later so that the stiffness matrix associated to these B-spline basis has a better condition number. The points s_{ij} are chosen as follows

$$s_{ij} = x_{i+j-4}, \quad 0 \leq j \leq k = 6.$$

Then the B-spline B_i is supported in $[x_{i-3}, x_{i+3}]$ and is centered around x_i . Since ω is odd in x , to impose this symmetry in the representation, we modify the first few basis

$$B_{1,i}(x) = B_i(x) - B_i(-x), \quad i \leq 2.$$

Then B_i is odd.

For the density $\bar{\theta}_2$, the representation is similar

$$\bar{\theta}_2 = x \sum_{ij} a_{ij} B_{1,i}(x) B_j(y).$$

Here, we multiply x since $\bar{\theta}$ is even and $\bar{\theta}(x, y)$ vanishes $O(x^2)$ near $x = 0$.

For the stream function $\bar{\psi}_{N,2}$, we represent it as follows

$$(E.3) \quad \bar{\psi}_{N,2} = \sum_{ij} a_{ij} B_{1,i}(x) B_{2,j}(y) \rho_p(y).$$

We multiply $\rho_p(y)$ given below to impose the Dirichlet boundary condition

$$(E.4) \quad \rho_p(y) = \arctan(1 + y) - 1.$$

We can obtain the exact formulas of $\partial_x^i \rho_p$ using symbolic computation. We use induction to obtain rigorous estimate of $\partial_x^i \rho_p$. See Section F.3.

E.2. Estimate of the derivatives of piecewise polynomials. Our approximate steady state is represented as piecewise polynomials. We discuss how to estimate its derivatives. Suppose that we can evaluate a function f on finite many points. For example, f is an explicit function or a polynomial. To obtain a piecewise sharp bound of f on $I = [x_l, x_u]$, we use the following estimate

$$(E.5) \quad \max_{x \in I} |f(x)| \leq \max(|f(x_l)|, |f(x_u)|) + \frac{h^2}{8} \|f_{xx}\|_{L^\infty(I)}, \quad h = x_u - x_l,$$

whose proof is simple. We refer to Section G. If we can obtain a rough bound for f_{xx} , as long as the interval I is small, i.e., h is small, the error part is small. Similarly, if we can obtain a rough bound for $\partial_x^{k+2} f$, using induction and the above estimate recursively,

$$\max_{x \in I} |\partial_x^i f(x)| \leq \max(|\partial_x^i f(x_l)|, |\partial_x^i f(x_u)|) + \frac{h^2}{8} \|\partial_x^{i+2} f\|_{L^\infty(I)},$$

for $i = k, k-1, \dots, 0$, we can obtain the sharp bound for $\partial_x^i f$ on I . We call the above method the second order method since the error term is second order in h .

E.2.1. Estimate a piecewise polynomial in 1D. Suppose that $p(x)$ is a piecewise polynomials on $x_0 < x_1 < \dots < x_n$ with degree d , e.g. Hermite spline. Denote $I_i = [x_i, x_{i+1}]$. Then $p(x)$ is a polynomial in each I_i with degree $\leq d$. Our goal is to estimate $\partial_x^k p(x)$ in I_i for all k by only finite many evaluations of $p(x)$ and its derivatives.

Firstly, we have

$$\partial_x^k p(x) = 0, \quad k > d, \quad \partial_x^d p(x) = c_p,$$

for some constant c_p in I_i .

Now, using induction from $k = d-1, d-2, \dots, 0$, we have

$$\max_{x \in I_i} |\partial_x^k p(x)| \leq \max(|\partial_x^k p(x_i)|, |\partial_x^k p(x_{i+1})|) + \frac{h_i^2}{8} \|\partial_x^{k+2} p\|_{L^\infty(I_i)}, \quad h_i = x_{i+1} - x_i.$$

Since we know $\partial_x^{d+1} p(x) = 0$ on I_i , using the above method, we can obtain the sharp piecewise bounds for all derivatives of $p(x)$ on I_i .

Using the above approach, we can estimate the derivatives of the angular profile in (5.2) rigorously.

E.2.2. Estimate a piecewise polynomial in 2D. Now, we generalize the above ideas to 2D so that we can estimate the approximate steady state (E.1). We assume that $p(x, y)$ is a piecewise polynomials in the mesh $Q_{ij} = [x_i, x_{i+1}] \times [y_j, y_{j+1}]$ with degree d . That is, in Q_{ij} , $p(x, y)$ can be written as a linear combination of

$$x^k y^l, \quad \max(k, l) \leq d,$$

e.g. (E.1). For (E.1), we have $d = 5$. Similar to the 1D case, we have

$$\partial_x^k \partial_y^l p(x, y) = 0, \quad \max(k, l) > d.$$

Moreover, we know $\partial_x^{d-1} \partial_y^{d-1}$ is linear in x, y .

We use the following generalization of (E.5) to 2d

$$(E.6) \quad \max_{(x, y) \in Q} |f(x, y)| \leq \max_{\alpha, \beta = l, u} |f(x_\alpha, y_\beta)| + \frac{\|f_{xx}\|_{L^\infty(Q)} (x_u - x_l)^2}{8} + \frac{\|f_{yy}\|_{L^\infty(Q)} (y_u - y_l)^2}{8},$$

$$Q = [x_l, x_u] \times [y_l, y_u].$$

The proof follows from (7.10) or the estimates in Appendix G.2.

Denote

$$A_{kl} \triangleq \max_{Q_{ij}} \|\partial_x^k \partial_y^l p\|_{L^\infty(Q_{ij})}, B_{kl} \triangleq \max_{\alpha, \beta = l, u} |\partial_x^k \partial_y^l p(x_\alpha, y_\beta)|, \quad h_1 = x_{i+1} - x_i, \quad h_2 = y_{j+1} - y_j.$$

Since p is given, we can evaluate B_{kl} . Clearly, we have $A_{kl} = 0$ for $\max(k, l) > d$. For $k = d-1, d$, using (E.6) and induction in the order $l = d, d-1, d-2, \dots, 0$, we can obtain

$$A_{kl} \leq B_{kl} + \frac{1}{8} (h_1^2 A_{k+2, l} + h_2^2 A_{k, l+2}).$$

This allows us to bound A_{kl} for $k = d, d-1$ and all l . Similarly, we can bound A_{kl} for $l = d, d-1$ and all k .

For the remaining cases, we can use induction on $n = \max(k, l) = d-2, d-1, \dots, 0$ to estimate

$$A_{kl} \leq B_{kl} + \frac{1}{8}(h_1^2 A_{k+2,l} + h_2^2 A_{k,l+2}).$$

This allows us to estimate all derivatives of $p(x, y)$ in Q_{ij} .

E.2.3. Estimate a piecewise polynomial in 2D with weights. We consider how to estimate the derivatives of $f = \rho(y)p(x, y)$, where ρ is a given weight in y and $p(x, y)$ is the piecewise polynomials in 2D. For example, our construction of the stream function (E.3) has such a form. Firstly, we can estimate the derivatives of $p(x, y)$ using the method in Appendix E.2.2. For the weight ρ , we estimate its derivatives in Section F.3. Then, using the Leibniz rule and the triangle inequality, we can estimate the derivatives f

$$|\partial_x^i \partial_y^j f| \leq \sum_{l \leq j} \binom{j}{l} |\partial_x^i \partial_y^l p(x, y)| |\partial_y^{j-l} \rho(y)|$$

for high enough derivatives.

Now, we plug the above bounds for $\partial_x^{i+2} \partial_y^j, \partial_x^i \partial_y^{j+2} f$ in (E.6) and evaluate $\partial_x^i \partial_y^j f$ on the grid points to obtain the sharp estimate of $\partial_x^i \partial_y^j f$.

E.3. Estimate of the far-field approximation. We estimate the derivatives of

$$g(x, y) = g(r, \beta) = A(r)B(\beta).$$

Note that the semi-analytic parts of $\bar{\omega}, \bar{\theta}$ have the above forms.

E.3.1. Formulas of the derivatives of g . Firstly, we use induction to establish

$$(E.7) \quad F_{i,j} \triangleq \partial_x^i \partial_y^j g(r, \beta) = \sum_{k+l \leq i+j} C_{i,j,k,l}(\beta) r^{-i-j+k} \partial_r^k A \partial_\beta^l B,$$

with $C_{i,j,k,l} = 0$, for $k < 0, l < 0$, or $k + l > i + j$. Let us motivate the above ansatz. Recall from (D.13) that

$$\partial_x = \cos \beta \partial_r - \frac{\sin \beta}{r} \partial_\beta, \quad \partial_y = \sin \beta \partial_r + \frac{\cos \beta}{r} \partial_\beta.$$

For each derivative ∂_x or ∂_y , we get the factor $\frac{1}{r}$ or a derivative ∂_r , which leads to the form $r^{-i-j+k} \partial_r^k A$. Moreover, we get a derivative ∂_β and some functions depending on β , which leads to the form $C_{i,j,k,l}(\beta) \partial_\beta^l B$.

For $D = \partial_x$ or ∂_y , a direct calculation yields

$$(E.8) \quad DF_{i,j} = \sum_{k+l \leq i+j} D(C_{i,j,k,l} r^{-i-j+k}) \cdot \partial_r^k A \partial_\beta^l B + C_{i,j,k,l} r^{-i-j+k} (D \partial_r^k A \cdot \partial_\beta^l B + \partial_r^k A \cdot D \partial_\beta^l B).$$

Using the formula of ∂_x, ∂_y , we get

$$\begin{aligned} \partial_x(C_{i,j,k,l}(\beta) r^{-i-j+k}) &= -\sin \beta \partial_\beta C_{i,j,k,l} r^{-i-j-1+k} + (k - i - j) \cos \beta C_{i,j,k,l} r^{-i-j-1+k}, \\ \partial_x \partial_r^k A &= \cos \beta \partial_r^{k+1} A, \quad \partial_x \partial_\beta^l B = -\frac{\sin \beta}{r} \partial_\beta^{l+1} B, \end{aligned}$$

Using $\partial_x F_{i,j} = F_{i+1,j}$ and comparing the above formulas and the ansatz (E.7), we yield

$$(E.9) \quad C_{i+1,j,k,l} = (k - i - j) \cos \beta C_{i,j,k,l} - \sin \beta \partial_\beta C_{i,j,k,l} + \cos \beta C_{i,j,k-1,l} - \sin \beta C_{i,j,k,l-1},$$

for $k \leq i + j$. Similarly, for $D = \partial_y$, plugging the following identities

$$\begin{aligned} \partial_y(C_{i,j,k,l}(\beta) r^{-i-j+k}) &= \cos \beta \partial_\beta C_{i,j,k,l} r^{-i-j-1+k} + (k - i - j) \sin \beta C_{i,j,k,l} r^{-i-j-1+k}, \\ \partial_y \partial_r^k A &= \sin \beta \partial_r^{k+1} A, \quad \partial_y \partial_\beta^l B = \frac{\cos \beta}{r} \partial_\beta^{l+1} B \end{aligned}$$

into (E.8) and then comparing (E.7) and (E.8), we yield

$$(E.10) \quad C_{i,j+1,k,l} = (k - i - j) \sin \beta C_{i,j,k,l} + \cos \beta \partial_\beta C_{i,j,k,l} + \sin \beta C_{i,j,k-1,l} + \cos \beta C_{i,j,k,l-1}.$$

The based case is given by

$$F_{0,0} = A(r)g(\beta), \quad C_{0,0,0,0} = 1.$$

Using induction and the above recursive formulas, we can derive $C_{i,j,k,l}(\beta)$ in (E.7).

E.3.2. Estimates of $F_{i,j}$. To estimate $F_{i,j}$, using (E.7) and triangle inequality, we only need to estimate $\partial_r^k A, \partial_\beta^l B(\beta)$, and $C_{i,j,k,l}(\beta)$. In our case, $B(\beta)$ is piecewise polynomials, whose estimates are simple. Function $A(r)$ is some explicit function, which will be constructed and estimated in Section F.1.

To estimate $C_{i,j,k,l}(\beta)$ on $\beta \in [\beta_1, \beta_2]$, we use the second order estimate in (E.5) and the induction ideas in Section E.2.1.

We can evaluate $C_{i,j,k,l}$ using its exact formula. It remains to bound $\partial_\beta^2 C_{i,j,k,l}$.

An important observation from (E.9), (E.8) is that $C_{i,j,k,l}$ is a polynomial on $\sin \beta$ and $\cos \beta$ with degree less than $i+j$, which can be proved easily using induction. In particular, we can write $C_{i,j,k,l}$ as follows

$$C_{i,j,k,l} = \sum_{0 \leq k \leq n} a_k \sin(k\beta) + b_k \cos(k\beta), \quad f \triangleq \partial_\beta^2 C_{i,j,k,l} = \sum_{1 \leq k \leq n} c_k \sin(k\beta) + d_k \cos(k\beta), \quad n = i+j$$

for some $a_k, b_k, c_k, d_k \in \mathbb{R}$. It is easy to see that $C_{i,j,k,l}$ is either odd or even in β , which implies $c_k \equiv 0$ or $d_k \equiv 0$. It follows

$$\|f\|_\infty \leq \sum_{1 \leq k \leq n} (|c_k| + |d_k|) \leq \left(n \sum_{k \leq n} (c_k^2 + d_k^2) \right)^{1/2} = \left(\frac{n}{\pi} \int_0^{2\pi} f^2 \right)^{1/2},$$

where we have used orthogonality of $\sin kx, \cos kx$ and $\|f\|_{L^2}^2 = \pi \sum_{k \leq n} (c_k^2 + d_k^2)$ in the last equality. It is easy to see that f^2 is again a polynomial in $\sin \beta, \cos \beta$ with degree $\leq 2n$. We fix $M > 2n$. For any $0 \leq k < M$, it is easy to obtain

$$\frac{1}{2\pi} \int_0^{2\pi} e^{ikx} = \frac{1}{M} \sum_{j=1}^M \exp(i \frac{2kj}{M} \pi) = \delta_{k0}.$$

Using the above identity, we establish

$$\|g\|_{L^2}^2 = \frac{2\pi}{M} \sum_{j=1}^M |g(\frac{2j\pi}{M})|^2,$$

for any polynomial g in $\sin \beta, \cos \beta$ with degree $< M$. Hence, we prove

$$\|f\|_\infty \leq \left(\frac{2n}{M} \sum_{k=1}^M f^2(\frac{2k\pi}{M}) \right)^{1/2}.$$

The advantage of the above estimate is that to obtain the sharp bound of $C_{i,j,k,l}$, we only need to evaluate $C_{i,j,k,l}, f = \partial_\beta^2 C_{i,j,k,l}$ on finite many points.

E.3.3. From polar coordinates to the Cartesian coordinate. We want to obtain the piecewise estimate of $F_{p,q} = \partial_x^p \partial_y^q (A(r)g(\beta))$ on $Q_{ij} = [x_i, x_{i+1}] \times [y_j, y_{j+1}], 1 \leq i, j \leq n$. Firstly, we partition the (r, β) coordinate into $r_1 < r_2 < \dots < r_{n_1}, 0 = \beta_0 < \beta_1 < \dots < \beta_{n_2} = \frac{\pi}{2}$. Then we apply the methods in Section E.3 to bound $F_{p,q}$ on $S_{ij} \triangleq [r_i, r_{i+1}] \times [\beta_j, \beta_{j+1}]$.

To estimate $F_{p,q}$, we cover Q_{ij} by $S_{k,l}$ and transfer the bound from (r, β) coordinate to (x, y) coordinate

$$\max_{x \in Q_{ij}} |F_{p,q}(x)| \leq \max_{S_{k,l} \cap Q_{ij} \neq \emptyset} \|F_{p,q}(r, \beta)\|_{L^\infty(S_{k,l})}$$

For $(r, \beta) \in Q_{ij}$, we get

$$r \in [(x_i^2 + y_j^2)^{1/2}, (x_{i+1}^2 + y_{j+1}^2)^{1/2}], \quad \beta \in [\arctan \frac{y_j}{x_{i+1}}, \arctan \frac{y_{j+1}}{x_i}].$$

Therefore, we yield the necessary conditions for $Q_{ij} \cap S_{k,l} \neq \emptyset$:

$$x_{i+1}^2 + y_{j+1}^2 \geq r_k^2, \quad x_i^2 + y_i^2 \leq r_u^2, \quad \arctan \frac{y_{j+1}}{x_i} \geq \beta_l, \quad \arctan \frac{y_j}{x_{i+1}} \leq \beta_{l+1}.$$

Given $Q_{i,j}$, we maximize $\|F_{p,q}\|_{L^\infty(S_{k,l})}$ over (k,l) satisfying the above bounds to control $\|F_{p,q}\|_{L^\infty(Q_{i,j})}$.

APPENDIX F. ESTIMATE OF EXPLICIT FUNCTIONS

In this section, we estimate the derivatives of several explicit or semi-explicit functions using induction, including several cutoff functions used in the estimates and the weight in the stream function (E.3).

F.1. Estimate of the radial functions.

F.1.1. *Estimate of the cutoff function.* We estimate the derivatives of the cutoff function

$$(F.1) \quad \chi_e(x) = \left(1 + \exp\left(\frac{1}{x} + \frac{1}{x-1}\right)\right)^{-1}$$

for $a > 0$, where e is short for *exponential*. In our verification, it involves high order derivatives of χ_e . Although χ_e is explicit, its formula is complicated and is difficult to estimate. Instead, we use the structure of $\partial_x^i \chi_e$ and induction to estimate $\partial_x^i \chi_e$. Denote

$$p(x) = \frac{1}{x} + \frac{1}{x-1}, \quad f = \frac{1}{1+x}, \quad \chi_e = f(e^p).$$

Firstly, we use induction to derive

$$d_x^k \chi_e = \sum_{i=1}^k (\partial^i f)(e^p) e^{ip} Q_{k,i}(x),$$

where $Q_{k,i} = 0$ for $i > k, i < 0$. A direct calculation yields

$$\begin{aligned} \partial \sum_{i=1}^k \partial^i f e^{ip} Q_{k,i}(x) &= \sum_{i=1}^k (\partial^{i+1} f)(e^p) \cdot p' e^p e^{ip} Q_{k,i} + (\partial^i f) \partial_x (e^{ip} Q_{k,i}) \\ &= \sum_{i=1}^k (\partial^{i+1} f)(e^p) \cdot e^{(i+1)p} Q_{k,i} + (\partial^i f) e^{ip} (ip' Q_{k,i} + Q'_{k,i}). \end{aligned}$$

Comparing the above two equations, we derive

$$Q_{k+1,i} = p' Q_{k,i-1} + ip' Q_{k,i} + Q'_{k,i}.$$

The first few terms in $Q_{k,i}$ are given by

$$Q_{0,0} = 1, \quad Q_{1,1} = p', \quad Q_{1,0} = 0.$$

It is not difficult to see that $Q_{k,i}$ is a polynomial of $\partial_x^j p$, $j \leq k$. Thus, using triangle inequality, we only need to bound $\partial_x^j p$. We have

$$|\partial_x^n p(x)| \leq n! (|x|^{-n-1} + |x-1|^{-n-1}) \leq n! (|z|^{-n-1} + 2^{n+1}), \quad z = \min(|x|, |1-x|).$$

Substituting the above bounds into the formula of $Q_{k,i}$, we can obtain the upper bound $Q_{k,i}^u(x)$ for $Q_{k,i}(x)$, which is a polynomial of z^{-1} with positive coefficient. Since each term in $Q_{k,i}$ is given by $c_{i_1, i_2, \dots, i_m} \prod_{j=1}^m \partial_x^{i_j} p$ with $\sum i_j = k$, the above estimate implies

$$|c_{i_1, i_2, \dots, i_m} \prod_{j=1}^m \partial_x^{i_j} p| \leq c_{i_1, i_2, \dots, i_m} \prod_{j=1}^m i_j! (|z|^{-i_j-1} + 2^{i_j+1}).$$

Since $m \leq k$, the highest order of z^{-1} in the upper bound is bounded by $2k$. Thus, we obtain that $Q_{k,i}^u$ is a polynomial in z with $\deg Q_{k,i}^u \leq 2k$. Next, we bound

$$|e^{ip} Q_{k,i}| \leq e^{ip} Q_{k,i}^u.$$

For $k \leq 20, x \geq \frac{1}{2}, z^{-1} = |x - 1|^{-1} \geq 2k$, a direct calculation implies that $e^{ip(x)}Q_{k,i}^u(x)$ is decreasing. In fact, for $l \leq 2k$, we have $z = |x - 1| = 1 - x$ and

$$\begin{aligned} \partial_x(\exp(ip(x))(1-x)^{-l}) &= \exp(ip(x))(ip'(1-x)^{-l} + l(1-x)^{-l-1}) \\ &= \exp(ip(x))\left(-\frac{i}{x^2} - \frac{i}{(x-1)^2} + l(1-x)^{-1}\right)(1-x)^{-l} \leq 0. \end{aligned}$$

In the last inequality, we have used $-\frac{i}{1-x} + l \leq -2ki + 2k \leq 0$.

Note that $|\partial_x^i f(e^p)| = i!|(1+e^p)^{-i-1}| \leq i!$. Thus, for $x \in [x_l, x_u]$ with x_l close to 1, we get

$$|\partial_x^k \chi_e(x)| \leq \sum_{i=1}^k |\partial^i f(x)| e^{ip(x_l)} Q_{k,i}^u(x_l) \leq \sum_{i=1}^k i! e^{ip(x_l)} Q_{k,i}^u(x_l).$$

Using the above derivatives bound, the symbolic formula of $\partial_x^k \chi_e$, and the refined second order estimate in Section E.2.1, we can obtain sharp bounds for $\partial_x^k \chi_e$.

F.1.2. Estimate of polynomial decay functions. For cutoff function $\chi_e(\frac{|x|-a}{b})$ based on the exponential cutoff function (F.1), it has rapid change from $|x| \leq a$ to $|x| \geq a+b$, which is not very smooth in the computational domain if there are not enough mesh for x with $a \leq |x| \leq b$. We apply these cutoff functions to the far-field, e.g. $|x| \geq 10$, where the mesh is relatively sparse. Thus, we need another function similar to a cutoff function that has a slower change than the exponential cutoff function. We consider

$$(F.2) \quad \chi(x) = \frac{x^7}{(1+x^2)^{7/2}}, \quad x \in \mathbb{R}_+.$$

and will use its rescaled version, e.g., $\chi(\frac{x-a}{b})$, in our verification.

Firstly, we use induction to derive

$$\partial_x^k \chi = \frac{p_k(x)}{(1+x^2)^{7/2+k}}, \quad p_0 = x^7.$$

where $p_k(x)$ is a polynomial. A direct calculation yields

$$\partial_x^{k+1} \chi = \frac{p'_k(x)(1+x^2) - (\frac{7}{2} + k) \cdot 2x p_k(x)}{(1+x^2)^{7/2+k+1}}.$$

Comparing the above two formulas, we yield

$$p_{k+1} = p'_k(1+x^2) - (7+2k)x p_k(x).$$

The first few terms are given by $p_0 = x^7$, $p_1 = 7x^6$. Using the recursive formula and $\deg p_1 = 6$, we yield

$$(F.3) \quad \deg p_{k+1} \leq \deg p_k + 1, \quad \deg p_k \leq k+5, \quad k \geq 1.$$

Since p_k is a polynomial, the above recursive formula shows that p_{k+1} is also a polynomial.

To estimate $\partial_x^k \chi$, we decompose p_k into the positive and the negative parts. Suppose that $p_k = \sum_i a_i x^i$. We have

$$p_k = p_k^+ - p_k^-, \quad p_k^+ = \sum a_i^+ x^i, \quad p_k^- = \sum a_i^- x^i.$$

For $x \geq 0$, p_k^+, p_k^- are increasing. Thus, for $x \in [x_l, x_u]$, we get

$$|\partial_x^k \chi| \leq \frac{\max(p_k^+(x_u) - p_k^-(x_l), p_k^-(x_u) - p_k^+(x_l))}{(1+x_l^2)^{7/2+k}}.$$

Next, we estimate $\partial_x^k \chi$ for large x . For $x \geq 2, k \geq 2$ and any polynomial $q(x)$ with non-negative coefficients and $\deg q \leq k+5$, we yield

$$xq' \leq (k+5)q, \quad \frac{q'(1+x^2)}{(7+2k)xq} \leq \frac{(1+x^2)(k+5)}{(7+2k)x^2} \leq \frac{5(k+5)}{4(7+2k)} < 1.$$

The first inequality follows by comparing the coefficients of xq' and $(k+5)q$, which are nonnegative. It follows

$$\partial_x \frac{q}{(1+x^2)^{7/2+k}} = \frac{q'(1+x^2) - (7/2+k)2xq}{(1+x^2)^{7/2+k+1}} \leq 0.$$

Thus $\frac{q}{(1+x^2)^{7/2+k}}$ is decreasing. For $k \geq 1$ and $x \geq x_l \geq 2$, using (F.3) and the monotonicity, we yield

$$|\partial_x^k(x)| \leq \frac{p_k^+(x) + p_k^-(x)}{(1+x^2)^{7/2+k}} \leq \frac{p_k^+(x_l) + p_k^-(x_l)}{(1+x_l^2)^{7/2+k}}$$

For $k = 0$, the estimate is trivial: $\chi(x) \leq 1$. Using these higher order derivative bounds, we can use the discrete values of $\partial_x^k \chi$ and the bound for $\partial_x^{k+2} \chi$ to obtain sharp bounds of $\partial_x^k \chi$.

Note that $\chi_1(x-a) = \frac{(x-a)_+^7}{(1+(x-a)^2)^{7/2}}$ is only $C^{6,1}$. Suppose that $a \in [x_l, x_u]$. Since χ_1 is smooth on $x \leq a$ and on $x \geq a$, we can still use first order estimate to estimate $\partial_x^k \chi_1$ as follows

$$|\partial_x^k \chi_1(x)| \leq \max_{\alpha \in \{l, u\}} |\partial_x^k \chi_1(x_\alpha)| + \|\partial_x^{k+1} \chi_1\|_{L^\infty[x_l, x_u]} |x_u - x_l|.$$

F.1.3. Radial cutoff function. Now, we construct the radial cutoff functions for the far-field approximation terms of ω and ψ as follows

$$(F.4) \quad \chi(r) = \chi_1(1 - \chi_2) + \chi_2, \quad \chi_1(r) = \chi_{rati}(\frac{x - a_1}{l_1^{1/2}}), \quad \chi_2(r) = \chi_{exp}(\frac{x - a_2}{9a_2}),$$

where χ_{exp} and χ_{rati} are defined in (F.1) and (F.2), respectively. Using the estimates of χ_{rati}, χ_{exp} established in the last two sections and the interval operations in (C.5), we can evaluate χ on the grid points and estimate its bounds.

F.2. Cutoff function near the origin. For the cutoff function $\kappa(x)$ used in Section 6, we choose it as follows

$$(F.5) \quad \kappa(x; \nu_1, \nu_2) = \kappa_1(x/\nu_1)(1 - \chi_e(\frac{x}{\nu_2})), \quad \kappa_1(x) = \frac{1}{1+x^4}, \quad \nu_1 = 1/3, \quad \nu_2 = 1.5,$$

where χ_e is the cutoff function chosen in (F.1). Since $\chi_e(y) = 1$ for $y \geq 1$ and $\chi_e(y) = 0$ for $y \leq 0$. The above cutoff function is supported in $x \leq a_2$. Using Taylor expansion, we have the following properties for κ

$$\kappa_1(x/a_1) = 1 + O(x^4), \quad \kappa(x) = 1 + O(x^4).$$

For $\kappa_1(x)$, we can use induction and the same method as that in Section F.1.2 to estimate the derivatives of $\partial_x^i \kappa_1(x)$. The estimate is simpler since κ_1 has a simpler form. Using the Leibniz rule and the triangle inequality, we can obtain estimate $\partial_x^l \kappa(x)$ in $[a, b]$. Then we use these derivative estimates for $\kappa_x^{l+2} \kappa(x)$, evaluate $\kappa(x; a_1, a_2)$ on the grid points, and then use (E.5) to obtain a sharp estimate of $\partial_x^l \kappa(x)$ on $[a, b]$.

F.3. Estimate of $\rho_p(y)$. We estimate the weight $\rho_p(y)$ (E.4) in the representation of the stream function. Using symbolic computation, e.g., Matlab or Mathematica, we yield

$$\begin{aligned} \partial_x^9 \rho_p(y) &= \frac{f_2(y) - f_1(y)}{(g(y))^8}, \quad g(y) = 2 + 2y + y^2, \\ f_1 &= 288y^2 + 672y^3 + 504y^4, \quad f_2 = 16 + 168y^6 + 72y^7 + 9y^8. \end{aligned}$$

Since $f_1, f_2, g \geq 0$ are increasing in $y \geq 0$, for $y \in [y_l, y_u]$, we yield

$$|\partial_x^9 \rho_p(y)| \leq \frac{\max(f_2(y_u) - f_1(y_l), f_1(y_u) - f_2(y_l))}{(g(y_l))^8}.$$

We have a trivial estimate similar to (E.5)

$$(F.6) \quad \max_{x \in I} |f(x)| \leq \max(|f(x_l)|, |f(x_u)|) + \frac{h}{2} \|f_x\|_{L^\infty(I)},$$

which is useful if we do not have bound for f_{xx} .

Based on the above estimates, using the estimates (E.5), (F.6), ideas in Section E.2.1, and evaluating ρ_p on some grid points, we can obtain piecewise sharp bounds for $\partial_x^i \rho_p$ for $i \leq 8$.

APPENDIX G. ESTIMATING THE L^∞ AND HÖLDER NORM OF FUNCTIONS

In this appendix, we estimate $\|f\|_{L^\infty(D)}$ in the domain $D = [a, b] \times [c, d]$ given the grid point values $f(x_i, y_j)$ in D and the derivatives bound $\|\partial_x^i \partial_y^j f\|_{L^\infty}$. We want to obtain an error term as small as possible, while we do not need to evaluate f on too many grid points and its high order derivatives, which are expensive for some complicated function f , e.g. $f = (\partial_t - \mathcal{L})\widehat{W}$ (6.14). Based on these L^∞ estimates, we further develop the Hölder estimate of a function in Section G.6. These estimates will be used to verify the smallness of the residual error, e.g. $f = (\partial_t - \mathcal{L})\widehat{W}$ (6.14), in suitable energy norm.

We will develop three estimates based on three interpolating polynomials: the Newton polynomial, the Lagrangian interpolating polynomial, and the Hermite interpolation. Each method has its own advantages. For the Newton and the Lagrangian method, to obtain 4-th order error estimates, we only need to evaluate 4×4 grid point values of f .

(a) For the Newton method, we have a sharp error bound with a much smaller constant than that of the Lagrangian method.

(b) For the Lagrangian method, it is easier and more efficient to estimate the Lagrangian interpolating polynomials for grid points (x_i, y_j) in a general position.

In some situation, we need to estimate both f and ∇f and evaluate f and ∇f on 4×4 grid points. In this case, we can use $f(x_i, y_j)$ and $\nabla f(x_i, y_j)$ to build fourth and fifth order interpolating polynomials based on the Hermite interpolation. The 4-th order error estimate is as sharp as the Newton method. Moreover, in the 4-th order Newton or Lagrangian interpolation, we need $f \in C^4[x_0, x_3]$. In the case where f is only piecewise smooth in $[x_i, x_{i+1}]$, we cannot use these two methods. Instead, we evaluate $f(x_i)$, $f'(x_i)$ and construct the Hermite interpolation in each interval $[x_i, x_{i+1}]$. One disadvantage is that the estimate of the interpolating polynomials is more complicated and takes longer time in practice.

We do not pursue higher order error estimates since most of these estimates are applied to estimate the errors in Section 6, e.g. $(\partial_t - \mathcal{L})\widehat{W}$ (6.14), which is only piecewise smooth, and we do not use very small h in the whole computational domain.

G.1. Estimates based on the Newton polynomials. Given $x_0, x_1, x_2, \dots, x_k$, we first define the divided differences recursively

$$f[x] = f(x), \quad f[x, y] = \frac{f(y) - f(x)}{y - x}, \quad f[x_i, x_1, \dots, x_{j+1}] = \frac{f[x_{i+1}, x_{i+2}, \dots, x_{j+1}] - f(x_i, x_{i+1}, \dots, x_j)}{x_{j+1} - x_i}.$$

G.1.1. The Newton polynomials in 1D. We first discuss how to bound $f(x)$ in 1D. We consider the domain $[a, b]$ and denote

$$z_0 = a, \quad h = (b - a)/3, \quad z_i = z_0 + ih.$$

Denote

$$(G.1) \quad \begin{aligned} D_{1,i}f &= f(z_{i+1}) - f(z_i), \quad i = 0, 1, 2, \quad D_{2,i}f = D_{1,i+1}f - D_{1,i}f, \quad i = 0, 1, \\ D_3f &= D_{2,1}f - D_{2,0}f = f(z_3) - 3f(z_2) + 3f(z_1) - f(z_0). \end{aligned}$$

Let $\{x_i\}_{i=0}^3$ be a permutation of $\{z_i\}_{i=0}^3$. We construct the Newton polynomial

$$(G.2) \quad \begin{aligned} P(x) &= (f[x_0] + f[x_0, x_1](x - x_0)) + f[x_0, x_1, x_2](x - x_0)(x - x_1) \\ &\quad + f[x_0, x_1, x_2, x_3](x - x_0)(x - x_1)(x - x_2) \triangleq l(x) + q(x) + c(x), \end{aligned}$$

where $l(x)$, $q(x)$, $c(x)$ denote the linear, quadratic, and the cubic parts, respectively.

By standard error analysis of the Newton interpolation, the error part $R(x)$ can be bounded as follows

$$(G.3) \quad |f(x) - P(x)| \leq \frac{1}{24} \|\partial_x^4 f\|_{L^\infty[a, b]} \max_{x \in [a, b]} |\Pi_{0 \leq i \leq 3}(x - x_i)| = \frac{1}{24} \|\partial_x^4 f\|_{L^\infty[a, b]} \frac{(b - a)^4}{81}.$$

To obtain the last equality, using the definition of x_i, z_i , we write $z = a + th, t \in [0, 3]$ and get

$$\max_{x \in [a, b]} |\Pi_{0 \leq i \leq 3}(x - x_i)| = \max_{z \in [a, b]} |\Pi_{0 \leq i \leq 3}(z - z_i)| = \max_{t \in [0, 3]} h^4 |\Pi_{0 \leq i \leq 3}(t - i)| \leq h^4,$$

where we have used (G.56) in Lemma G.3 in the last inequality.

To bound $f(x)$, given the derivative bound of f and the above estimate, we only need to control $P(x)$. We choose different permutation $\{x_i\}_{i=0}^3$ of $\{z_i\}_{i=0}^3$ for z in different part of $[a, b]$:

$$\begin{aligned} x_i = z_i, \quad z \in [z_0, z_1], \quad (x_0, x_1, x_2, x_3) &= (z_2, z_1, z_0, z_3), \quad z \in [z_1, z_2], \\ (x_0, x_1, x_2, x_3) &= (z_3, z_2, z_1, z_0), \quad z \in [z_2, z_3]. \end{aligned}$$

Let I_z be the interval with endpoints x_0, x_1 . We have $z_0 \in I_z$. Since $l(x)$ in (G.2) is linear with $l(x_i) = f(x_i)$ and $|(x - x_0)(x - x_1)| \leq \frac{(x_1 - x_0)^2}{4}$, we get

$$|l(z)| \leq \max(|f(x_0)|, |f(x_1)|), \quad \max_{z \in I_z} |q(x)| \leq |f[x_0, x_1, x_2]| \frac{(x_1 - x_0)^2}{4} = |f[x_0, x_1, x_2]| \frac{h^2}{4}.$$

Since x_0, x_1, x_2 are three consecutive points with distance h and $I = [\min(x_0, x_1, x_2), \max(x_0, x_1, x_2)]$ covers z . In particular, we have

$$(G.4) \quad \max_{z \in I} |(z - x_0)(z - x_1)(z - x_2)| = \max_{z \in [0, 2h]} |z(z - h)(z - 2h)| \leq \frac{2}{3\sqrt{3}} h^3,$$

where we have used (G.54) in Lemma G.3 in the last inequality.

Next, we use (G.1) to simplify $f[x_i, x_{i+1}, \dots, x_j]$. For each case, a direct calculation yields

$$\begin{aligned} z \in [z_0, z_1] : |f[z_0, z_1, z_2]| &= \left| \frac{f[z_2, z_1] - f[z_1, z_0]}{z_2 - z_0} \right| = \left| \frac{1}{2h^2} (D_{1,1}f - D_{1,0}f) \right| = \frac{1}{2h^2} |D_{2,0}f|, \\ z \in [z_1, z_2] : |f(z_2, z_1, z_0)| &= \left| \frac{f[z_0, z_1] - f[z_1, z_2]}{z_0 - z_2} \right| = \left| \frac{1}{2h^2} (D_{1,1}f - D_{1,0}f) \right| = \frac{1}{2h^2} |D_{2,0}f|. \end{aligned}$$

Similarly, for $z \in [z_2, z_3]$, we get

$$|f(z_3, z_2, z_1)| = \frac{1}{2h^2} |D_{2,1}f|.$$

A direct calculation yields $|f[x_0, x_1, x_2, x_3]| = \frac{1}{6h^3} |D_3f|$. Thus, we get

$$\max_{z \in [a, b]} |c(x)| \leq \frac{2}{3\sqrt{3}} h^3 |f[x_0, x_1, x_2, x_3]| = \frac{2}{3\sqrt{3}} h^3 \cdot \frac{1}{6h^3} |D_3f| = \frac{1}{9\sqrt{3}} |D_3f|.$$

Combining the above estimates, we obtain

$$(G.5) \quad |P(x)| \leq \max \left(\max_{i=0,1,2} |f(z_i)| + c_1 |D_{2,0}f|, \max_{i=1,2,3} |f(z_i)| + c_1 |D_{2,1}f| \right) + c_2 |D_3f|.$$

where

$$c_1 = \frac{1}{8}, \quad c_2 = \frac{1}{9\sqrt{3}}.$$

G.1.2. A quadratic interpolation. We also need a cubic interpolation in the Hermite interpolation in Section G.4. Given $x_0 < x_1 < x_2$ with $x_2 - x_1 = x_1 - x_0$, we define

$$(G.6) \quad N_2(f, x_0, x_1, x_2)(x) \triangleq f(x_0) + f[x_0, x_1](x - x_0) + f[x_0, x_1, x_2](x - x_0)(x - x_1),$$

and construct $P(x) = N_2(f, x_0, x_1, x_2)(x)$.

We have an error estimate similar to (G.3) for $x \in [x_0, x_2]$

$$(G.7) \quad |P(x) - f(x)| \leq \frac{\|\partial_x^3 f\|_{L^\infty[x_0, x_2]}}{6} \max_{x \in [x_0, x_2]} |\Pi_{i=0,1,2}(x - x_i)| \leq \frac{\|\partial_x^3 f\|_{L^\infty[x_0, x_2]}}{6} \frac{2h^3}{3\sqrt{3}} = \frac{\|\partial_x^3 f\|_{L^\infty[x_0, x_2]} h^3}{9\sqrt{3}},$$

where we have used (G.4) in the last inequality.

Using the same estimates in Section G.1.1 for the linear part and quadratic part, we obtain

$$\begin{aligned} x \in [x_0, x_1] : |P(x)| &\leq \max(|f(x_0)|, |f(x_1)|) + \frac{1}{8} |f(x_0) - 2f(x_1) + f(x_2)|, \\ (G.8) \quad x \in [x_0, x_1] : |P(x)| &\leq \max(|f(x_0)|, |f(x_1)|) + \frac{1}{8} |f(x_0) - 2f(x_1) + f(x_2)|. \end{aligned}$$

Note that using the notation (G.1), we have $|D_{2,0}f| = |f(x_0) - 2f(x_1) + f(x_2)|$.

G.1.3. Generalization to 2D. Denote

$$D = [a, b] \times [c, d], \quad x_i = a + ih_1, \quad y_j = c + jh_2, \quad h_1 = (b - a)/3, \quad h_2 = (d - c)/3.$$

Suppose that $f(x_i, y_j)$ and $\|\partial_x^k \partial^l f\|_{L^\infty}, k + l \leq 4$ are given. Firstly, we treat y as a parameter and interpolate $f(x, y)$ in x . Denote

$$\begin{aligned} D_{i,1}f(y) &= f(x_{i+1}, y) - f(x_i, y), \quad 0 \leq i \leq 2, \quad D_{i,2}f(y) = D_{i+1,1}f(y) - D_{i,1}f(y), \quad 0 \leq i \leq 1, \\ D_3f(y) &= D_{2,1}f(y) - D_{2,0}f(y). \end{aligned}$$

Applying (G.3), (G.5), we get

$$\begin{aligned} \max_{x \in [a, b]} |f(x, y)| &\leq \max \left(\max_{i=0,1,2} |f(x_i, y)| + c_1 |D_{2,0}f(y)|, \max_{i=1,2,3} |f(x_i, y)| + c_1 |D_{2,1}f(y)| \right) \\ &\quad + c_2 |D_3f(y)| + \frac{1}{24} h_1^4 \|\partial_x^4 f\|_{L^\infty(D)}. \end{aligned}$$

Note that $f(x_i, y), D_{i,j}f(y)$ are 1D functions in y and their grid point values on y_j can be obtained from $f(x_i, y_j)$. We further apply (G.3), (G.5) to estimating $\|g\|_{L^\infty[c,d]}$ with $g = f(x_i, y), D_{i,j}f(y)$. Maximizing the above estimate over y yields the bound for f .

G.2. Estimates based on the Lagrangian interpolation. If the grid points x_i are not uniform, the estimates of the Newton polynomials can be more complicated. We develop another estimate based on the Lagrangian interpolating polynomials. Although these two interpolating polynomials for given grid points $f(x_i)$ are equivalent, the Lagrangian formulation is sometimes easier to estimate.

Firstly, let $p_i(x), q_j(y)$ be the Lagrange interpolating polynomials associated to the points $x_1 < \dots < x_k \in [a, b], y_1 < y_2 < \dots < y_k \in [c, d]$

$$(G.9) \quad p_i(x) = \prod_{j \neq i} \frac{x - x_j}{x_i - x_j}, \quad q_i(y) = \prod_{j \neq i} \frac{y - y_j}{y_i - y_j}.$$

For any $(x, y) \in D$, we consider the following decomposition by first interpolating f in x and then in y

$$\begin{aligned} (G.10) \quad f(x, y) &= \sum_{i=1}^k f(x_i, y) p_i(x) + R_1(x, y) = \sum_{i=1}^k \left(\sum_{j=1}^k f(x_i, y_j) q_j(y) + R_2(x_i, y) \right) p_i(x) + R_1(x, y) \\ &= \sum_{i,j=1}^k p_i(x) q_j(y) f(x_i, y_j) + \left(\sum_i R_2(x_i, y) p_i(x) + R_1(x, y) \right) \triangleq I + II. \end{aligned}$$

By standard error analysis of the Lagrange interpolation, the error part $R_1(x, y), R_2(x, y)$ can be bounded as follows

$$\begin{aligned} (G.11) \quad |R_1(x, y)| &\leq \frac{1}{k!} \|\partial_x^k f(x, y)\|_{L^\infty(D)} \max_{x \in [a, b]} \left| \prod_{i=1}^k (x - x_i) \right|, \\ |R_2(x_i, y)| &\leq \frac{1}{k!} \|\partial_y^k f(x, y)\|_{L^\infty(D)} \max_{y \in [c, d]} \left| \prod_{j=1}^k (y - y_j) \right|. \end{aligned}$$

Denote

$$C_1 = \max_{x \in [a, b]} \sum_{i=1}^k |p_i(x)|, \quad a_{ij} = f(x_i, y_j).$$

Note that the value C_1 only depends on the ratio $\frac{x_{i+1} - x_i}{b - a}, i = 1, \dots, k$, since from (G.9), we have

$$p_i(x) = \prod_{j \neq i} \frac{x - x_j}{x_i - x_j} = \prod_{j \neq i} \frac{t - t_j}{t_i - t_j}, \quad t = \frac{x - a}{b - a}, \quad t_j = \frac{x_j - a}{b - a}.$$

We will choose the grid points so that we also have $C_1 = \max_{y \in [c, d]} \sum_{i=1}^k |q_j(y)|$. See (G.15). We have the following trivial estimate for any c_j

$$(G.12) \quad \left| \sum_i p_i(x) c_i \right| \leq \sum_i |p_i(x)| \max |c_i| \leq C_1 \max |c_i|, \quad \left| \sum_j q_j(y) c_j \right| \leq C_1 \max |c_i|.$$

Next, we estimate I . Since $\sum_i p_i(x) = \sum_j q_j(y) = 1$, we expect that $I \approx f(x_i, y_j) + O(\max(h_1, h_2))$, where $h_1 = b - a, h_2 = d - c$. Thus, for some m to be chosen, we further decompose it into the mean and the variation and apply (G.12) to obtain

$$\begin{aligned} |I| &= |m + \sum_{i,j=1}^k p_i(x) q_j(y) (a_{ij} - m)| \leq |m| + \max_{i,j} |a_{ij} - m| \sum_i |p_i(x)| \sum_j |q_j(y)| \\ &= |m| + C_1^2 \max_{i,j} |a_{ij} - m|. \end{aligned}$$

We use the following trivial inequality for b_1, b_2, \dots, b_n

$$(G.13) \quad \max_i |b_i - b| = \frac{1}{2}(\max b_i - \min b_i), \quad b = \frac{1}{2}(\max b_i + \min b_i),$$

which can be proved by ordering b_i .

Thus, we optimize the estimate of I by choosing $m = \frac{1}{2}(\max_{i,j} a_{ij} + \min_{i,j} a_{ij})$.

We can obtain a sharper estimate as follows

$$\begin{aligned} (G.14) \quad |I| &= \left| \sum_j q_j(y) \left(\bar{a}_j + \sum_i p_i(x) (a_{ij} - \bar{a}_j) \right) \right| = \left| \sum_j q_j(y) (\bar{a}_j + S_j(x)) \right| \\ &\leq |\bar{a}| + \left| \sum_j q_j(y) (\bar{a}_j - \bar{a}) \right| + \left| \sum_j q_j(y) S_j(x) \right|, \quad S_j(x) = \sum_i p_i(x) (a_{ij} - \bar{a}_j). \end{aligned}$$

For a fixed j , we choose

$$\bar{a}_j = \frac{\max_i a_{ij} + \min_i a_{ij}}{2}, \quad \bar{a} = \frac{\max_j \bar{a}_j + \min \bar{a}_j}{2}.$$

Applying (G.12), (G.13), and the definition of $S_j(x)$ in (G.14), we yield

$$\left| \sum_j l_j(y) S_j(x) \right| \leq C_1 \cdot \max_j |S_j(x)|, \quad |S_j(x)| \leq C_1 \max_i |a_{ij} - \bar{a}_j| = \frac{C_1}{2} \left| \max_i a_{ij} - \min_i a_{ij} \right|.$$

Similarly, we have

$$\left| \sum_j l_j(x) (\bar{a}_j - \bar{a}) \right| \leq C_1 \max_j |\bar{a}_j - \bar{a}| = \frac{C_1}{2} (\max_j \bar{a}_j - \min_j \bar{a}_j).$$

Combining two parts, we yield an improved estimate for $|I|$

$$|I| \leq \frac{1}{2} \left| \max_j \bar{a}_j + \min_j \bar{a}_j \right| + \frac{C_1}{2} (\max_j \bar{a}_j - \min_j \bar{a}_j) + \frac{C_1^2}{2} \max_j \left| \max_i a_{ij} - \min_i a_{ij} \right|.$$

The above estimate is better if $a_{ij} = f(x_i, y_j)$ is smooth in x . Similarly, we can first sum over $p_i(x)$ and then sum over $q_j(y)$ in (G.14) to obtain another improved estimate.

In practice, we apply the above method to the third order estimate of f on $[a, b] \times [c, d]$, we choose

$$(G.15) \quad (x_1, x_2, x_3) = (a + \frac{1}{32}h_1, a + \frac{1}{2}h_1, a + \frac{31}{32}h_1), \quad (y_1, y_2, y_3) = (c + \frac{1}{32}h_2, c + \frac{1}{2}h_2, c + \frac{31}{32}h_2),$$

where $h_1 = b - a, h_2 = d - c$. Then we get

$$C_1 \leq 1.28, \quad \max_{x \in [a, b]} \prod_{i=1}^3 |x - x_i| \leq 0.04h_1^3, \quad \max_{x \in [a, b]} \prod_{i=1}^3 |y - y_i| \leq 0.04h_2^3.$$

Using (G.11), (G.12), and the above estimate, we get

$$|II| \leq C_1 \max_i \|R_2(x_i, y)\|_{L^\infty} + \|R_1\|_{L^\infty} \leq \frac{1}{6} \cdot 0.04 (C_1 \|\partial_y^3 f\|_{L^\infty(D)} h_2^3 + \|\partial_x^3 f\|_{L^\infty(D)} h_1^3).$$

We can also first interpolate f in y and then in x (G.10) to obtain another form of II . Similar estimates yield

$$|II| \leq \frac{1}{6} \cdot 0.04(C_1 \|\partial_x^3 f\|_{L^\infty(D)} h_1^3 + \|\partial_y^3 f\|_{L^\infty(D)} h_2^3).$$

We minimize the above two estimates to bound II .

G.3. Hermite interpolation in 1D. We first discuss the Hermite interpolation in 1D, and then generalize it to 2D.

Consider $x_0 < x_1 < x_2$ with $x_2 - x_1 = x_1 - x_0$. Denote by p_i, q_i the cubic polynomials such that

$$\begin{aligned} p_i(x_i) &= 1, & p_i(x_{1-i}) &= 0, & i &= 0, 1, & p'_i(x_j) &= 0, & j &= 0, 1, \\ q'_i(x_i) &= 1, & q'_i(x_{1-i}) &= 0, & i &= 0, 1, & q_i(x_j) &= 0, & j &= 0, 1, \end{aligned}$$

and

$$(G.16) \quad l_i = f(x_i), \quad m_i = h f'(x_i), \quad h = x_1 - x_0.$$

We consider the $4 - th$ and $5 - th$ order Hermite interpolations for f

$$\begin{aligned} (G.17) \quad H_4(f, x_0, x_1)(x) &= \sum_{i=0,1} (f(x_i)p_i(x) + f'(x_i)q_i(x)), \\ H_5(f, x_0, x_1, x_2)(x) &= H_4(x) + (f(x_2) - H_4(x_2)) \frac{(x - x_0)^2(x - x_1)^2}{(x_2 - x_0)^2(x_2 - x_1)^2}. \end{aligned}$$

For simplicity, we drop the dependence of f, x_i . Note that the coefficients of the polynomials p_i, q_i depend on x_0, x_1, x_2 only. It is easy to see that

$$H_4(x_i) = H_5(x_i) = f(x_i), \quad H'_4(x_i) = H'_5(x_i) = f'(x_i), \quad i = 0, 1, \quad H_5(x_2) = f(x_2).$$

G.3.1. Estimates of the interpolation error. For $[x_0, x_2]$, we have the following error estimate

$$(G.18) \quad |f(x) - H_4(x)| \leq \frac{1}{24} \|\partial_x^4 f\|_{L^\infty([x_0, x_2])} (x - x_0)^2 (x - x_1)^2, \quad x \in [x_0, x_2].$$

For $x \in [x_0, x_1]$, we have the following error estimates with further simplifications

$$\begin{aligned} |f(x) - H_4(x)| &\leq \frac{1}{24} \|\partial_x^4 f\|_{L^\infty([x_0, x_1])} (x - x_0)^2 (x - x_1)^2 \leq \frac{h^4}{384} \|\partial_x^4 f\|_{L^\infty([x_0, x_1])}, \\ |f(x) - H_5(x)| &\leq \frac{\|\partial_x^5 f\|_{L^\infty([x_0, x_2])}}{120} |(x - x_0)^2 (x - x_1)^2 (x - x_2)| \leq \frac{h^5}{1200} \|\partial_x^5 f\|_{L^\infty([x_0, x_2])}, \end{aligned}$$

where we have used (G.52), (G.57) in Lemma G.3 in the last inequality. The proof of the first inequality is standard. We consider the second estimate. For any $t \in [x_0, x_2]$, denote

$$R_t(x) = f(x) - H_5(x) - (f(t) - H_5(t)) \frac{(x - x_0)^2 (x - x_1)^2 (x - x_2)}{(t - x_0)^2 (t - x_1)^2 (t - x_2)}.$$

Clearly, we have $R_t(x_i) = 0, i = 0, 1, 2, R'_t(x_i) = 0, i = 0, 1, R_t(t) = 0$, and R_t has 6 zeros. For $f \in C^{4,1}$, applying the Rolle's theorem repeatedly up to $\partial_x^4 f$, we yield $\xi_1 \neq \xi_2 \in (x_0, x_2)$ with

$$0 = \partial_x^4 f(\xi_i) - C_1 - \frac{(f(t) - H_5(t))(120\xi_i - C_2)}{(t - x_0)^2 (t - x_1)^2 (t - x_2)},$$

where we have used $\partial_x^4 H_5(x) = C_1, \partial_x^4 (x - x_0)^2 (x - x_1)^2 (x - x_2) = 120x - C_2$. Rewriting the above identities and computing the difference, we obtain

$$|f(t) - H_5(t)| = \left| \frac{\partial_x^4 f(\xi_2) - \partial_x^4 f(\xi_1)}{120(\xi_2 - \xi_1)} (t - x_0)^2 (t - x_1)^2 (t - x_2) \right| \leq \frac{\|\partial_x^5 f\|_{L^\infty([x_0, x_1])}}{120} |(t - x_0)^2 (t - x_1)^2 (t - x_2)|.$$

Since t is arbitrary, this proves the second estimate in (G.19). The first estimate can be proved similarly. Next, we estimate the interpolating polynomials H_4, H_5 .

We should compare the first estimate (G.19) with (G.3). In (G.3), $x_1 - x_0 = \frac{b-a}{3} = h$ and the upper bound is $\frac{1}{24} \|\partial_x^4 f\|_\infty h^4$. In (G.19), for $x \in [x_0, x_1]$, using $|(x - x_0)(x - x_1)| \leq \frac{(x_1 - x_0)^2}{4}$, we obtain an extra small factor $\frac{1}{16}$. This is one of the main advantages of the Hermite interpolation.

G.3.2. *Estimate H_4, H_5 .* We consider $x \in [x_0, x_1]$ and introduce $t = \frac{x-x_0}{h}$. Recall l_i, m_i from (G.16). We have

$$\begin{aligned} G_4(t) &\triangleq H_4(x_0 + th) = H_4(x), \\ (G.20) \quad G_4(t) &= \left(l_0(1-t) + l_1t \right) + \left(t^2(t-1)(m_1 - (l_1 - l_0)) + (t-1)^2t(m_0 - (l_1 - l_0)) \right) \\ &\triangleq I(t) + II(t). \end{aligned}$$

To show that G_4 defined via the first identity has the second expression, it suffices to verify that the expression satisfies $G_4(i) = l_i = f(x_i), \partial_t G_4(i) = m_i = hf'(x_i)$, which is obvious. To estimate $H_4(x)$ on $[x_0, x_1]$, we only need to estimate $G_4(t)$ on $[0, 1]$.

The estimate of the linear part is trivial

$$|I(t)| = |l_0(1-t) + l_1t| \leq \max(|l_0|, |l_1|).$$

Denote

$$(G.21) \quad M_1 = \max(|m_1 - m_0|, |m_1 - (l_1 - l_0)|, |m_0 - (l_1 - l_0)|).$$

For $0 \leq t \leq \frac{1}{2}$, using (G.55) for $t(t-1)^2$, we have

$$\begin{aligned} II(t) &= t(t-1)(t(m_1 - (l_1 - l_0)) + (t-1)(m_0 - (l_1 - l_0))) \\ &= t(t-1)(t(m_1 - m_0) + (2t-1)(m_0 - (l_1 - l_0))), \\ |II(t)| &\leq M_1|t(t-1)|(t + |1-2t|) = M_1t(1-t)^2 \leq \frac{4}{27}M_1. \end{aligned}$$

Similarly, for $t \in [1/2, 1]$, writting $m_0 - (l_1 - l_0) = m_0 - m_1 + (m_1 - (l_1 - l_0))$, we get

$$II(t) = t(t-1)((t-1)(m_0 - m_1) + (2t-1)(m_1 - (l_1 - l_0))),$$

$$|II(t)| \leq |t(t-1)|(|t-1| + |2t-1|)M_1 = t(1-t)(1-t+2t-1)M_1 = t^2(1-t)M_1 \leq \frac{4}{27}M_1.$$

To obtain the last inequality, we apply (G.55) with $s = 1-t$. Therefore, we prove

$$(G.22) \quad |H_4(x)| = |G(t)| \leq \max(|l_0|, |l_1|) + \frac{4}{27} \max(|m_1 - m_0|, |m_1 - (l_1 - l_0)|, |m_0 - (l_1 - l_0)|).$$

For H_5 , since $x_2 - x_1 = x_1 - x_0 = h$, we have

$$H_4(x_2) = G_4(2) = -l_0 + 2l_1 + 4(m_0 - (l_1 - l_0)) + 2(m_0 - (l_1 - l_0)) = l_0 + 2m_0 + 4(m_1 - (l_1 - l_0)).$$

For $x \in [x_0, x_1]$ or $t \in [0, 1]$, since $|t(1-t)| \leq \frac{1}{4}$, we have

$$\frac{(x-x_0)^2(x-x_1)^2}{(x_2-x_0)^2(x_1-x_0)^2} = \frac{t^2(t-1)^2}{4} \leq \frac{1}{64}.$$

We obtain

$$(G.23) \quad \max_{x \in [x_0, x_1]} |H_5| \leq \max_{x \in [x_0, x_1]} |H_4(x)| + \frac{1}{64} |f(x_2) - H_4(x_2)|.$$

G.3.3. *Estimate derivatives in 1D.* In this subsection, we discuss how to estimate $\partial f(x)$ using the Hermite interpolation $\partial H_5(x)$. We consider ∂_x without loss of generality. Firstly, since $f(x) - H_5(x)$ has five zeros: two zeros at x_0 , two zeros at x_1 , and one zero at x_2 , we know that $\partial_x(f(x) - H_5(x))$ has four zeros: $x_0 < \xi < x_1 < \eta$. Using the Rolle's theorem and an argument similar to that in Section G.3.1, we get

$$|\partial_x(f(x) - H_5(x))| \leq \frac{1}{24} \|\partial_x^5 f\|_{L^\infty[x_0, x_2]} |(x-x_0)(x-x_1)(x-\xi)(x-\eta)|.$$

Next, for $x \in [x_0, x_1]$, we simplify the upper bound. Clearly, we have

$$|x - \xi| \leq \max(|x - x_0|, |x_1 - x|), |x - \eta| \leq |x - x_2|. \text{ We yield}$$

$$\begin{aligned} p(x) &\triangleq |(x-x_0)(x-x_1)(x-\xi)(x-\eta)| \leq |(x-x_0)(x-x_1)(x-x_2)| \max(|x-x_0|, |x-x_1|) \\ &= h^4 |t(1-t)(2-t)| \max(|1-t|, t) \triangleq h^4 q(t), \quad t = (x-x_0)h^{-1}. \end{aligned}$$

If $t \leq \frac{1}{2}$, we denote $s = (1-t)^2 \in [0, 1]$ and get

$$q(t) = t(1-t)^2(2-t) = (2t-t^2)s = (1-s)s \leq \frac{1}{4}.$$

If $t \in [1/2, 1]$, we get

$$q(t) = t(1-t) \cdot t(2-t) \leq \frac{1}{4} \cdot 1 = \frac{1}{4}.$$

Thus, for $x \in [x_0, x_1]$, we prove the error estimate

$$(G.24) \quad |\partial_x(f(x) - H_5(x))| \leq \frac{h^4}{96} \|\partial_x^5 f\|_{L^\infty[x_0, x_2]}.$$

Next, we estimate $\partial_x H_5$. Recall $t = \frac{x-x_0}{h}$. Using (G.17) and the chain rule, we get

$$(G.25) \quad \begin{aligned} H_5(x) &= H_4(x) + (f(x_2) - H_4(x_2)) \frac{t^2(t-1)^2}{4} = G_4(t) + (f(x_2) - H_4(x_2)) \frac{t^2(t-1)^2}{4}, \\ \partial_x H_5(x) &= \frac{1}{h} (\partial_t G_4(t) + (f(x_2) - H_4(x_2)) \partial_t \frac{t^2(t-1)^2}{4}) \triangleq \frac{1}{h} (I(t) + II(t)). \end{aligned}$$

We estimate two parts separately. Using (G.20), we get

$$(G.26) \quad I(t) \triangleq \partial_t G_4 = (l_1 - l_0) + (3t^2 - 2t)(m_1 - (l_1 - l_0)) + (3t^2 - 4t + 1)(m_0 - (l_1 - l_0)).$$

Note that $l_1 - l_0, m_1, m_0$ are approximations of $hf'(x)$ and have cancellations. We discuss different $t \in [0, 1]$ to exploit the cancellations.

Denote $a \vee b = \max(a, b)$. If $t \leq \frac{1}{3}$, we get

$$I(t) = (4t - 3t^2)(l_1 - l_0) + (3t^2 - 4t + 1)m_0 + (2t - 3t^2)(l_1 - l_0 - m_1).$$

Since $t \leq \frac{1}{3}$, we get

$$4t - 3t^2 > 0, \quad 3t^2 - 4t + 1 = (1 - 3t)(1 - t) \geq 0, \quad 2t - 3t^2 = 3t\left(\frac{2}{3} - t\right) \leq \frac{1}{3},$$

where the last inequality is equivalent to $(t - \frac{1}{3})^2 \geq 0$. It follows

$$(G.27) \quad |I(t)| \leq |l_1 - l_0| \vee m_0 (4t - 3t^2 + 3t^2 - 4t + 1) + \frac{1}{3} |l_1 - l_0 - m_1| = |l_1 - l_0| \vee m_0 + \frac{1}{3} |l_1 - l_0 - m_1|.$$

The estimate of $t \in [2/3, 1]$ is similar by swapping t and $1-t$, m_0 and m_1 , p_0 and p_1 . We get

$$(G.28) \quad |I(t)| \leq |l_1 - l_0| \vee m_1 + \frac{1}{3} |l_1 - l_0 - m_0|.$$

For $t \in [1/3, 2/3]$, we rewrite $I(t)$ as follows

$$I(t) = l_1 - l_0 + (4t - 3t^2 - 1)(l_1 - l_0 - m_0) + (2t - 3t^2)(l_1 - l_0 - m_1).$$

Since $t \in [1/3, 2/3]$, we get

$$4t - 3t^2 - 1 = (3t - 1)(1 - t) \geq 0, \quad 2t - 3t^2 = t(2 - 3t) \geq 0,$$

$$4t - 3t^2 - 1 + 2t - 3t^2 = 6t - 6t^2 - 1 = 6t(1 - t) - 1 \leq \frac{3}{2} - 1 \leq \frac{1}{2}.$$

Thus, using $4t - 3t^2 - 1 + 2t - 3t^2 = 6t - 6t^2 - 1 \leq \frac{1}{2}$, we obtain

$$(G.29) \quad I(t) \leq |l_1 - l_0| + \frac{1}{2} (|l_1 - l_0 - m_0| \vee |l_1 - l_0 - m_1|).$$

Combining three cases (G.27)-(G.28), we obtain the bound for $\partial_t G_4$.

For the second term in (G.25), using (G.54), we get

$$(G.30) \quad \partial_t \frac{t^2(t-1)^2}{4} = t(t-1)(t-\frac{1}{2}), \quad |t(t-1)(t-\frac{1}{2})| = \frac{1}{8} |2t(1-2t)(2-2t)| \leq \frac{1}{8} \cdot \frac{2}{3\sqrt{3}} \leq \frac{1}{12\sqrt{3}},$$

which implies

$$(G.31) \quad \left| \frac{1}{h} II(t) \right| \leq \frac{1}{12\sqrt{3}h} |f(x_2) - H_4(x_2)|.$$

Combining the estimates (G.27)-(G.31), we obtain the estimate for $\partial_x H_5$.

G.4. Hermite interpolation in 2D. The estimate in 2D is more involved. Consider $x_0 < x_1 < x_2, y_0 < y_1 < y_2$ with $x_2 - x_1 = x_1 - x_0, y_2 - y_1 = y_1 - y_0$. The domain D can be decomposed into 4 blocks with size $h_1 \times h_2$. For the 5-th order interpolation, we assume $(x, y) \in [x_0, x_1] \times [y_0, y_1]$ without loss of generality. For the 4-th order interpolation, we only need 1 block. Denote

$$(G.32) \quad \begin{aligned} D &= [x_0, x_2] \times [y_0, y_2], \quad h_1 = x_1 - x_0, \quad h_2 = y_1 - y_0, \\ t &= (x - x_0)h_1^{-1}, \quad s = (y - y_0)h_2^{-1}. \end{aligned}$$

G.4.1. Estimate the L^∞ norm. We first consider the estimate of $\|f\|_{L^\infty}$. We treat y as a parameter and use (G.17) to construct the 4-th and 5-th order interpolations in x : $H_4(x, y), H_5(x, y)$. Using the formula in (G.20), we have

$$(G.33) \quad \begin{aligned} G_5(t, s) &\triangleq H_5(x, y) = H_4(x, y) + (f(x_2, y) - H_4(x_2, y)) \frac{t^2(t-1)^2}{4}, \\ H_4(x, y) &= f(x_0, y)(1-t) + f(x_1, y)t + t^2(t-1)(hf'(x_1, y) - (f(x_1, y) - f(x_0, y))) \\ &\quad + (t-1)^2t(hf'(x_0, y) - (f(x_1, y) - f(x_0, y))). \end{aligned}$$

Using (G.19), we have the error bound in x

$$(G.34) \quad |H_5(x, y) - f(x, y)| \leq \frac{1}{1200} \|\partial_x^5 f\|_{L^\infty(D)} h_1^5.$$

We need to further interpolate $G_5(t, s), H_5(x, y)$ in the y direction. To achieve the overall 5-th order error, we do not need to apply a high order interpolation to each coefficient. In particular, for the linear term, we apply the 5-th order Hermite interpolation to $f(x_i, y)$ in y using $f(x_i, y_j), j = 0, 1, 2$ and $\partial_y f(x_i, y_j), j = 0, 1$ for $i = 0, 1$ and denote it by $A_i(y)$, i.e.

$$(G.35) \quad A_i(y) = H_5(f(x_i, \cdot), y_0, y_1, y_2)(y)$$

using the notation in (G.17). Applying (G.22), we have the error bound in y

$$(G.36) \quad |f(x_i, y) - A_i(y)| \leq \frac{1}{1200} \|\partial_y^5 f\|_{L^\infty(D)} h_2^5.$$

Denote

$$(G.37) \quad M_i(y) \triangleq h f'(x_i, y) - (f(x_1, y) - f(x_0, y)).$$

For $M_i(y), i = 1, 2$, it is of order h_1^2 . Thus, we apply the cubic interpolation in Section G.1.2 to these functions in y direction on grids y_0, y_1, y_2 and denote it by $Q_i(y)$. Using the notation (G.6), we have

$$(G.38) \quad Q_i(y) = N_2(M_i, y_0, y_1, y_2)(y).$$

Applying (G.7), we have the error bound

$$(G.39) \quad |M_i(y) - Q_i(y)| \leq \frac{h_2^3}{9\sqrt{3}} \|\partial_y^3 M_i(y)\|_{L^\infty([y_0, y_2])} \leq \frac{h_2^3 h_1^2}{18\sqrt{3}} \|\partial_x^2 \partial_y^3 f\|_{L^\infty(D)},$$

where we have used the following estimate with $c = a, b, g = \partial_y^3 f(\cdot, y)$ in the last inequality

$$\left| (b-a)g'(c) - (g(b) - g(a)) \right| = \left| \int_a^b g'(c) - g'(s) ds \right| \leq \|g''\|_{L^\infty[a, b]} \int_a^b |c-a| ds = \frac{(b-a)^2}{2} \|g''\|_{L^\infty[a, b]}.$$

For the last term $f(x_2, y) - H_4(x_2, y)$, it is already very small and of order h_1^4 . We use first order estimate and then (G.18) with $x = x_2$ to bound it directly

$$(G.40) \quad \begin{aligned} |f(x_2, y) - H_4(x_2, y)| &\leq \max_{j=0,1} |f(x_2, y_j) - H_4(x_2, y_j)| + \frac{h_2}{2} |\partial_y(f(x_2, y) - H_4(x_2, y))| \\ &\leq \max_{j=0,1} |f(x_2, y_j) - H_4(x_2, y_j)| + \frac{h_2 h_1^4}{2 \cdot 6} \|\partial_y \partial_x^4 f\|_{L^\infty(D)}. \end{aligned}$$

Estimate the 2D interpolating polynomials for f . We obtain the 2D interpolating polynomials in x, y for $H_4(x, y)$ as follows

$$(G.41) \quad P_4(x, y) = \left(A_0(y)(1-t) + A_1(y)t \right) + \left(t^2(t-1)Q_1(y) + t(t-1)^2Q_0(y) \right) = I(t, y) + II(t, y).$$

Combining (G.34)-(G.40) and using $t + (1-t) = 1$, $|t^2(1-t)| + |(1-t)^2t| = (1-t)t \leq \frac{1}{4}$, we have the following error bound

$$(G.42) \quad \begin{aligned} |P_4(x, y) - f(x, y)| &\leq \frac{1}{64} \max_{j=0,1} |f(x_2, y_j) - H_4(x_2, y_j)| + \frac{1}{72\sqrt{3}} h_1^2 h_2^3 \|\partial_x^2 \partial_y^3 f\|_{L^\infty(D)} \\ &\quad + \frac{1}{1200} (h_1^5 \|\partial_x^5 f\|_{L^\infty(D)} + h_2^5 \|\partial_y^5 f\|_{L^\infty(D)}) + \frac{h_2 h_1^4}{768} \|\partial_y \partial_x^4 f\|_{L^\infty(D)}, \end{aligned}$$

where the constant $\frac{1}{768}$ comes from (G.40) and $\frac{1}{768} = \frac{1}{64} \cdot \frac{1}{16}$.

To estimate $P_4(x, y)$ (G.41), we use estimates similar to (G.22). The estimate of the linear part is trivial

$$|I(t, y)| \leq \max_{i=0,1} \|A_i(y)\|_{L^\infty[y_0, y_1]}, \quad y \in [y_0, y_1].$$

Since $A_i(y)$ (G.35) is the Hermite polynomial in y , we can use the method in Section G.3 to estimate it. For II , following the derivations between (G.21) to (G.22) and by considering two cases: $t \leq \frac{1}{2}$ and $t > \frac{1}{2}$, we obtain

$$|II(t, t)| \leq \frac{4}{27} \max(|Q_1(y) - Q_0(y)|, |Q_1(y)|, |Q_0(y)|).$$

Since $Q_i, Q_1 - Q_0$ are quadratic interpolating polynomials of $M_i, M_1 - M_0$ (G.37) on y_0, y_1, y_2 , we can use (G.8) to estimate the $L^\infty[y_0, y_1]$ norm.

G.4.2. Estimates of the $\partial f(x, y)$ in 2D. Now, we consider how to estimate $\partial f(x, y)$ using the Hermite interpolation. We consider ∂_x without loss of generality. Recall the notation (G.32). We first fix y as a parameter and interpolate $f(x, y)$ in x using the same method as (G.33). Using the error estimate (G.24), we yield

$$(G.43) \quad |\partial_x(f(x, y) - H_5(x, y))| \leq \frac{h_1^4}{96} \|\partial_x^5 f\|_{L^\infty(D)}.$$

Using the computation (G.25), (G.26), (G.30) in Section G.3.3 and the notation (G.16) for m_i, l_i , we have

$$\begin{aligned} h_1 \partial_x H_5(x, y) &= h_1 \partial_x H_4(x, y) + (f(x_2, y) - H_4(x_2, y))t(t-1)(t-\frac{1}{2}), \\ h_1 \partial_x H_4(x, y) &= f(x_1, y) - f(x_0, y) + (3t^2 - 2t)(hf'(x_1, y) - (f(x_1, y) - f(x_0, y))) \\ &\quad + (3t^2 - 4t + 1)(hf'(x_0, y) - (f(x_1, y) - f(x_0, y))) \\ &= f(x_0, y) - f(x_1, y) + (3t^2 - 2t)M_1(y) + (3t^2 - 4t + 1)(M_0(y)), \end{aligned}$$

where $t = \frac{x-x_0}{h_1}$ (G.32), and we have used (G.37) to simplify the presentation.

Next, we interpolate the above functions in y . We want to achieve an overall 4-th order approximation for $\partial_x H_4(x, y)$. For $f(x_1, y) - f(x_0, y)$, we use the 4-th order Hermite interpolation in y based on the grid point values $f(x_1, y_j) - f(x_0, y_j), \partial_y(f(x_1, y_j) - f(x_0, y_j)), j = 0, 1$ and denote it as $B(y)$, i.e.

$$(G.44) \quad B(y) \triangleq H_4(f(x_1, \cdot) - f(x_0, \cdot), y_0, y_1)$$

using the notation (G.17). By (G.19), we have the error estimate

$$(G.45) \quad \left| \frac{B(y)}{h_1} - \frac{f(x_1, y) - f(x_0, y)}{h_1} \right| \leq \frac{1}{384} \left\| \partial_y^4 \frac{f(x_1, y) - f(x_0, y)}{h_1} \right\|_{L^\infty([y_0, y_1])} \leq \frac{1}{384} \left\| \partial_y^4 \partial_x f \right\|_{L^\infty(D)}.$$

For M_i , we apply the same quadratic interpolation Q_i in y (G.38). It satisfies the error bound (G.39).

For $f(x_2, y) - H_4(x_2, y)$, we use the same estimate (G.40), which along with (G.30) implies

$$(G.46) \quad \begin{aligned} \frac{1}{h_1} \left| (f(x_2, y) - H_4(x_2, y))t(t-1)(t-\frac{1}{2}) \right| &\leq \frac{1}{12h_1} \max_{j=0,1} |f(x_2, y_j) - H_4(x_2, y_j)| \\ &\quad + \frac{h_2 h_1^3}{12 \cdot 12\sqrt{3}} \|\partial_y \partial_x^4 f\|_{L^\infty(D)}. \end{aligned}$$

Estimate the 2D interpolating polynomials for $\partial_x f$. Now, we construct the interpolating polynomials for $h_1 \partial_x H_4$ as follows

$$S_4(x, y) = B(y) + (3t^2 - 2t)Q_1(y) + (3t^2 - 4t + 1)Q_0(y).$$

Combining the estimate (G.45) and using the triangle inequality, we can estimate the error $\frac{1}{h_1} S_4(x, y) - f(x, y)$.

It remains to estimate $S_4(x, y)$. We further decompose the above approximation as the linear part and the nonlinear part. The linear part is the main term, and we want to obtain a sharper estimate. The nonlinear part is smaller, which will be estimated using the triangle inequality. Since B is the 4-th order Hermite interpolation in y (G.44), we can apply the decomposition (G.20) to B . Since Q_i is the quadratic interpolation of M_i (G.37), (G.38), we can apply the decomposition (G.6) to Q_i .

$$(G.47) \quad S_4 = S_{lin} + S_{nlin}, \quad S_\sigma(y) \triangleq B_\sigma(y) + (3t^2 - 2t)Q_{1,\sigma}(y) + (3t^2 - 4(t+1))Q_{0,\sigma}(y)$$

where $\sigma \in \{lin, nlin\}$, f_{lin} denotes the linear part, and f_{nlin} denotes the nonlinear part.

Since S_{lin} is linear in y and $B(y_j) = f(x_1, y_j) - f(x_0, y_j)$, $Q_i(y_j) = M_i(y_j)$ for $j = 0, 1$ (the interpolating polynomials agree with the functions on the grid points), we get

$$\begin{aligned} |S_{lin}(y)| &\leq \max_{i=0,1} \left| B_{lin}(y) + (3t^2 - 2t)Q_{1,lin}(y_i) + (3t^2 - 4(t+1))Q_{0,lin}(y_i) \right|, \\ &= \max_{i=0,1} \left| f(x_1, y_i) - f(x_0, y_i) + (3t^2 - 2t)M_1(y_i) + (3t^2 - 4(t+1))M_0(y_i) \right|. \end{aligned}$$

Recall the definition of M_i in (G.37). The polynomials inside $|\cdot|$ is the 1D polynomial in t with the same form as $I(t)$ (G.26). Thus it can be estimated using the method in Section G.3.3 for 1D Hermite interpolation of the derivative.

For the nonlinear part,

$$(G.48) \quad S_{nlin} = B_{nlin}(y) + (3t^2 - 2t)Q_{1,nlin}(y) + (3t^2 - 4t + 1)Q_{0,nlin}(y),$$

we recall the definition of B (G.44) and Q (G.38). The estimate of B_{nlin} follows the method of estimating $II(t)$ in (G.20), (G.22) with l_i, m_i replacing by

$$\tilde{l}_i = f(x_1, y_i) - f(x_0, y_i), \quad \tilde{m}_i = h_2 \partial_y(f(x_1, y_i) - f(x_0, y_i)),$$

which gives

$$|B_{nlin}(y)| \leq \frac{4}{27} \max(|\tilde{m}_0, \tilde{m}_1|, |\tilde{m}_0 - (\tilde{l}_1 - \tilde{l}_0)|, |\tilde{m}_1 - (\tilde{l}_1 - \tilde{l}_0)|).$$

The estimate of the Q_{nlin} follows that in (G.8) and Section G.1.2, which gives

$$|Q_{i,nlin}| \leq \frac{1}{8} |M_i(y_0) - 2M_i(y_1) + M_i(y_2)|.$$

Using (G.53) in Lemma G.3, for $t \in [0, 1]$, we prove

$$\begin{aligned} &|(3t^2 - 2t)Q_{1,nlin}(y) + (3t^2 - 4t + 1)Q_{0,nlin}(y)| \\ &\leq (|3t^2 - 2t| + |3t^2 - 4t + 1|) \max_{i=0,1} |Q_{i,nlin}(y)| \leq \frac{1}{8} \max_{i=0,1} |M_i(y_0) - 2M_i(y_1) + M_i(y_2)|. \end{aligned}$$

Thus, we yield the estimate of S_{nlin} . Combining the above estimates of S_{lin} and S_{nlin} and using (G.47), we obtain the estimate of S_4 . We remark that one needs to further divide the above bounds by $\frac{1}{h_1}$ to get the bound for $\frac{S_4}{h_1}$.

G.5. Weighted estimates of a function using derivatives. In our estimate of the residual error or some norms, we need to estimate $F(x)\rho(x)$ near $x = 0$ with singular weight ρ rigorously. In this section, we discuss how to use the estimate of the derivatives of F to estimate the weighted norm of F . Note that the estimate of $\partial_x^i \partial_y^j F$ can be established using the methods in Sections G.1-G.4.

Typical behaviors of ρ near $x = 0$ is $|x|^{-k}$, $k = 2, \frac{5}{2}, 3$ or $|x|^{-k} x_1^{-1/2}$. By decomposing ρ into the singular part $|x|^{-i} x_1^{-j/2}$ and the regular part, we only need to estimate $F|x|^{-i} x^{-j/2}$. Denote

$$E_x(F, i)(x, y) \triangleq \frac{1}{x^{i+1}} \int_0^x F(z, y)(x-z)^i dz, \quad E_y(F, i)(x, y) \triangleq \frac{1}{y^{i+1}} \int_0^y F(x, z)(y-z)^i dz.$$

Due to the Fubini's Theorem, we get

$$E_x(E_y(F, j), i) = E_y(E_x(F, i), j) = \frac{1}{x^{i+1} y^{j+1}} \int_0^x \int_0^y F(x-t)^i (y-s)^j dt ds \triangleq E_{ij}(F)(x, y).$$

Using the piecewise bound of F , we can bound these functions easily.

For $F(x, y)$ odd in x and $\nabla^k F(0) = 0$ for $k \leq 2$, we have the following identities

$$\begin{aligned} F(x, y) &= \int_0^y F_y(x, z) dz + F(x, 0) \\ &= \int_0^x \int_0^y F_{xyy}(t, s)(y-s) dt ds + y \int_0^x F_{xxy}(t, 0)(x-t) dt + \frac{1}{2} \int_0^x F_{xxx}(t, 0)(x-t)^2 dt. \end{aligned}$$

Using the average operators, we yield

$$|F(x, y)| \leq E_{xy}(|F_{xyy}|, 0, 1) xy^2 + x^2 y E_x(|F_{xxy}|, 1) + \frac{x^3}{2} E_x(|F_{xxx}|, 2).$$

Denote $\beta = \arctan(\frac{y}{x})$, $r = (x^2 + y^2)^{1/2}$. Using these estimates, for $a + b = 3, b \leq 1$, we get

$$\begin{aligned} (G.49) \quad \frac{|F(x, y)|}{r^a x^b} &\leq \frac{1}{2} E_x(|F_{xxx}|, 1) \cos^{3-b}(\beta) + E_{xy}(|F_{xxy}|, 0, 1) \cos \beta^{1-b} \sin^2 \beta \\ &\quad + E_x(|F_{xxy}|, 1) \cos^{2-b} \sin \beta. \end{aligned}$$

Since we have the bounds for these coefficients, e.g., $E_{xy}(|F_{xxy}|, 0, 1)$, by maximizing $\beta \in [0, \pi/2]$, we obtain the bounds for $\frac{F}{r^3}$ and $\frac{F}{r^{5/2} x^{1/2}}$.

Similarly, we can bound $\frac{\partial_x^i \partial_y^j F}{r^k}$, $i + j + k \leq 3$. For odd F , we have

$$\begin{aligned} (G.50) \quad |F| &= \left| \int_0^x F_x(z, y) dz \right| \leq E_x(|F_x|, 0) x, \\ |F| &= \left| \int_0^y F_y(x, z) dz + F(x, 0) \right| = \left| \int_0^x \int_0^y F_{xy}(t, s) dx dy + \int_0^x F_{xx}(t, 0)(x-t) dt \right| \\ &\leq E_{xy}(|F_{xy}|, 0, 0) xy + E_x(|F_{xx}|, 1)(x, 0) x^2, \quad \nabla^k F(0) = 0, k = 0, 1. \end{aligned}$$

Using estimate similar to (G.49), we can bound $\frac{F}{|x|^2}, \frac{F}{|x|}$.

Weighted derivatives. Similarly, we estimate $\frac{\partial_{x_i} F}{|x|^2}, \frac{\partial_{x_i} F x_j^{1/2}}{|x|^{5/2}}$. For odd F with $\nabla^k F = 0, k \leq 2$, using (G.49) with F replaced by F_y , we get

$$|F_y| \leq E_{xy}(|F_{xyy}|, 0, 0) xy + E_x(|F_{xxy}|, 1)(x, 0) x^2.$$

Then, we can use the method in (G.49) to estimate

$$\frac{|x_j|^\alpha \partial_{x_i} F}{|x|^{2+\alpha}} = (g(\beta))^\alpha \frac{\partial_{x_i} F}{|x|^2}, \quad g(\beta) = \cos \beta, \text{ or } \sin \beta.$$

We also need to estimate $\frac{F_x}{|x|}$ and $\frac{F_y}{|x|}$. Using (G.50) with F replaced by F_y , we get

$$|F_y| \leq E_x(|F_{xy}|, 0) x.$$

For $\frac{F_x}{|x|}$, we have two cases. If $F(x, 0) \equiv 0$, e.g., F satisfies the Dirichlet boundary condition, we yield

$$|F_x| \leq E_y(|F_{xy}|, 0) y.$$

Without the vanishing conditions, we require $\nabla F = 0$ and yield

$$\begin{aligned} |F_x(x, y)| &= \left| \int_0^y F_{xy}(x, z) dz + F_x(x, 0) \right| = \left| \int_0^y F_{xy}(x, z) dz + \int_0^x F_{xx}(z, 0) dz \right| \\ &\leq E_y(|F_{xy}|, 0)y + E_x(|F_{xx}|, 0)(x, 0)x. \end{aligned}$$

Then we apply the method in (G.49) to estimate $\frac{\partial_{x_i} F}{|x|}$.

G.6. Hölder estimate of the functions. In the following two sections, we estimate the Hölder seminorms $[f]_{C_x^{1/2}}$ or $[f]_{C_y^{1/2}}$ of some function f , e.g. $f = (\partial_t - \mathcal{L})\widehat{W}$ in (6.14), based on the previous L^∞ estimates. We will develop two approaches.

Suppose that we have bounds for $\partial_x f, \partial_y f$ and f . Firstly, we consider the $C_x^{1/2}$ estimate. For $x_1 < y_1$ and $x_2 = y_2$, we have

$$I = \frac{|f(x) - f(y)|}{|x - y|^{1/2}} \leq |x - y|^{1/2} \frac{1}{|x - y|} \int_{x_1}^{y_1} |f_x(z_1, x_2)| dz_1.$$

We further bound the average of f_x to obtain the first estimate. We have a second estimate

$$\begin{aligned} |I| &= \left| \int_{x_1}^{y_1} f_x(z_1, x_2) dz_1 \right| \cdot \frac{1}{|x - y|^{1/2}} \leq \|f_x x^{1/2}\|_\infty \int_{x_1}^{y_1} z_1^{-1/2} dz_1 \cdot \frac{1}{|x - y|^{1/2}} \\ &\leq \|f_x x^{1/2}\|_\infty 2 \frac{y_1^{1/2} - x_1^{1/2}}{|x - y|^{1/2}} = \|f_x x^{1/2}\|_\infty \frac{2\sqrt{y_1 - x_1}}{\sqrt{x_1} + \sqrt{y_1}}. \end{aligned}$$

We also have a trivial L^∞ estimate

$$|I| \leq \|f x_1^{-1/2}\|_\infty \frac{x_1^{1/2} + y_1^{1/2}}{|x - y|^{1/2}}, \quad |I| \leq \|f\|_\infty \frac{2}{|x - y|^{1/2}}.$$

Similar L^∞ and Lipschitz estimates apply to $\|f\|_{C_y^{1/2}}$.

Near the origin, optimizing the above estimates, for $x_2 = y_2$, we obtain

$$\left| \frac{f(x) - f(y)}{|x - y|^{1/2}} \right| \leq \min(\|f_x x^{1/2}\|_\infty 2t, \|f x_1^{-1/2}\|_\infty t^{-1}), \quad t = \frac{\sqrt{y_1 - x_1}}{\sqrt{x_1} + \sqrt{y_1}}.$$

In the Y -direction, $x_1 = y_1, x_2 \leq y_2$, we use

$$\begin{aligned} I_Y &= \left| \frac{f(x) - f(y)}{|x - y|^{1/2}} \right| \leq \frac{1}{|x_2 - y_2|^{1/2}} \int_{x_2}^{y_2} |f_y(x_1, z_2)| |z|^{1/2} \cdot |z|^{-1/2} dz_2 \leq \|f_y x|^{1/2}\|_\infty \frac{|x_2 - y_2|^{1/2}}{|x|^{1/2}}, \\ I_Y &\leq \|f x^{-1/2}\|_\infty \frac{2x_1^{1/2}}{|x_2 - y_2|^{1/2}}. \end{aligned}$$

Since $x_1 \leq |x|$, the minimum of these two estimates are not singular near $x = 0$. In particular, we optimize two estimates to estimate I_Y .

From the above estimates, to obtain sharp Hölder estimate of f , we estimate the piecewise bounds of $f, f x_1^{-1/2}, f|x|^{-1/2}, f_x, f_y, f_x|x_1|^{1/2}, f_y|x|^{1/2}$, which are local quantities. These estimates can be established using the methods in Sections G.1-G.4.

G.7. The second approach of Hölder estimate of a given function. We develop an additional approach to estimate $I(f) = \frac{|f(x) - f(z)|}{|x - z|^{1/2}}$ that is sharper if $|x - z|$ is not small and f is smooth. Suppose that we can evaluate the grid point value of f and have derivatives bound of f .

We estimate $I(f) = \frac{|f(x) - f(z)|}{|x - z|^{1/2}}$ for $x \in [x_l, x_u], z \in [z_l, z_u]$. Denote by \hat{f} the linear approximation of f with $\hat{f}(x_i) = f(x_i)$ on the grid point x_i . We have the following Lemma.

Lemma G.1. *Suppose that f is linear on $[x_l, x_u], [z_l, z_u]$ and $x_l \leq x_u \leq z_l \leq z_u$. Then we have*

$$\max_{x \in [x_l, x_u], z \in [z_l, z_u]} \frac{|f(x) - f(z)|}{|x - z|^{1/2}} = \max_{\alpha, \beta \in \{l, u\}} \frac{|f(x_\alpha) - f(z_\beta)|}{|x_\alpha - z_\beta|^{1/2}}.$$

The above Lemma shows that for the linear interpolation of f , the maximum of the Hölder norm is achieved at the grid point.

Proof. Denote by M the right hand side in the Lemma. Clearly, it suffices to prove that the left hand side is bounded by M . We fix $x \in [x_l, x_u], z \in [z_l, z_u]$. Suppose that

$$x = a_l x_l + a_u x_u, \quad z = b_l z_l + b_u z_u, \quad a_u + a_l = 1, \quad b_l + b_u = 1,$$

for $a_l, b_l \in [0, 1]$. Denote

$$m_{\alpha\beta} = a_\alpha b_\beta, \quad \alpha, \beta \in \{l, u\}.$$

Since $f(x)$ is linear on $[x_l, x_u]$ and $[z_l, z_u]$, we get

$$f(x) = a_l f(x_l) + a_u f(x_u), \quad f(z) = b_l f(z_l) + b_u f(z_u).$$

For any function g linear on $[x_l, x_u], [z_l, z_u]$, e.g., $g(x) = 1, g(x) = x, g(x) = f(x)$, we have

$$(G.51) \quad g(x) = \sum_{\alpha, \beta \in \{l, u\}} m_{\alpha\beta} g(x_\alpha), \quad g(z) - g(x) = \sum_{\alpha, \beta \in \{l, u\}} m_{\alpha\beta} (g(z_\beta) - g(x_\alpha)),$$

Using the above identities and the triangle inequality and the definition of M , we yield

$$|f(x) - f(z)| = \left| \sum_{\alpha, \beta \in \{l, u\}} m_{\alpha\beta} (f(x_\alpha) - f(z_\beta)) \right| \leq \sum_{\alpha, \beta \in \{l, u\}} m_{\alpha\beta} M |x_\alpha - z_\beta|^{1/2}.$$

Using the Cauchy-Schwarz inequality, $|x_\alpha - z_\beta| = z_\beta - x_\alpha$ and (G.51), we establish

$$\begin{aligned} |f(x) - f(z)| &\leq \sum_{\alpha, \beta \in \{l, u\}} m_{\alpha\beta} \sum_{\alpha, \beta \in \{l, u\}} m_{\alpha\beta} M |x_\alpha - z_\beta|^{1/2} = \sum_{\alpha, \beta \in \{l, u\}} m_{\alpha\beta} M |x_\alpha - z_\beta|^{1/2} \\ &= M \left(\sum_{\alpha, \beta \in \{l, u\}} m_{\alpha\beta} (z_\beta - x_\alpha) \right)^{1/2} = M (z - x)^{1/2}. \end{aligned}$$

The desired result follows. \square

We generalize Lemma G.1 to 2D as follows.

Lemma G.2. *Let $I_x = [x_l, x_u], I_z = [z_l, z_u], I_y = [y_l, y_u]$ with $x_l \leq x_u \leq z_l \leq z_u$. Suppose that f is linear on $I_x \times I_y$ and $I_z \times I_y$. Then we have*

$$\max_{x \in I_x, z \in I_z, y \in I_y} \frac{|f(x, y) - f(z, y)|}{|x - z|^{1/2}} = \max_{\alpha, \beta, \gamma \in \{l, u\}} \frac{|f(x_\alpha, y_\gamma) - f(z_\beta, y_\gamma)|}{|x_\alpha - z_\beta|^{1/2}}.$$

Proof. Note that the function $I(x, z, y) = \frac{f(x, y) - f(z, y)}{|x - z|^{1/2}}$ is linear in y . We get

$$|I(x, z, y)| = \max(|I(x, z, y_l)|, |I(x, z, y_u)|).$$

Applying Lemma G.1 completes the proof. \square

Let \hat{f} be the linear interpolation of f . Suppose that $x \in I_x, z \in I_z, y \in I_y$ with $x_u \leq z_l$. Using the above estimates and notations, we can bound $I(f)$ as follows

$$\begin{aligned} I(f) &= \frac{|f(z, y) - f(x, y)|}{|x - z|^{1/2}} \leq \frac{|\hat{f}(x, y) - f(x, y)| + |\hat{f}(z, y) - f(z, y)|}{|x - z|^{1/2}} + \max_{\alpha, \beta, \gamma \in \{l, u\}} \frac{|f(x_\alpha, y_\gamma) - f(z_\beta, y_\gamma)|}{|x_\alpha - z_\beta|^{1/2}} \\ &\leq \left(\frac{h_x^2}{8} \|f_{xx}\|_{I_x \times I_y} + \frac{h_y^2}{8} (\|f_{yy}\|_{I_x \times I_y} + \|f_{yy}\|_{I_z \times I_y}) + \frac{h_z^2}{8} \|f_{xx}\|_{I_z \times I_y} \right) |x - z|^{-1/2} + M. \end{aligned}$$

G.8. Estimate of some explicit polynomials. We use the following bounds for some polynomials in the error estimate of the interpolation.

Lemma G.3. *We have the following estimates*

$$(G.52) \quad |(t-a)(t-b)| \leq \frac{(b-a)^2}{4}, \quad t \in [a, b],$$

$$(G.53) \quad |3t^2 - 2t| + |3t^2 - 4t + 1| \leq 1, \quad t \in [0, 1],$$

$$(G.54) \quad |t(t-1)(t-2)| \leq \frac{2}{3\sqrt{3}}, \quad t \in [0, 2],$$

$$(G.55) \quad t(t-1)^2 \leq \frac{4}{27}, \quad t \in [0, 1/2],$$

$$(G.56) \quad |t(t-1)(t-2)(t-3)| \leq 1, \quad t \in [0, 3],$$

$$(G.57) \quad |t^2(t-1)^2(t-2)| \leq \frac{1}{10}, \quad t \in [0, 1].$$

We will use the computer assisted method to verify the following estimate

$$\sum_{1 \leq i \leq 3} |p_i(x)| \leq 1.28, \quad \max_{x \in [0, 1]} |(x - \frac{1}{32})(x - \frac{1}{2})(x - \frac{31}{32})| \leq 0.04,$$

where p_i is the Lagrangian interpolating polynomials associated with $(\frac{1}{32}, \frac{1}{2}, \frac{31}{32})$.

Proof. The proof of (G.52) follows from the inequality of arithmetic and geometric means (AM-GM) or a direct calculation.

For (G.53), firstly, we note that $|a| + |b| = |a + b|$ or $|a - b|$. It suffices to prove $|a + b| \leq 1$ and $|a - b| \leq 1$ for $a = 3t^2 - 2t$, $b = 3t^2 - 4t + 1$. Since $t^2 - t \in [-1/4, 0]$, $2t - 1 \in [-1, 1]$, we have

$$a + b = 6t^2 - 6t + 1 \in [-1/2, 1], \quad a - b = 2t - 1 \in [-1, 1],$$

which implies $|a + b|, |a - b| \leq 1$. We prove the desired result.

Denote $s = t - 1 \in [-1, 1]$. Then using the AM-GM inequality, we have

$$t^2(t-1)^2(t-2)^2 = (t-1)^2(t^2-2t)^2 = \frac{1}{2}2s^2(1-s^2)^2 \leq \frac{1}{2}(\frac{2s^2+2(1-s^2)}{3})^3 = \frac{4}{27}.$$

Taking the square root on both sides proves (G.54).

To prove (G.55), applying the AM-GM inequality, we get

$$t(1-t)^2 = \frac{1}{2}2t(1-t)^2 \leq \frac{1}{2}(\frac{2t+2(1-t)}{3})^3 = \frac{4}{27}.$$

Denote $s = t(3-t) \in [0, \frac{9}{4}]$. Then we have $|s-1|^2 \in [0, 2]$ and

$$|(t-1)(t-2)t(t-3)| = |s(t^2-3t+2)| = |(2-s)s| = |1-(s-1)^2| \leq 1,$$

which implies (G.56).

To prove (G.57), we use (G.52) with $a = 0, b = 1$ and (G.54) to obtain

$$|t^2(t-1)^2(t-2)| \leq \frac{1}{4} \frac{2}{3\sqrt{3}} = \frac{1}{6\sqrt{3}} < \frac{1}{10},$$

where the last inequality follows from $(6\sqrt{3})^2 = 108 > 100 = 10^2$. \square

Acknowledgments. The research was in part supported by NSF Grants DMS-1907977 and DMS-2205590. We would like to acknowledge the generous support from Mr. K. C. Choi through the Choi Family Gift Fund and the Choi Family Postdoc Gift Fund.

REFERENCES

- [1] Franck Barthe. On a reverse form of the brascamp-lieb inequality. *Inventiones mathematicae*, 134(2):335–361, 1998.
- [2] Tristan Buckmaster, Steve Shkoller, and Vlad Vicol. Formation of shocks for 2D isentropic compressible Euler. *Communications on Pure and Applied Mathematics*.
- [3] Tristan Buckmaster, Steve Shkoller, and Vlad Vicol. Formation of point shocks for 3D compressible Euler. *arXiv preprint arXiv:1912.04429*, 2019.

- [4] Roberto Castelli, Marcio Gameiro, and Jean-Philippe Lessard. Rigorous numerics for ill-posed PDEs: periodic orbits in the Boussinesq equation. *Archive for Rational Mechanics and Analysis*, 228(1):129–157, 2018.
- [5] A Castro and D Córdoba. Infinite energy solutions of the surface quasi-geostrophic equation. *Advances in Mathematics*, 225(4):1820–1829, 2010.
- [6] Angel Castro, Diego Córdoba, and Javier Gómez-Serrano. Global smooth solutions for the inviscid sqg equation. 2020.
- [7] Angel Castro, Diego Córdoba, Javier Gómez-Serrano, and Alberto Martín Zamora. Remarks on geometric properties of SQG sharp fronts and α -patches. *arXiv preprint arXiv:1401.5376*, 2014.
- [8] Jiajie Chen. Singularity formation and global well-posedness for the generalized Constantin–Lax–Majda equation with dissipation. *Nonlinearity*, 33(5):2502, 2020.
- [9] Jiajie Chen. On the regularity of the De gregorio model for the 3D Euler equations. *To appear in J. Eur. Math. Soc., arXiv preprint arXiv:2107.04777*, 2021.
- [10] Jiajie Chen. On the slightly perturbed De Gregorio model on S^1 . *Arch. Ration. Mech. Anal.*, 241(3):1843–1869, 2021.
- [11] Jiajie Chen and Thomas Y Hou. On stability and instability of $C^{1,\alpha}$ singular solutions to the 3D Euler and 2D Boussinesq equations. *arXiv preprint: arXiv:2206.01296 [math.AP]*.
- [12] Jiajie Chen and Thomas Y Hou. Finite time blowup of 2D Boussinesq and 3D Euler equations with $C^{1,\alpha}$ velocity and boundary. *Communications in Mathematical Physics*, 383(3):1559–1667, 2021.
- [13] Jiajie Chen, Thomas Y Hou, and De Huang. Asymptotically self-similar blowup of the Hou–Luo model for the 3D Euler equations. *arXiv preprint arXiv:2106.05422*.
- [14] Jiajie Chen, Thomas Y Hou, and De Huang. On the finite time blowup of the De Gregorio model for the 3D Euler equations. *Communications on Pure and Applied Mathematics*, 74(6):1282–1350, 2021.
- [15] K Choi, TY Hou, A Kiselev, G Luo, V Sverak, and Y Yao. On the finite-time blowup of a 1D model for the 3D axisymmetric Euler equations. *CPAM*, 70(11):2218–2243, 2017.
- [16] K Choi, A Kiselev, and Y Yao. Finite time blow up for a 1D model of 2D Boussinesq system. *Comm. Math. Phys.*, 334(3):1667–1679, 2015.
- [17] P Constantin. On the Euler equations of incompressible fluids. *Bulletin of the American Mathematical Society*, 44(4):603–621, 2007.
- [18] P Constantin, C Fefferman, and AJ Majda. Geometric constraints on potentially singular solutions for the 3D Euler equations. *Communications in Partial Differential Equations*, 21(3–4), 1996.
- [19] P Constantin, P. D. Lax, and A. Majda. A simple one-dimensional model for the three-dimensional vorticity equation. *CPAM*, 38(6):715–724, 1985.
- [20] Dario Cordero-Erausquin, Bruno Nazaret, and Cédric Villani. A mass-transportation approach to sharp sobolev and gagliardo–nirenberg inequalities. *Advances in Mathematics*, 182(2):307–332, 2004.
- [21] Diego Córdoba, Javier Gómez-Serrano, and Andrej Zlatoš. A note on stability shifting for the Muskat problem, II: From stable to unstable and back to stable. *Analysis & PDE*, 10(2):367–378, 2017.
- [22] Guy David and Jean-Lin Journé. A boundedness criterion for generalized calderón-zygmund operators. *Annals of Mathematics*, pages 371–397, 1984.
- [23] Guy David, Jean-Lin Journé, and Stephen Semmes. Opérateurs de calderón-zygmund, fonctions para-acrétives et interpolation. *Revista Matemática Iberoamericana*, 1(4):1–56, 1985.
- [24] S De Gregorio. On a one-dimensional model for the three-dimensional vorticity equation. *Journal of Statistical Physics*, 59(5–6):1251–1263, 1990.
- [25] S De Gregorio. A partial differential equation arising in a 1D model for the 3D vorticity equation. *Mathematical Methods in the Applied Sciences*, 19(15):1233–1255, 1996.
- [26] J Deng, TY Hou, and X Yu. Geometric properties and nonblowup of 3D incompressible Euler flow. *Communications in Partial Difference Equations*, 30(1–2):225–243, 2005.
- [27] Tarek M Elgindi. Finite-time singularity formation for $C^{1,\alpha}$ solutions to the incompressible Euler equations on \mathbb{R}^3 . *Annals of Mathematics*, 194(3):647–727, 2021.
- [28] Tarek M Elgindi, Tej-Eddine Ghoul, and Nader Masmoudi. On the stability of self-similar blow-up for $C^{1,\alpha}$ solutions to the incompressible Euler equations on \mathbb{R}^3 . *arXiv preprint arXiv:1910.14071*, 2019.
- [29] Tarek M Elgindi, Tej-eddine Ghoul, and Nader Masmoudi. Stable self-similar blow-up for a family of nonlocal transport equations. *Analysis & PDE*, 14(3):891–908, 2021.
- [30] Tarek M Elgindi and In-Jee Jeong. Finite-time singularity formation for strong solutions to the axi-symmetric 3D Euler equations. *Annals of PDE*, 5(2):1–51, 2019.
- [31] Tarek M. Elgindi and In-Jee Jeong. On the effects of advection and vortex stretching. *Archive for Rational Mechanics and Analysis*, Oct 2019.
- [32] Tarek M Elgindi and In-Jee Jeong. Finite-time singularity formation for strong solutions to the Boussinesq system. *Annals of PDE*, 6:1–50, 2020.
- [33] Alberto Enciso, Javier Gómez-Serrano, and Bruno Vergara. Convexity of Whitham’s highest cusped wave. *arXiv preprint arXiv:1810.10935*, 2018.
- [34] Alessio Figalli, Francesco Maggi, and Aldo Pratelli. A mass transportation approach to quantitative isoperimetric inequalities. *Inventiones mathematicae*, 182(1):167–211, 2010.
- [35] JD Gibon. The three-dimensional Euler equations: Where do we stand? *Physica D: Nonlinear Phenomena*, 237(14):1894–1904, 2008.

- [36] Javier Gómez-Serrano. Computer-assisted proofs in pde: a survey. *SeMA Journal*, 76(3):459–484, 2019.
- [37] Javier Gómez-Serrano and Rafael Granero-Belinchón. On turning waves for the inhomogeneous Muskat problem: a computer-assisted proof. *Nonlinearity*, 27(6):1471, 2014.
- [38] Vu Hoang, Betul Orcan-Ekmekci, Maria Radosz, and Hang Yang. Blowup with vorticity control for a 2D model of the Boussinesq equations. *Journal of Differential Equations*, 264(12):7328–7356, 2018.
- [39] Vu Hoang and Maria Radosz. Singular solutions for nonlocal systems of evolution equations with vorticity stretching. *SIAM Journal on Mathematical Analysis*, 52(2):2158–2178, 2020.
- [40] T Y Hou. The potentially singular behavior of the 3D Navier–Stokes equations. *Foundation of Computational Mathematics*, published online on 9/7/2022, DOI: <https://doi.org/10.1007/s10208-022-09578-4>, 2021.
- [41] T Y Hou. Potential singularity of the 3D Euler equations in the interior domain. *Foundation of Computational Mathematics*, published online on 9/7/2022, DOI: <https://doi.org/10.1007/s10208-022-09585-5>, 2022.
- [42] T Y Hou and D Huang. Potential singularity formation of 3D axisymmetric Euler equations with degenerate variable viscosity coefficients. *MMS*, accepted, 2022, [arXiv:2102.06663](https://arxiv.org/abs/2102.06663), 2021.
- [43] T. Y. Hou and D Huang. A potential two-scale traveling wave asingularity for 3D incompressible Euler equations. *Physica D*, 435:133257, 2022.
- [44] TY Hou. Blow-up or no blow-up? a unified computational and analytic approach to 3D incompressible Euler and Navier–Stokes equations. *Acta Numerica*, 18(1):277–346, 2009.
- [45] TY Hou and C Li. Dynamic stability of the three-dimensional axisymmetric Navier–Stokes equations with swirl. *Communications on Pure and Applied Mathematics*, 61(5):661–697, 2008.
- [46] TY Hou and R Li. Dynamic depletion of vortex stretching and non-blowup of the 3D incompressible Euler equations. *Journal of Nonlinear Science*, 16(6):639–664, 2006.
- [47] Carlos E Kenig and Frank Merle. Global well-posedness, scattering and blow-up for the energy-critical, focusing, non-linear Schrödinger equation in the radial case. *Inventiones mathematicae*, 166(3):645–675, 2006.
- [48] A Kiselev and V Sverak. Small scale creation for solutions of the incompressible two dimensional Euler equation. *Annals of Mathematics*, 180:1205–1220, 2014.
- [49] Alexander Kiselev. Small scales and singularity formation in fluid dynamics. In *Proceedings of the International Congress of Mathematicians*, volume 3, 2018.
- [50] Alexander Kiselev and Changhui Tan. Finite time blow up in the hyperbolic Boussinesq system. *Adv. Math.*, 325:34–55, 2018.
- [51] Laurent Lafleche, Alexis F Vasseur, and Misha Vishik. Instability for axisymmetric blow-up solutions to incompressible Euler equations. *Journal de Mathématiques Pures et Appliquées*, 155:140–154, 2021.
- [52] Michael J. Landman, George C. Papanicolaou, Catherine Sulem, and Pierre-Louis Sulem. Rate of blowup for solutions of the nonlinear Schrödinger equation at critical dimension. *Phys. Rev. A (3)*, 38(8):3837–3843, 1988.
- [53] Pengfei Liu. *Spatial Profiles in the Singular Solutions of the 3D Euler Equations and Simplified Models*. PhD thesis, California Institute of Technology, 2017. <https://resolver.caltech.edu/CaltechTHESIS:09092016-000915850>.
- [54] G Luo and TY Hou. Toward the finite-time blowup of the 3D incompressible Euler equations: a numerical investigation. *SIAM Multiscale Modeling and Simulation*, 12(4):1722–1776, 2014.
- [55] Guo Luo and Thomas Y Hou. Potentially singular solutions of the 3D axisymmetric Euler equations. *Proceedings of the National Academy of Sciences*, 111(36):12968–12973, 2014.
- [56] AJ Majda and AL Bertozzi. *Vorticity and incompressible flow*, volume 27. Cambridge University Press, 2002.
- [57] Yvan Martel, Frank Merle, and Pierre Raphaël. Blow up for the critical generalized Korteweg–de Vries equation. I: Dynamics near the soliton. *Acta Mathematica*, 212(1):59–140, 2014.
- [58] Nader Masmoudi and Hatem Zaag. Blow-up profile for the complex Ginzburg–Landau equation. *Journal of Functional Analysis*, 255(7):1613–1666, 2008.
- [59] Alan McIntosh. Algèbres d’opérateurs définis par des intégrales singulières. *CR Acad. Sci. Paris Sér. I Math.*, 301:395–397, 1985.
- [60] David W. McLaughlin, George C. Papanicolaou, Catherine Sulem, and Pierre-Louis Sulem. Focusing singularity of the cubic Schrödinger equation. *Phys. Rev. A*, 34(2):1200, 1986.
- [61] Frank Merle and Pierre Raphael. The blow-up dynamic and upper bound on the blow-up rate for critical nonlinear Schrödinger equation. *Annals of mathematics*, pages 157–222, 2005.
- [62] Frank Merle, Pierre Raphaël, Igor Rodnianski, and Jeremie Szeftel. On blow up for the energy super critical defocusing nonlinear Schrödinger equations. *Inventiones mathematicae*, 227(1):247–413, 2022.
- [63] Frank Merle, Pierre Raphaël, Igor Rodnianski, and Jeremie Szeftel. On the implosion of a compressible fluid i: smooth self-similar inviscid profile. *Ann. of Math. (2)*, 196(2):567–778, 2022.
- [64] Frank Merle, Pierre Raphaël, Igor Rodnianski, and Jeremie Szeftel. On the implosion of a compressible fluid ii: singularity formation. *Ann. of Math. (2)*, 196(2):779–889, 2022.
- [65] Frank Merle and Hatem Zaag. Stability of the blow-up profile for equations of the type $u_t = \Delta u + |u|^{p-1}u$. *Duke Math. J.*, 86(1):143–195, 1997.
- [66] Frank Merle and Hatem Zaag. On the stability of the notion of non-characteristic point and blow-up profile for semilinear wave equations. *Communications in Mathematical Physics*, 333(3):1529–1562, 2015.

- [67] Ramon E Moore, R Baker Kearfott, and Michael J Cloud. *Introduction to interval analysis*, volume 110. Siam, 2009.
- [68] H Okamoto, T Sakajo, and M Wunsch. On a generalization of the constantin–lax–majda equation. *Nonlinearity*, 21(10):2447–2461, 2008.
- [69] Siegfried M Rump. Verification methods: Rigorous results using floating-point arithmetic. *Acta Numerica*, 19:287–449, 2010.
- [70] Steven Schochet. Explicit solutions of the viscous model vorticity equation. *Communications on pure and applied mathematics*, 39(4):531–537, 1986.
- [71] Jack Sherman and Winifred J Morrison. Adjustment of an inverse matrix corresponding to a change in one element of a given matrix. *The Annals of Mathematical Statistics*, 21(1):124–127, 1950.
- [72] Alexis F Vasseur and Misha Vishik. Blow-up solutions to 3D Euler are hydrodynamically unstable. *Communications in Mathematical Physics*, 378(1):557–568, 2020.
- [73] Cédric Villani. *Optimal transport: old and new*, volume 338. Springer, 2009.
- [74] Cédric Villani. *Topics in optimal transportation*, volume 58. American Mathematical Soc., 2021.
- [75] Yongji Wang, Ching-Yao Lai, Javier Gomez-Serrano, and Tristan Buckmaster. Self-similar blow-up profile for the Boussinesq equations via a physics-informed neural network. *arXiv:2201.06780v1 [math.AP]*, 2022.

COURANT INSTITUTE AND APPLIED AND COMPUTATIONAL MATHEMATICS, CALTECH, PASADENA, CA 91125.
 EMAILS: JIAJIE.CHEN@CIMS.NYU.EDU, HOU@CMS.CALTECH.EDU,